# The role of *rdc1/cxcr7b* in the migration of the zebrafish posterior lateral line

Duncan Bruce Wilson

Division of Developmental Biology,

National Institute for Medical Research and

Department of Anatomy and Developmental Biology,

University College London

Thesis submitted to University College London for the degree of Doctor of Philosophy





ProQuest LLC
789 East Eisenhower Parkway
P.O. Box 1346
Ann Arbor, MI 48106-1346

I, Duncan Bruce Wilson, do hereby confirm that the work presented in this thesis is my own work. Where information has been derived from other sources, I confirm that this has been indicated in the thesis.

# Abstract

The posterior lateral line primordium migrates along the horizontal myoseptum to the tip of the tail. The migration of the primordium utilises the CXC-type chemokine receptor *cxcr4b* which is expressed in a graded fashion within the primordium; with strongest expression at the leading edge. The ligand for CXCR4b is stromal-derived factor 1a (SDF1a). *sdf1a* is expressed along the length of the horizontal myoseptum. Loss of *cxcr4b*, or *sdf1a*, results in defects in migration. However, various observations suggest additional systems guiding the primordium.

We have performed an expression screen to identify genes with differential expression in the migrating primordium and as a result have identified the chemokine receptor *cxcr7b*, which is expressed in a complimentary fashion to *cxcr4b*. Functional analyses reveal that *cxcr7b* is essential for initiation and guidance of primordium migration.

This work reveals that the posterior lateral line primordium is formed by fusion of several distinct groups of placodal cells and the fusion of these groups correlates with the initiation of directional migration. Inhibition of *cxcr7b* function leads to retarded primordium migration and failure to complete coalescence. Ectopic expression of *cxcr7b* on the path results in stalled migration of the leading cells; suggesting a role for *cxcr7b* in altering the response of the primordium to *sdf1a*, possibly by inhibiting its effect. It is likely that expression of *cxcr7b* in the trailing part of the primordium acts to render it incapable of responding to the underlying *sdf1a* stripe, thus producing directional guidance of migration.

Preliminary results from this work also demonstrate the presence of FGF signalling in parallel to the *cxcr4b*/*cxcr7b*/*sdf1a* pathways which may have roles in the initiation and guidance of the migration of the posterior lateral line primordium. In the absence of *cxcr4b*/*cxcr7b*/*sdf1a* pathways the primordium often migrates aberrantly towards the pectoral fin bud due to the presence of FGF signalling.

# Table of contents

# Acknowledgements

There are many to thank for making my study at the NIMR so enjoyable and rewarding. Particularly I thank my supervisor, Qiling Xu, for her help, advice, discussion and support. Her aid in the preparation of this thesis has been invaluable and I have learnt a great deal. Thanks must also go to all the lab members past and present for their counsel and their fantastic scientific assistance, in particular Betty Bennett for her help during the *in situ* hybridisation screen. I am grateful to everyone in Developmental Biology for taking an interest in my work, their friendship, help, advice, and emergency supply of reagents has been invaluable.

Outside of Development Biology thanks and praise must go to the Wilkinson Lab for their help with reagents and general advice, Daan Zhu and Kate Sullivan for their help with acquisition and processing of confocal microscopy data, and Darren Gilmour for supplying the *Odysseus* mutant and CldnB:LynEGFP transgenic zebrafish lines.

Finally, my deepest thanks go to my mother, sister and Sharon for their support, encouragement and everything else that has made my studies possible. I could not have done it without them.

# Abbreviations

| | |
|---|---|
| BCIP | 5-bromo-4-chloro-3-indolyl phosphate |
| BLAST | Basic Local Alignment and Searching Tool |
| bp | Base pair |
| cAMP | Cyclic adenosine monophosphate |
| CBLD | Cascade Blue lysinated dextran |
| cDNA | Complementary DNA |
| CXCR4 | CXC-type chemokine receptor 4 |
| CXCR7 | CXC-type chemokine receptor 7 |
| CXCL11 | CXC-type ligand 11 (ITAC) |
| CXCL12 | CXC-type ligand 12 (SDF1) |
| DAPI | 4',6-diaminobenzidine |
| DIG | Digoxigenin |
| DMSO | Dimethyl sulphoxide |
| DNA | Deoxyribonucleic acid |
| dNTP | Deoxyribonucleotide triphosphate |
| dpf | Days post fertilisation |
| DTT | Dithiothreitol |
| ECM | Extracellular matrix |
| EGFP | Enhanced green fluorescent protein |
| ERK | Extracellular signal-regulated kinase |
| ERM | ETS related molecule |
| EST | Expressed sequence tag |
| EtOH | Ethanol |
| EYFP | Enhanced yellow fluorescent protein |
| FAK | Focal adhesion kinase |
| FGF | Fibroblast growth factor |
| FGF10 | Fibroblast growth factor 10 |
| FGFR | Fibroblast growth factor receptor |
| FGFR1 | Fibroblast growth factor receptor 1 |
| GEFs | Guanine exchange factors |
| GPCR | G-protein coupled receptor |
| GS | Goat serum |
| HISS | Heat inactivated sheep serum |
| hm | Horizontal myoseptum |
| hpf | Hours post fertilisation |

| | |
|---|---|
| IMAGE | Integrated Molecular Analysis of Genomes and their Expression Consortium |
| ITAC | Interferon-inducible T-cell alpha chemoattractant |
| inc | Interneuromast cell |
| JAK | Janus kinase |
| LB | Luria-Bertani |
| LRD | Lysinated rhodamine dextran |
| MAPK | Mitogen activated protein kinase |
| MeOH | Methanol |
| MLCK | Myosin light chain kinase |
| MO | Morpholino |
| mp | Migrating primordium |
| NaAc | Sodium acetate |
| NBT | Nitro blue tetrazolium |
| NCBI | National Centre for Biotechnology Information |
| NIH | National Institutes of Health |
| NIMR | National Institute for Medical Research |
| NM | Neuromast |
| NTP | Nucleotide triphosphate |
| ov | Otic vesicle |
| PBS | Phosphate buffered saline |
| PBT | PBS-0.1% Tween20 |
| PCR | Polymerase chain reaction |
| PDGF | Platelet derived growth factor |
| PEA3 | Polyomavirus enhancer activator 3 |
| PFA | Paraformaldehyde |
| PGC | Primordial germ cell |
| PI3K | Phosphoinositide-3 kinase |
| PKB | Protein kinase B |
| pllg | Posterior lateral line ganglion |
| plln | Posterior lateral line nerve |
| pllp | Posterior lateral line primordium |
| PTEN | Phosphatase and tensin |
| RFP | Red fluorescent protein |
| RNA | Ribonucleic acid |
| s | Somite |

| | |
|---|---|
| SC | Separated cells |
| SDF1 | Stromal-derived factor 1 (CXCL12) |
| SHIP1 | Src homology 2 domain-containing inositol 5-phosphatase |
| SSC | Saline sodium citrate |
| STAT | Signal transducers and activators of transcription |
| Tricaine | Tricaine methane sulphonate |
| TRITC | Tetramethylrhodamine isothiocyanate |
| VEGF | Vascular endothelial-derived growth factor |
| WHIM | Warts, Hypogammaglobulinemia, Infections, and Myleokathexis syndrome |
| ZFIN | Zebrafish Information Network |

# Chapter 1: Introduction

Directed cell migration is the ability of a cell, or cells, to migrate from one location to another by responding to attractive and/or repulsive cues present in their environment by a process termed chemotaxis. Chemotactic cell movement is an indispensable component of many biological processes including embryogenesis, organogenesis, wound healing and immune responses. As such it is a tightly regulated process and defective migration is associated with a number of human diseases including cancer metastasis, craniofacial defects and WHIM (Warts, Hypogammaglobulinemia, Infections, and Myleokathexis) syndrome. Due to the biological importance of cell migration it has been widely studied in a range of model systems.

## 1.1 Molecules involved in directional cell migration

Chemotaxis is the process by which a cell senses the signals present in its environment and converts that information into a migratory response. Much of our understanding of chemotaxis comes from studies conducted in *Dictyostelium discoidium* and neutrophils. The response of a cell to a chemoattractant can be broken down into three phases. First the extracellular signal must be detected and the cell must determine whether it should move toward or away from the stimulus. Next the cell must reorganise its cytoskeleton and polarise to be able to move in a specific direction. Finally, the cell must extend protrusions in the appropriate direction create new attachments to the extracellular matrix at its leading edge, disassemble attachments at its trailing edge and retract its trailing edge to move forward.

Many molecules are known to act as attractive and/or repulsive cues for migratory cells and the responses they elicit are essential for many biological processes. The following are examples of some of these molecules and the systems in which they exert their influence: Cyclic-adenosine monophosphate (cAMP) is a chemoattractant for the slime mould *D. discoidium* used in the hunting of bacteria and the formation of the fruiting body in response to starvation (Bonner, 1970; Goidl et al., 1972; Konijn et al., 1969). Fibroblast growth factors (FGFs) have been shown to act as both attractants and repellents during chick gastrulation (Yang et al., 2002), and are required for completion of gastrulation in mouse (Sun et al., 1999). Migration of sex myoblast cells in *Caenorhabditis elegans* is guided by the FGF-family member *egl-17* (Burdine et al., 1997), and trachea formation in *Drosophila melanogaster* requires the FGF homologue *bnl* (*branchless*) (Ribeiro et al., 2002). Semaphorins have been

shown to act as both repellents and attractants of neural axons in zebrafish and mammals (Wolman et al., 2004) (Kantor et al., 2004). Vascular endothelial derived growth factor (VEGF) guides the migration of haematopoietic precursor cells in the mouse embryo (Hiratsuka et al., 2005). The chemokine stromal derived factor 1 (SDF1), and its receptor CXC-type chemokine receptor 4 (CXCR4) have been implicated in blood cell maturation and migration (Cherla and Ganju, 2001), motor neurone cell body migration in the hindbrain (Sapede et al., 2005), primordial germ cell migration to the gonad (Ara et al., 2003; Doitsidou et al., 2002; Dumstrei et al., 2004), neural crest migration and melanophore patterning (Svetic et al., 2007), and metastasis of a wide range of cancers (Zlotnik, 2006). In short there are many ligands and receptors that are capable of guiding cell migration and their effects can be cell context specific.

When exposed to an attractive, or repulsive, cue the signal has to be transduced from the exterior to the interior of the cell. The resultant signalling cascades then facilitate migration.

### 1.1.1 G-protein coupled receptor mediated migration

The G-protein coupled receptor (GPCR) superfamily is very large and diverse in structure and function. It represents the largest class of membrane proteins in the human genome with more than 800 human GPCR sequences identified in a recent survey (Fredriksson et al., 2003).

GPCRs have a common structural signature, consisting of seven hydrophobic transmembrane domains, an extracellular amino-terminus and an intracellular carboxy-terminus. However, their protein sequences are highly variable and much of our understanding of GPCR structure depends on high-resolution structures of bovine rhodopsin (Kobilka, 2007). The structural conformity of GPCRs is in stark contrast to the diversity of their natural ligands which range from subatomic particles (photons), to ions, small organic molecules, peptides and proteins (Ji et al., 1998).

The GPCR superfamily can be subdivided into five smaller families: the rhodopsin family, adhesion family, frizzled/taste family, glutamate family, and secretin family. The physiological function of many GPCRs is as yet unknown; these receptors are referred to as the orphan GPCRs (Kobilka, 2007). Orphan GPCRs are widely studied as potential targets for pharmaceutical drug design. Hence, the number of orphan GPCRs is in continual decline as they are reassigned to new sub-families (Kobilka, 2007).

Within the rhodopsin subfamily lie the chemokine receptors. The chemokines, or **chemo**attractive cyto**kines**, have diverse roles in directed cell migration (Fredriksson et al., 2003). Chemokines are classified, depending on the number and spacing of amino-terminal cystein residues, into four subgroups: C, CC, CXC and CX3C. The chemokine receptors are split into four corresponding subfamilies dependent upon the family of the ligands they bind. Thus there are CC-chemokine receptors, CXC-chemokine receptors, CX3C-chemokine receptors and C-chemokine receptors (Procko and McColl, 2005). Each receptor class binds only one class of ligand; however, many bind multiple ligands from within one class. Chemokines, and chemokine receptors, play important roles in inflammation, cell migration, wound healing, haematopoiesis, embryogenesis and metastasis (See (Horuk, 2001) for review).

Activation of chemokine receptors is thought to have a similar mechanism to other GPCRs. The ligand binds to the extracellular domains resulting in conformational changes in the receptor that allow intracellular signalling (Kobilka and Deupi, 2007). The ternary complex model of GPCR activation postulates that receptors have a limited number of conformations representing inactive, active and limited intermediate states. However, the link between conformation and activity is not well understood (Berchiche et al., 2007).

GPCRs are so named because of their ability to interact with the heterotrimeric G-proteins consisting of the Gα, Gβ and Gγ subunits (Neves et al., 2002). There are several different types of each G-protein subunit and dependent upon which combination of heterotrimeric G-proteins a GPCR couples to they can affect multiple pathways including transcriptional machinery and motility pathways (Neves et al., 2002; Ye, 2001).

Ligand binding causes conformational changes in the GPCR that allow it to signal through the heterotrimeric G-protein complex composed of the Gα and Gβγ subunits. The Gβγ subunit is thought not to dissociate under physiological conditions and so the G-protein complex essentially functions as a dimer (Alberts B, 1998; Neves et al., 2002). The Gα subunit activates adenylcyclase leading to the production of cyclic adenosine monophosphate (cAMP), activation of protein kinase A (PKA) and activation of $Ca^{2+}$ channels leading to an increase in intracellular $Ca^{2+}$ and activation of many signalling cascades including cytoskeletal rearrangement and gene transcription (Alberts B, 1998).

There is also mounting evidence that GPCRs can signal through non-G-protein linked pathways by signalling via β-arrestin to activate the extracellular signal-regulated kinase (ERK1/2) pathway and mitogen activated protein kinase (MAPK) pathway (Kang et al., 2005; Lefkowitz and Shenoy, 2005; Luttrell, 2002). Activation of the ERK or MAPK signalling pathways leads to activation of myosin light chain kinase (MLCK), paxillin, focal adhesion kinase (FAK) and the proteolytic enzyme calpain resulting in membrane protrusions and altered cell adhesion properties that allow cell migration to occur (Huang et al., 2004). This non-G-protein mediated signalling has led to the proposal that GPCRs should be referred to as seven-transmembrane (7-TM) receptors (Kobilka, 2007). However, for the purposes of this thesis they shall retain the name G-protein coupled receptors. In addition, there is evidence that homo- and hetero-dimerisation of GPCRs can alter their responses to ligands and their signalling properties (Levoye et al., 2006; Mellado et al., 2001a; Mellado et al., 2001b; Springael et al., 2005). Following signalling GPCRs are desensitised by internalisation of the receptor which is then either degraded or recycled to the cell surface (Ferguson, 2001; Marchese et al., 2003) though this process may not necessarily require ligand binding (Futahashi et al., 2007).

The molecular mechanisms underlying G-protein coupled receptor mediated migration have been widely studied in neutrophils and *Dictyostelium* (Charest and Firtel, 2007). Following G-protein coupled receptor signalling phosphoinositol-3 kinase (PI3K) localises to the leading edge of the cell where it catalyses the conversion of phosphatidylinositol 3,4 bisphosphate ($PIP_2$) to phosphatidylinositol 3,4,5 trisphosphate ($PIP_3$) (Funamoto et al., 2002). Meanwhile phosphatase and tensin (PTEN), which catalyses the reverse reaction, translocates to the back and sides of the cell where it inhibits the formation of membrane protrusions (Funamoto et al., 2002; Iijima and Devreotes, 2002). The opposing localisation of PI3K and PTEN facilitates the formation of an internal $PIP_3$ gradient which allows the cell to become polarised (Funamoto et al., 2002; Iijima and Devreotes, 2002).

The localised increase in $PIP_3$ at the front of the cell leads to the recruitment of pleckstrin homology (PH) domain containing proteins to the membrane (Funamoto et al., 2002). This ultimately leads to actin and microtubule branching, and polymerisation, resulting in the extension of filopodia and lamellopodia from the leading edge of the cell and the formation of new adhesions to the extracellular matrix at the advancing edge (Affolter and Weijer, 2005; Ridley et al., 2003; Van Haastert and Devreotes, 2004). Meanwhile type-II myosin localises to the trailing region of the cell where it is thought to generate the force necessary to disassemble

the existing adhesions to the extracellular matrix and retract the trailing part of the cell (Chung et al., 2001). Disruption of the intracellular $PIP_2/PIP_3$ gradient inhibits polarisation and leads to the production of random cell protrusions and hindered migration (Chung et al., 2001; Devreotes and Janetopoulos, 2003; Funamoto et al., 2002; Iijima and Devreotes, 2002).

### 1.1.2 Fibroblast growth factor mediated migration

Fibroblasts growth factors (FGFs) were originally identified as growth promoters for cultured fibroblasts (Gospodarowicz et al., 1974) however, they have since been shown to have roles in development, metabolism and disease (See (Eswarakumar et al., 2005; Itoh, 2007; Thisse and Thisse, 2005) for reviews). FGFs represent a large family of polypeptide signalling molecules identified in a number of multicellular organisms from the nematode to humans (see (Itoh and Ornitz, 2004) for a review).

The FGF family consists of 22 members in human and mouse, and 27 members, including six paralogs, in zebrafish (Itoh, 2007). Though FGFs vary in size from 17 to 34 kDa, they share a conserved core of 120 amino acids (Itoh, 2007). FGFs mediate their responses through a family of four tyrosine kinase receptors; fibroblast growth factor receptors 1-4 (FGFR1-4). FGFRs comprise of an extracellular ligand binding domain, a single transmembrane domain and a cytoplasmic domain which contains catalytic tyrosine kinase and regulatory sequences (Eswarakumar et al., 2005). The ligand binding domain consists of three immunoglobulin like domains designated D1-D3. *fgfr1-fgfr3* encode two alternate versions of immunoglobulin-like domain three (D3II and D3III) that are generated by alternative mRNA splicing thereby resulting in seven different FGFR proteins (FGFRs1b, 1c, 2b, 2c, 3b, 3c, and 4) (Eswarakumar et al., 2005; Itoh, 2007). These alternate splicing events alter the ligand binding specificity of the individual receptors (Johnson and Williams, 1993; Zhang et al., 2006). FGF binding to an FGFR causes receptor dimerisation, trans-activation of receptor tyrosine kinases and autophosphorylation of the cytoplasmic domain of the receptors leading to activation of many downstream pathways including PI3K, MAPK, ERK1/2 (Boilly et al., 2000; Eswarakumar et al., 2005) and regulation of transcription through the transcription factors ETS related molecule (ERM) and polyomavirus enhancer activator 3 (PEA3) (Raible and Brand, 2001; Roehl and Nusslein-Volhard, 2001). These pathways mediate multiple cellular responses including chemotactic responses and cell proliferation (Eswarakumar et al., 2005).

FGFs have been implicated as chemoattractants in *Drosophila* trachea formation and border cell migration. The migration of tracheal cells during the development of the embryonic tracheal system is dependent upon Branchless/FGF (Bnl/FGF) signalling through the Breathless/FGFR (Btl/FGFR). The migrating tracheal cells express *btl/fgfr* while *bnl/fgf* is expressed in groups of ectodermal and mesodermal cells in a dynamic pattern which coordinates tracheal branch formation and outgrowth (Affolter and Weijer, 2005; Ribeiro et al., 2002). FGFR signalling is

required at the tip of the migrating tracheal primordium (Sato and Kornberg, 2002). Loss of *bnl* mediated signalling leads to a reduction in the formation of filopodia and subsequent extension of the tracheal cells (Ribeiro et al., 2002). In border cells the Btl /FGFR is expressed by the ovary and mutations in Btl/FGFR result in retarded migration of the border cells. Furthermore, over-expression of Btl/FGFR in null backgrounds can partially rescue migration, however, the partial rescue indicates that additional signalling pathways are involved in border cell migration (Murphy et al., 1995). Indeed a *Drosophila* protein related to platelet derived growth factor (PDGF) and vascular endothelial growth factor (VEGF), PVF1, is also required for normal migration of the border cells (Duchek and Rorth, 2001; Duchek et al., 2001).

In addition, FGF mediated signalling via FGFRs has been implicated in a wide range of cell migration events including; mouse germ cell migration (Takeuchi et al., 2005), sex myoblast migration in *C. elegans* (Burdine et al., 1997), Ciona heart formation (Davidson et al., 2005), and mutations are associated with increased cancer cell motility (Bange et al., 2002). However, it is not yet clear whether cell migration is a direct response to ligand binding or as a result of downstream gene activation (Yang et al., 2002).

### 1.1.3 Wnt/planar cell polarity pathway

Wnts bind 7-transmembrane receptors of the Frizzled (Fz) GPCR sub-family. Activation of the non-canonical Wnt pathways; the Wnt/PCP and Wnt/$Ca^{2+}$ pathways, leads to signalling cascades that in turn regulate cell movement and polarity (Rohde and Heisenberg, 2007; Seifert and Mlodzik, 2007). The activity of Wnt/PCP factors leads to polarisation of a field of cells along a specific axis. This is reflected by differential distribution of molecular markers and members of the Wnt/PCP pathway in the polarised cells (Fanto and McNeill, 2004; Seifert and Mlodzik, 2007). The Wnt/PCP pathway has been widely studied for its roles in establishing the polarity of a wide range of tissues including the directionality of hairs on both the *Drosophila* wing, and mammalian limbs together with the orientation of photoreceptor cells in the *Drosophila* eye (See (Fanto and McNeill, 2004) for review). In addition to establishing polarity Wnt/PCP signalling has been implicated in a number of cell migration events; during vertebrate gastrulation the Wnt/PCP pathway has been shown to coordinate the medially directed movement of cells (Seifert and Mlodzik, 2007); in zebrafish the *silberblick* (*wnt11*) and *pipetail* (*wnt5*) mutants disrupt convergent extension and result in a shortened body axis (Kilian et al., 2003; Ulrich et al., 2003). In addition, the Wnt/PCP pathway has been implicated

in controlling differential cell adhesion during the rotation of ommatidia in the *Drosophila* eye (Mirkovic and Mlodzik, 2006).

### 1.1.4 Semaphorins

Semaphorins are secreted, membrane bound or transmembrane glycoproteins of which more than 20 types have been described (Kruger et al., 2005; Tamagnone and Comoglio, 2004). Thus they can mediate both long- and short-range signalling (Tamagnone and Comoglio, 2004). In addition, some transmembrane semaphorins can act as receptors leading to 'reverse signalling' (Godenschwege et al., 2002).

Semaphorins act through interactions with plexins and neuropilins which often form oligomers that allow cross-talk between different signalling pathways (Tamagnone and Comoglio, 2004). Typically semaphorins act to collapse neural growth cones and pseudopodia (Tamagnone and Comoglio, 2004) and have roles in axon pathfinding where they have been shown to prevent axons crossing the midline of the brain and are required for guidance of motor axons to limbs (Poliakov et al., 2004). However, the effect of a semaphorin on a tissue may depend on the composition of its receptor and they may act as a chemoattractant, or chemorepellant, depending on their cellular context (Wolman et al., 2004). Furthermore, signalling mediated by the chemokine SDF1 has been shown to reduce the collapse of growth cones mediated by semaphorins (Chalasani et al., 2003). Thus cross-talk between receptor families can also alter the effect of semaphorins. In addition to their roles in axon guidance semaphorins have roles in vascular remodelling and act to exclude vasculature from the forming somites (Klagsbrun and Eichmann, 2005; Kruger et al., 2005). Furthermore, semaphorins have been implicated in tissue invasion by cancer cells and the vascularisation of tumours (Klagsbrun and Eichmann, 2005; Tamagnone and Comoglio, 2004).

### 1.1.5 Ephrins and ephrin receptors

Ephrins are classified into two groups depending on whether they are anchored to the membrane or have a transmembrane/cytoplasmic domain (Klagsbrun and Eichmann, 2005). Eph receptors are transmembrane proteins with an extracellular N-terminal ephrin binding domain and intracellular tyrosine kinases. Binding of ephrins to Eph receptors leads to receptor and ligand complex formation resulting in tyrosine kinase phosphorylation and activation of signal transduction cascades (Klagsbrun and Eichmann, 2005; Sela-Donenfeld and Wilkinson, 2005). Importantly, the transmembrane ephrins are also capable of mediating signalling, allowing both forward and reverse signalling following interaction with Eph receptors. Forward and reverse signalling has been shown to be important in the sorting of cells into distinct

populations and the control of gap junction formation, thereby controlling intercellular signalling between populations (Mellitzer et al., 1999). Ephrins and Ephs are poor activators of the MAPK and PI3K pathways, however, their activation of Rho GTPases leads to remodelling of the actin cytoskeleton (Egea and Klein, 2007). Depending on the cell type and the Eph/ephrin family involved interactions can either result in attraction or repulsion of the cells (Davy and Soriano, 2005). Ephrin signalling has roles in contact mediated repulsion which prevents cells from migrating into ligand expressing regions thus confining them to a restricted pathway (Poliakov et al., 2004) and is particularly important in neuron guidance (Wilkinson, 2001). For example the sorting of cells and formation of rhombomere boundaries in the zebrafish hindbrain has been shown to require forward and reverse signalling by Ephs and transmembrane ephrins (Xu et al., 1999). In addition, ephrin signalling has roles in preventing neural crest cells, and motor axons, from entering the caudal-most region of forming somites (Krull et al., 1997; Wang and Anderson, 1997).

## 1.2 Directional cell migration

Gradients formed by chemotropic factors act as essential guides in the development, function and regeneration of multicellular organisms. The directional and positional information they provide is essential for the guidance of migrating cells. Here we present several systems and examples to illustrate the processes and regulation of directional cell migration.

### 1.2.1 Neutrophils and *Dictyostelium*

The sensation of gradients by *Dictyostelium* is essential for feeding behaviour as well as aggregation and spore formation in response to starvation. Neutrophils sense a range of chemotropic signals and they migrate in response to infection or inflammation (von Philipsborn and Bastmeyer, 2007). Although distant in evolutionary terms neutrophils and *Dictyostelium* are single celled and morphologically similar. In addition, they share common pathways for gradient detection and migration (Charest and Firtel, 2007; Dormann and Weijer, 2006).

*Dictyostelium* are attracted by cyclic adenosine monophosphate (cAMP) and ascend gradients of cAMP in their environment. In order to migrate *Dictyostelium* translate the extracellular gradient to an internal one of $PIP_3$ along the cell membrane (von Philipsborn and Bastmeyer, 2007). cAMP is detected by the 7-transmembrane receptor cAMP receptor 1 (cAR1) which transduces the signal through the heterotrimeric G-proteins leading to recruitment of phosphoinositide-3 kinase (PI3K) to the cell membrane increasing the local concentration of $PIP_3$ at the leading edge.

This in turn leads to recruitment of PH domain containing proteins including protein kinase B (PKB) and guanine nucleotide exchange factors (GEFs) which regulates cytoskeletal rearrangements leading to actin polymerisation and branching in turn leading to the production of filopodia and lamellopodia from the leading edge (Affolter and Weijer, 2005; Chung et al., 2001). Intriguingly the cAR1 receptor does not show signs of polarisation and remains evenly distributed in polarised cells (Xiao et al., 1997). So how is polarity established? In *Dictyostelium* PTEN localises to the sides and trailing regions of the cell where it converts $PIP_3$ to $PIP_2$ which inhibits the formation of pseudopodia in these regions (Funamoto et al., 2002; Iijima and Devreotes, 2002) and in cells deficient for PTEN polarity is disrupted, leading to random pseudopodia formation and inhibited directional migration (Funamoto et al., 2002).

The detection of gradients by mammalian neutrophils is surprisingly similar to that of *Dictyostelium*. The extracellular chemotropic gradient is converted into an amplified internal gradient by PI3K activation and PIP3 localisation at the leading edge, with an intracellular feedback mechanism to maintain polarity once established (von Philipsborn and Bastmeyer, 2007). However, neutrophils have to navigate in multiple chemotactic signals which are imposed on top of one another and the exact method of signal transduction differs from *Dictyostelium*. Such chemotactic signals may be bacterially derived (e.g. formyl-MetLeuPhe (fMLP)) or host derived (e.g. Interleukin 8 (IL-8),or stromal derived factor 1a (SDF1a)) (von Philipsborn and Bastmeyer, 2007). Chemotactic signals in neutrophils are transduced by G-protein coupled receptors and lead to the localised increase of PIP3 and the recruitment of PH-domain containing proteins at the leading edge (Servant et al., 2000). This internal polarisation again results in the remodelling of the cytoskeleton and the production of pseudopodia from the leading edge, in a process dependant on localised activation of Rac at the leading edge and the inhibition of pseudopodia formation at the trailing edges by Rho. Rho in turn activates myosin contraction and retraction of the trailing edge of the cell (von Philipsborn and Bastmeyer, 2007). Interestingly, unlike *Dictyostelium*, neutrophils do not show polarised localisation of PTEN. However, it is proposed that SH2 domain-containing inositol 5-phosphatase 1 (SHIP1) serves the function of converting PIP3 to PIP2 in neutrophils and restricts pseudopodia formation to the leading edge. Furthermore, neutrophils lacking SHIP1 show similar defects in their ability to respond to extracellular signals as with *Dictyostelium* deficient for PTEN suggesting they share the same role (Nishio et al., 2007).

### 1.2.2 Gastrulation

In the embryos of multicellular organisms gastrulation is the morphogenetic process by which the future mesoderm and endoderm move inside the ectoderm to form a three layered embryo with ectoderm on the outside, endoderm on the inside and mesoderm between the two. Whilst the process of gastrulation varies from organism to organism, it involves the migration of many individual cells and the remodelling of tissues as the result of collective behaviours of cells within the tissue. During gastrulation cells show coordinated migration, collective changes in cell shape and cell rearrangements (Keller, 2005; Solnica-Krezel, 2006). Directional cell migration plays an intrinsic role in gastrulation however the underlying guidance cues have been elusive (Keller, 2005). In amphibian gastrulation the endodermal cells involute to form the presumptive mesendodermal cells that migrate on the endoderm back toward the animal pole (Keller, 2005). This migration is reliant upon expression of platelet derived growth factor (PDGF), which is expressed in a vegetal-to-animal gradient, and the PDGF receptor (PDGFR). PDGF acts via PI3K to promote cell protrusions and inhibition of PDGF signalling randomises cell migration (Ataliotis et al., 1995; Nagel et al., 2004). In fish PDGF and PDGFR are not expressed in a graded fashion and blockade of PDGF or PI3K function leads to loss of polarisation but cells remain motile and move in a directional manner (Montero et al., 2003). However, disruption of the Wnt11/planar cell polarity (PCP) pathway in the *Silberblick* mutant leads to migratory cells that remain polarised with individual cells being misdirected in their migration (Ulrich et al., 2003).

In chick the use of timelapse microscopy to study the migration of primitive streak cells has shown that FGF4 can act as a chemoattractant to attract cells anteriorly. While FGF8 expressed in the middle of the primitive streaks acts to repel cells which are forced to migrate out from the primitive streak (Yang et al., 2002). In addition the *Drosophila* fibroblast growth factor receptor (FGFR) *heartless* (*htl*) is required for mesoderm cell adhesion and migration (Schumacher et al., 2004) whilst *fgf24* and *fgf8* expression are required for posterior mesoderm formation in zebrafish (Draper et al., 2003).

Additionally, G-protein mediated signalling in response to an unknown ligand has been implicated in convergent extension movements during zebrafish gastrulation, such that interference with the function of $G\alpha_{12/13}$ disrupts gastrulation movements and efficient directed cell migration (Lin et al., 2005).

### 1.2.3 Border cell migration

*Drosophila* border cells are a group of 6-10 follicle cells specified at the posterior of the egg chamber. The border cells form as a cluster of two cell types: an outer group of motile cells and a central pair of non-motile cells. Border cells must become competent to migrate and mutants for the janus kinase/ signal transducers and activators of transcription (JAK/STAT) pathway, the cytokine receptor *dome* or its ligand *unpaired* frequently fail to initiate migration (Starz-Gaiano and Montell, 2004). Once instructed to become motile the border cells wait to receive a steroid hormone signal in the form of ecdysone to signal them to commence migration (Montell, 2003; Starz-Gaiano and Montell, 2004). The border cell cluster then extends processes between the nurse cells and migrates through the midline of the egg chamber to the anterior border of the oocyte (Montell, 2003; Starz-Gaiano and Montell, 2004). Subsequent border cell migration is in part guided by epidermal growth factor receptor (EGFR) and PVR receptor activity (Duchek and Rorth, 2001; Starz-Gaiano and Montell, 2004). Mutations in the EGFR receptor *gurken* inhibit border cell migration, however, EGFR activity is only required for the posterior migration toward the oocyte but not the subsequent dorsal movement to the oocyte nucleus (Duchek and Rorth, 2001). Effective border cell migration also required the expression of the *Drosophila* FGFR homologue *breathless* (*btl*) (Murphy et al., 1995). In addition the planar polarity pathway is required for coordinated migration of the border cells and mutations in *frizzled*, *strabismus*, *dashund* and *prickles* cause delays in border cell migration (Bastock and Strutt, 2007).

## 1.3 Lateral line development

The lateral line is a superficial sensory system found on the head and body of fish and aquatic amphibians. The lateral line systems are composed of sensory structures termed neuromasts that are distributed in unique patterns depending upon species and can be divided into mechanoreceptive and electroreceptive. The mechanoreceptors enable detection of water displacement in the vicinity allowing a sense of touch at a distance, while the electroreceptors allow detection of weak electrical currents in the vicinity. Both systems are important for prey capture, predator evasion and shoaling behaviour (see (Cernuda-Cernuda and Garcia-Fernandez, 1996) for review).

Of particular interest to our lab is the formation of the primary posterior lateral line which is derived from the posterior lateral line placode; a localised thickening of the ectoderm posterior to the ear. The placodal origins of the posterior lateral line are thought to be similar in amphibians and teleosts, however, the specific details of

how this process occurs are essentially unknown (see (Baker and Bronner-Fraser, 2001) for review).

Much of what is known about the development of the lateral line placodes is derived from a series of reports published by L. S. Stone (Yale University) in the 1920s and 1930s examining the lateral line sense organs in amphibia. These studies demonstrated that the lateral line placodes are polarised such that one pole gives rise to the glia and nerves, and the other to the migratory primordium (Stone, 1922). The primordia migrate away from their place of origin along well defined routes and deposit in their wake the sensory neuromasts which are innervated by the lateral line nerve (Stone, 1928; Winklbauer, 1989).

### 1.3.1 Formation of the primary posterior lateral line in zebrafish

The posterior lateral line placode of zebrafish can first be identified from approximately 4-somite stage using the molecular marker *nkx5.1/hmx3.* It is located posterior to the otic placode and extends over the first 1-3 somites (Adamska et al., 2000; Gompel et al., 2001; Kimmel et al., 1995; Metcalfe, 1985). The posterior lateral line placode gives rise to the primary posterior lateral line primordium which migrates along the horizontal myoseptum, between the epidermis and basement membrane, to the very tip of the tail (Metcalfe, 1985). This process commences at approximately 20hpf (26-somite stage) and takes approximately 20-hours to complete (Metcalfe, 1985). As the primordium migrates, clusters of cells are deposited from the trailing end to form the neuromast precursors, which differentiate into mechanosensory neuromasts 6 to 9 hours post deposition (Metcalfe, 1985). In addition to the primordium the posterior lateral line placode also generates the posterior lateral line ganglion and sensory neurons (Metcalfe, 1985). The lateral line ganglion remains more or less stationary posterior to the ear and extends two processes; one toward the hindbrain; and the other into the primordium (Metcalfe, 1985). The neural processes comigrate with the primordium to the tip of the tail and innervate the sensory neuromasts (Gilmour et al., 2004; Metcalfe, 1985; Metcalfe et al., 1985).

The neuromasts deposited by the migratory primordium are termed the primary neuromasts and form a stereotypical pattern of 5-6 neuromasts along the trunk and a cluster of 2-3 neuromasts at the tip of the tail (Gompel et al., 2001; Ledent, 2002). The position of each neuromast is variable and the position of deposition is a property intrinsic to the primordium (Gompel et al., 2001), which may involve the expression of proneural genes within the primordium (Itoh and Chitnis, 2001).

A second group of cells are also deposited by the migrating primordium these cells (termed interneuromast cells) form a thin chain the length of the horizontal myoseptum. These cells lie quiescent for a period before they begin to form 'secondary' neuromasts (Lopez-Schier and Hudspeth, 2005). In addition there is evidence to suggest the presence of a second primordium which migrates along the same route as the primary primordium and deposits additional secondary neuromasts (Sapede et al., 2002). The process of embryonic lateral line development is summarized in Figure 1. The number of neuromasts increases as the larvae develops such that the adult zebrafish has a complex pattern comprising several hundred neuromasts arranged in rows termed 'stitches' (Metcalfe et al., 1985).

**Figure 1: Schematic summary of zebrafish posterior lateral line development**

Summary of the development of the embryonic posterior lateral line of zebrafish.

(a) The posterior lateral line placode can be identified posterior to the otic placode from 4 somite stage. (b) The placode differentiates to form the lateral line ganglion and the lateral line primordium at approximately 18-somite stage. (c) The primordium begins to migrate posteriorly along the horizontal myoseptum together with the lateral line nerve at approximately 22hpf. (d-e) As the primordium continues its posterior-ward migration small clusters of cells are deposited that later form the primary neuromasts (1), in addition the primordium deposits a thin chain of cells termed the interneuromast cells. The migration is complete by approximately 48hpf. Additional neuromasts are added by the migration of a second primordium and the differentiation of interneuromast cells such that by four days postfertilisation both primary and secondary neuromasts (2) can be identified.

Abbreviations: **ov**, otic vesicle; **pllp**, posterior lateral line primordium; **mp**, migrating primordium; **pllg**, posterior lateral line ganglion; **plln**, posterior lateral line nerve; **hm**, horizontal myoseptum; **nm**, neuromast; **inc**, interneuromast cells; **1**, primary neuromast; **2**, secondary neuromast . Images a-d adapted from Kimmel *et al.* (Kimmel et al., 1995).

**Figure 1**

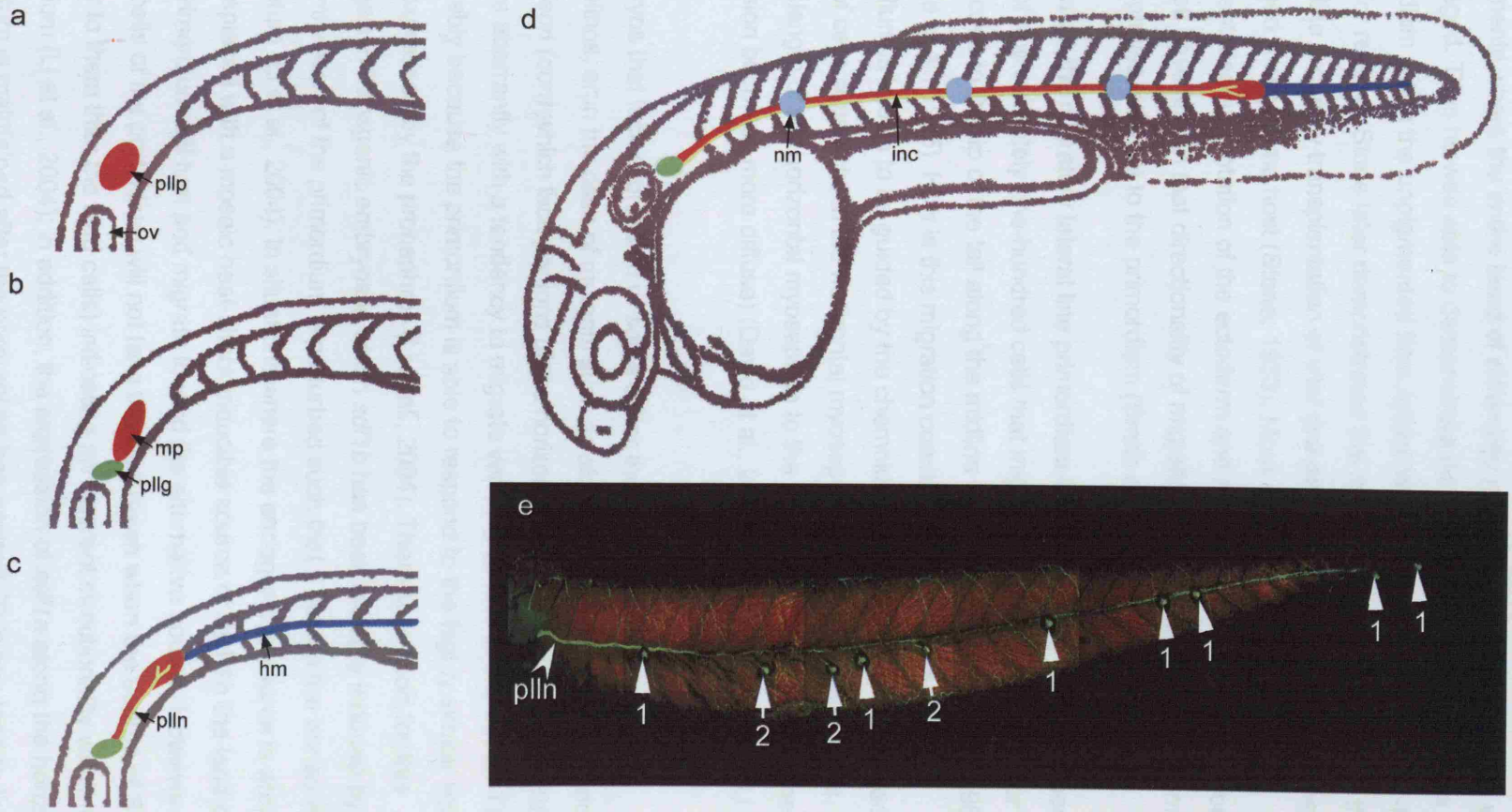

### 1.3.2 Guidance of migration

The migration of lateral line placodes was first demonstrated by R. G. Harrison in experiments where the entire head of differently pigmented species of *Rana* were exchanged. Thus he was able to demonstrate the migration of the lateral line primordium within the unpigmented host epidermis (see (Baker and Bronner-Fraser, 2001) for review). Stone later demonstrated the migration, and formation, of the lateral line organ by transplantation of vital dye-stained epidermis into regions of unstained Amblystoma host (Stone, 1933). More recent experiments using transplantation and rotation of the ectoderm and epidermis along the migration route in axolotl have shown that directionality of migration and deposition of neuromasts are properties inherent to the primordium (Smith et al., 1990).

In zebrafish the migratory lateral line primordium is composed of a small cohesive group of approximately one-hundred cells that migrate from a region posterior to the otic placode to the tip of the tail along the midline of the somites (Metcalfe, 1985; Metcalfe et al., 1985). How is this migration coordinated? Migration of the primordium is known to be guided by the chemokine *sdf1a. sdf1a* is expressed in a group of cells superficial to the horizontal myoseptum, beneath the epidermis, that run the length of the horizontal myoseptum to the very tip of the tail (where the expression becomes more diffuse) (David et al., 2002; Hollway et al., 2007; Li et al., 2004).

In embryos that lack expression of *sdf1a* either through microinjection with morpholinos, or in the case of mutants such as *slow-muscle-omitted (smu)* and *chameleon (con)* which lack portions of the horizontal myoseptum, the primordium migrates aberrantly with a tendency to migrate ventrally (David et al., 2002). This is presumably because the primordium is able to respond to the highly similar ligand *sdf1b,* expressed by the pronephros (Li et al., 2004). There is support for this hypothesis in transgenic embryos in which *sdf1b* has been globally induced by heat-shock; migration of the primordium is perturbed such that it leaves the horizontal myoseptum (Li et al., 2004). In situations where the endogenous source is absent and is replaced with a mosaic heat-shock inducible source of SDF1b the lead cells of the primordium will turn and migrate toward the alternative source. However, the trailing cells of the primodium will not take the lead (even when the source of SDF1b is closer to them than the lead cells) indicating an inherent directionality within the primordium (Li et al., 2004); in addition, the expression of *sdf1a* along the horizontal myoseptum is maintained after the primordium has passed. This has lead to the hypothesis that the *sdf1a* stripe demarcates the pathway of migration but does not

form a gradient, therefore, the directionality of migration is most likely an innate property of the primordium (David et al., 2002).

The receptor for SDF1a in zebrafish is thought to be CXCR4b which is expressed within the posterior lateral line primordium (Chong et al., 2001; David et al., 2002). Expression of *cxcr4b* is in a graded fashion such that it is strongly expressed in the cells at the leading edge of the primordium; it is down regulated in the trailing cells (David et al., 2002; Li et al., 2004). In embryos that have been injected with morpholino against *cxcr4b*, or in the mutant *Odysseus (Ody)* which expresses a severely truncated form of *cxcr4b* (Knaut et al., 2003), the migration of the primordium is greatly retarded (David et al., 2002; Li et al., 2004). However, published data indicates that in the majority of cases the primordium remains on the horizontal myoseptum which may indicate a second mechanism is potentially capable of guiding migration (Li et al., 2004).

During the migration the lateral line nerve remains associated with the migrating primordium and is prevented from entering the somites by expression of *semaphorin3a1* in the somites. *semaphorin3a1* causes neural growth cone collapse and is also expressed in the lead cells of the primordium where it is believed to prevent the growth cone from overtaking the primordium (Shoji et al., 1998). It has also been speculated that expression of *semaphorin3a1* in the somites may act to guide migration of the primordium (Shoji et al., 1998).

More recent work has shown that cells expressing *cxcr4b* are only required at the very tip of the primordium for migration to occur. When wildtype cells are transplanted into the *Odysseus* mutant background they move to the front of the primordium where they appear to organise the entire primordium and rescue migration (Haas and Gilmour, 2006). Conversely, *Ody* -/- cells transplanted into a wildtype background are excluded from the leading edge of the primordium but are capable of migrating with the primordium (Haas and Gilmour, 2006). Guidance of the migration of the posterior lateral line is summarised in Figure 2.

**Figure 2: Schematic summary of known guidance cues during the migration of the posterior lateral line primordium**

Summary of the guidance of primordium migration in zebrafish embryos.

(a) The chemokine receptor *cxcr4b* is expressed in a graded fashion within the migrating primordium with strong expression in the leading region of the primordium. The presumed ligand for *cxcr4b* is *sdf1a* which is expressed along the horizontal myoseptum and its expression is maintained when the primordium has passed. (b) In embryos in which *sdf1a* expression is inhibited primordium migration is greatly retarded and may go ventrally (David et al., 2002; Li et al., 2004). (d) Similarly in mutant embryos that lack portions of the *sdf1a* stripe the primordium migrates aberrantly in regions lacking *sdf1a* expression (David et al., 2002). (c) When *cxcr4b* signalling is abrogated primordium migration is greatly retarded and may go ventrally (David et al., 2002; Haas and Gilmour, 2006). (e) Migration of *Ody -/-* primordia may be rescued by transplantation of wildtype cells into the primordium which migrate to the front of the primordium leading to organisation of the primordium and rescue of migration (Haas and Gilmour, 2006). (f) When *sdf1b*, a close homologue of *sdf1a*, is globally expressed the primordium migrates aberrantly (Li et al., 2004). (g) In cases where *sdf1b* is mosaically induced in backgrounds lacking *sdf1a* the primordium will turn and migrate toward the ectopic sources of *sdf1b* (Li et al., 2004). (h) In addition, the chemorepellant *sema3a1* is expressed in the somites and leading region of the primordium where it acts to prevent the lateral line nerve overtaking the primordium. It may also function to keep the primordium on the horizontal myoseptum (Shoji et al., 1998).

Abbreviations: **mp,** migrating primordium; **inc**, interneuromast cells; **hm**, horizontal myoseptum. Blue arrows indicate direction(s) of migration.

**Figure 2**

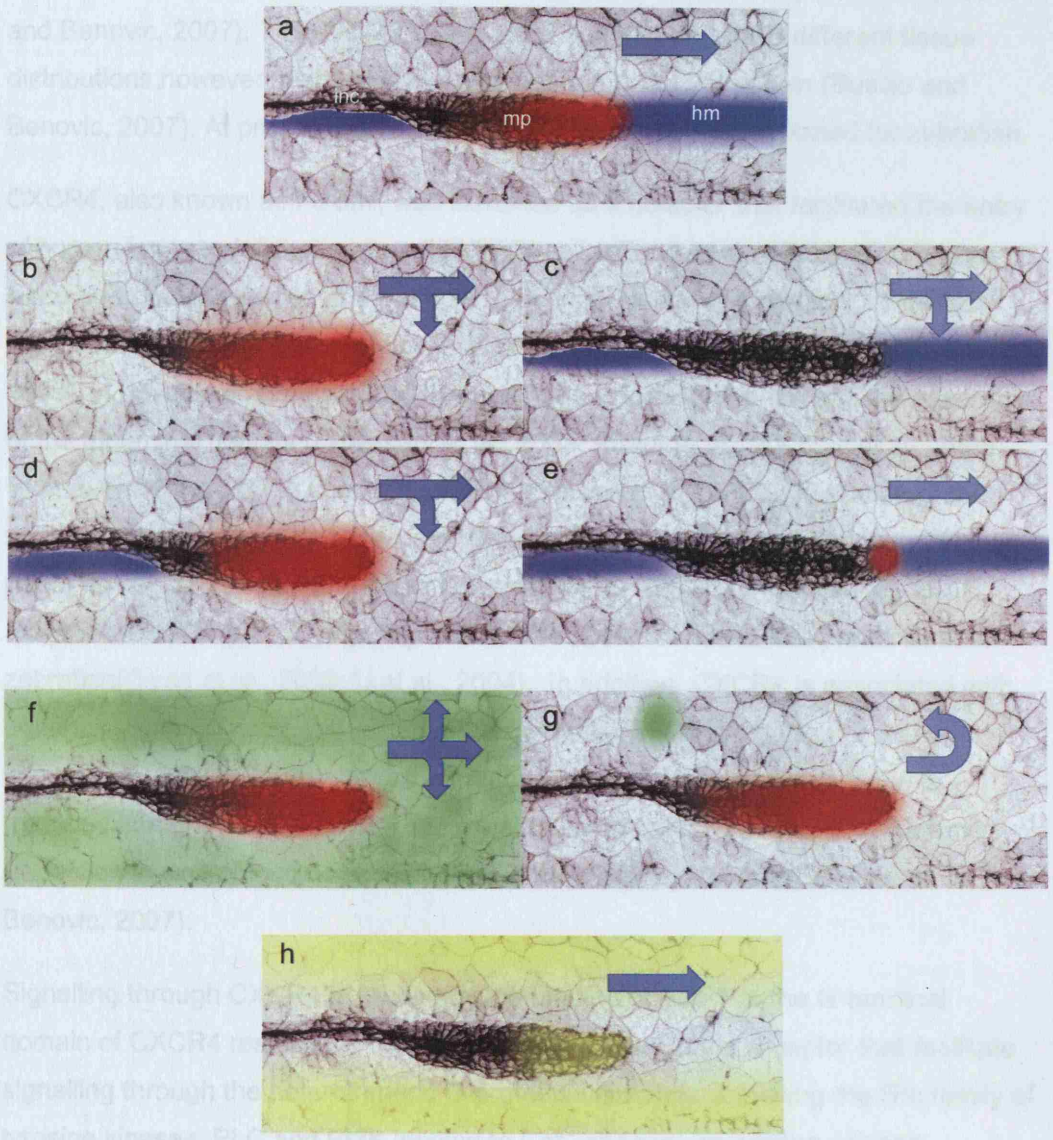

## 1.4 The CXCR4-SDF1 chemokine pathway

Within the CXC-type chemokine receptor family lies the receptor CXCR4. CXCR4 is relatively unique within this family as it has only one known ligand; SDF1, also known as CXC-type ligand 12 (CXCL12). However, six splice variants of SDF1 have been identified with varying amino acid extensions at the carboxy terminus (Busillo and Benovic, 2007). The 6 splice-forms are functional and have different tissue distributions however their functional significance is not yet known (Busillo and Benovic, 2007). At present *sdf1a* splice-forms have not been reported for zebrafish.

CXCR4, also known as FUSIN, was identified as a cofactor that facilitated the entry of human immunodeficiency virus (HIV) into cells (Feng et al., 1996). CXCR4 has since been widely studied and has roles in a wide variety of biological processes; the guidance of T-cells to sites of infection and blood cell maturation (Baird et al., 1999); in developing embryos CXCR4 has roles in axon guidance and the assembly of the trigeminal ganglia (Chalasani et al., 2003; Knaut et al., 2005; Li et al., 2005; Stumm and Hollt, 2007); somite formation (Hollway et al., 2007); migration of the primordial germ cells in zebrafish and mice (Ara et al., 2003, vascularisation of the gut in mice {Tachibana, 1998 #400; Doitsidou et al., 2002; Dumstrei et al., 2004; Molyneaux and Wylie, 2004)}; migration of the posterior lateral line primordium in zebrafish(David et al., 2002; Li et al., 2004). In addition, CXCR4 is associated with enhancing motility and proliferation of cancer cells, and an inherited immunodeficiency disease characterized by **W**arts, **H**ypogammaglobulinemia (reduced immunoglobulin levels), recurrent bacterial **I**nfection, and **M**yelokathexis (reduction in white blood cell count), known as **WHIM** syndrome (Busillo and Benovic, 2007).

Signalling through CXCR4 is elicited by the binding of SDF1 to the N-terminal domain of CXCR4 resulting in conformational changes in the receptor that facilitate signalling through the heterotrimeric G-proteins ultimately activating the Src family of tyrosine kinases, PLC and PI3K leading to $Ca^{2+}$ release, regulation of gene transcription and cell migration (Busillo and Benovic, 2007). In addition SDF1 binding can cause CXCR4 dimerisation resulting in activation of the janus kinase signal transducers and activators of transcription (JAK/STAT) pathway independent of the heterotrimeric G-proteins (Vila-Coro et al., 1999).

Following activation serine and threonine residues in the C-terminal tail of CXCR4 are phosphorylated leading to internalisation of the receptor (Haribabu et al., 1997; Orsini et al., 1999). Removal of the C-terminal tail results in abrogation of ligand

induced internalisation (Haribabu et al., 1997; Signoret et al., 1997). Following internalisation the receptor is either degraded in lysosomes or recycled to the cell surface (Marchese et al., 2003). Deletion of the C-terminal domain has also been implicated in down-regulation of cell-cell contact and enhanced motility in breast carcinoma cells possibly due to altered signalling characteristics (Ueda et al., 2006).

## 1.5 Zebrafish primordial germ cell migration

In addition to the migration of the lateral line primordium, *cxcr4* and *sdf1* are required for the migration of the primordial germ cells (PGCs) to the gonad in zebrafish (Doitsidou et al., 2002; Knaut et al., 2003). Germ cells are the immortal cells which are set aside from the somatic tissue and later differentiate into gametes to allow the production of the next generation of an organism. In most animals germ cell specification occurs at a position distant from the forming gonad (see (Starz-Gaiano and Lehmann, 2001) for a review). In zebrafish, germ cells form in a maternally synthesised cytoplasm, 'germ' plasm, which is thought to contain germ cell determinants (Knaut et al., 2002). Germ plasm can be identified by the presence of *vas* (*vasa*) transcripts which are initially expressed throughout the embryo (Yoon et al., 1997). The *vas* transcript localises to the cleavage planes at two- and four-cell stages and becomes progressively restricted to just four cells by the 1000-cell stage, apparently at random with regard to the developing body axis (Yoon et al., 1997). The PGCs then migrate from these random positions to their future site in the gonad (Weidinger et al., 1999; Yoon et al., 1997). This migration requires both the presence of *cxcr4b* and *sdf1a* (Doitsidou et al., 2002; Knaut et al., 2003). Expression of *sdf1a* acts as a pathway for the *cxcr4b* expressing PGCs to migrate along. As the embryo develops the PGCs migrate to a series of intermediate targets defined by expression of *sdf1a* (Doitsidou et al., 2002). The *sdf1a* pathway gradually shifts to the gonad and the PGCs migrate to remain associated with the expression domain (Doitsidou et al., 2002). Disruption of either pathway (Doitsidou et al., 2002; Knaut et al., 2003), or G-protein receptor signalling (Dumstrei et al., 2004), results in scattering of the PGCs throughout the embryo.

The CXCR4/SDF1 pathway is an evolutionarily conserved system for the guidance of PGCs; CXCR4 and SDF1a have been implicated in PGC migration in chick (Stebler et al., 2004), mouse (Ara et al., 2003) and *Xenopus* (Nishiumi et al., 2005).

## 1.6 Project overview

The posterior lateral line primordium is known to be guided by the interactions of *cxcr4b* and *sdf1a*. It is interesting to note that *sdf1a* is expressed along the entire

length of the horizontal myoseptum and its expression is maintained in regions the primordium has migrated past. *cxcr4b* is expressed in the trailing part of the primordium at much lower levels compared with the leading part. So, what prevents the trailing cells from responding to the source of *sdf1a* behind the primordium in the normal situation? Furthermore, what prevents the trailing cells from migrating toward exogenous sources of SDF1b in the experimental situation? We reasoned that there must be additional genes expressed in the trailing part of the primordium that were responsible for these observations. We set out to identify these additional genes by carrying out an *in situ* hybridisation screen for genes with differential expression patterns in the migrating primordium.

As a result of this screen we identified one gene encoding a G-protein coupled receptor expressed in the trailing part of the primordium. Subsequent phylogenetic analysis revealed this gene to be *rdc1/cxcr7b*, a close relative of *cxcr4b*, the human homologues of which have both been shown to bind SDF1.

In this thesis we will provide evidence that *cxcr7b* is required for the formation and migration of the posterior lateral line primordium, and provide evidence that *cxcr7b* also has a role in primordial germ cell migration in zebrafish. In addition, as a result of our efforts to elucidate the role of the *cxcr7b* we have identified a potential role for fibroblast growth factor mediated signalling in primordium migration.

To better understand the initiation and guidance of the migrating primordium we set out to learn more about the cell behavioural changes using timelapse microscopy and cell tracking analyses. This approach has also been used to evaluate the phenotypes observed in gain- and loss-of-function analysis of the *cxcr7b* gene.

# Chapter 2: Materials and methods

## 2.1 Embryological techniques

### 2.1.1 Zebrafish embryo collection and staging

Zebrafish (*Danio rerio*) embryos were produced by natural spawning of adult zebrafish pairs, kept under 10-hour dark and 14-hour light cycles. Embryos were raised in the fish water and were incubated at 28.5°C, however temperatures ranging between 18°C and 31°C were used to advance or slow embryo development where necessary. Embryos were staged in accordance with the criteria outlined in Kimmel *et al.* (Kimmel et al., 1995). Stages are stated according to morphological features or in hours post fertilisation (hpf) or days post fertilisation (dpf) at 28.5°C.

### 2.1.2 PTU Treatment

To inhibit melanin production in embryos 0.03% 1-phenyl-2-thiourea was added to the fish water from approximately 22hpf (Westerfield, 1995).

### 2.1.3 SU5402 treatment

SU5402 was dissolved in DMSO to make a stock solution of 3.2mM and stored at 4°C. Prior to treatment embryos were manually dechorionated and transferred to a 0.3x Danieau's solution (see 2.7). Embryos were then transferred to a 0.3x Danieau's 1%DMSO solution. Once embryos had developed to the appropriate stage the SU5402 stock solution was added to a final concentration of 32μM. Embryos were kept in the dark and allowed to develop to the appropriate stage at 28.5°C. The SU5402 was removed by rinsing with 0.3x Danieau's 1%DMSO solution and the embryos fixed in 4% PFA (see 2.7) overnight at 4°C.

### 2.1.4 Microinjection

Embryos were injected utilising a pulled GC100F-15 borosilicate glass capillary (Harvard Apparatus, UK) connected to an InjectMatic microinjection compressor (InjectMatic, Switzerland). The injection needle was mounted on a MN-153 micromanipulator (Narishige, Japan) to facilitate movement in three dimensions. Injection volumes were calculated using a graticule.

DNA constructs were diluted to between 10ng and 20ng per μL in RNase/DNase free water (Sigma). 3nL of the DNA solution was injected directly into the cell of 1-cell stage embryos.

Capped-RNA was diluted to approximately 100ng/μL using RNase/DNase free water (Sigma) and injected at a volume of approximately 3nL directly into the cell of 1-cell stage embryos.

Morpholino oligonucleotides were injected into the yolk below the cell of 1-4 cell stage embryos. Morpholinos were diluted in RNase/DNase free water (Sigma). When capped-RNA and morpholinos were co-injected the solution was made up to volume using RNase/DNase free water (Sigma), 3nl of the solution was injected into the yolk below the cell of one-cell stage embryos.

### 2.1.5 Mounting of embryos for live microscopy

Embryos were manually dechorionated and anaesthetised by incubation in a 0.65x Danieau's (see 2.7) solution containing 5% tricaine (see 2.7). While embryos were being anaesthetised microscope slides were prepared. A small drop (approximately 30 μL) of 4% methylcellulose (Sigma)/ 0.65x Danieau's solution was placed on a slide. The drop was then flattened using a piece of narrow gauge tungsten wire. A single anaesthetised embryo was then placed on top of the methylcellulose solution in a small volume (approximately 50 μL) of the anaesthesia solution. The embryo was oriented such that the region of interest was uppermost. Silicon grease (Dow Corning) was then used to create a chamber around the embryo and a cover slip placed on top. The cover slip was pressed onto the embryo with suitable force so as to hold the embryo in place without damaging it.

### 2.1.6 Zebrafish lines utilised

Wildtype embryos were the Lon/AB strain. Additional zebrafish lines are outlined in Table 1.

**Table 1: Additional mutant and transgenic lines used**

| Line Used | Synopsis |
|---|---|
| $H_2A.F/Z$:GFP | A transgenic zebrafish line containing a constitutively expressed histone $H_2A.F/Z$ variant protein fused to green-fluorescent protein. Line provided by Dr Campos-Ortega's lab (Pauls et al., 2001). |
| CldnB:LynEGFP | A transgenic line containing an 8kb sequence upstream of the Claudin B start codon driving the expression of LynEGFP. The line has robust membrane-EGFP expression in the lateral line and other tissues including the epithelium. Provided by Dr Darren Gilmour's lab (Haas and Gilmour, 2006). |
| Hypersensitive tc288d (*hps*) | A mutant line that lacks the posterior lateral line glia which results in supernumerary neuromasts from 3dpf (Grant et al., 2005). |
| *Odysseus* (*Ody*) | A mutant line in which *cxcr4b* contains a nonsense mutation (Lys 239 to stop) resulting in the deletion of part of the third intracellular loop and the last two transmembrane domains. The mutation is thought to result in a non-functional protein, however, offspring are homozygous viable (Knaut et al., 2003). |
| *Ody*/CldnB:LynEGFP | The result of crossbreeding of the *Odysseus* mutant line with the CldnB:LynEGFP transgenic line. The resultant line expresses the truncated *cxcr4b* and the CldnB:LynEGFP transgene (Haas and Gilmour, 2006). Double transgenic embryos are identifiable by LynEGFP expression in the primordium which displays severely retarded migration. |
| hsp70:dn-*fgfr1*-EGFP | Transgenic line with a dominant-negative version of *fgfr1*, in which the tyrosine kinase domain has been replaced with an *egfp* coding sequence, under the transcriptional regulation of the heat-shock *hsp70* promoter (Lee et al., 2005). |

## 2.2 DNA techniques

### 2.2.1 Bacterial transformation

For routine DNA transformation DH5α chemically competent cells (Bioline) were thawed on ice and dispensed (80µL) into pre-chilled 1.5mL Eppendorf tubes, to which 1-5µL of DNA solution was added, and mixed gently. Cells were incubated on ice for 20 minutes and heat-shocked for 1 min at 42°C. 1mL of Luria-Bertani (LB) broth was added and the cells incubated at 37°C for 1 hour with agitation. 100µL of cells were plated onto pre-warmed LB-agar plates containing the appropriate selective antibiotic (ampicillin or kanamycin, used at a concentration of 100µg/mL). Bacterial plates were incubated at 37°C overnight. For ligations 10µL of the DNA ligation reaction was transformed by the above method.

When higher efficiency transformation was required ElectroMax (Promega) electro-competent cells were transformed following the manufacturers protocol. Cells were plated onto pre-warmed LB-agar plates containing appropriate antibiotic (as above). Bacterial plates were incubated at 37°C overnight.

### 2.2.2 Small scale DNA preparation

3mL LB-broth cultures, containing the appropriate selective antibiotic (ampicillin or kanamycin, used at a concentration of 100µg/mL) were grown from single colonies overnight at 37°C. 1.5mL of the resulting culture was pelleted by centrifugation in a desktop centrifuge at 13,000rpm for 1 minute in 1.5mL Eppendorf tubes. Supernatant was removed by aspiration and isolation of DNA was performed using the NucleoSpin Plasmid Kit (Machery-Nagel) following the manufacturer's protocol. DNA was eluted with 30µL-50µL of RNase/DNase-free water (Sigma) and stored at -20°C.

### 2.2.3 Large scale DNA preparation

100mL LB-broth cultures, containing the appropriate selective antibiotic, were seeded from small-scale cultures (approximately 3mL) overnight at 37°C. Extraction of DNA was carried out using the Nucleobond AX PC500 Kit (Machery-Nagel) following the manufacturer's protocol. DNA pellets were resuspended in 200-400µL sterile low TE buffer (see 2.7) and stored at -20°C.

### 2.2.4 Restriction endonuclease digestion

Plasmid DNA was excised using appropriate restriction endonucleases in accordance with the manufacturers' instructions using an appropriate supplied buffer

(Roche, New England Biolabs). Enzyme volumes were typically less than 5% of the total reaction volume. DNA digestion was confirmed by running a small sample of the digest product on a 1% agarose gel. Where necessary protein and salt contaminants were removed as described below.

### 2.2.5 Removal of contaminants from DNA

Prior to using DNA for *in vitro* transcription (i.e. synthesis of capped-RNA or *in situ* hybridisation probe), or subcloning, contaminants were removed as follows:

An equal volume of phenol-chloroform-isoamyl alcohol (49.5:49.5:1 *v/v/v* 100mM TRIS pH8.0) (Fluka) was added to the DNA and vortexed prior to centrifugation at 13,000rpm in a bench top centrifuge for 4 minutes. The aqueous phase was removed and the non-aqueous phase discarded. To the aqueous phase a 10% volume of 3M sodium acetate (pH 5.5) and a 250% volume of 100% ethanol was added in a 1.5mL Eppendorf tube. The solution was vortexed briefly and incubated at -20°C for 2 hours to precipitate the DNA. Subsequently the solution was centrifuged at 13,000rpm in a bench top centrifuge for 10 minutes. The supernatant was removed and discarded, and the DNA pellet washed by addition of 400 µL of 70% ethanol to remove excess salts. Following a brief vortex the solution was again centrifuged at 13,000rpm in a bench top centrifuge for 10 minutes. The supernatant was removed and the DNA pellet allowed to air dry before being resuspended in a suitable volume of RNase/DNase free $H_2O$ (Sigma).

### 2.2.6 Gel purification of DNA

Where a DNA fragment required isolation from other fragments, following restriction digest or PCR, DNA was gel purified. Samples of up to 100µL were run on a 1% agarose electrophoresis gel made with 1xTBE (see 2.7) to which a suitable volume of Ethidium Bromide had been added. DNA bands were excised from the gel and purified using the QIAquick Gel Extraction Kit (Qiagen).

### 2.2.7 DNA ligation

Isolated DNA fragments were ligated into prepared vector using the Rapid DNA Ligation Kit (Roche) according to the manufacturer's guidelines.

### 2.2.8 DNA sequencing and sequence analysis

Sequencing was performed by GATC Sequencing, Germany. Approximately 30ng of DNA was prepared in accordance with instructions on the website: http://www.gatc-biotech.com.

DNA sequence analysis and alignment was conducted using the DNAStar (LaserGene) group of sequence analysis programs. Identification of ESTs was performed using Basic Local Alignment and Searching Tool (BLAST, NCBI). Homology and sequence alignment was conducted using the MegAlign program (LaserGene). Translated protein sequence alignments were performed using the NeedlemanP global sequence alignment algorithm (http://srs.ebi.ac.uk).

### 2.2.9 Generation of constructs

Three constructs were generated to analyse the function of zebrafish CXCR7b; full-length or C-terminally truncated CXCR7b with C-terminal fusion to enhanced-yellow-fluorescent-protein (EYFP) (CXC7bEYFP and CXC7bΔCEYFP) and full-length CXCR7b fusion with red-fluorescent-protein (RFP) (CXC7bRFP). A further construct was generated to act as positive control for the internalisation assay; full-length CXCR4b C-terminally fused with RFP (CXCR4bRFP).

Constructs were generated by PCR amplification of plasmid DNA using primer pairs containing restriction enzyme sites for sticky ended ligation into the appropriate vector. All constructs were subsequently sequenced to ensure no mutations were introduced by the PCR amplification.

### 2.2.10 Incorporation of restriction sites using PCR

PCR primer pairs were designed to amplify the desired region of DNA and incorporate a unique restriction enzyme site at each end of the amplified sequence. Primer sequences were as long as necessary to provide an annealing temperature of between 50°C and 65°C. A 6 base pair (bp) site corresponding to the 6-cutter restriction enzyme site was added at the 5'-end of the 5'-primer and the 3'-end of the 3'-primer with a 2-6 bp flanking region to aid enzymatic restriction digests where necessary.

PCR primers were diluted using RNase/DNase-free water (Sigma) to make 100μM stock solutions. Two forms of PCR reaction mix were used:

The first utilised the PFU DNA polymerase and was used for basic DNA amplification and the fabrication of CXCR7b constructs. The reaction mix was as follows:

| | |
|---|---|
| 2.5μL | 10x PFU DNA polymerase buffer (Promega), |
| 1.5μL | 25mM $MgCl_2$ (Sigma) |
| 1.0μL | dNTPs (10mM each of GTP, TTP, ATP and CTP) (Roche) |
| 2.5μL | 5' primer (0.1mM) |
| 2.5μL | 3' primer (0.1mM) |
| 10ng | Plasmid containing *cxcr7b* or *cxcr4b* |
| 1.0μL | PFU DNA polymerase (Promega) |
| Make up to 20μL with RNase/DNase-free water (Sigma) | |

The second, used to generate the CXCR4b construct, utilised the TaqMan (Roche) DNA polymerase substituted for the PFU DNA polymerase in the above reaction mix. Use of Taq DNA polymerase results in the addition of an overhanging 3' adenine residue on both DNA strands and was used for cloning of DNA into the pCR2.1-TOPO Vector using the TopoTA Cloning Kit (Invitrogen).

The PCR reaction was performed in a Peltier Thermal Cycler 100. The PCR machine was programmed as follows: Step1- 94°C for 4.00min, Step2- 94°C for 0.30min, Step3- 55°C for 0.30min, Step4- 72°C for 1.30min, Step5- Goto 2 for 30 repetitions, Step6- 72°C for 10.00min, Step7- END.

### 2.2.11 Generation of CXCR7bEYFP tagged constructs

Full-length *cxcr7b* including 108bp of the 5'UTR, which contains both *cxcr7b* morpholino sites, was amplified by PCR from the IMAGE clone: 7067778. The primers against *cxcr7b* were designed to incorporate an EcoRI and XbaI restriction sites at the 5' and 3' termini respectively (underlined):

5' primer: 5'-ttcgaattccatcctgtctctcgcacggatatc-3'

3' primer: 5'-agtggatcccctaatggtccctggttttccacggc-3'

A C-terminally truncated *cxcr7b* including 108bp of the 5'UTR containing both cxcr7b morpholino sites was amplified by PCR from the IMAGE clone: 7067778. The primers against *cxcr7b* were designed to incorporate EcoRI and XbaI restriction sites at the 5' and 3' termini respectively (underlined):

5' primer: 5'-ttcgaattccatcctgtctctcgcacggatatc-3'

3' primer: 5'-agtggatccccgtatcggtagttcttgttgatgaagttg-3'

The 3' primer sequence results in the C-terminal truncation of the CXCR7b protein at amino acid 323 resulting in the loss of the C-terminal 39 amino acids, removing serine residues whose phosphorylation has been shown to be necessary for ligand induced internalisation of CXCR4 (Signoret et al., 1997).

PCR products were restriction digested using enzymes specific for the added restriction sites. The digested fragments were gel purified (see 2.2.6) and ligated (see 2.2.7) into the pEYFP-N1 vector (Clontech) at the corresponding restriction sites 5' to the EYFP sequence such that EYFP was in-frame with CXCR7b. The CXCR7bEYFP/CXCR7bΔCEYFP sequences were then excised from EYFP-N1 by digestion with EcoRI and BamHI. The fragments were gel purified and subcloned into the EcoRI and BamHI sites of pCS2+.

The constructs were sequenced with the primers outlined below.

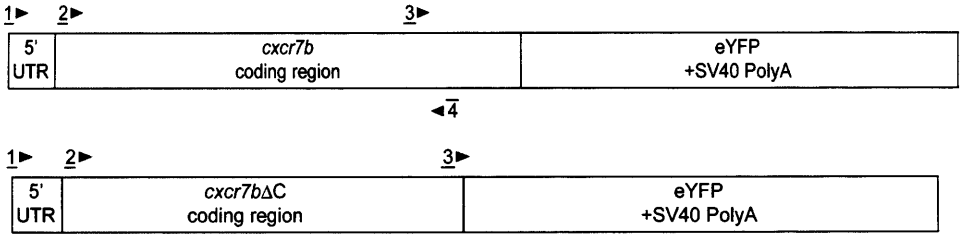


1: 5'-ttcgaattccatcctgtctctcgcacggatatc

2: 5'- atgagtgtgaacgtgaatgat

3: 5'- ggacactctagcctttctcaatgtgc

4: 5'- agtggatccccgtatcggtagttcttgttgatgaagttg

### 2.2.12 Generation of CXCR7bRFP tagged constructs

Full-length *cxcr7b*, including 55bp of the 5'UTR containing the *cxcr7b*-AUG morpholino site but lacking the *cxcr7b* morpholino site, was amplified by PCR from the IMAGE clone: 7067778. The primers against *cxcr7b* were designed to incorporate XbaI and AgeI restriction sites at the 5' and 3' termini respectively (underlined):

5' primer: 5'- ttctctagacatcctgtctctcgcacggatatc-3'

3' primer: 5'- agtaccggtcctaatggtccctggttttccacggc-3'

PCR products were restriction digested using the enzymes specific for the added restriction sites under appropriate conditions. The PCR product was gel purified and ligated into the pCS2+ vector, with an RFP coding region already present, at the corresponding restriction sites 5' to the RFP sequence such that RFP was C-terminal and in-frame with *cxcr7b*.

The construct was verified by DNA sequencing with the primers outlined below.

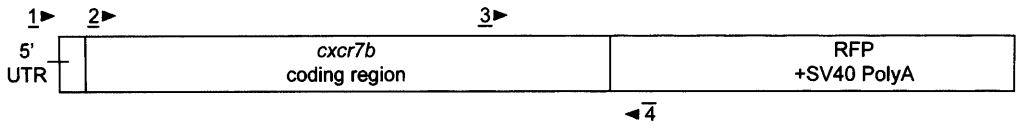


1: 5'-ttcgaattccatcctgtctctcgcacggatatc (SP6)

2: 5'- atgagtgtgaacgtgaatgat

3: 5'- ggacactctagcctttctcaatgtgc

4: 5'- agcgcatgaactccttgat

### 2.2.13 Generation of CXCR7bRFP tagged heat-shock inducible construct

To generate a heat-shock inducible version of the CXCR7bRFP fusion protein the construct, including the poly-A tail, was excised from the pCS2+ vector using the 5' BstBI site and the 3' Asp718 site. The pCS2+ HSP7-4 MCS9 vector, provided by Dr Sebastian Gerety (NIMR), was digested using a 5' ClaI site and a 3' Asp718 site. Both vector and insert were gel purified prior to ligation. Ligation resulted in the destruction of the BstBI and ClaI sites. The resulting construct placed the *cxcr7brfp* construct under the transcriptional regulation of the *hsp70* promoter as shown below. The construct was tested for *in vivo* expression of CXCR7bRFP by heat-shock at 37°C for one hour. The RFP signal was first detectable approximately 1 hour after heat-shock.

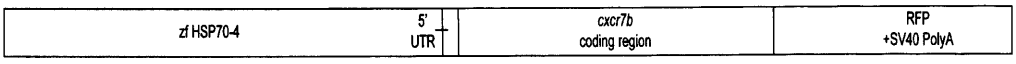

### 2.2.14 Generation of the CXCR4bRFP tagged construct

Full-length *cxcr4b* including 3bp of 5'-UTR was amplified by PCR from the clone CB403 (GenBank: CA408048) using the TaqMan PCR method as described previously. Primers were designed to incorporate XbaI and AgeI restriction sites at the 5' and 3' termini respectively (underlined):

5' primer: 5'-gtctagatgcgccttttgagcacact-3'

3' primer: 5'-gaccggtttactcgtcagtgcactggacgac-3'

The PCR product was cloned into the TopoTA vector (Invitrogen) following the manufacturers protocol. The amplified fragment was then excised from the TopoTA vector by restriction digest with XbaI and AgeI. The PCR product was gel purified and ligated into the pCS2+ vector, with an RFP coding region already present, at the corresponding restriction sites 5' to the RFP sequence such that RFP was C-terminal and in-frame with *cxcr4b*.

The CXCR4bRFP construct was sequenced using the following primers:

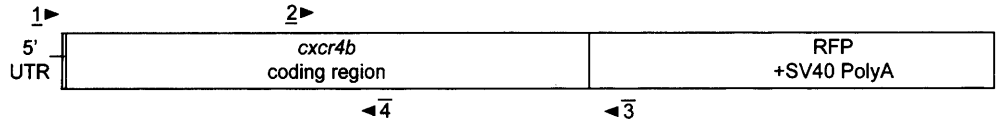


1: 5'- gaatttaggtgacactataga (SP6)

2: 5'- tgcgggaagggtgatctacattg

3: 5'- agcgcatgaactccttgat

4: 5'- gatacagtaacaggtcaaaa

## 2.3 RNA techniques

### 2.3.1 Antisense RNA probe synthesis

Plasmids containing zebrafish cDNA for genes of interest were linearised by restriction digest and used as templates for *in vitro* synthesis of labelled anti-sense RNA. Some CB clones required PCR amplification and addition of polymerase recognition sites prior to probe synthesis. Details of PCR primers can be found on the ZFIN website (www.zfin.org). The ribose of the RNA used was chemically modified and labelled with either digoxigenin (Roche) or fluorescein (Roche). RNA synthesis utilised RNA-polymerases that recognise the T3, T7 or SP6 recognition

sites present in the cDNA containing plasmids. A list of plasmids, restriction enzymes and RNA-polymerases can be found in Table 2. Transcription was performed at 37°C for 2 hours using the reaction mix that follows:

| | |
|---|---|
| 2 µL | 10x transcription buffer (Roche) |
| 2 µL | Digoxigenin or fluorescein labelled nucleotide mix (10mM ATP, CTP, GTP (each), 6.5mM UTP, 3.5mM DIG/Fluorescein-11-UTP) (Roche) |
| 1 µL | RNAse inhibitor (Promega) |
| (1 µg) 1 or 2 µL | Linearised template DNA |
| 1 µL | SP6/T3/T7 RNA polymerase (Roche) |
| Make up to 20µL $dH_2O$ | |

Once synthesis of RNA was complete the template cDNA was removed by digestion with RNase-free DNaseI (Promega) for 20 minutes at 37°C. Unincorporated nucleic acids were removed by filtration through G50 columns (GE Healthcare). Probe synthesis and approximate concentration were determined by agarose gel electrophoresis prior to dilution in 50µL hybridisation mix (see 2.7) and stored at -20°C.

**Table 2: Conditions for *in situ* hybridisation probe synthesis**

| Clone/ Gene Name | Vector | 5' Linearisation Enzyme | RNA Polymerase Used | PCR Amplification Required |
|---|---|---|---|---|
| cb6 | pBluescript II SK+ | N/A | N/A | Yes |
| cb97 | pBluescript II SK+ | NotI | T7 | No |
| cb117 | pBluescript II SK+ | NotI | T7 | No |
| cb299 | pBluescript II SK+ | NotI | T7 | No |
| cb308 | pSPORT1 | N/A | N/A | Yes |
| cb341 | pSPORT1 | N/A | N/A | Yes |
| cb376 | pSPORT1 | N/A | N/A | Yes |
| cb386 | pSPORT1 | N/A | N/A | Yes |
| cb387 | pSPORT1 | N/A | N/A | Yes |
| cb388 | pSPORT1 | N/A | N/A | Yes |
| cb486 | pSPORT1 | N/A | N/A | Yes |
| cb488 | pSPORT1 | N/A | N/A | Yes |
| cb521 | pSPORT1 | N/A | N/A | Yes |
| cb747 | pBluescript II SK+ | NotI | T7 | No |
| cb766 | pBluescript II SK+ | NotI | T7 | No |
| cb786 | pBluescript II SK+ | NotI | T7 | No |
| cb837 | pBluescript II SK+ | NotI | T7 | No |
| cb900 (*rdc1/cxcr7b*) | pBluescript II SK+ | NotI | T7 | No |
| cb915 | pBluescript II SK+ | NotI | T7 | No |
| cb967 | pBluescript II SK+ | NotI | T7 | No |
| cb1016 | pBK-CMV | N/A | N/A | Yes |
| cb1018 | pBK-CMV | EcoRI | T7 | No |
| cb1077 | pBK-CMV | EcoRI | T7 | No |
| *hmx3* | pBluescript II SK+ | EcoRI | T7 | No |
| *nanos* | pSP64T | NotI | T7 | No |
| *sdf1a* | pBluescript KS+ | BamHI | T3 | No |
| *cxcr4b* | pBluescript SK+ | BamHI | T7 | No |
| *keratin 15* | pBluescript KS+ | EcoRI | T7 | No |
| *fgfr1* | pCS2+ | XhoI | T3 | No |
| *fgf10* | pCS2+ | HindIII | T7 | No |
| *pea3* | pBluescript SK+ | NotI | T3 | No |

### 2.3.2 Whole mount *in situ* hybridisation

Whole mount *in situ* hybridisation was performed essentially as described by Thisse *et al.* (Thisse et al., 2004). All washes were performed in 1.5mL Eppendorf tubes. Proteinase-K digestion was performed using 2μg/mL proteinase K (Boehringer) diluted in PBT (see 2.7) for 5 minutes at room temperature for embryos up to 48hpf. Probes were used at a working dilution of 1:200 in hybridisation mix (see 2.7), however, the dilution was titrated to give the best result. Hybridisation was performed at 65-67°C overnight in a water bath. Detection of RNA hybridisation was performed using NBT-BCIP Developer (see 2.7) following 3x 5min washes with NBT-BCIP buffer (see 2.7). Once colour had developed sufficiently embryos were washed extensively (6x 10min) in PBT and re-fixed in 4% PFA (see 2.7) for 20 minutes at room temperature. Fixative was removed by rinsing with PBT before embryos were stored in 70% glycerol/PBS at 4°C.

### 2.3.3 Whole mount double fluorescent *in situ* hybridisation

The initial treatment of embryos prior to hybridisation was as described above. Two probes were used during the hybridisation step one fluorescein-labelled probe and one digoxigenin-labelled probe. The probe with the most robust signal would be made as fluorescein and the weaker probe as digoxigenin. Probes were combined and used at a working dilution of 1:200 in hybridisation mix (see 2.7). Hybridisation was performed at 65-67°C overnight in a water bath. Post hybridisation washes were as Thisse *et al.* (Thisse et al., 2004). mRNA localisation was detected as follows: Embryos were blocked in 5% heat-inactivated sheep serum (HISS)/PBT for 1 hour at room temperature. The fluorescein probe was detected first using an anti-fluorescein horseradish peroxidase (HRP) conjugated antibody (PerkinElmer) at 1:1000 dilution incubated at 4°C overnight. Unbound antibody was removed by 10x 30 minute washes in PBT (see 2.7). Colour was developed as a CY5 product using the Tyramide TSA-Plus Palette System (PerkinElmer) in accordance with the manufacturer's instructions (volumes used for the reaction were 100 μL with a developing period of one hour). The reaction was stopped by 3x 5 minute washes in PBT followed by a 45-minute incubation in a 1% $H_2O_2$/PBS solution (see 2.7) to inactivate the HRP. Following 3x 5 minute washes with PBT the embryos were once again blocked using a 5% HISS/PBT solution for 1-hour then the digoxigenin probe was detected using an anti-digoxigenin HRP-conjugated antibody (Roche) at 1:1000 dilution. The colour development procedure was repeated using the CY3-product of the Tyramide TSA-Plus Palette System (PerkinElmer) in accordance with the manufacturer's instructions (volumes used for the reaction were 100 μL with a

developing period of one hour). The reaction was stopped by 3x 5 minute washes in PBT followed by fixation in 4% PFA at room temperature for 20 minutes. Fixative was removed by 3x 15 minute washes in PBT and embryos were either stored in 70% glycerol/ PBS, or if the CldnB:LynEGFP lines were used embryos were processed for immunostaining to detect GFP expression (see 2.3.4).

### 2.3.4 Post *in situ* hybridisation antibody staining

Where the CldnB:LynEGFP transgenic line had been processed for *in situ* hybridisation it was possible to further process the embryos to detect GFP expression thereby identifying the posterior lateral line primordium. Embryos were blocked in a 5% heat inactivated sheep serum (HISS)/PBT solution for 1-hour at room temperature. GFP was detected by overnight incubation with an anti-GFP antibody (Torrey Pines Biolabs) at 1:400 dilution in 5%HISS/PBT at 4°C overnight. The primary antibody was removed by 8x 15 minute PBT washes and an anti-rabbit FITC-conjugated secondary antibody (Jackson Immuno Research Labs Inc.) added at 1:400 dilution overnight in 5%HISS/PBT at 4°C. and unbound secondary antibody was removed by 8x 15 minute washes in PBT. Embryos were then stored in 70% glycerol/PBS at 4°C.

### 2.3.5 Synthesis of capped RNA

Capped-structure RNA for microinjection was transcribed *in vitro* from plasmid DNA linearised 3' to the polyA tail of the gene/construct required. Transcription was performed in a 50µL reaction volume at 37°C for 2 hours. The reaction composition was as follows:

| | |
|---|---|
| 5 µL | 10x Transcription buffer (Roche) |
| 5 µL | rNTPs (1mM GTP with 10mM each of ATP, CTP and UTP) (Roche) |
| 5 µL | 5mM m7G(ppp)G capped structure RNA analogue (New England Biolabs) |
| 2 µL | RNase inhibitor (Promega) |
| 2 µL | RNA polymerase (SP6, T3 or T7) |
| 2 µg | Linearised DNA |
| Made up to 50 µL with RNase/DNase-free water (Sigma) | |

The linearisation and transcription enzymes are listed in Table 3. The capped mRNA synthesis reaction was performed at 37°C for two hours. Successful synthesis was checked by running 1 µL of the reaction on a 1% agarose gel. Following synthesis template DNA was removed by addition of 1µL RNase-free DNaseI (Promega) and

a further 20 minute incubation at 37°C. Unincorporated nucleic acids were removed by filtration through a S300HR column (GE Healthcare). Probe synthesis was confirmed by agarose gel electrophoresis. Concentration of capped-RNA was determined using a ND-1000 Nanodrop spectrophotometer (Nanodrop) before being aliquoted and stored at -80°C.

**Table 3: Conditions for capped-RNA synthesis**

| Capped RNA Injected | Transcription Enzyme | Linearisation Enzyme |
|---|---|---|
| *h2brfp* | SP6 | NotI |
| *gapgfp* | SP6 | BssHII |
| *cxcr7beyfp* | SP6 | Asp718 |
| *cxcr7bΔceyfp* | SP6 | Asp718 |
| *cxcr7brfp* | SP6 | NotI |
| *cxcr4brfp* | SP6 | Asp718 |

## 2.4 Antisense morpholino oligonucleotides

### 2.4.1 Anti-sense morpholino oligonucleotide design

Anti-sense morpholino oligonucleotides were obtained from GeneTools LLC, Oregon. Sequences were designed by the manufacturer against regions we specified.

The *cxcr7b-aug* morpholino is designed against the translation initiation site (AUG) of *cxcr7b*:

*cxcr7b-aug* MO 5'-atcattcacgttcacactcatcttg-3'

The *cxcr7b* morpholino is designed against an AUG site approximately 100bp 5' of the translation initiation site:

*cxcr7b* MO 5'-ggtaatgagattccgatgcctggag-3'

The *cxcr4b* morpholino sequence was designed, and published by Li *et al.* (Li et al., 2004). The morpholino is designed against the translation initiation site (AUG) of *cxcr4b*:

*cxcr4b* MO 5'-aaatgaatgctatcgtaaaattccat-3'

The *sdf1a* morpholino sequence was designed, and published by David *et al.* (David et al., 2002). The morpholino is designed against the translation initiation site (AUG) of *sdf1a*:

*sdf1a* MO 5'-atcactttgagatccatgtttgca-3'

The control morpholino used was the standard control morpholino provided by GeneTools LLC:

control MO 5'- cctcttacctcagttacaatttata-3'

Details of the design procedure can be found on the GeneTools LLC website: www.gene-tools.com.

Some of the morpholinos appeared to have high toxicity following initial testing. To reduce toxicity an aliquot of the morpholino was passed through an S-300 HR Sepharose column (GE Helathcare) to remove unincorporated nucleotides.

## 2.5 Embryo staining techniques

### 2.5.1 Whole mount immunohistochemistry

Embryos were fixed for 2-hours at room temperature in 4%PFA. Fixative was removed by 4x 15 minute washes with PBT. Embryos were then blocked for one hour at room temperature with 5% goat serum (Sigma)/PBT. The blocking solution was replaced with a 2% goat serum containing the primary antibody (see Table 4). The primary antibody was incubated overnight at 4°C. Unbound antibody was removed by 10x 15 minute washes in PBT prior to the addition of the secondary antibody 2% goat serum/PBS (see Table 4). Following an overnight incubation the secondary antibody was removed by 10x 15 minute washes in PBT and the embryos stored in 70% glycerol/PBS at 4°C.

**Table 4: Antibodies used**

| Primary antibody | Dilution used | Secondary antibody | Dilution used |
|---|---|---|---|
| Mouse anti-acetylated tubulin (Sigma) | 1:1000 | Anti-mouse IgG FITC-conjugated antibody (Jackson Immuno Research) | 1:500 |
| Mouse anti-ERK1/2P (Sigma) | 1:200 | Anti-mouse IgG CY3-conjugated antibody (Jackson Immuno Research) | 1:500 |

| | | | |
|---|---|---|---|
| Rabbit anti-GFP (Torrey Pines Biolabs) | 1:200 | Anti-Rabbit IgG FITC-conjugated antibody (Jackson Immuno Research) | 1:500 |

Where necessary embryos were counterstained by incubation in a PBT solution, containing 1:500 TRITC-conjugated phalloidin (Sigma), for 20 minutes to visualise the somites. Unbound phalloidin was then removed by 3x 5 minute washes in PBT.

Embryos were stored in 70% glycerol/PBS at 4°C.

### 2.5.2 Staining for endogenous alkaline phosphatase activity

Neuromasts contain high levels of endogenous alkaline phosphatase activity. This provides an easy method to visualise the number and distribution of posterior lateral line neuromasts in the embryo. Embryos were fixed at 4 dpf in 4% PFA (see 2.7) for 15 minutes at room temperature. Fixed embryos were washed in PBT and equilibrated in NBT/BCIP buffer (see 2.7). Endogenous alkaline phosphatase activity was detected by immersion of the embryos in NBT/BCIP developer solution for approximately 8 minutes, or until the colour had developed sufficiently. The reaction was stopped by washing in PBT. Embryos were then re-fixed in 4% PFA at room temperature. Fixative was removed by washes in PBT and the embryos stored in 70% glycerol/PBS at 4°C.

## 2.6 Microscopy and image analysis

### 2.6.1 Photomicrography

Flat mounted embryos were imaged using the Zeiss Axiophot microscope with a Jenoptik ProgRes C14 camera attachment and Openlab software.

### 2.6.2 Confocal microscopy

Fluorescent images of flat mounted embryos and timelapse of live embryos were collected using either a Leica DMRXE upright microscope and Leica TCS-NT software, or a Zeiss Pascal confocal microscope and accompanying software.

### 2.6.3 Image processing and analysis

Processing of confocal image stacks and confocal timelapse sequences was performed using the ImageJ V 1.38 open-source program (NIH). Sequences were z-projected then aligned using the ROI RGB align plugin (Dr Daan Zhu, NIMR). Cell migration sequences were tracked manually using the cell tracker 4 and cell tracker 5 plugins (Dr Daan Zhu, NIMR). Timelapse image sequences were exported as .AVI

(Audio Video Interleave) files. Cell migration speeds were calculated using the Cell Mov Visual plugin and the results exported to Microsoft Excel in order to calculate the average speed over the period examined. The resultant data was entered into GraphPad Prism statistical analysis software. GraphPad Prism was used to plot graphs of average cell speeds, and P-values were calculated using one-tailed paired t-tests.

## 2.7 Solutions list

| | |
|---|---|
| 1x Danieau's Solution | 58mM NaCl, 0.7mM KCl, 0.4mM $MgSO_4$ 0.6mM $Ca(NO_3)_2$, 0.5mM HEPES (Shih and Fraser, 1995). |
| 1x Tricaine | 400mg 3-amino benzoic acid ethylester, 97.9mL $H_2O$ adjust pH to 7.0 with 2.1mL TRIS pH9 (Westerfield, 1995). |
| 4% Methyl Cellulose Solution | 4% Methyl cellulose w/v dissolved in 1x Danieau's Solution |
| Low TE buffer | 0.1mM Ethlene-diamine-tetra-acetate (EDTA), 10mM Tris-HCl (pH 7.5) |
| Phosphate Buffered Saline (PBS) | 0.8% NaCl, 0.02% KCl, 0.02M $PO_4$ (pH 7.3). |
| Phosphate Buffered Saline / Tween-20 (PBT) | PBS, 0.1% Tween-20 (Sigma). |
| 4% Paraformaldehyde (PFA) Solution | PBS, 4% paraformaldehyde, aliquoted and stored at -20°C. |
| Hybridisation Mix | 50% formamide, 5xSSC, pH 6.0 (adjusted using 1M citric acid), 50µg/mL heparin, 0.1% Triton X-100 (Sigma). Stored at -20°C. |
| NBT-BCIP Buffer | 100mM Tris-HCl (pH9.5), 50mM MgCl2, 100mM NaCl, 0.1% Tween 20. |
| NBT-BCIP Developer | 100mM Tris-HCl (pH9.5), 50mM $MgCl_2$, 100mM NaCl, 0.1% Tween 20, 0.45% NBT (50 mg/mL), 0.35% BCIP (50mg/mL). |

# Chapter 3: *In situ* hybridisation screen

## 3.1 Introduction

The Xu lab is primarily interested in revealing and understanding the molecular mechanisms underlying directed cell migration *in vivo*. Directed cell migration is the method by which a cell, or cells, are guided to migrate to a target location. The balance between attractive and repulsive cues present in the environment guides the migration. To study this process we utilise the zebrafish posterior lateral line primordium as our model system.

As discussed in the introduction directionality is an essential component of directed cell migration and when directionality is disrupted migration fails (Funamoto et al., 2002; Iijima and Devreotes, 2002). With regards to the primordium there are several lines of evidence which suggest an inherent directionality.

Firstly, there are the observed behavioural differences within different regions of the primordium. The cells at the leading edge of the primordium play a specific role in responding to the guidance cue, SDF1a (Haas and Gilmour, 2006). In the absence of SDF1a the leading cells can lead the entire primordium to exogenous sources of SDF1b (Li et al., 2004). Additionally, the presence of *cxcr4b* positive cells at the very tip of the primordium is required for normal migration (Haas and Gilmour, 2006). However, the leading cells ability to migrate is dependent upon contact with the trailing cells; if cells are ablated behind the leading edge the lead cells fail to migrate until contact is re-established (Gilmour, 2005); meanwhile the cells at the back of the primordium follow wherever they are led (Li et al., 2004).

Secondly, the regions of the primordium differentiate independently. This is first apparent at the placodal stage when the posterior lateral line placode differentiates to form the ganglion and primordium (Stone, 1922). During the migration of the primordium, cells in the middle and trailing part of the primordium form transient rosette structures which are later deposited as neuromast precursors, while cells at the trailing edge of the primordium are deposited as interneuromast cells and neuromast precursors (Gompel et al., 2001; Grant et al., 2005; Haas and Gilmour, 2006; Lopez-Schier and Hudspeth, 2005).

Thirdly, there are many known genes with restricted expression domains within the primordium. *semaphorin3A1* is expressed by the cells in the leading part of the primordium, and causes collapse of neural growth cones which is thought to prevent the lateral line nerve overtaking the primordium (Shoji et al., 1998). The chemokine

receptor *cxcr4b* shows strong expression in the leading half of the primordium and weaker expression in the trailing half. In addition, *selenophosphate synthetase 2* (cb701), *delta a*, *delta b*, *zath1, notch3, eyes absent 1* and *keratin 15* all show differential expression patterns within the primordium and neuromasts (Gompel et al., 2001; Itoh and Chitnis, 2001; Sahly et al., 1999).

## 3.2 Aims

In light of the evidence for the differences in cell behaviour and differentiation, as well as the differential gene expression within the primordium, we set out to identify novel genes that have differential expression within the migrating primordium. To this end an *in situ* hybridisation screen was performed. We first conducted a search of the ZFIN (Zebrafish Information Network (Sprague et al., 2006)) EST expression database and identified 23 ESTs that appeared to have differential expression in the posterior lateral line system from the available images. These ESTs were obtained from the I.M.A.G.E. Consortium. *In situ* hybridisation was carried out to obtain more precise expression data on these genes. DNA sequence homology searches were then used in an attempt to identify the genes encoded by the ESTs in order to better assess which to pursue further.

## 3.3 Results

EST plasmid DNA was isolated for each of the 23 clones and *in situ* hybridisation probes produced (see: 2.3.1; 2.3.2). Probe synthesis was attempted a maximum of three times. Successfully synthesised probes were used to perform *in situ* hybridisation on wildtype embryos at three developmental stages: prior to primordium migration (20-somites) and two points during migration (24hpf and 28hpf). The procedure was repeated a maximum of three times for each probe. Any ESTs that failed to produce a probe, or a distinct expression pattern, on each of the three occasions were not examined further.

Of the 23 ESTs screened, twelve clones produced specific expression patterns. Five of these twelve were found to be expressed in the posterior lateral line: cb388, cb486, cb900, cb967 and cb1077. DNA sequence analysis by BLAST search identified these clones as having high homology to: *claudin-7* (cb388), PAR interacting protein (cb486), G-protein coupled receptors (cb900), filamin (cb967) and *myosin5b* (cb1077). These results are summarised in Table 5. Following the completion of this work the zebrafish genome project and ZFIN database have identified these ESTs as: cb388; *claudin-7 (cldn7)*, cb486; *myb binding protein (p160) 1a (mybbp1a)*, cb900; *rdc1/cxc-type chemokine receptor 7b (rdc1/cxcr7b)*,

cb967; *filamin b-like (flnbl)*, and cb1077; *myosin5b (myo5b)* respectively. cb900 has undergone several name changes during the course of this project including: *rdc1, cxcr7* and *cxcr7b*.

To determine if these ESTs demonstrated spatially restricted expression within the primordium, embryos were flat mounted and examined by brightfield microscopy. cb388 (*cldn7*) showed restricted expression in the migrating primordium and deposited neuromast precursor structures (Figure 3a-a'). cb486 (*mybbp1a*), cb967 (*flnbl*) and cb1077 (*myo5b*) displayed weak, punctate, expression restricted to the migrating primordium. The domain was highly dynamic and no reproducible pattern of expression could be identified (Figure 3b-b', d-e'). cb900 (*rdc1/cxcr7b*) exhibited strong spatially restricted expression throughout the posterior lateral line. Expression of cb900 was present in the trailing cells of the primordium, the deposited neuromast precursors and in a thin chain of deposited cells in the wake of the primordium; most probably the interneuromast cells (Figure 3c-c'). Expression of cb900 was only visible at the 24hpf and 28hpf stages; no expression was detectable at 20hpf stage.

## Table 5: Summary of the *in situ* hybridisation screen

| Clone name | EST homologous to | Probe synthesised successfully | Probe tested | Probe found to produce specific signal | Expression in the posterior lateral line | Expression pattern within posterior lateral line |
|---|---|---|---|---|---|---|
| cb6 | trop-2 | Yes | Yes | No | | |
| cb97 | p62 ras-gap | Yes | Yes | Yes | No | |
| cb117 | cingulin | Yes | Yes | No | | |
| cb299 | rin zf | Yes | Yes | No | | |
| cb308 | amot-like 2 | Yes | Yes | No | | |
| cb341 | hox c8 | Yes | Yes | No | | |
| cb376 | hgf activator inhibitor | Yes | Yes | No | | |
| cb386 | thrombospondin | Yes | Yes | No | | |
| cb387 | matrix metalloproteinase14a | No | | | | |
| cb388 | claudin-7 | Yes | Yes | Yes | Yes | Primordium and neuromast precursors |
| cb486 | myb binding protein (p160) 1a | Yes | Yes | Yes | Yes | Weak punctate expression throughout primordium |
| cb488 | calcium binding protein | Yes | Yes | Yes | No | |
| cb521 | lethal giant larvae 2 | Yes | Yes | Yes | No | |
| cb747 | unknown | Yes | Yes | No | | |
| cb766 | tight junction 3 | Yes | Yes | No | | |
| cb786 | unknown | Yes | Yes | No | | |
| cb837 | eva1 | Yes | Yes | No | | |
| cb900 | rdc1/ cxc-chemokine receptor7b | Yes | Yes | Yes | Yes | Trailing cells of primordium, neuromast precursor cells and chain of deposited cells |
| cb915 | unknown | Yes | Yes | No | | |
| cb967 | filamin b-like | Yes | Yes | Yes | Yes | Weak punctate expression throughout primordium |
| cb1016 | unknown | Yes | Yes | Yes | No | |
| cb1018 | zf erv | Yes | Yes | No | | |
| cb1077 | myosin 5b | Yes | Yes | Yes | Yes | Weak punctate expression throughout primordium |

**Figure 3: EST clones and their expression patterns in the zebrafish posterior lateral line**

EST expression domains were visualised by *in situ* hybridisation on 28hpf wildtype embryos. All images are lateral views with anterior to the left and dorsal up

(a-a') cb388/*cldn7* is expressed throughout the primordium and deposited neuromast precursors. (b-b') cb486/*mybbp1a*, (d-d') cb967/*flnbl* and (e-e') cb1077/*myo5b* are dynamically expressed throughout the primordium. (c-c') cb900/*rdc1/cxcr7b* is expressed in the trailing cells of the primordium, a thin trail of cells deposited in the wake of the primordium and the neuromast precursors.

The migrating primordium is outlined in all cases. Abbreviations: **mp**, migrating primordium; **nm**, neuromasts; **inc**, interneuromast cells. Scale bars are 200μm in a-e and 100μm a'-e'.

**Figure 3**

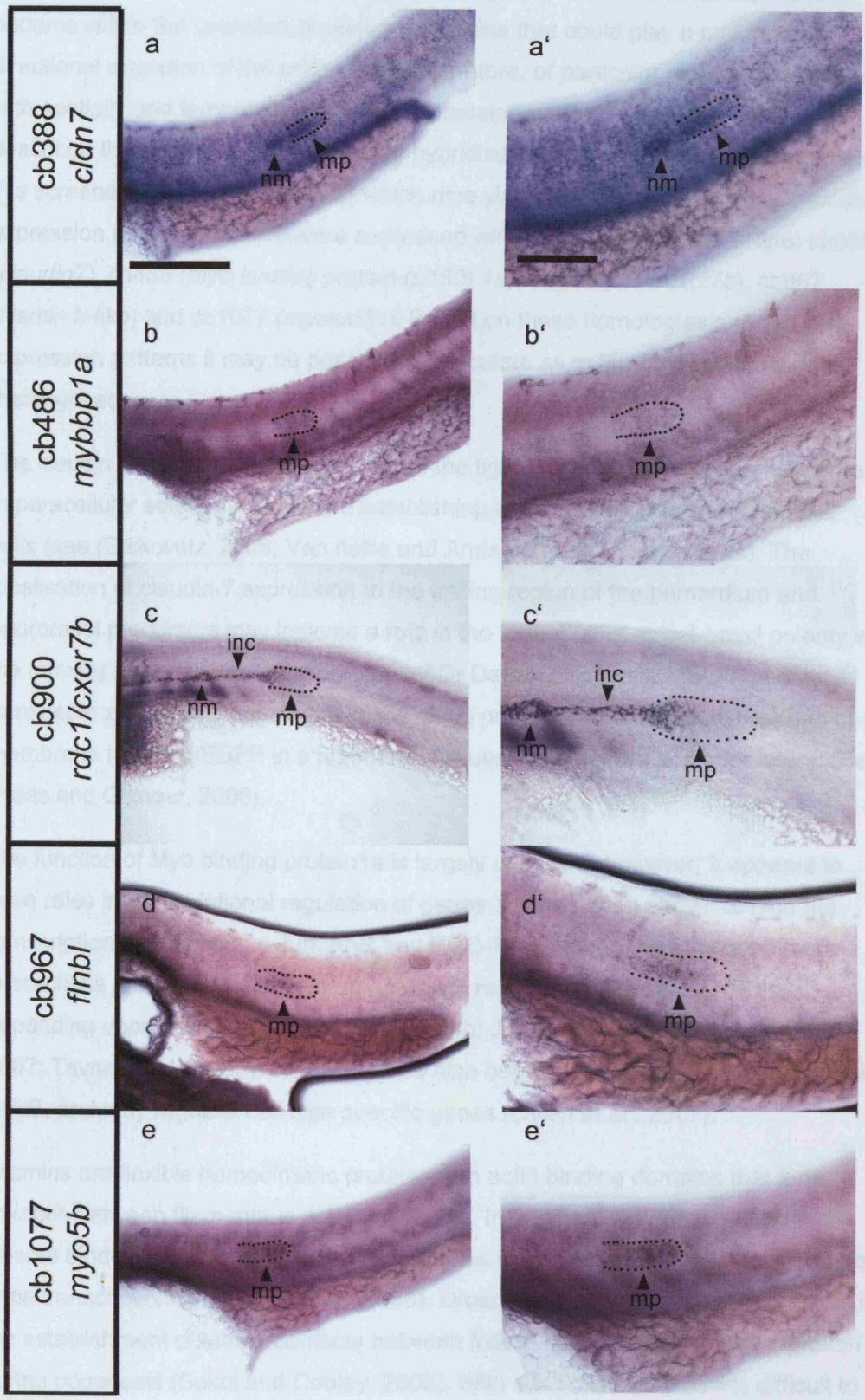
cb388
cldn7
cb486
mybbp1a
cb900
rdc1/cxcr7b
cb967
flnbl
cb1077
myo5b
a
a'
b
b'
c
c'
d
d'
e
e'
nm
mp
inc

## 3.4 Discussion

The aim of this section of work was to identify genes with differential expression patterns within the zebrafish posterior lateral line that could play a role in the directional migration of the primordium. Therefore, of particular interest were genes with spatially and temporally restricted expression patterns. This chapter has described the results of a limited *in situ* hybridisation screen to identify such genes. We screened a total of 23 ESTs of which nine yielded viable probes with identifiable expression patterns and five were expressed within the posterior lateral line: cb388 (*claudin7*), cb486 (*myb binding protein (p160) 1a*), cb900 (*rdc1/cxcr7b*), cb967 (*filamin b-like*) and cb1077 (*myosin5b*). Based on these homologies and the gene expression patterns it may be possible to speculate as to the possible function of these genes.

The claudin family of proteins form part of the tight-junction complex and have roles in paracellular solute transport and establishing apical-basal polarity in epithelial cells (see (Balkovetz, 2006; Van Itallie and Anderson, 2006) for reviews). The localisation of claudin-7 expression to the trailing region of the primordium and neuromast precursors may indicate a role in the formation of apical-basal polarity in the forming neuromasts. The laboratory of Dr Darren Gilmour (EMBL) has created a transgenic zebrafish line that utilises the *cldnb* promoter to drive the expression of membrane targeted EGFP in a number of tissues including the posterior lateral line (Haas and Gilmour, 2006).

The function of Myb binding protein1a is largely unknown, however, it appears to have roles in transcriptional regulation of genes and has been shown to bind the transcription factors Myb, c-Jun, AhR and PGC-1α, although the effects of these interactions are varied leading to up, or down, regulation of gene expression depending upon cell context (Fan et al., 2004b; Jones et al., 2002; Owen et al., 2007; Tavner et al., 1998). MYBBP1a has also been shown to be a co-repressor of NFκB, and may regulate cell type specific genes (Owen et al., 2007).

Filamins are flexible homodimeric proteins with actin binding domains that form linkages between filamentous actin molecules. In addition, they have multiple diverse binding partners with wide ranging roles in cell migration, cell adhesion and gene transcription (Popowicz et al., 2006). *Drosophila* filamin has been implicated in the establishment of stable contacts between follicle cells and follicle cell migration during oogenesis (Sokol and Cooley, 2003). With such diverse roles it is difficult to

speculate on a function for *flnbl*, however, it may play roles in cytoskeleton organisation, cell adhesion and cell migration in the trailing region of the primordium.

Myosin5b, like other myosins, is a motor protein capable of moving along actin filaments. MYO5b is thought to have roles in molecular transport (Thirumurugan et al., 2006; Watanabe et al., 2006). There is evidence that MYO5b colocalises with CXCR2 and may be involved in recycling of CXCR2 to the cell membrane. In addition, over-expression of the tail region of *myo5b* is reported to inhibit both CXCR4 and CXCR2 mediated chemotaxis probably by inhibiting receptor recycling following internalisation (Fan et al., 2004a). It may therefore be that *myo5b* plays a role in recycling of CXC-type receptors in the primordium.

It is likely that there are more EST clones within our search panel that are expressed in the posterior lateral line, that have not been identified by this screen, as several of the clones failed to yield viable probes or produce specific *in situ* hybridisation signals. DNA extraction, probe synthesis and subsequent *in situ* hybridisations were conducted manually and performed in a batch format to increase the speed of the screening process; errors may have occurred as a result. It is also possible that some of the ESTs examined failed to produce an *in situ* hybridisation probe and/or signal due to inaccurate vector data provided with them. These clones were not pursued due to time constraints and it was deemed that cb900/*rdc1*/*cxcr7b* fulfilled the criteria for this section of work for the reasons outlined below. However, it may be worthwhile at a future date to re-examine our EST panel for additional genes with differential expression patterns.

Our initial BLAST searches had identified cb900 as a G-protein coupled receptor. Further sequence analysis (see Chapter 4) showed that cb900 was closely related to the orphan GPCR *rdc1* and showed strong homology to the CXC-type GPCR family. GPCRs have well documented roles in the chemotaxis of migratory cells (Dormann and Weijer, 2003; Fanto and McNeill, 2004; Wang et al., 2006) and *cxcr4b*, a member of the CXC-type GPCR family, has an established role in primordium migration (David et al., 2002; Li et al., 2004). Thus, we set out to characterise the expression pattern and study the function of cb900 in the developing posterior lateral line.

# Chapter 4: Characterisation of cb900

## 4.1 Introduction

The EST clone cb900 showed robust expression within the trailing region of the primordium and cells deposited in its wake. Our initial sequence analysis identified cb900 as a G-protein coupled receptor with high homology to the CXCR-family of G-protein coupled receptors. This was intriguing as the CXCR-family member *cxcr4b* is known to be required for primordium migration and is expressed in a graded fashion with high levels in the leading part of the primordium (David et al., 2002; Li et al., 2004). In addition, the CXCR-family of chemokine receptors have well-established roles in directed cell migration (Horuk, 2001; Kucia et al., 2004; Kulbe et al., 2004; Zlotnik, 2006). The relationship between these two receptors intrigued us and detailed sequence analysis was carried out to further characterise cb900. We were also curious as to the temporal and spatial expression of the two receptors during primordium migration.

## 4.2 Aims

The aim of this section of work was to conduct DNA-sequence analysis, protein-sequence analysis and phylogenetic examination of cb900 in order to assign it to a specific subfamily of G-protein coupled receptors. This was necessary in order to build an hypothesis as to the possible function of cb900 within the posterior lateral line primordium.

We also performed an *in situ* hybridisation time course to better characterise the spatial and temporal elements of cb900 expression. We were particularly interested in the initiation of expression within the primordium and the identity of the cells in which it is expressed. *In situ* hybridisation was also used to examine the relationship between the expression domains of *cxcr4b* and cb900 during the development of the posterior lateral line.

## 4.3 Results

### 4.3.1 Homology and phylogenetic analysis of clone cb900

To identify the gene encoded by the clone cb900 further DNA sequence analysis was performed using the Vertebrate Genome Annotation database (VEGA, Sanger Institute) and the UniGene (NCBI) database. cb900 was identified as a partial length clone of the zebrafish homologue of *rdc1* encoding the 5'-most region; a result confirmed by both databases (data not shown). During the course of our

investigations we identified an EST encoding the full-length open reading frame of *rdc1* in the I.M.A.G.E Consortium database (IMAGE clone: 7067778). This clone was obtained and utilised for all subsequent work.

DNA sequencing of the full-length clone revealed several polymorphisms when compared to the sequence held on the VEGA database (Version 28). *rdc1* encodes a peptide of 362 amino acid residues. The majority of the polymorphisms were silent, however, there was a substitution of a phenylalanine for a leucine at amino acid 172 (F172L), and an isoleucine for a valine at amino acid 232 (I232V). These substitutions were not considered likely to affect the protein as the phenylalanine is a more conserved residue when compared to mammalian RDC1s, and the isoleucine substitution appeared to be in a region of variability (data not shown).

The predicted zebrafish RDC1 protein is conserved compared to RDC1 homologues in other species (Figure 4a). Zebrafish RDC1 shows 72.6% similarity (54.5% identity) to human, 70.0% similarity (52.5% identity) to mouse and 70.0% similarity (52.3% identity) to rat. This is comparable to the conservation between human CXCR4 and zebrafish CXCR4b; 74.7% similarity (60.0% identity). Phylogenetic comparison of zebrafish RDC1 to representative receptors of several G-protein coupled receptor families revealed a strong homology between RDC1 and the chemokine receptor family (data not shown), particularly the CXCR-family of receptors with strong homology to CXCR1 and CXCR2 (Figure 4b).

Protein sequence comparison between zebrafish RDC1 and human CXCR4 shows the conservation of several known functional domains which include: DRY, G-protein binding motif (Doranz et al., 1999): NPxxY motif, believed to be involved in receptor internalisation (Kalatskaya et al., 2004) and four conserved cystein residues, thought to form internal structural disulphide bonds (Heesen et al., 1996) (Figure 4a; Figure 5). One interesting feature shared by the RDC1 homologues is that they lack the SSLKILSKGK motif present in other GPCRs and required for degradation by targeting the receptors to lysosomes (Marchese and Benovic, 2001) (Figure 4a; Figure 5).

Study of the ENSEMBL (EMBL-EBI and Sanger Institute) genome browser revealed a conserved genomic structure between human, mouse and zebrafish *rdc1/cxcr7*. There is one intron 5' to the transcription start site (Figure 6a-c). In addition, the presence of the *iqca* (*IQ motif containing with AAA domain*) gene is conserved 5' to *rdc1* on the antisense DNA strand in all three species (Figure 6a'-c').

Our phylogenetic analysis and identification of cb900 as *rdc1* is in agreement with the recently published work of several groups (Dambly-Chaudiere et al., 2007; Infantino et al., 2006; Miyasaka et al., 2007). In addition, our assessment that RDC1 shows high homology to the CXC-receptor family is in agreement with published data (Heesen et al., 1998). Since the completion of this section of work it has been shown that RDC1 can bind CXC-type chemokines, the defining feature of CXC-type receptors, which has lead to its reclassification as CXCR7 (Balabanian et al., 2005; Burns et al., 2006; Proost et al., 2007). In zebrafish, two homologues of *cxcr7* have been identified *cxcr7a* and *cxcr7b* (Miyasaka et al., 2007). cb900 corresponds to *cxcr7b* and will be referred to as such for the remainder of this thesis.

**Figure 4: CB900/RDC1 shows high homology to the CXCR-receptor family**

Summary of CB900/RDC1 sequence homology to RDC1 in other species.

(a) The predicted protein sequence for cb900 was aligned against the sequences for human, mouse and *Xenopus laevis* RDC1 obtained from the UniGene database. Residues identical to zebrafish CB900/RDC1 are shaded grey. DRY G-protein binding domain and NPxxY internalisation motif are conserved (red shading). Conserved cysteine residues are thought to form structural disulphide bonds (yellow shading). The position of the absent SSLKILSKGK degradation motif is indicated (blue shading).

(b) Protein sequences for a range of CXCR-family G-protein coupled receptors were obtained by BLAST alignments and a phylogenetic tree compiled. Zebrafish CB900/RDC1 (black arrow) shows high homology to the CXCR-family especially CXCR1 and CXCR2.

# Figure 4

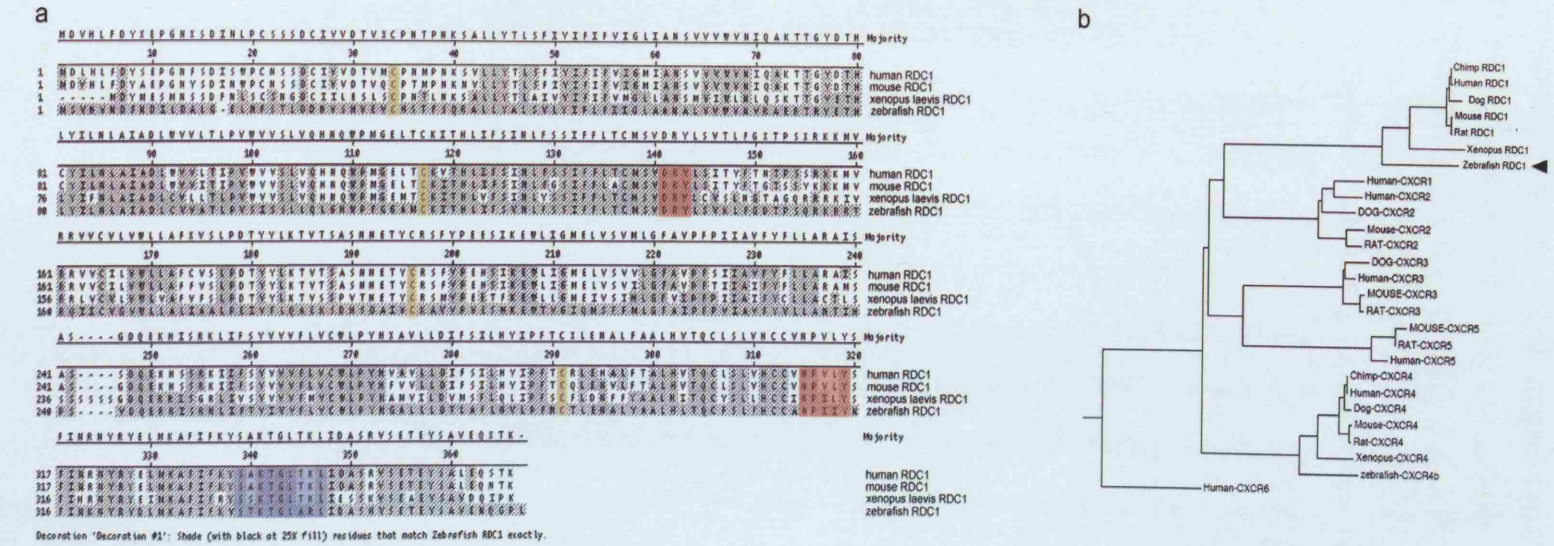
a
Majority
human RDC1
mouse RDC1
xenopus laevis RDC1
zebrafish RDC1
Decoration 'Decoration #1': Shade (with black at 25% fill) residues that match Zebrafish RDC1 exactly.
b
Chimp RDC1
Human RDC1
Dog RDC1
Mouse RDC1
Rat RDC1
Xenopus RDC1
Zebrafish RDC1
Human-CXCR1
Human-CXCR2
DOG-CXCR2
Mouse-CXCR2
RAT-CXCR2
DOG-CXCR3
Human-CXCR3
MOUSE-CXCR3
RAT-CXCR3
MOUSE-CXCR5
RAT-CXCR5
Human-CXCR5
Chimp-CXCR4
Human-CXCR4
Dog-CXCR4
Mouse-CXCR4
Rat-CXCR4
Xenopus-CXCR4
zebrafish-CXCR4b
Human-CXCR6

**Figure 5: Protein alignment reveals the presence of several conserved domains**

Zebrafish CXCR7b was compared to human CXCR4 using the Needleman P global alignment algorithm (NCBI). Known transmembrane domains of CXCR4 were superimposed onto zebrafish CXCR7b (yellow shading). DRY and NPxxY motifs are conserved (red shading) as are four conserved cysteine residues (orange shading). However, the SSLKILSKGK domain of CXCR4 is absent from zebrafish CXCR7b (blue shading).

Figure 5

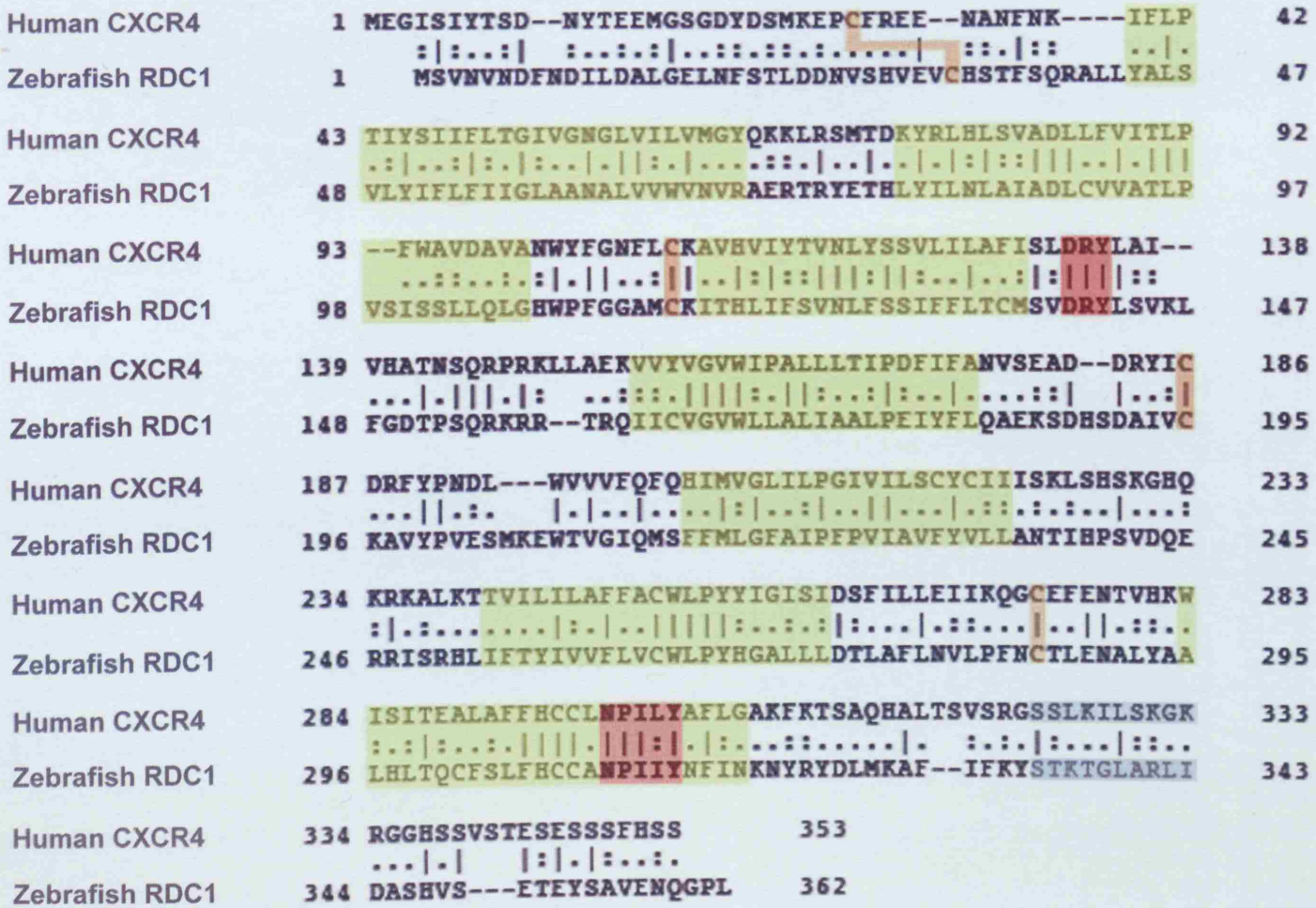
Human CXCR4 1 MEGISIYTSD--NYTEEMGSGDYDSMKEPCFREE--NANFNK----IFLP 42
Zebrafish RDC1 1 MSVNVNDFNDILDALGELNFSTLDDNVSHVEVCHSTFSQRALLYALS 47
Human CXCR4 43 TIYSIIFLTGIVGNGLVILVMGYQKKLRSMTDKYRLHLSVADLLFVITLP 92
Zebrafish RDC1 48 VLYIFLFIIGLAANALVVWVNVRAERTRYETHLYILNLAIADLCVVATLP 97
Human CXCR4 93 --FWAVDAVANWYFGNFLCKAVHVIYTVNLYSSVLILAFISLDRYLAI-- 138
Zebrafish RDC1 98 VSISSLLQLGHWPFGGAMCKITHLIFSVNLFSSIFFLTCMSVDRYLSVKL 147
Human CXCR4 139 VHATNSQRPRKLLAEKVVYVGVWIPALLLTIPDFIFANVSEAD--DRYIC 186
Zebrafish RDC1 148 FGDTPSQRKRR--TRQIICVGVWLLALIAALPEIYFLQAEKSDHSDAIVC 195
Human CXCR4 187 DRFYPNDL---WVVVFQFQHIMVGLILPGIVILSCYCIIISKLSHSKGHQ 233
Zebrafish RDC1 196 KAVYPVESMKEWTVGIQMSFFMLGFAIPFPVIAVFYVLLANTIHPSVDQE 245
Human CXCR4 234 KRKALKTTVILILAFFACWLPYYIGISIDSFILLEIIKQGCEFENTVHKW 283
Zebrafish RDC1 246 RRISRHLIFTYIVVFLVCWLPYHGALLLDTLAFLNVLPFNCTLENALYAA 295
Human CXCR4 284 ISITEALAFFHCCLNPILYAFLGAKFKTSAQHALTSVSRGSSLKILSKGK 333
Zebrafish RDC1 296 LHLTQCFSLFHCCANPIIYNFINKNYRYDLMKAF--IFKYSTKTGLARLI 343
Human CXCR4 334 RGGHSSVSTESESSSFHSS 353
Zebrafish RDC1 344 DASHVS---ETEYSAVENQGPL 362

**Figure 6: *rdc1/cxcr7* transcript and genomic structure are conserved**

The DNA encoding *rdc1/cxcr7* in human, mouse and zebrafish was identified using the ENSEMBL (EMBL, Sanger Institute) genome browser.

(a) The transcript structure of RDC1 is conserved in human, mouse and zebrafish with one intron 5' to the transcription start site, though the size of the intron varies. (b) Examination of neighbouring genes reveals the conservation of the *iqca* (*IQ motif containing with AAA domain*) (black arrow) gene 5' to *rdc1/cxcr7* (black arrowhead) on the antisense DNA strand.

## Figure 6

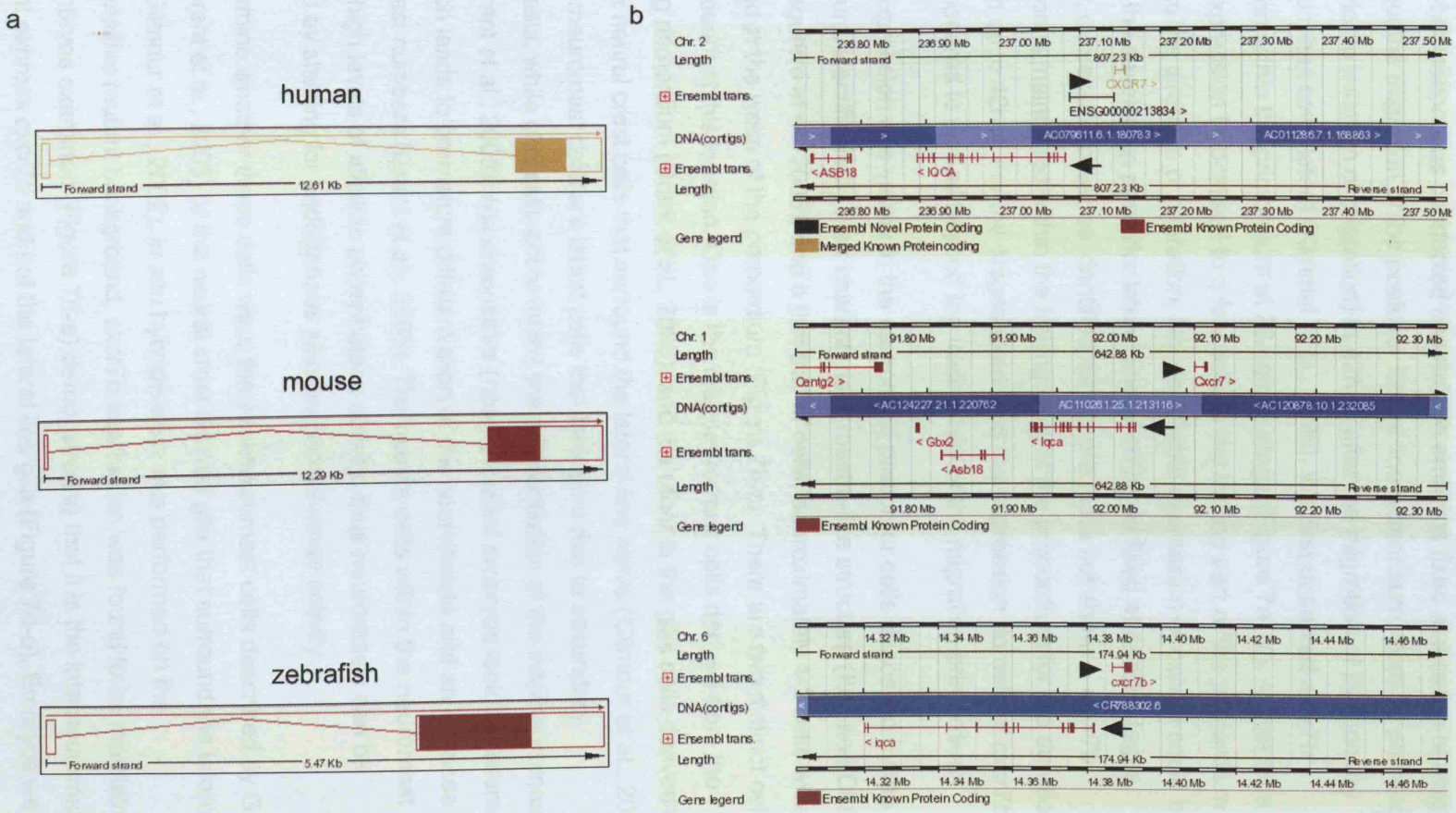
a
human
Forward strand
12.61 Kb
mouse
Forward strand
12.29 Kb
zebrafish
Forward strand
5.47 Kb
b
Chr. 2
Length
Forward strand
807.23 Kb
Ensembl trans.
CXCR7 >
ENSG00000213834 >
DNA(contigs)
AC079611.6.1.18078.3 >
AC011286.7.1.168863 >
< ASB18
< IQCA
Reverse strand
Gene legend
Ensembl Novel Protein Coding
Ensembl Known Protein Coding
Merged Known Protein coding
Chr. 1
642.88 Kb
Cxcr7 >
Cxcr2 >
< AC124227.21.1.220762
AC110261.25.1.213116 >
< AC120878.10.1.232085
< Gbx2
< Iqca
< Asb18
Chr. 6
174.94 Kb
cxcr7b >
< CR788302.6
< iqca

### 4.3.2 Characterisation of *cxcr7b* expression within the posterior lateral line

*In situ* hybridisation was conducted on wildtype embryos fixed at a range of stages throughout the migration of the posterior lateral line primordium, from 18-somites stage (prior to initiation of migration) to 42hpf (after the migration of the primary primordium has completed) (Kimmel et al., 1995). We first observed *cxcr7b* expression within the primordium at 26-somite stage (Figure 7a, a'). At that time *cxcr7b* expression is localised to a few cells in the trailing part of the primordium with respect to the direction of migration. No identifiable expression of *cxcr7b* could be found in the developing posterior lateral line of embryos fixed at earlier stages, however, expression could be identified elsewhere (data not shown). *cxcr7b* expression is maintained within the trailing cells of the primordium for the duration of migration up to 42hpf. For the stages examined the expression domain of *cxcr7b* never appeared to spread beyond the trailing half of the migrating primordium.

*cxcr7b* expression was visible in the neuromast precursor cells deposited by the primordium, identifiable by their characteristic rosette-like structure (Itoh and Chitnis, 2001; Laguerre et al., 2005), and a thin trail of cells, approximately 1-2 cells wide deposited in the wake of the primordium (Figure 7b-c). There are two distinct cell types present at this location. One is the interneuromast cells derived from the migrating primordium (Grant et al., 2005), and the other is the glial cells derived from the trunk neural crest cells that surround the lateral line nerve (Gilmour et al., 2002). The interneuromast cells are latent cells that later give rise to secondary neuromasts, while glial cells act to inhibit the differentiation of the interneuromast cells (Grant et al., 2005). *Hypersensitive* (*hps-/-*) mutant embryos lack the lateral line glia which leads to premature differentiation of the neuromasts and an increase in neuromast numbers (Grant et al., 2005). The mantle cells within the neuromast contain high levels of alkaline phosphatase activity, thus neuromasts can be detected by staining for endogenous alkaline phosphatase activity.

To determine whether these cells were the interneuromast cells described by Grant *et al.* (Grant et al., 2005) or the neural crest derived glia that surround the lateral line nerve (Gilmour et al., 2002), *in situ* hybridisation was performed on the *hypersensitive* mutant background. *cxcr7b* expression was found to be maintained in all embryos examined (Figure 7d-e) demonstrating that it is the interneuromast cells that express *cxcr7b* and not the lateral line glia (Figure 7d-e). Embryos were confirmed as mutants by alkaline phosphatase staining of both the mutant and wildtype siblings at 5dpf where approximately 25% of embryos displayed the

phenotypic supernumerary neuromasts of the *hypersensitive* mutant (Grant et al., 2005).

**Figure 7: *cxcr7b* expression is spatially restricted throughout migration**

Expression of *cxcr7b* in the posterior lateral line primordium. Images a and a' are dorsal views with anterior to the left. Images b-e are lateral views with dorsal up and anterior to the left.

(a-a') *cxcr7b* expression within the posterior lateral line primordium is first visible at the 26-somite stage where it is localised to the trailing region of the primordium with regards to the direction of migration. (b-b') Expression of *cxcr7b* is restricted to the trailing cells of the primordium, neuromast precursor cells and the interneuromast cells. (c-c') These domains of expression were maintained throughout the migration of the primordium and following the completion of migration until 42hpf. (d-e) Examples of *cxcr7b* expression in the *hps* mutant background at 28hpf.

The primordium is outlined in all images. Abbreviations: **mp**, migrating primordium; **nm**, neuromasts; **inc**, interneuromast cells. Scale bars are 100μm, except a' where it is 50μm.

**Figure 7**

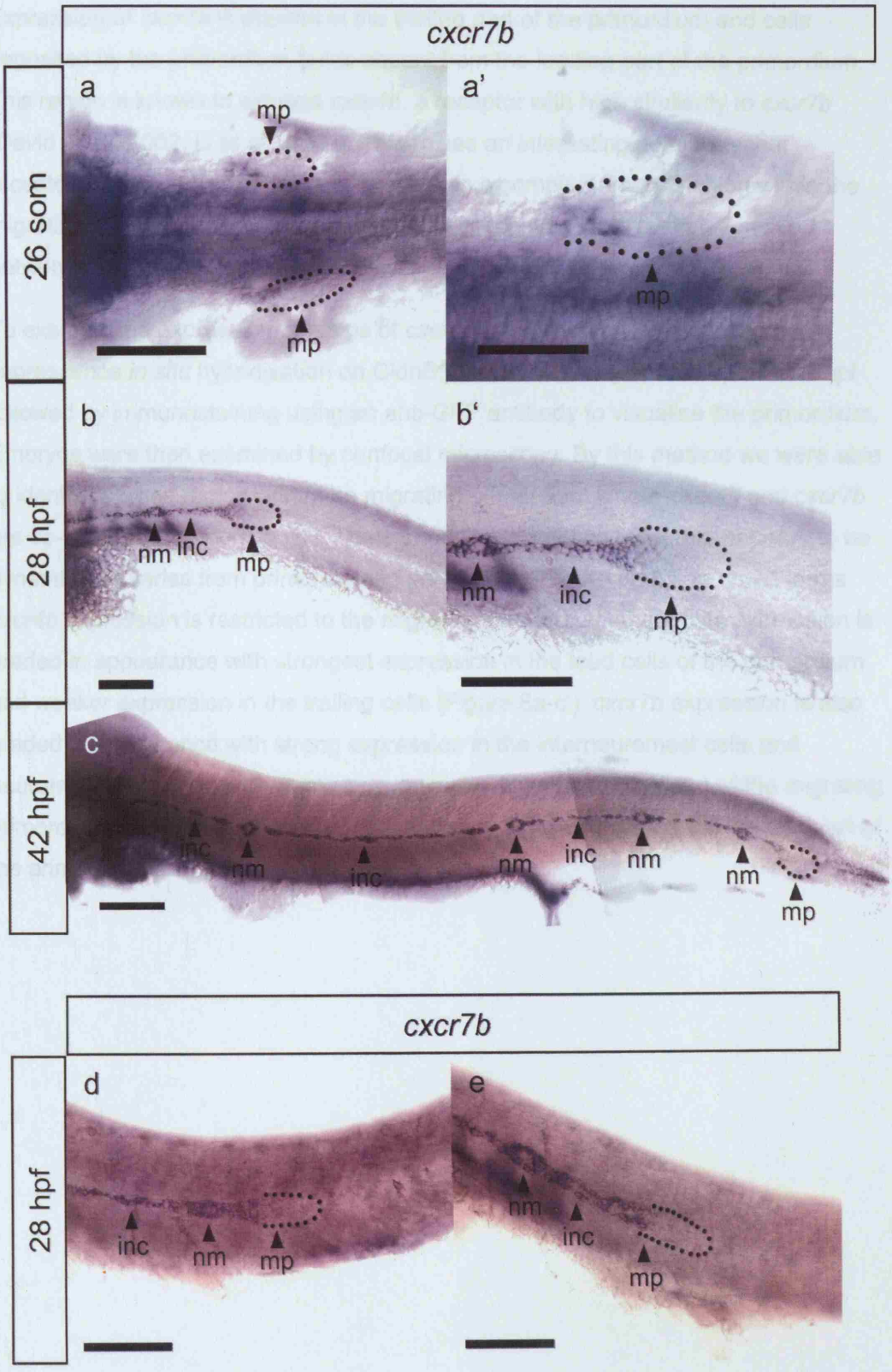

### 4.3.3 Spatial expression of *cxcr4b* and *cxcr7b* in the developing posterior lateral line

Expression of *cxcr7b* is present in the trailing part of the primordium and cells deposited by the primordium but is absent from the leading part of the primordium. This region is known to express *cxcr4b*, a receptor with high similarity to *cxcr7b* (David et al., 2002; Li et al., 2004). This raises an interesting possibility that receptors of the same family are expressed in a complementary fashion within the migrating primordium. We were therefore keen to investigate the relationship between the two expression patterns.

To examine the expression domains of *cxcr4b* and *cxcr7b* we utilised double fluorescence *in situ* hybridisation on CldnB:LynEGFP embryos at 24hpf and 28hpf followed by immunostaining using an anti-GFP antibody to visualise the primordium. Embryos were then examined by confocal microscopy. By this method we were able to identify a broad region within the migrating primordium where *cxcr4b* and *cxcr7b* are co-expressed (Figure 8a-c'). The expression of the two receptors appears to be dynamic and varies from primordium to primordium (Figure 8a-c'). In broad terms *cxcr4b* expression is restricted to the migrating primordium, though its expression is graded in appearance with strongest expression in the lead cells of the primordium and weaker expression in the trailing cells (Figure 8a-c'). *cxcr7b* expression is also graded in appearance with strong expression in the interneuromast cells and neuromast precursors with weaker expression within the trailing part of the migrating primordium (Figure 8a-c'). *cxcr7b* transcripts were not detected in the leading part of the primordium at the stages examined.

**Figure 8: Dynamic expression of *cxcr7b* and *cxcr4b***

Expression domains of *cxcr7b* and *cxcr4b* at 28hpf in CldnB:LynEGFP embryos. All images are lateral views with anterior to the left and dorsal up. *cxcr7b* and *cxcr4b* mRNA expression are red and blue respectively. EGFP was revealed by antibody staining after *in situ* hybridisation thus visualising the primordium.

(a-c') Several examples of *cxcr7b* and *cxcr4b* expression in the primordium are shown. Expression of *cxcr7b* and *cxcr4b* is not mutually exclusive within the posterior lateral line primordium. The expression domains overlap and the boundaries of expression are individual to each primordium.

Abbreviations: **mp**, migrating primordium; **nm**, neuromasts; **inc**, interneuromast cells. The scale bar is 50μm in a, b, and c, and 25μm in a', b', and c'.

**Figure 8**

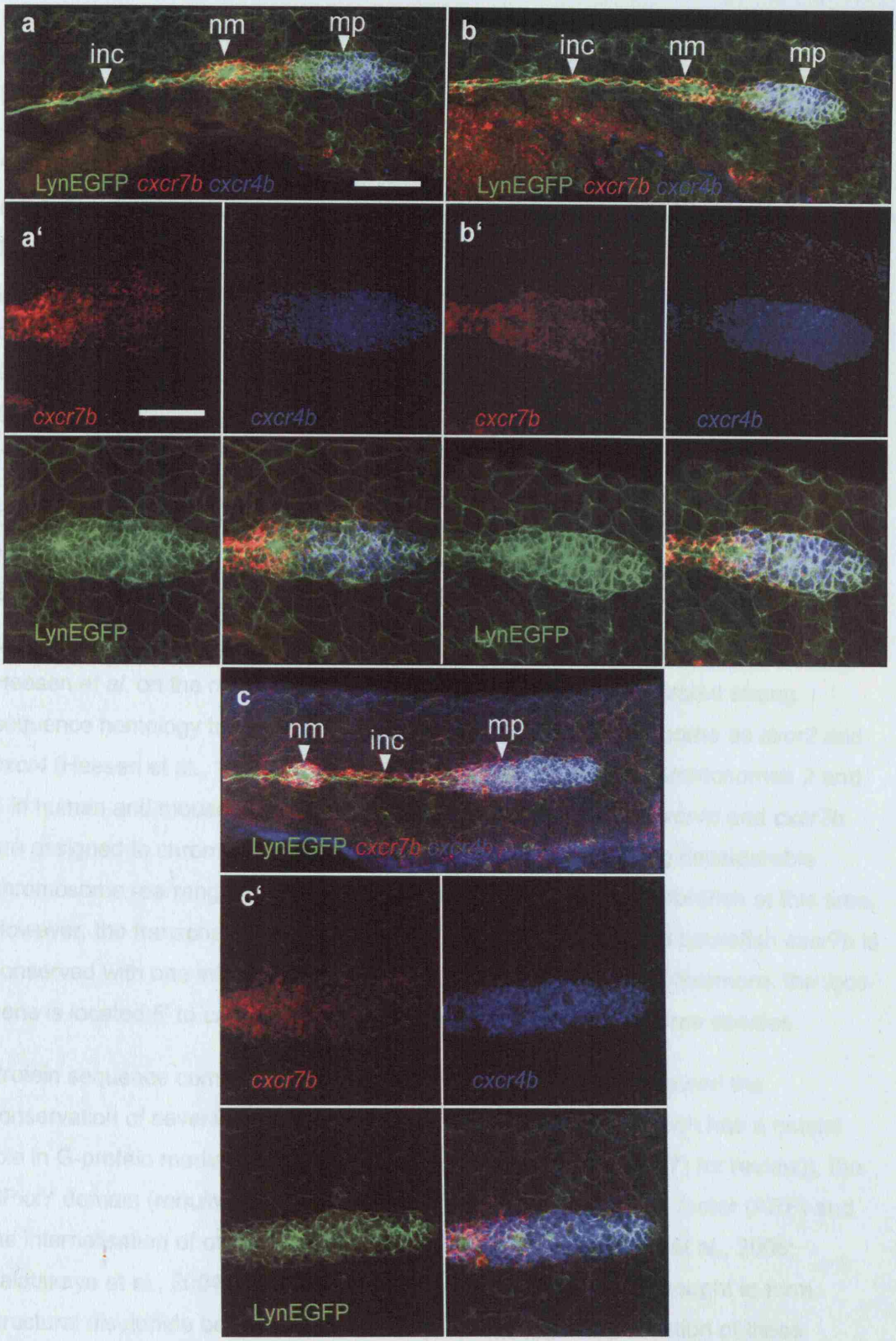
a
inc
nm
mp
LynEGFP cxcr7b cxcr4b
b
inc
nm
mp
LynEGFP cxcr7b cxcr4b
a'
cxcr7b
cxcr4b
b'
cxcr7b
cxcr4b
LynEGFP
LynEGFP
c
nm
inc
mp
LynEGFP cxcr7b
c'
cxcr7b
cxcr4b
LynEGFP

## 4.4 Discussion

We selected cb900 for further examination based on its intriguing expression pattern and its high homology to the G-protein coupled receptor superfamily. Detailed sequence analysis and whole mount *in situ* hybridisation was carried out to gain a better understanding of its possible function in the developing posterior lateral line.

### 4.4.1 cb900 is a member of the CXCR-family of G-protein coupled receptors

In this chapter we have conducted DNA sequence, protein sequence and phylogenetic analysis of cb900. These methods provided strong evidence that cb900 encodes *rdc1*. At the time that this work was conducted RDC1 was an orphan G-protein coupled with no assigned ligand, function or role in development. Sequence comparison indicated that RDC1 was highly homologous to the CXC-receptor subfamily of G-protein coupled receptors.

Our phylogenetic comparisons of RDC1 to a variety of G-protein coupled receptors from a number of species (human, mouse, rat, dog and *Xenopus*) demonstrated that RDC1 was highly homologous to the CXC-type chemokine receptor family, particularly CXCR1 and CXCR2. This was in agreement with work performed by Heesen *et al.* on the mouse homologue of RDC1 which demonstrated strong sequence homology to CXCR2 and linkage to the same chromosome as *cxcr2* and *cxcr4* (Heesen et al., 1998). *cxcr2*, *cxcr4* and *cxcr7* localise to chromosomes 2 and 1 in human and mouse respectively, while in zebrafish *cxcr4a*, *cxcr4b* and *cxcr7b* are assigned to chromosomes 6, 16 and 9 respectively indicating considerable chromosome rearrangements. *cxcr2* has not been identified in zebrafish at this time. However, the transcript structure of human and mouse *cxcr7* and zebrafish *cxcr7b* is conserved with one intron 5' to the transcription initiation site. Furthermore, the *iqca* gene is located 5' to *cxcr7b* on the antisense DNA strand in all three species.

Protein sequence comparison between CXCR7b and CXCR4 showed the conservation of several domains, including: the DRY domain (which has a crucial role in G-protein mediated GPCR activity (See (Rovati et al., 2007) for review)), the NPxxY domain (required for interaction with the ADP-ribosylation factor (ARF) and the internalisation of other GPCRs (Bouley et al., 2003; Johnson et al., 2006; Kalatskaya et al., 2004)), and four conserved cystein residues (thought to form structural disulphide bonds (Infantino et al., 2006)). The conservation of these domains combined with published evidence that both CXCR4 and CXCR7 act as cofactors that allow human immunodeficiency virus (HIV) to enter cells (Brelot et al.,

1997; Shimizu et al., 2000) led us to hypothesise that they could share SDF1a as a ligand in zebrafish.

Interestingly, CXCR7b, like homologues of CXCR7 in other species, lacks the SSLKILSKGK (equivalent region: STKTGLARLI) degradation motif that targets receptors to lysosomes for destruction present in CXCR4 and other G-protein coupled receptors (Marchese and Benovic, 2001; Ueda et al., 2006). This may indicate that CXCR7 is not degraded following internalisation and may suggest that the protein is more stable and possibly able to elicit its effect over a longer period of time (Sierro et al., 2007). Furthermore, zebrafish CXCR7b, like its homologues from other species, also lacks the conserved DRYLAIV, altered to DRYLSVK, motif thought to be associated with G-protein activation and calcium signalling (Sierro et al., 2007). This may help to explain the varied effects observed following CXCR7 activation with some groups finding that binding of SDF1 to CXCR7 does not cause $Ca^{2+}$ release while others find that it does cause $Ca^{2+}$ release (Balabanian et al., 2005; Burns et al., 2006; Infantino et al., 2006; Proost et al., 2007). However, in zebrafish CXCR4b the DRYLAIV motif is altered to DRYLAVV therefore the motifs may not have the same function in humans and zebrafish.

Based upon the DNA and protein sequence homology, conserved transcript and genomic structures we are confident that *cxcr7b* is a true homologue of mammalian *cxcr7*.

### 4.4.2 Possible ligand for CXCR7

Libert *et al.* first identified *rdc1* in 1989 during a degenerate RT-PCR search for G-protein coupled receptors in dog thyroid tissue. *rdc1* is not an acronym and no mention is made of the reasoning behind the name (Libert et al., 1989). The following year Libert *et al.* published the full *rdc1* cDNA sequence identifying *rdc1* as a seven transmembrane receptor (Libert et al., 1990). Initial characterisation of RDC1 identified it as a receptor for vasointestinal peptide (VIP) in transfected cell lines due to increased cyclic-AMP levels (Sreedharan et al., 1991). However, this possibility was later dismissed due to the low protein homology of RDC1 to the existing VIP receptors and an inability to show a correlation between the increased expression levels of RDC1 and increased binding of VIP on cellular membranes (Cook et al., 1992). RDC1 has also been proposed to be a receptor for calcitonin gene-related peptide (CGRP) (Kapas and Clark, 1995) and adrenomedullin (Martinez et al., 2000), however, these possibilities have since been dismissed as RDC1 could not account for the majority of the cellular binding of CGRP or adrenomedullin (Chakravarty et al., 2000).

The defining feature of CXC-receptors is their ability to bind ligands with an N-terminal CXC-motif. The ligand for CXCR4 is SDF1, also known as CXCL12 (Bleul et al., 1996). The link between RDC1 and the CXCR-family of GPCRs was strengthened when RDC1 and CXCR4 were identified as cofactors that aided the entry of the HIV and simian immunodeficiency virus (SIV) into brain derived cells, CD4+-cells and a T-cell line (Brelot et al., 1997; Shimizu et al., 2000) suggesting similarities in the extracellular domains. It has since been demonstrated that RDC1 can bind CXCL12 in T-lymphocytes (Balabanian et al., 2005) and the human mammary adenocarcinoma MCF-7 cell line (Burns et al., 2006). However, additional ligands have also been identified that are recognised by CXCR7 which include CXCL11/I-TAC in transfected Chinese hamster ovary (CHO) cells (Proost et al., 2007) and MCF-7 cells (Burns et al., 2006), and a distinct, as yet unidentified, ligand secreted by stimulated plasmacytoid dendritic cells (pDCs) that is capable of internalising CXCR7 in pDCs (Infantino et al., 2006). This may suggest a tissue dependent element to the binding and internalisation of RDC1/CXCR7, and, unlike CXCR4, CXCR7 may have affinity for several ligands.

Until relatively recently GPCRs were thought to function as monomeric units. However, it is now largely accepted that most, if not all, GPCRs form dimers or higher order structures and that oligomerisation may be essential for their function (Levoye et al., 2006; Springael et al., 2005). Indeed it has been suggested that dimerisation may be necessary for protein folding and transport to the cell membrane (Bulenger et al., 2005; Milligan et al., 2006). Both CXCR1 and CXCR2 have been shown to be capable of forming homodimers as well as heterodimers with one another (Wilson et al., 2005). Furthermore, it has been suggested that CXCR4 can form homodimers that activate the JAK/STAT pathway (Vila-Coro et al., 1999) though whether this is ligand dependent remains controversial (Busillo and Benovic, 2007). However, the effect of heterodimerisation on the signalling properties of GPCRs remains controversial as it is difficult to ascertain which effects are due to homodimerisation of the individual receptors and which may be due to heterodimer formation (Milligan et al., 2006).

Fluorescence resonance energy transfer (FRET) analysis of HEK293 cells transfected with fluorescently tagged versions of CXCR4 and CXCR7 has been used to indicate an interaction between the two receptors (Sierro et al., 2007). Furthermore, addition of SDF1/CXCL12 to cells transfected with CXCR7 and CXCR4 produces a greater calcium influx in response to ligand binding than cells transfected with CXCR4 alone (Sierro et al., 2007). Formation of CXCR4/CXCR7

heterodimers is also reported to alter downstream ERK1 and ERK2 phosphorylation in transfected HEK293 cells (Sierro et al., 2007). While the potential interaction of the two receptors is intriguing, the situation in tissue culture where both receptors are over-expressed may not be representative of the *in vivo* situation, and any effect may be dependent on cell context and the level of protein expression.

The demonstration of CXC-type ligand binding combined with the strong phylogenetic similarity between RDC1 and the CXCR-family of G-protein coupled receptors has led to the reclassification of *rdc1* as *cxcr7*. However, the exact mode of action of CXCR7 remains controversial as different groups claim different effects following stimulation of CXCR7: on the one hand CXCR7 has been shown not to cause calcium influx following activation by CXCL12 (Burns et al., 2006; Sierro et al., 2007) and has been implicated in increased cell adhesion and improved cell survival (Burns et al., 2006); alternatively activation of CXCR7 by CXCL12 has been shown to result in calcium influx (Jones et al., 2006) and increased cell motility (Balabanian et al., 2005). Activation by CXCL11 has also been shown to not result in calcium influx, and ERK or AKT phosphorylation (Proost et al., 2007). *Cxcr7* deficient mice die within 24 hours of birth and display defects in heart development and B-cell maturation, however, vascular development and development of the nervous system are grossly normal (Sierro et al., 2007). In addition, *cxcr7* is associated with growth and invasion of breast carcinoma and prostate cancers (Miao et al., 2007; Wang et al., 2007).

### 4.4.3 Temporal and spatial expression of *cxcr7b* in the developing posterior lateral line

To gain insights into the possible function during the migration of the primordium we further characterised the expression profile of *cxcr7b*. We were first able to identify *cxcr7b* expression in the posterior lateral line at approximately 26-somite stage; at this stage expression was restricted to the trailing cells of the primordium. Expression of *cxcr7b* was maintained in the trailing part of the primordium throughout the migration to the tip of the tail. Interestingly, expression of *cxcr7b* correlates well with the initiation of migration of the primordium (Kimmel et al., 1995). Additionally, we have shown that *cxcr7b* is expressed not only in the trailing part of the primordium but also in the neuromast precursors and the interneuromast cells. This expression profile led us to consider the possibility that *cxcr7b* may be required during the initiation and/or guidance of migration.

Double *in situ* hybridisation revealed an overlapping expression pattern between *cxcr4b* and *cxcr7b* thus providing us with a potentially interesting situation.

Heterodimerisation can occur in other G-protein coupled receptors and may alter the signalling properties of the receptors involved (Bulenger et al., 2005; Jordan and Devi, 1999; Mellado et al., 2001a; Sierro et al., 2007; Springael et al., 2005); though this had not been reported for CXCR4 and CXCR7 at the time we were intrigued by any possible relationship between the two receptors. Heterodimerisation between CXCR4 and CXCR7 has since been suggested, with evidence for altered signalling characteristics, when both receptors are over-expressed in HEK293 cells (Sierro et al., 2007), thus there may be altered signalling characteristics where the two receptors overlap. In addition, the complimentary expression may indicate transcriptional regulation between them.

# Chapter 5: Initiation of primordium migration

## 5.1 Introduction

The posterior lateral line placode can be identified from 4-somite stage due to the expression of the transcription factor *hmx3/nkx5.1* (Adamska et al., 2000). By 20-somite stage the placode is identifiable under Nomarski optics (Kimmel et al., 1995), and by approximately 26-somite stage the primordium commences its migration (Kimmel et al., 1995). However, little if anything is known about the process by which the primordium initiates its migration in zebrafish.

## 5.2 Aims

The aims of this section of work were to examine the early migration of the primordium in order to gain a better understanding of the process of the initiation of directed migration along the horizontal myoseptum. To do this we performed confocal timelapse analysis of the primordium to analyse cell behaviour during the early stages of migration. We also made use of *in situ* hybridisation to relate the expression of *hmx3*, *cxcr4b*, *sdf1a* and *cxcr7b* to the initiation of primordium migration.

## 5.3 Results

### 5.3.1 Timelapse analysis reveals the presence of separated cell clusters

To obtain a better understanding of the cellular process of migration initiation in the posterior lateral line we conducted confocal timelapse analysis of zebrafish embryos from approximately 18-somite stage onwards. At this stage the primordium is identifiable as a large cluster of cells posterior to the otic vesicle that extends to approximately somite 1 (Figure 9a) (Kimmel et al., 1995).

Our initial experiments utilised the $H_2A.F/Z$:GFP (Pauls et al., 2001) transgenic line in which all nuclei are labelled with green fluorescent protein (GFP). By this method we were able to observe the condensation and coalescence of cells scattered over a wide area to form the visible cell mass that constitutes the primordium. However, it is difficult to say for certain using this line where the boundary between primordium cells, and cells exterior to the primordium, lies.

Later in the project the CldnB:LynEGFP transgenic line was published and became available (Haas and Gilmour, 2006). In this line cells of the primordium (among others) are demarcated by membrane-bound LynEGFP thus making identification of the primordium simpler and more reliable. We injected embryos with capped-RNA

encoding H2BRFP, a nuclear localising red fluorescent protein (RFP), (Megason and Fraser, 2003) in order to label the cell nuclei. By combining the membrane GFP with the nuclear RFP we were able to not only examine cell behaviour but also to track individual cells in order to better quantify migration. However, development of the embryo and migration of the primordium was slower than normal as timelapse was conducted at room temperature (~24°C).

Utilising the above methods we have been able to study the earliest stages of primordium migration and revealed new insight into the formation of the migrating primordium. The CldnB:LynEGFP transgenic line expresses LynEGFP in a number of structures including the epidermis and posterior lateral line. The posterior lateral line primordium migrates beneath the epidermis and can be easily distinguished, due to the compact nature of the cells within it, when compared to the larger cells of the epidermis.

The main body of the primordium was visible as a placodal region located posterior to the otic vesicle extending to approximately somite 1 beneath the epidermis (Figure 9a; Figure 10a-b; Supplemental Data S1-S3) (Kimmel et al., 1995; Metcalfe, 1985). The timelapse analysis revealed small clusters of cells at the boundary of somite 1 and somite 2 (Figure 9a; Figure 10b and f), and in one case at the boundary between somite 2 and somite 3 (Figure 10c). These cell clusters are LynEGFP positive and are located beneath the epidermis and exterior to the somites suggesting that they are part of the primordium. Close study of the behaviour of the separated cells revealed that they form membrane protrusions with the more posterior cell cluster appearing to migrate a short distance along the horizontal myoseptum before stalling and displaying a wheeling behaviour (Figure 9; Supplemental Data S1), suggesting that they are motile. Furthermore, upon contact with the main primordium the separated cells become incorporated into the primordium as it continued its posterior-ward migration along the horizontal myoseptum (Figure 9f and j; Figure 10e and h). Thus it appears that the primordium forms from several distinct parts (Figure 9; Figure 10; Supplemental Data S1-S3). Interestingly the incorporation of the separated cells also appears to correlate with an increase in migration speed of the primordium and the commencement of deposition of cells from the trailing edge of the primordium (Figure 9; Figure 10; Supplemental Data S1-S3).

**Figure 9: Timelapse analysis reveals that the primordium forms from several parts**

An overview of a confocal timelapse sequence showing early primordium migration from approximately 18-somite stage. Anterior is to the left and dorsal is up in each image.

(a-k) The primordium forms from cells derived from several different regions. The main body of the primordium (outlined) extends from the region of the lateral line ganglion posteriorly. (a-e; g-l) Posterior to the main primordium two additional clusters of LynEGFP positive cells can be identified at the boundaries between somite 1 and somite 2, and somite 2 and somite 3 (white arrowheads). (e-i) As the primordium migrates posteriorly these clusters of cells become incorporated into the primordium. (e-k) The primordium continues its posterior-ward migration away from the lateral line ganglion and begins to deposit cells in its wake.

The total elapsed time, in minutes, is indicated. The primordium is outlined in all cases. Abbreviations: **mp**, migrating primordium; **ov**, otic vesicle; **pllg**, posterior lateral line ganglion; **S1**, somite 1; **S2**, somite 2. The scale bar is 50μm. The corresponding video can be found in **Supplemental Data S1**.

**Figure 9**

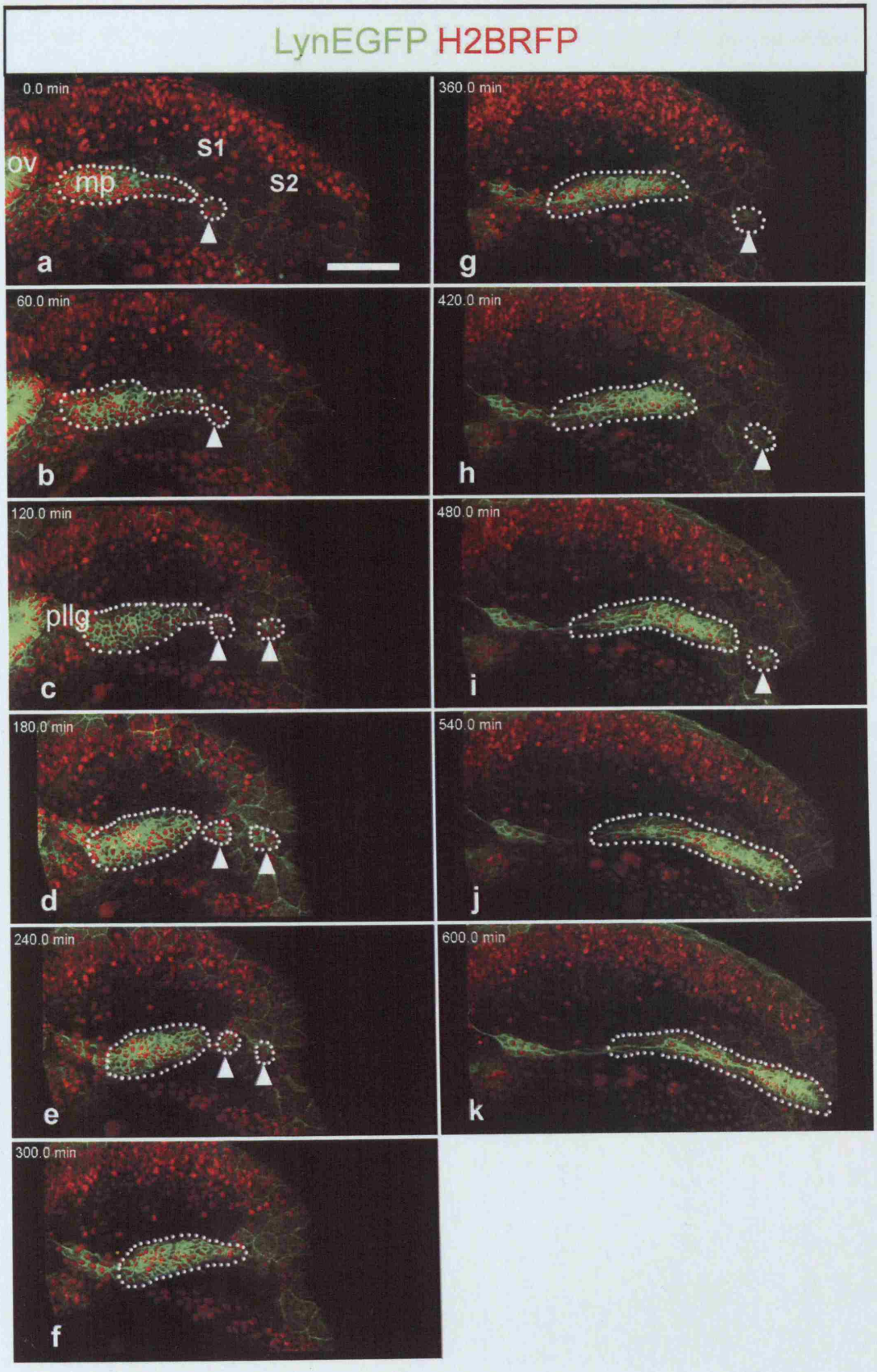
LynEGFP H2BRFP
0.0 min
ov
mp
S1
S2
a
60.0 min
b
120.0 min
pllg
c
180.0 min
d
240.0 min
e
300.0 min
f
360.0 min
g
420.0 min
h
480.0 min
i
540.0 min
j
600.0 min
k

**Figure 10: Timelapse analysis reveals that the primordium forms from several parts**

Additional examples of confocal timelapse sequences examining early primordium migration. Anterior is to the left and ventral is up in each image.

(a-e) Analysis of a primordium from approximately 18-somite stage in an H2A.F/Z embryo reveals the presence of a small cluster of cells posterior to the main primordium (white arrowhead). These cells are incorporated into the main primordium as it migrates posteriorly.

(f-m) Timelapse analysis of CldnB:LynEGFP from approximately 24-somite stage reveals a cluster of cells posterior to the main primordium that are incorporated into the primordium as it migrates posterior-ward.

The total elapsed time, in minutes, is indicated. The primordium is outlined in all cases. Abbreviations: **mp**, migrating primordium; **ov**, otic vesicle; **pllg**, posterior lateral line ganglion; **S1**, somite 1; **S2**, somite 2. The scale bar is 50μm. The corresponding video can be found in **Supplemental Data S2-S3**.

**Figure 10**

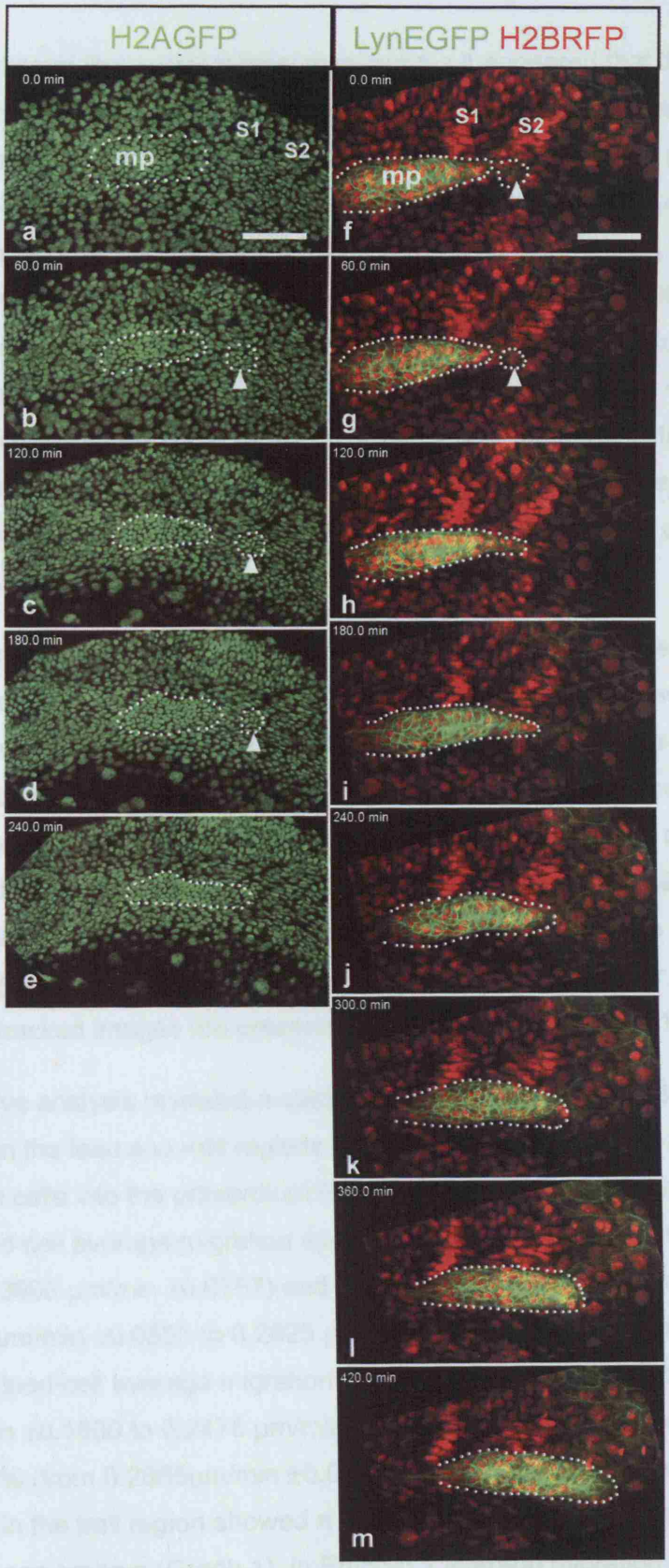
H2AGFP
LynEGFP H2BRFP
0.0 min
S1
S2
mp
a
f
60.0 min
b
g
120.0 min
c
h
180.0 min
d
i
240.0 min
e
j
300.0 min
k
360.0 min
l
420.0 min
m

### 5.3.2 Incorporation of the separated cells into the main body of the primordium correlates with an increase in the speed of primordium migration

From examination of the confocal timelapse images it appeared that the speed of migration of the primordium increased following incorporation of the separated cells into the main primordium. To determine the speed of cells within the primordium individual cells were manually tracked using the Cell Tracker 4 and Cell Tracker 5 plugins for ImageJ (NIH) developed by Dr Daan Zhu (NIMR). Manual tracking was used as automated programs proved unreliable. The speed of the cells at each time point was then calculated using the Cell Mov Visual plugin (Daan Zhu, NIMR). The primordium was divided into three portions; lead, mid and trail. A few cells were randomly selected from each portion and their movements manually tracked. To facilitate tracking the membrane data (green channel) was removed and the images converted from RGB-colour to 8-bit greyscale images to improve the contrast between the nuclei and increase the reliability of tracking.

The timelapse data was examined to determine the point at which the separated cells first fused with the main primordium. The average migration speeds of the chosen cells were calculated for a period of one-hour before and one-hour after fusion had occurred using Microsoft Excel. The average migration speeds were then used to conduct statistical analysis using GraphPad Prism statistical analysis software. To determine whether the change in velocity was statistically significant the p-value was calculated using a paired one-tailed t-test. A p-value $\leq 0.05$ was taken as being statistically significant. This process was repeated for a second embryo. The tracked images are presented in Figure 11 and Figure 12.

Our quantitative analysis revealed a statistically significant increase in the velocity of cells located in the lead and mid regions of the primordium following incorporation of the separated cells into the primordium (Graph 1; Supplemental Data S4-S5). In Embryo 1 lead-cell average migration speed increased by 55% (from 0.2583μm/min ±0.0452 to 0.3993 μm/min ±0.0757) and mid-cell average speed increased by 16% (from 0.2433μm/min ±0.0553 to 0.2825 μm/min ±0.5586). Increases were also seen in Embryo 2; lead-cell average migration speed increased by 9% (from 0.2277μm/min ±0.1680 to 0.2476 μm/min ±0.1613) and mid-cell average speed increased 13% (from 0.2885μm/min ±0.0937 to 0.3263 μm/min ±0.0698). Whilst cells located in the trail region showed a decrease in speed which was only significant in one embryo (Graph 1), in Embryo 1 average migration speed decreased 12% (from 0.2075μm/min ±0.0512 to 0.0.1832 μm/min ±0.0612), while in

Embryo 2 speed decreased 18% (from 0.3342μm/min ±0.0143 to 0.2744 μm/min ±0.0259). The decrease in speed is probably due to deposition of the cells in the trailing part of the primordium. As the incorporation of the separated cells correlated with an increase in migration speed we were intrigued as to whether the separated cells could possess a distinct function. We were particularly curious as to whether the separated cells could have a role in guiding primordium migration.

Therefore we attempted to track the separated cells to determine their position within the migrating primordium. The main primordium tended to move over the separated cells making tracking in a 2-dimensional image extremely difficult and inaccurate. On the limited occasions when we felt we had tracked a separated cell with reasonable accuracy the cells appeared to remain stationary while the leading cells of the main primordium migrated over them. Following which the separated cells began to migrate and seemed to become incorporated into the lead or mid region of the primordium behind the cells at the leading edge (Figure 11a; Figure 12a; Supplemental Data S4-S5).

**Figure 11: Cell tracking reveals an increase in velocity following incorporation of the separated cells.**

Results of manual tracking of cells from within the lead, mid and trail regions of the primordium during the initial stages of primordium migration. All images are lateral views.

(a-c) The migration routes of the individual cells tracked are indicated for each of the three regions of the primordium examined by the coloured trace lines. (a) The separated cells (white arrowheads) tracked do not remain at the leading edge of the primordium following their incorporation.

The tracked image is a greyscale version of the embryo in **Figure 9**, and **Supplemental Data S1**. Scale bars are 50μm. See **Graph 1** for details of migration speeds. The tracked timelapse images can be found in **Supplemental Data S4a-c**.

**Figure 11**

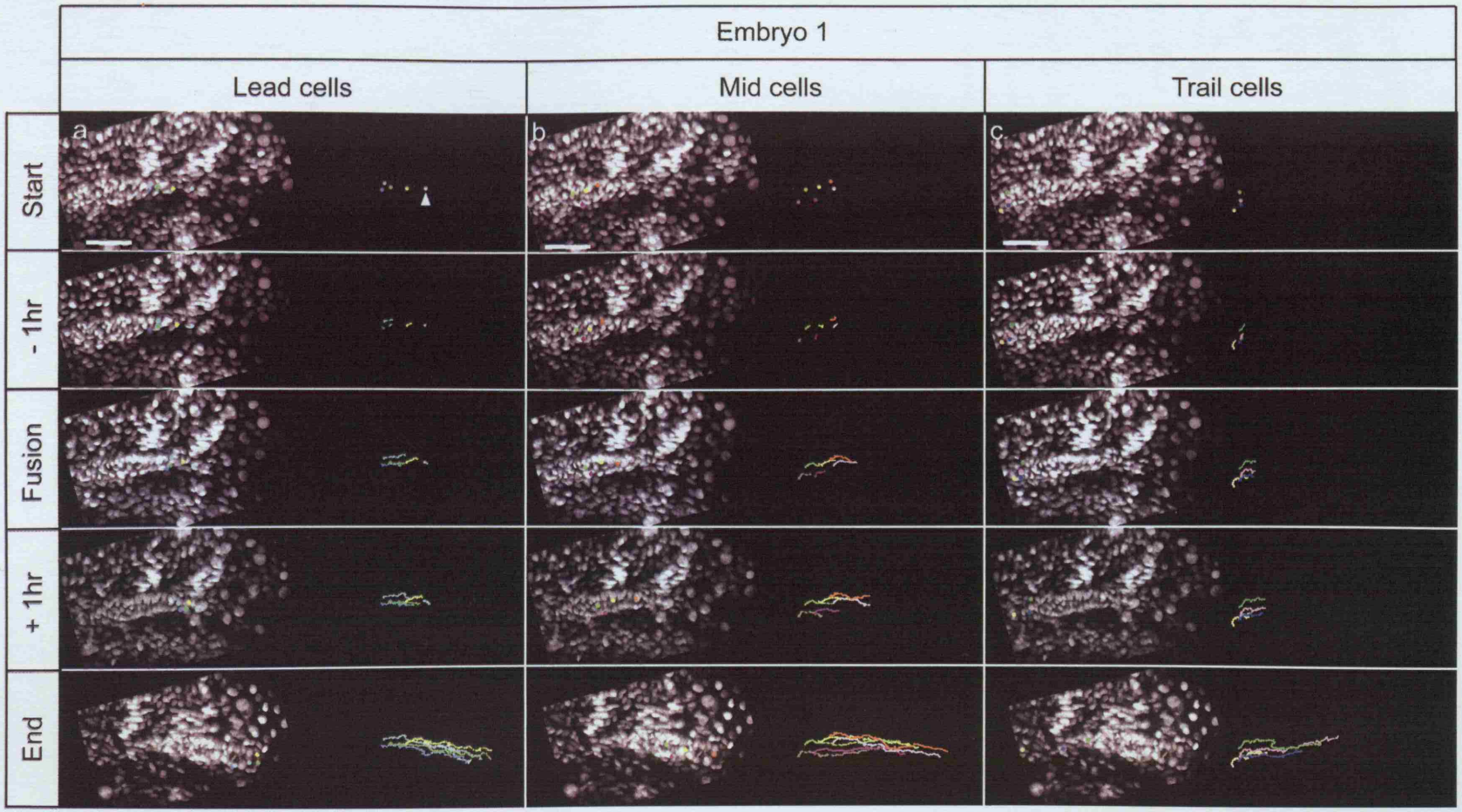
Embryo 1
Lead cells
Mid cells
Trail cells
a
b
c
Start
- 1hr
Fusion
+ 1hr
End

**Figure 12: Cell tracking reveals an increase in velocity following incorporation of the separated cells.**

Results of manual tracking of cells from within the lead, mid and trail regions of the primordium during the initial stages of primordium migration. All images are lateral views.

(a-c) The migration routes of the individual cells tracked are indicated for each of the three regions of the primordium examined by the coloured trace lines. (a) The separated cells (white arrowheads) tracked do not remain at the leading edge of the primordium following their incorporation.

The tracked image is a greyscale version of the embryo in **Figure 10f-m**, and **Supplemental Data S3**. Scale bars are 50μm. See **Graph 1** for details of migration speeds. The tracked timelapse images can be found in **Supplemental Data S5a-c**.

**Figure 12**

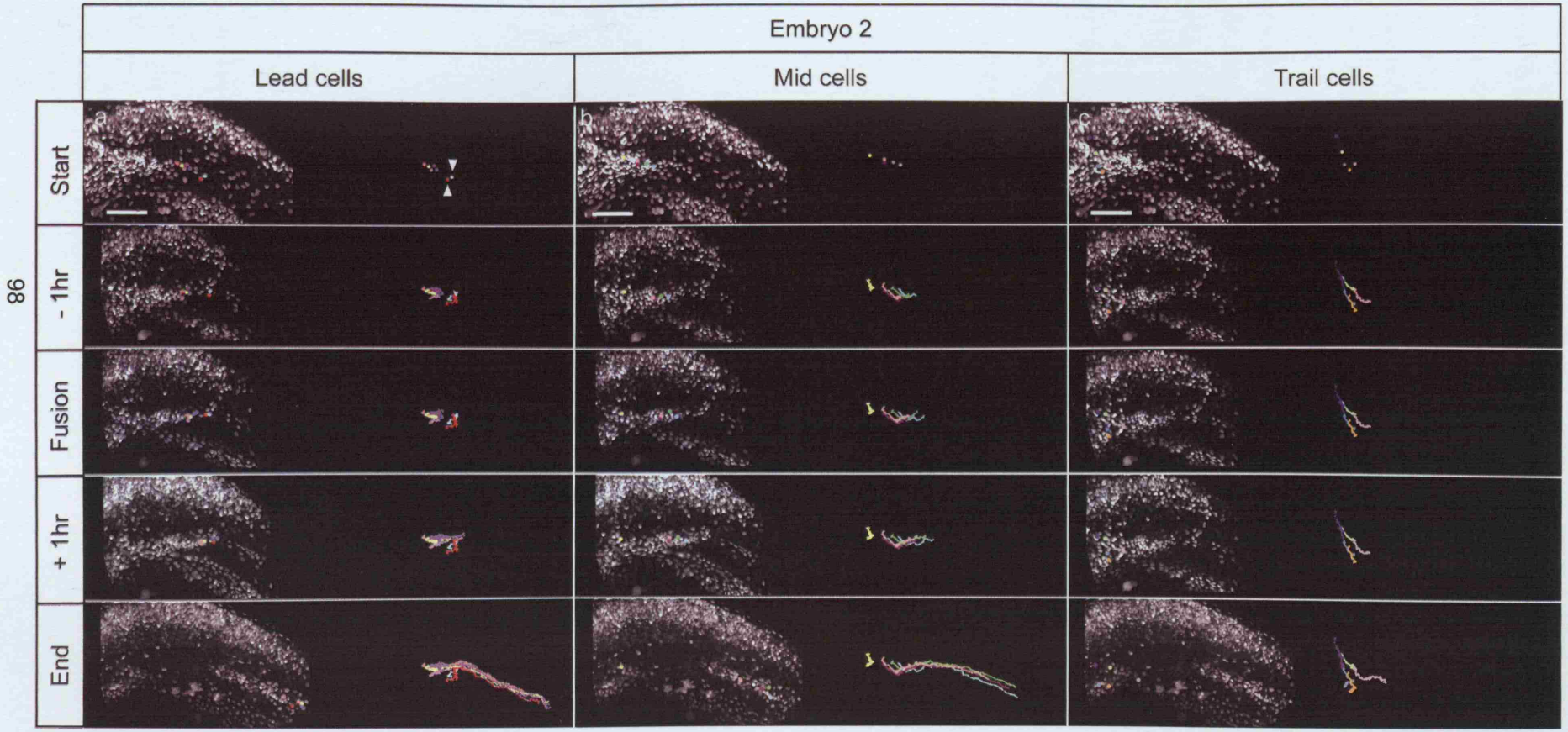
Embryo 2
Lead cells
Mid cells
Trail cells
Start
- 1hr
Fusion
+ 1hr
End
a
b
c

**Graph 1: Statistical analysis of the migration speed of cells in three separate regions of the primordium one-hour before and after fusion of the separated cells.**

The average migration speeds of the cells chosen from each of the three regions of the primordium were calculated for a period of one hour before and one hour after incorporation of the separated cells into the main primordium. The average speed of each cell before and after fusion was compared for a statistically significant difference using a paired one-tailed t-test. T-test p-values: 1=0.0183, 2=0.0287, 3=0.0156, 4=0.0001, 5=0.0400 and 6=0.2585. A p-value <0.05 was taken as statistically significant.

Embryo 1 relates to the Embryo in **Figure 11** and **Supplemental Data S4a-c**, Embryo 2 relates to **Figure 12** and **Supplemental Data S5a-c**.

**Graph 1: Effect of fusion with seperated cells on the speed of migration**

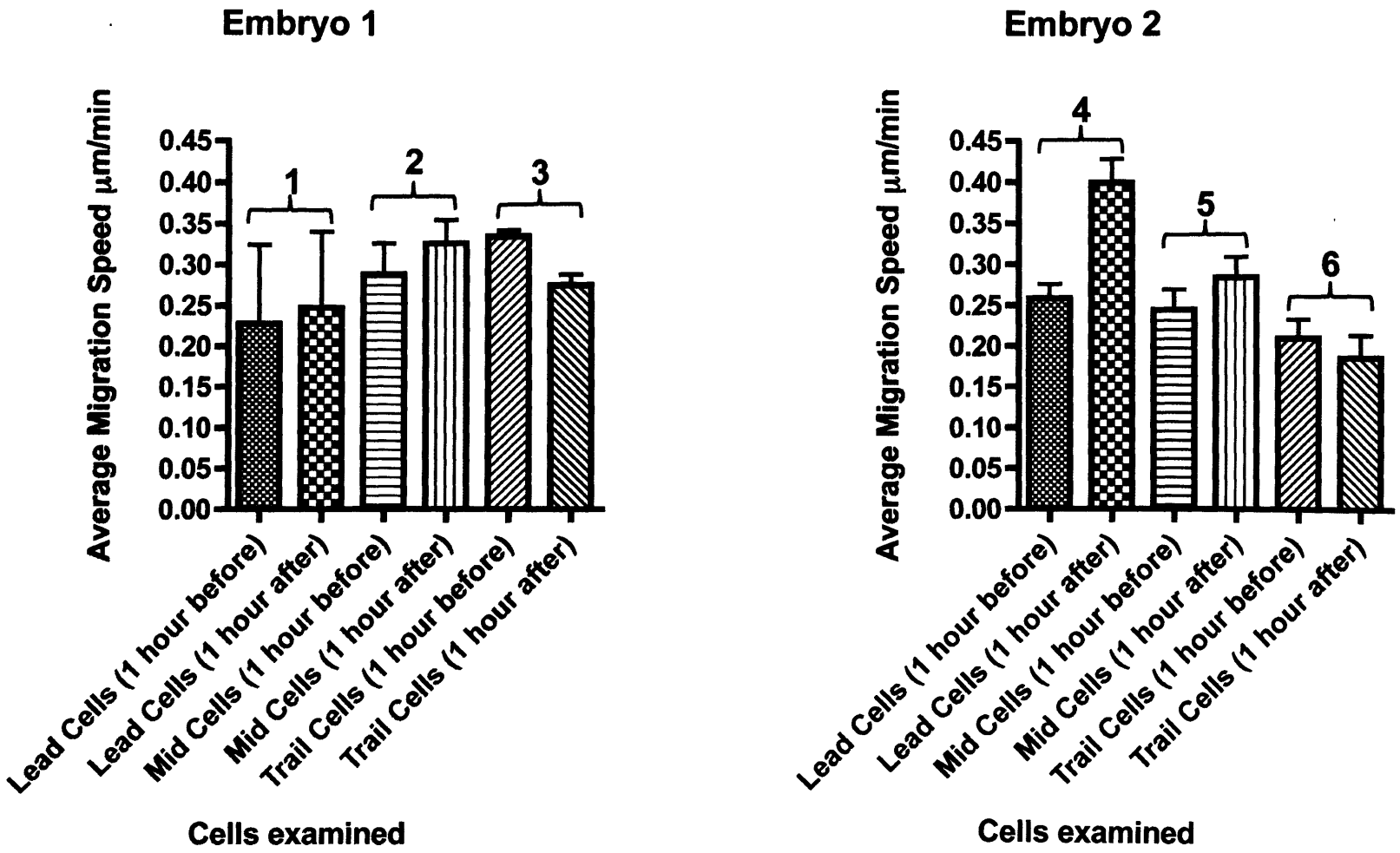

### 5.3.3 Separated cells are part of the posterior lateral line primordium

Confocal timelapse microscopy had revealed the presence of small cell clusters that are separate and distinct from the main body of the primordium. We were curious as to whether these cells were part of the primordium or a distinct cell type. Whole mount *in situ* hybridisation was carried out using the marker for the posterior lateral line primordium *hmx3* on embryos fixed at 2-somite intervals from 18-somite stage to 28-somite stage.

It is clear that the separated cells express *hmx3* like the rest of the primordium and are clearly visible separated from the main body of the primordium from approximately 18-somite stage to 24-somite stage (Figure 13a-d'). Typically these cell clusters were located at the boundaries between somite 2 and somite 3 (Figure 13a-d'). Thus it is confirmed that the separated cells are part of the primordium. However, the timing of incorporation into the main body of the primordium is variable with regard to the population as a whole and the individual primordia of an embryo (Figure 13a-d').

Our analysis also revealed changes in the morphology of the primordium over the period analysed. At early stages (18-somite to 22-somite stage) the primordium has a teardrop shape with the bulbous end located anteriorly (Figure 13a-c'). By 24-somite stage the primordium has adopted a more uniform finger-like structure (Figure 13d-e'). This morphology has altered by 26-somite stage to a teardrop shape once again, however, at this stage the bulbous end is posterior-ward (Figure 13f-f'). This change of morphology correlates not only with the incorporation of the separated cells into the main primordium, but also with the commencement of migration and deposition by the primordium (Figure 13f-f'). These morphological changes are consistent with our timelapse observations (Figure 8; Figure 9).

**Figure 13: Incorporation of the separated cell clusters coincides with morphological changes in the primordium.**

Whole mount *hmx3 in situ* hybridisation reveals the presence of small clusters of cells located posteriorly to the main body of the posterior lateral line primordium. All images are dorsal views with anterior to the left.

(a-d') Small clusters of *hmx3* expressing cells (black arrowheads) are located posterior to the main body of the posterior lateral line primordium. The timing of incorporation of the cell clusters into the primordium is variable with regard to individual primordia. (a-c') Fusion of the primordium appears to correlate with a morphological alteration in the primordium. At early stages the primordium is teardrop shaped with the bulbous end located anteriorly. (d-e') Following fusion of the main body of the primordium with the separated cells the primordium adopts a more uniform finger-like structure. (f-f') As the primordium commences its migration along the horizontal myoseptum the morphology returns to a teardrop shape, however, the bulbous end is located posteriorly and cells have begun to be deposited from the anterior region of the primordium (red arrowheads).

Scale bars are 100μm in a-f and 50μm in a'-f'. The primordium and cell clusters are outlined in images a-f; a'-f' are higher magnification views of the same embryos. Abbreviations: **S1**, somite 1; **S3**, somite 3.

**Figure 13**

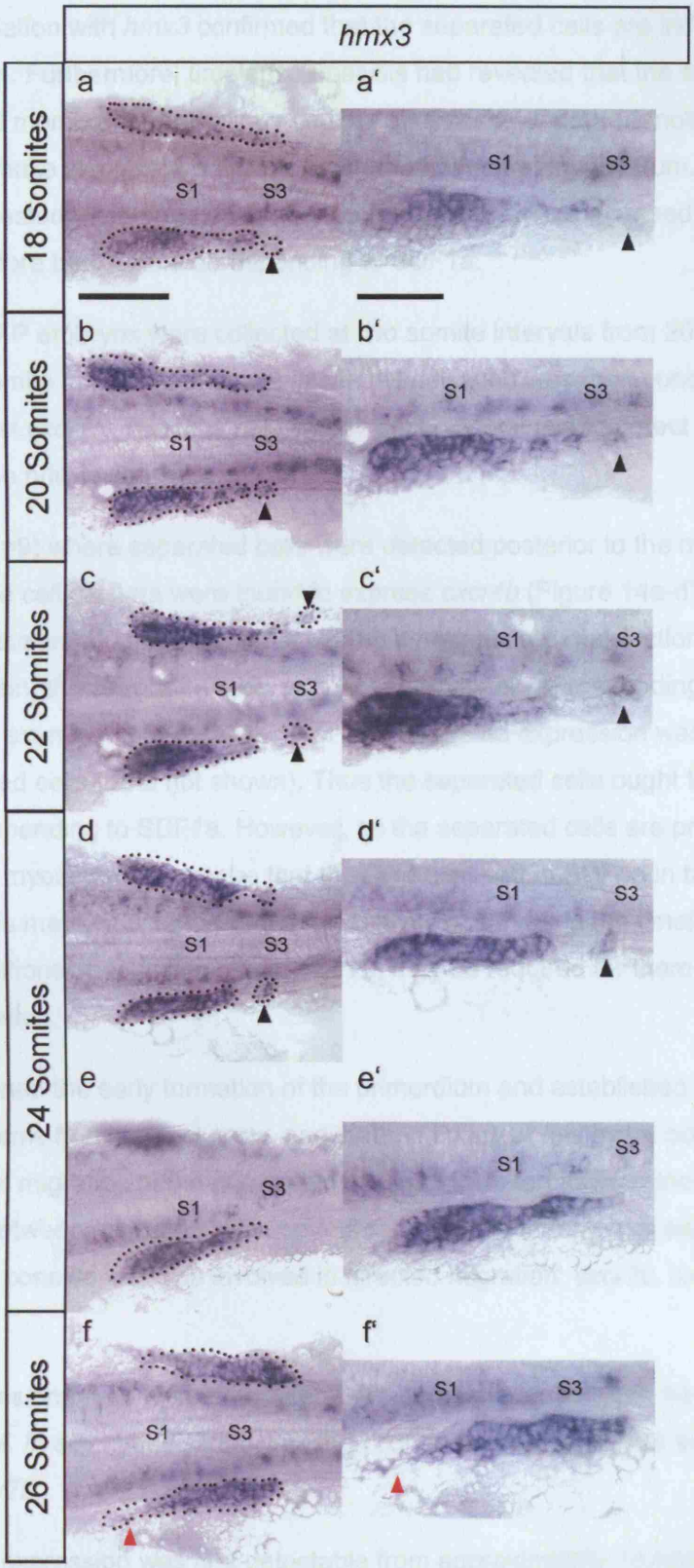
hmx3
18 Somites
20 Somites
22 Somites
24 Somites
26 Somites
a
a'
b
b'
c
c'
d
d'
e
e'
f
f'
S1
S3

### 5.3.4 Molecular characterisation of the primordium during initiation of migration

*In situ* hybridisation with *hmx3* confirmed that the separated cells are indeed part of the primordium. Furthermore; timelapse analysis had revealed that the separated cells displayed membrane protrusions and in some cases appeared motile and yet they failed to make significant progress along the horizontal myoseptum. We were therefore interested to determine whether the separated cells expressed *cxcr4b* and ought to therefore be capable of responding to SDF1a.

CldnB:LynEGFP embryos were collected at two somite intervals from 20-somite stage to 26-somite stage. Fluorescent *in situ* hybridisation was then conducted using a probe against *cxcr4b*. This was followed by antibody staining to detect LynEGFP and identify the primordium.

In all cases (n=9) where separated cells were detected posterior to the main primordium the cell clusters were found to express *cxcr4b* (Figure 14a-d'). Therefore, assuming that expression of *cxcr4b* correlates with production of the CXCR4b protein, the separated cells appear to be capable of responding to SDF1a. We have also examined the expression of *cxcr7b* and no expression was detected in the separated cells (data not shown). Thus the separated cells ought to be capable of responding to SDF1a. However, as the separated cells are present on the horizontal myoseptum it may be that they are exposed to SDF1a in both directions. This may underlie the protrusive activity observed in the timelapse. However, additional mechanisms, e.g. *cxcr7b*, may be required for them to undergo directed migration.

Having examined the early formation of the primordium and established that the primordium forms from several parts, and that the timing of this event correlates with the initiation of migration of the primordium. We next wanted to examine the relationship between migration initiation and the spatial and temporal expression of the genes we considered to be involved in directed migration; *cxcr7b*, *cxcr4b* and *sdf1a*.

To facilitate this embryos were collected at two somite intervals from 18-somite stage to 24hpf. *In situ* hybridisation was then conducted using probes against *sdf1a*, *cxcr4b* or *cxcr7b*.

Weak *cxcr4b* expression was first detectable from approximately 18-somite stage. At this stage expression was punctate and appeared to be distributed throughout the primordium (Figure 15f). However, it is difficult to identify the primordium at this

stage under Nomarski optics, therefore expression may be polarised but we could not confirm this. c*xcr4b* expression intensified in subsequent stages and became more polarised to the leading region of the primordium (Figure 15g-j). By 26-somite stage *cxcr4b* expression was not detected in the hindmost region of the primordium (Figure 15j), these cells are most likely the interneuromast cells which have started to be deposited.

The expression of the presumed ligand for *cxcr4b*, *sdf1a*, was first identified in the horizontal myoseptum of the most anterior somites (approximately somites 1-3) from approximately 20-somite stage (Figure 15l). Somitic expression of *sdf1a* then proceeded to increase in intensity and expand posteriorly along the horizontal myoseptum (Figure 15l-o).

The earliest expression of *cxcr7b* in the posterior lateral line primordium is from approximately 26-somite stage and expression is localised to the trailing region of the primordium (Figure 15a-e). This temporal expression of *cxcr7b* correlates well with the initiation of primordium migration (relative timings of expression are summarised in Figure 15p).

**Figure 14: Separated cells express *cxcr4b***

Several examples of *cxcr4b* expression in the primordium of CldnB:LynEGFP embryos at 24-somite stage. All images are lateral views with anterior to the left and dorsal up.

(a-d') Expression of cxcr4b is detectable throughout the primordium and separated cells (white arrowheads).

The primordium is outlined in all cases. Abbreviations: **mp**, migrating primordium. Scale bars are 50μm.

**Figure 14**

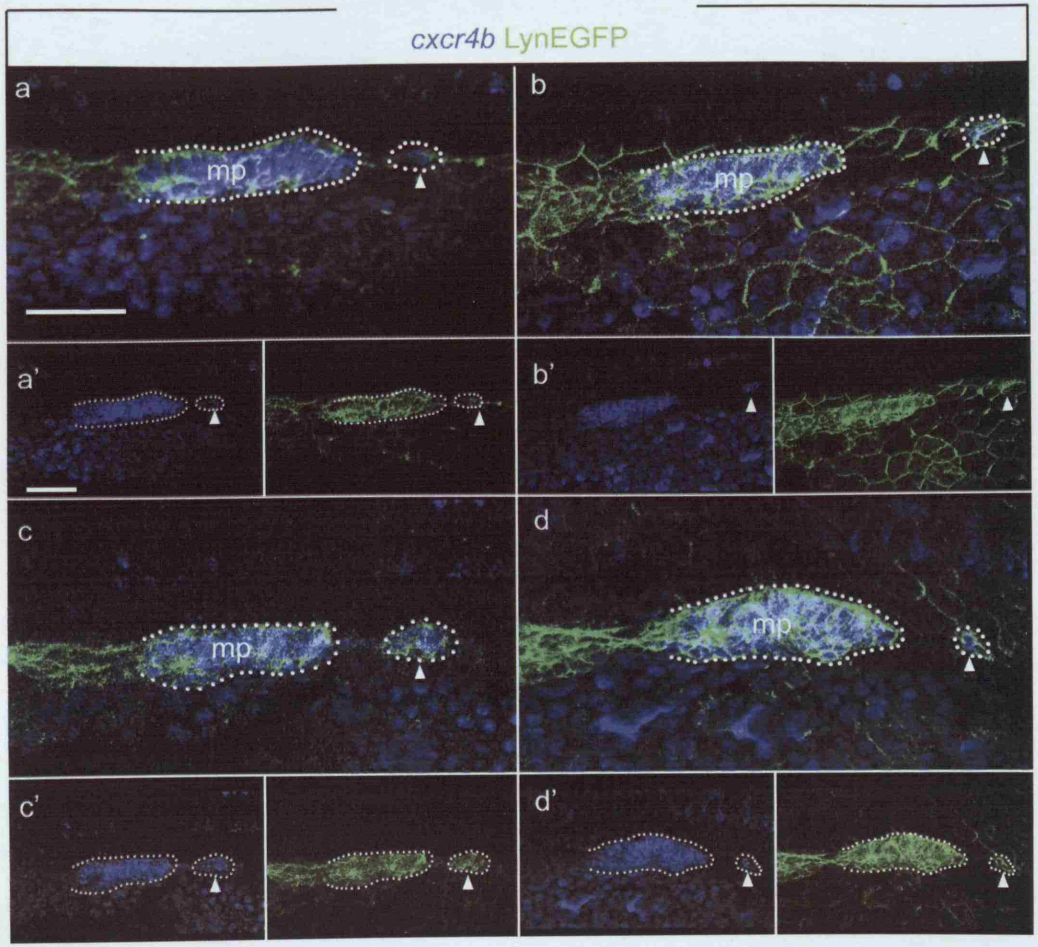

**Figure 15: Expression of *cxcr7b* correlates with the initiation of primordium migration.**

Gene expression profiles in the posterior lateral line primordium. All images are dorsal views with anterior to the left.

(a-d) Expression of *cxcr7b* in the primordium. *cxcr7b* expression is not detectable in the primordium prior to 26-somite. (e) At 26-somite stage *cxcr7b* expression is present in the trailing cells of the primordium.

(f-j) *cxcr4b* expression in the primordium. (f) *cxcr4b* expression can be detected in the posterior lateral line primordium from as early as 18-somite stage. (g-j) At subsequent stages *cxcr4b* expression intensifies and becomes polarised to the leading edge of the primordium such that by 26-somite stage expression is not detected in the trailing cells of the primordium.

(k-o) Expression of *sdf1a* in the somites. Expression *sdf1a*, is first identifiable in the most anterior somites from approximately 20-somite stage (black arrowhead). Subsequently expression of *sdf1a* intensifies and expands posteriorly along the horizontal myoseptum.

(p) Summary of the relative timings of expression of the *hmx3*, *cxcr4b*,*cxcr7b* and *sdf1a* and their relationship to the development of the primordium .

Scale bars are 50μm. The primordium is outlined in all cases. Abbreviations: **s**, somite stage; **hpf**, hours post fertilisation.

**Figure 15**

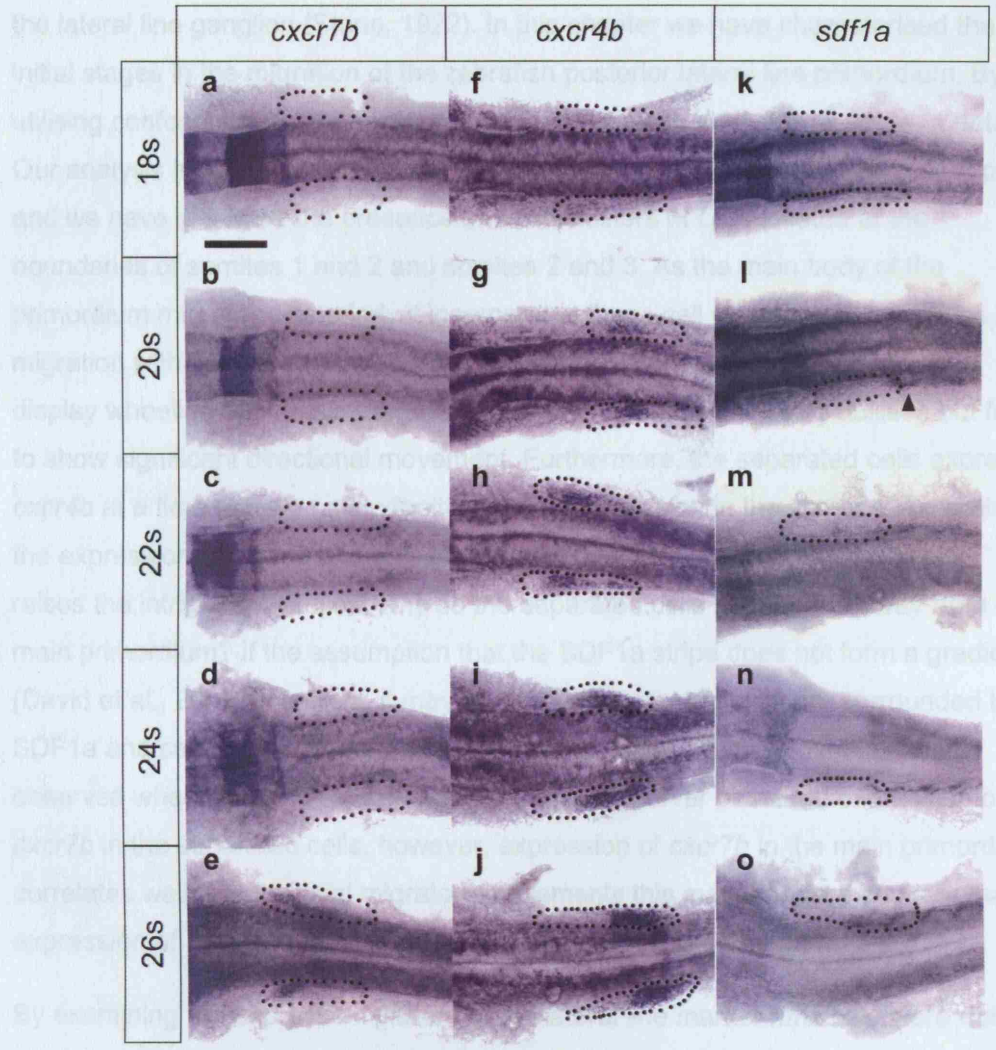
cxcr7b
cxcr4b
sdf1a
18s
20s
22s
24s
26s
a
b
c
d
e
f
g
h
i
j
k
l
m
n
o
p
Specification of primordium
Initiation of migration
Migration and deposition
End of migration
hmx3
cxcr4b
sdf1a
cxcr7b
Stage:
4s
18s
20s
26s
40hpf

## 5.4 Discussion

The posterior lateral line placode forms posterior to the otic placode and extends to approximately somite one as previously observed (Kimmel et al., 1995). The placode later differentiates to form the main body of the migratory primordium and the lateral line ganglion (Stone, 1922). In this chapter we have characterised the initial stages in the migration of the zebrafish posterior lateral line primordium. By utilising confocal timelapse microscopy we were able to study the process in detail. Our analysis has demonstrated that the primordium forms from several distinct parts and we have identified the presence of small clusters of cells located at the boundaries of somites 1 and 2 and somites 2 and 3. As the main body of the primordium migrates posteriorly it incorporates these cell clusters and continues its migration with increased velocity. The cell clusters appear to be protrusive and display wheeling behaviour suggesting that they possess migratory abilities but fail to show significant directional movement. Furthermore, the separated cells express *cxcr4b* at a time that we have identified *sdf1a* expression in the somites. Assuming the expression of *cxcr4b* and *sdf1a* correlates with production of the proteins it raises the intriguing question: why do the separated cells not migrate away from the main primordium? If the assumption that the SDF1a stripe does not form a gradient (David et al., 2002) is correct, it may be that the separated cells are surrounded by SDF1a and cannot determine which direction to migrate. This could explain the observed wheeling behaviour. In addition, we have never observed expression of *cxcr7b* in the separated cells, however, expression of *cxcr7b* in the main primordium correlates well with its initial migratory movements this may therefore suggest that expression of *cxcr7b* is necessary for directed migration of the primordium.

By examining the expression pattern of the lateral line marker *hmx3* we were able to confirm that the separated cell clusters were *hmx3* positive and are part of the primordium. By using manual cell tracking techniques and statistically analysing the migration velocity of cells from several regions of the primordium we have been able to show that there is a significant increase in the migration speed of the leading two thirds of the primordium. This coincides with the incorporation of the cell clusters into the main primordium. Furthermore, incorporation of the separated cells into the main primordium correlates with changes in the morphology of the primordium and the deposition of cells from the trailing edge of the primordium. As the two events occur within a short period of one another it is possible that the deposition of cells from the trailing edge of the primordium may affect migration velocity. Alternatively, migration of the main primordium posterior-ward onto the somites may result in organisational

changes within the primordium that allow an increase in migration speed and the deposition of cells from the training edge. Further work will be required to dissect the relationship between these events and determine their significance to the initiation of primordium migration.

Tip cells are specialist cells that have been identified in the developing *C.elegans* reproductive system (Kimble and White, 1981), the mammalian vascular system (Gerhardt et al., 2003) and the developing *Drosophila* tracheal system (Samakovlis et al., 1996). In each of these systems the tip cells are specialised cells that display distinct behaviour and gene expression profiles. The tip cells appear to exert an organisational effect over cells that migrate in their wake and their presence is required for successful migration to occur (Gerhardt et al., 2003; Kimble and White, 1981; Samakovlis et al., 1996).

In *C. elegans* hermaphrodites the gonad forms from a 4-cell primordium positioned in the ventral midline. These cells replicate to form a bi-lobed structure with a specialised cell called the distal tip cell (DTC) at each tip of the structure (Hubbard and Greenstein, 2000; Su et al., 2000). The DTCs act to guide the migration of the two arms of the gonad on characteristic three stage migration route along the ventral surface, towards dorsal surface and back towards the midline resulting in the formation of U-shaped gonadal arms (Blelloch et al., 1999; Su et al., 2000). Laser ablation of the DTCs results in severely defective migration of the gonadal arms indicating a specialist function which cannot be mimicked by other cells in the gonad (Kimble and White, 1981).

In the posterior lateral line primordium there is evidence for a potential role for tip cells though the function may not be mediated by single cells. Recent work by Haas *et al.* has shown that the transplantation of as few as 3 wildtype cells into the *Ody* (*cxcr4b -/-*) mutant background will rescue the normally severely retarded migration. In this instance the wildtype cells migrate to the very tip of the primordium where they appear to exert an organizing effect over the rest of the primordium that facilitates a rescue of migration (Haas and Gilmour, 2006). In the converse experiments *Ody -/-* cells transplanted into a wildtype background are always excluded from the leading edge of the primordium (Haas and Gilmour, 2006).

Our cell tracking experiments do not appear to be in agreement with this possibility for the separated cell clusters as they do not remain at the leading edge of the primordium following their incorporation. However, tracking of these cells proved difficult as they move through different confocal planes and owing to technological

constraints we were only able to track them in 2-dimensional projections therefore not all separated cells were tracked. Thus, it is possible that some of the separated cells may adopt positions at the leading edge of the primordium. Better tracking may be possible by mosaic expression of fluorescent constructs so that cells can be tracked with greater accuracy. It would also be interesting to examine the effect of ablation of the separated cells on the behaviour of the primordium. This would be technologically challenging as it requires the elimination of these cells without causing damage to the underlying horizontal myoseptum. This would be difficult using laser ablation, however, if specific gene expression can be identified in the separated cells, and promoter regions identified, it may be possible to conditionally target cell death to the separated cells (Pisharath et al., 2007). Time constraints have prevented further investigation of the separated cell clusters at this time.

# Chapter 6: The role of *cxcr7b* in initiation of migration

## 6.1 Introduction

The posterior lateral line primordium of zebrafish begins to migrate along the horizontal myoseptum at approximately 26-somite stage (Kimmel et al., 1995). We observed that by this stage both *cxcr4b* and *sdf1a* have been expressed for approximately 2 hours but migration does not occur. However, migration does correlate well with initiation of expression of *cxcr7b* in the trailing region of the primordium. This led us to postulate that *cxcr7b* could have a role in the commencement of primordium migration.

There are no known mutants for *cxcr7b* in zebrafish. Therefore, to investigate the possibility of a role in primordium formation we opted to use antisense morpholino oligonucleotide technology to knock-down synthesis of the CXCR7b protein.

Antisense morpholino phosphorodiamidate oligonucleotides (morpholinos) are short complementary oligonucleotides in which the ribose sugar of the backbone has been substituted with a morpholine ring. Antisense morpholinos have been demonstrated to effectively knock down gene translation *in vitro* (Summerton, 1999) and in zebrafish (Nasevicius and Ekker, 2000). Morpholinos have become widely used as a method of mediating gene knockdown in a wide variety of developmental systems (Ekker and Larson, 2001). Effective knockdown of the gene of interest is achieved in one of two ways. Firstly, complimentary morpholino sequences can be designed to target a region 5' to the translation initiation (AUG) site in the RNA thus hindering protein translation (Summerton, 1999). The second method is to design complementary sequences to the splice-donor or splice-acceptor sites present in RNA thereby inhibiting post-translational RNA modification (Draper et al., 2001).

There are however difficulties associated with the use of morpholinos. It has been estimated that 15-20% of morpholino oligonucleotides used in zebrafish produce non-specific effects (Ekker and Larson, 2001). These effects are target independent and are not associated with the characterised mutants of the same gene (Ekker and Larson, 2001). Recently these off-target effects have been shown to be mediated through p53-induced apoptosis (Robu et al., 2007). Thus the major difficulties associated with the use of morpholinos are demonstrating specificity, i.e. the gene of interest is knocked down, and demonstrating that the phenotypes observed are solely due to a deficiency in the gene of interest. This can be achieved by several methods including: RNA mediated rescue of the morphant phenotype utilising an

RNA encoding the gene of interest with an altered sequence so as to be impervious to the effects of the morpholino (Ekker and Larson, 2001). Use of multiple morpholinos against independent sequences targeted to the gene of interest, either alone or in combination (Ekker and Larson, 2001). Additionally, where antibodies are available Western blot analysis can be used to demonstrate that levels of the target protein have been effectively reduced (Ekker and Larson, 2001). Where splice blocking morpholinos have been used reverse transcriptase polymerase chain reaction (RT-PCR) can be used to demonstrate aberrant splicing of mRNA (Draper et al., 2001).

## 6.2 Aims

In this chapter we will use antisense morpholino oligonucleotide technology to knock-down the expression of *cxcr7b* in order to investigate the possible function of *cxcr7b* during primordium migration.

## 6.3 Results

### 6.3.1 Titration of morpholinos

Prior to the commencement of experimentation it was necessary to titrate the dilution of morpholino administered to embryos so as to deliver the highest dose possible to achieve specific gene knockdown without off-target effects. Off-target defects associated with morpholinos include: abnormal cell death (particularly associated with the eyes, ventricles of the brain and somites), severely reduced body axes and abnormal, or absent, notochord (Nasevicius and Ekker, 2000; Robu et al., 2007). To facilitate this morpholino oligonucleotide stock solutions were tested by injection over a range of dilutions into one-cell stage embryos at a volume of approximately 4nl. The concentration and hence quantity of morpholino injected was then determined by spectrophotometry in accordance with the manufacturers instructions (www.gene-tools.com). Details of the quantities found to be effective are detailed in Table 5. For our experiments in this and subsequent chapters we have utilised four morpholinos. Two of which are directed against non-overlapping regions of *cxcr7b* (*cxcr7b* MO and *cxcr7b-AUG* MO) and were used at two different concentrations. In addition, we have utilised morpholinos against *cxcr4b* (Li et al., 2004), and *sdf1a* (David et al., 2002) (See 2.4).

**Table 5: Quantities of morpholinos delivered by microinjection**

| Morpholino injected | Dilution | Quantity injected |
|---|---|---|
| *cxcr7b* MO | 1:12 | ~7ng |
| | 1:10 | ~8.4ng |
| *cxcr7b-AUG* MO | Neat | ~40ng |
| | 3:4 | ~30ng |
| *cxcr4b* MO | 1:4 | ~12ng |
| *sdf1a* MO | 1:10 | ~10ng |
| control MO | 1:10 | ~10ng |

### 6.3.2 Demonstration of *cxcr7b* morpholino efficacy

In an attempt to ensure that the phenotypes we observed were attributable to knockdown of *cxcr7b* we have utilised two non-overlapping morpholinos designed against the 5' UTR of *cxcr7b*. *cxcr7b-AUG* MO morpholino is designed against the transcription start site of *cxcr7b*. The second morpholino, *cxcr7b* MO, is designed against a region approximately 100bp 5' of the transcriptions start site. Through our initial experiments we found that both morpholinos resulted in very similar defects in posterior lateral line formation, however, they do not appear to affect development of the anterior lateral lines, where *cxcr7b* is not expressed, suggesting the effect is specific. In addition, two recently published papers examining the role of *cxcr7b* in primordium migration have utilised a morpholino similar to *cxcr7b-AUG* MO (sequence shifted 1bp 3') and have reported similar defects (Dambly-Chaudiere et al., 2007; Valentin et al., 2007).

To demonstrate specific knockdown of CXCR7b by morpholinos embryos were injected at one-cell stage with *CXCR7bEYFP* mRNA, which contains both morpholinos sequences, or *GAPGFP* mRNA. These embryos were then mosaically injected into one cell of an eight-cell stage embryo with *cxcr7b* MO, or control morpholino, in combination with lysinated rhodamine dextran (LRD) in order to detect cells containing the morpholino. Live embryos were mounted at approximately dome stage and levels of expression examined by confocal microscopy. The control morpholino had no effect on CXCR7bEYFP expression (Figure 16b), similarly *cxcr7b* morpholino had no effect on GAPGFP expression (Figure 16a). However, all embryos expressing CXCR7bEYFP co-injected with *cxcr7b* morpholino showed a dramatic decrease in CXCR7bEYFP in regions where

cells were positive for LRD and by inference *cxcr7b* MO (n=15) (Figure 16c). The experiment was repeated with *cxcr7b*-AUG morpholino with the same result (data not shown).

Due to the lack of an antibody against CXCR7b in zebrafish we have been unable to demonstrate knockdown of the CXCR7b protein. Antibodies are available against human CXCR7 however they interact with regions not conserved in zebrafish CXCR7b.

We have attempted to rescue the morphant phenotype by coinjection of *cxcr7brfp* mRNA. This construct lacks the morpholino sequence of *cxcr7b* MO (see 2.2.13). However, we found that the protein was rapidly degraded and was not visible by approximately 20hpf thus we were unable to rescue the morphant phenotype by this method (data not shown). We utilised a heat-shock inducible *hsp:cxcr7brfp* DNA construct (see 2.2.13) in an attempt to circumvent these problems. Unfortunately this proved unsuccessful due to gain-of-function effects that will be discussed in Chapter 9.

**Figure 16: *cxcr7b* morpholino inhibits CXCR7bEYFP production**

Effect of morpholino treatment on fluorescently tagged protein production in embryos at approximately dome stage.

(a) Expression of GAPGFP is unaffected in embryos co-injected with *cxcr7b* morpholino and LRD. (b) Expression levels of CXCR7bEYFP are normal in embryos co-injected with control morpholino and LRD. (c) In embryos co-injected with *cxcr7b* morpholino and LRD levels of CXCR7bEYFP expression are greatly reduced in cells that are positive for lysinated rhodamine dextran.

Abbreviations: LRD, lysinated rhodamine dextran.

**Figure 16**

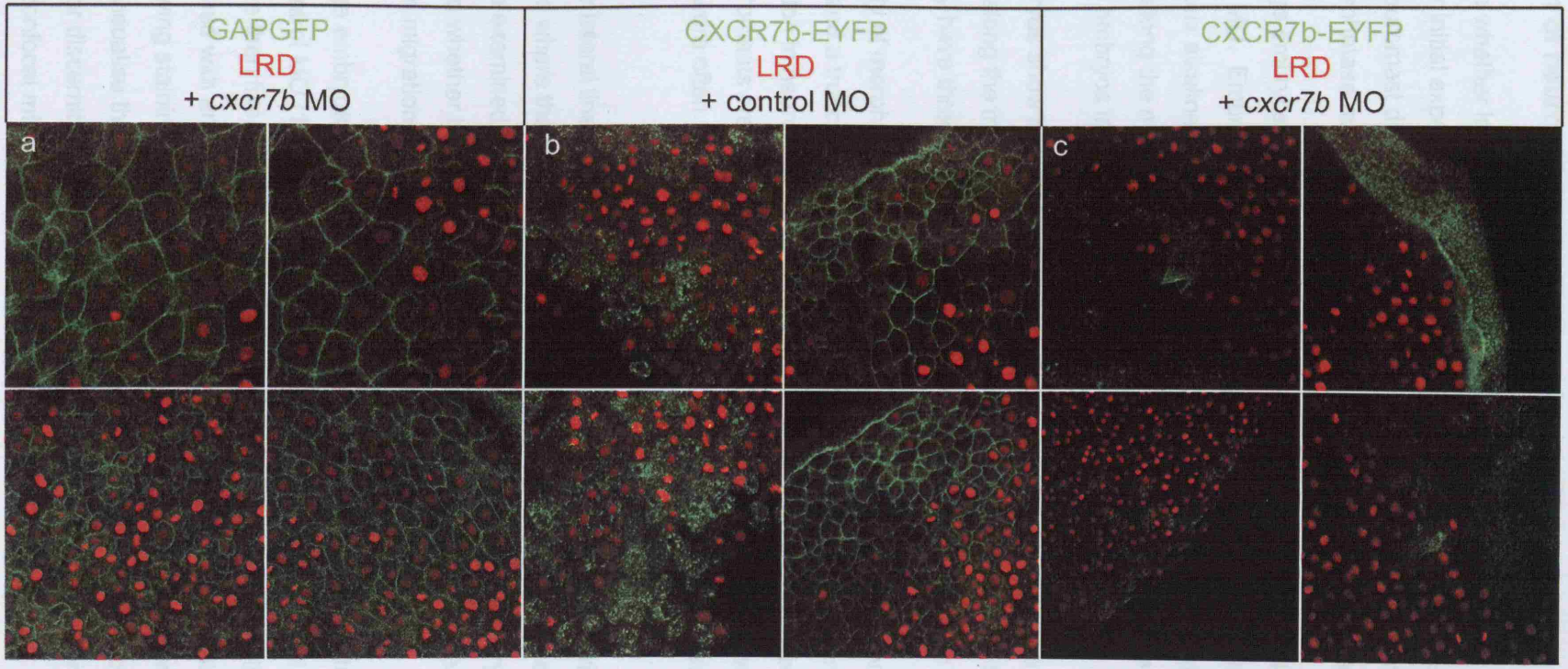
GAPGFP
LRD
+ cxcr7b MO
CXCR7b-EYFP
LRD
+ control MO
CXCR7b-EYFP
LRD
+ cxcr7b MO
a
b
c

### 6.3.3 *cxcr7b* morphant embryos display reduced number and abnormal distribution of neuromasts.

To determine whether knockdown of *cxcr7b* had a deleterious effect on primordium migration our initial experiments assessed the distribution of neuromasts in 4dpf embryos. Neuromast distribution can be visualised using staining for endogenous alkaline phosphatase activity present in the mantle cells of the neuromast.

One-cell stage embryos were injected with either 7ng of *cxcr7b* MO or 40ng of *cxcr7b-AUG* MO. Embryos were allowed to develop to 4dpf and were then stained for endogenous alkaline phosphatase activity. The number and distribution of neuromasts along the midline was assessed by brightfield microscopy and compared to embryos injected with 10ng of control MO.

Control embryos show normal neuromast distribution at 4dpf with five to six primary neuromasts along the midline, and an additional two to three at the tip of the tail. In addition, they have three to four smaller secondary neuromasts anterior to the anus.

In the majority of morphant embryos we found a reduction in the number of neuromasts and a truncated distribution along the midline, this was often associated with a reduction in neuromast number (Figure 17b). In more severe cases there were no neuromasts present along the midline (Figure 17c-d) and ectopic neuromasts were often found on the yolk (Figure 17c). The results are summarised in Graph 2.

The posterior lateral line nerve has been shown to comigrate with the primordium even in cases where the primordium takes an abnormal route (Gilmour et al., 2004). Therefore we examined the lateral line nerves of *cxcr7b* morphant embryos to gain an insight into whether the truncated distribution of neuromasts was due to a failure of primordium migration or neuromast deposition.

One-cell stage embryos were injected with *cxcr7b* MO (7ng), *cxcr7b*-AUG MO (40ng), or control MO (10ng) and were allowed to develop normally until 4dpf. Embryos were then fixed, stained for alkaline phosphatase activity and then antibody stained with an anti-acetylated tubulin antibody to detect the lateral line nerve. Following staining the embryos were counterstained with rhodamine-labelled phalloidin to visualise the somites. Embryos were examined by fluorescence microscopy for discernible phenotypes and images obtained of flat mounted embryos by confocal microscopy.

Examination of the morphant embryos revealed four distinct phenotypes. The majority of embryos showed varying degrees of nerve truncation along the midline (Figure 18b-c). Several more phenotypes were observed including; misrouting of the nerve, typically ventrally (Figure 18d), splitting of the nerve into several parts with one part being misrouted (Figure 18e), and no detectable lateral line nerve in the trunk (Figure 18f). Results are summarised in Graph 2.

As neuromasts were often visible associated with a truncated or aberrantly migrated lateral line nerve (Figure 18b-e) it was reasonable to assume that the neuromast distribution observed in *cxcr7b* morphants was due to abnormal migration of the primordium which resulted in abnormal deposition. Furthermore, *in situ* hybridisation of *cxcr7b* morphant embryos with the neuronal marker *ngn1*, expressed by the lateral line ganglion (Andermann et al., 2002), confirmed that the lateral line ganglion was present and grossly normal in all embryos (data not shown). Closer examination of the most severe embryos, which lacked a lateral line nerve in the trunk, confirmed the presence of the lateral line ganglion, however it was not possible to trace the route of the nerve due to the number of other nerves in that region (data not shown).

**Figure 17: *cxcr7b* morphants show reduced number and altered distribution of neuromasts.**

Neuromast distribution visualised by staining for endogenous alkaline phosphatase. All images are lateral views with anterior to the left and dorsal up.

(a) Control embryos show normal neuromast distribution at 4dpf with five to six primary neuromasts along the midline, and an additional two to three at the tip of the tail, and three to four secondary neuromasts anterior to the anus. (b-d) *cxcr7b* morphants show severely truncated neuromast distribution along the midline. (c-d) In severe cases no neuromasts can be identified along the midline and ectopic neuromasts are often present on the yolk posterior to the pectoral fin.

The scale bar is 200μm. Green arrowheads indicate neuromasts.

**Graph 2: Summary of the distribution of the posterior lateral neuromasts in *cxcr7b* morphants**

Embryos were examined for neuromast distribution at 4dpf. Neuromast distribution was noted independently for each side of the embryo.

**Figure 17**


Graph 2: Summary of the distribution of the posterior lateral neuromasts in cxcr7b morphants

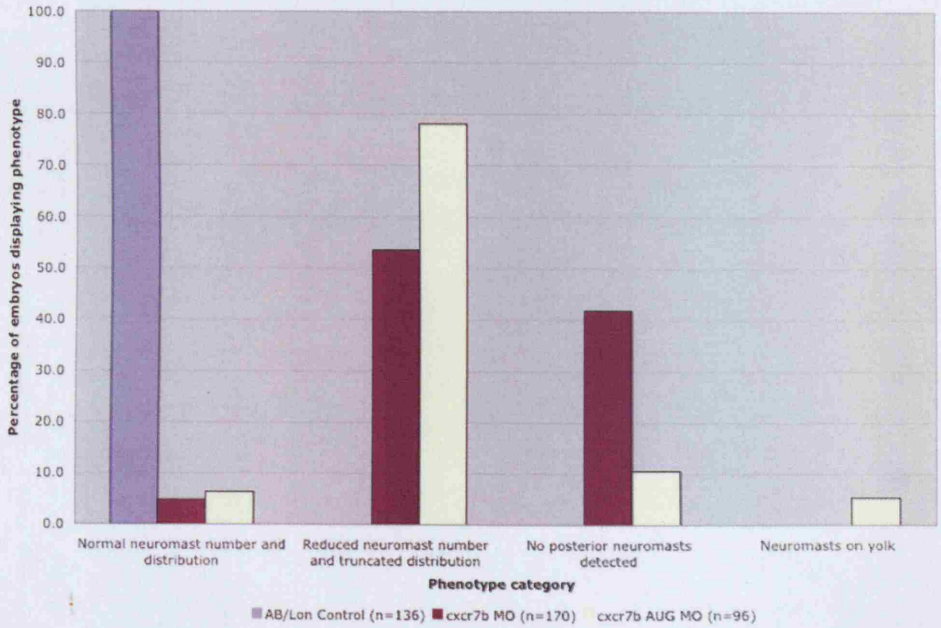

**Figure 18: *cxcr7b* morphant embryos exhibit truncated and aberrantly migrated lateral line nerves**

Primordium migration route visualised by examining the migration route of the posterior lateral line nerve. All images are lateral views with anterior to the left and dorsal up.

(a) Control embryos display normal lateral line nerve routing along the horizontal myoseptum to the tip of the tail at 4dpf. (b-f) *cxcr7b* morphant embryos display several phenotypes including; truncation of the lateral line nerve (b-c), aberrant routing of the nerve (d), splitting of the nerve into multiple parts (e) or absence of the nerve from the somites (f).

The scale bar is 200μm. The lateral line nerve is indicated by plln.

**Graph 3: Summary of the lateral line nerve routing in *cxcr7b* morphants**

Nerve routing was examined at 4dpf by fluorescence microscopy. Both flanks of the embryo were examined and counted separately.

**Figure 18**

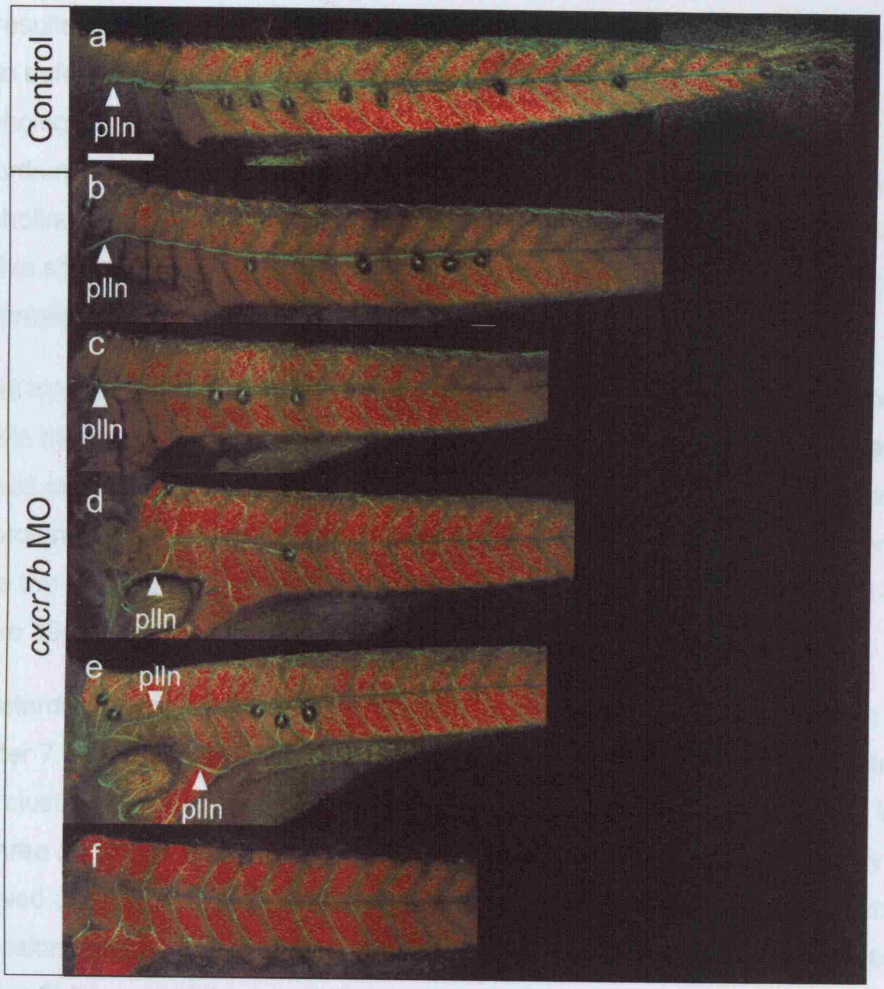


**Graph 3: Summary of the lateral line nerve routing in cxcr7b morphants**

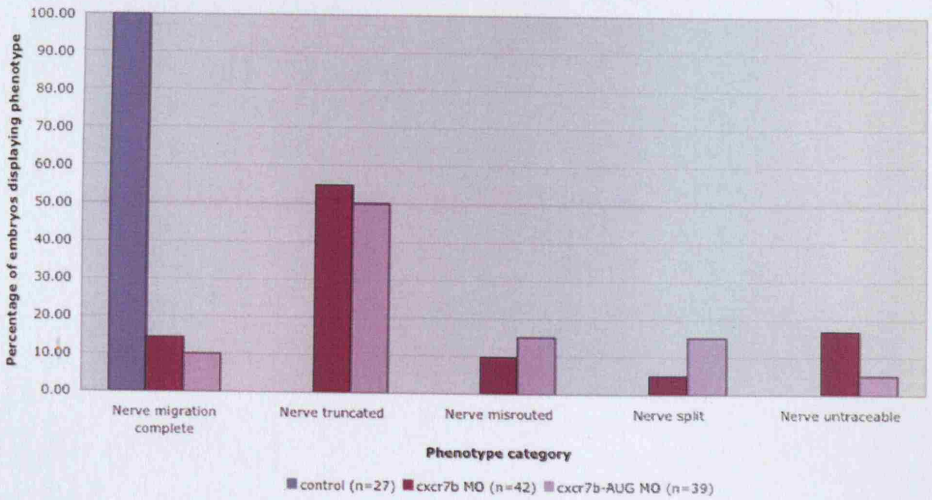

### 6.3.4 Retarded migration and split primordium phenotype in *cxcr7b* morphant embryos

Our results indicated that the truncated distribution of lateral line neuromasts was due to defective primordium migration. To gain a better understanding of the morphological defects underlying the retarded and aberrant migration of the primordium embryos were injected at one cell stage with *cxcr7b*, or *cxcr7b-AUG*, morpholino and allowed to develop to 28hpf. The primordium was then detected by hmx3 in situ hybridisation. In control embryos the primordium had typically migrated to approximately somite 10.

By this method we observed three major primordium phenotypes: retarded migration wherein the primordium had migrated along the horizontal myoseptum but had reached somite 9 or less (data not shown), a split primordium phenotype where the primordium was in several pieces (Figure 19e-f), and a ventral migration phenotype where the primordium had migrated onto the yolk at approximately somites 1-3 (Figure 19c-d). The results are summarised in Graph 4.

The retarded migration and ventral migration phenotypes will be discussed in Chapter 7. The split primordium phenotype was intriguing as it typically resulted in small clusters of cells at the boundaries of somites one and two and somites two and three (Figure 19e-f). These were the same locations that we had typically observed clusters of cells during the early migration of the primordium. As *cxcr7b* expression appeared to correlate with the initiation of primordium migration (see Chapter 5) this raised the possibility that *cxcr7b* had a role in initiation of migration of the primordium.

**Figure 19: *cxcr7b* morphant primordia display a split primordium phenotype**

Primordium morphology visualised by wholemount *in situ* hybridisation to detect *hmx3* expression. Images a and b are lateral views with anterior to the left and dorsal up. All other images are dorsal views with anterior to the left.

(a-b) *hmx3 in situ* hybridisation on control embryos at 28hpf. The primordia of control embryos had typically migrated to approximately somite 10.

(c-f) *hmx3 in situ* hybridisation on *cxcr7b* morphant primordia. (c-d) Primordia were found at ventral positions from approximately somite 1 to somite 3; the region of the forming pectoral fin bud. (e-f) Small clusters of cells were observed posterior to the main primordium typically at the boundaries of somites one and two and somites three and four.

The scale bar is 50μm. Insets in e and f are high magnification views. The primordium is indicated by black arrows, and separated clusters of cells by black arrowheads.

**Graph 4: Summary of the effect of *cxcr7b* morpholino treatment on the posterior lateral line primordium**

Morphant embryos were examined at 28hpf. Primordia were examined individually and assigned to one phenotype category. Abbreviations: **N**, number of experiments; **n**, number of primordia examined.

**Figure 19**

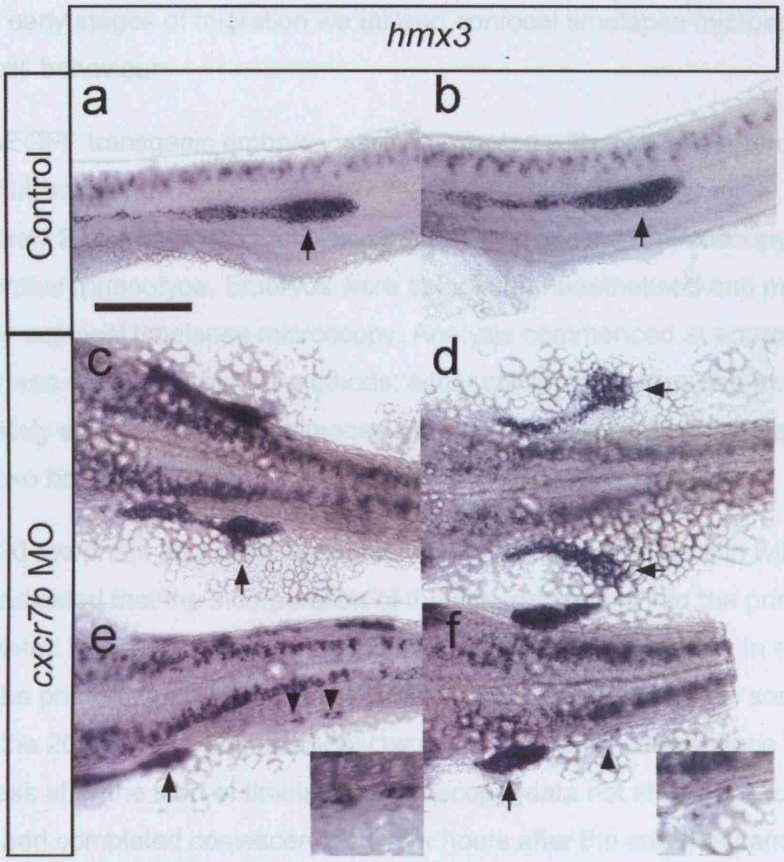


Graph 4: Summary of the effect of *cxcr7b* morpholino treatment on the posterior lateral line primordium

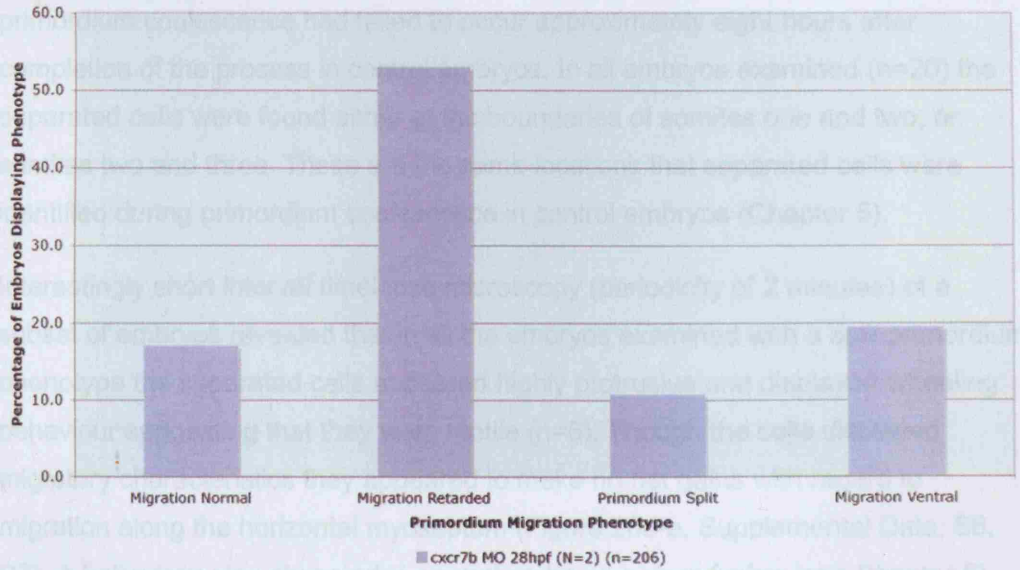

### 6.3.5 Retarded migration in *cxcr7b* morphant embryos

To assess the effect of loss of *cxcr7b* function on the behaviour of the primordium during the early stages of migration we utilised confocal timelapse microscopy to visualise cell behaviour.

CldnB:LynEGFP transgenic embryos were co-injected with *cxcr7b* morpholino and capped-RNA encoding H2BRFP. Embryos were allowed to develop to approximately 22hpf and were then examined by fluorescence microscopy for the split primordium phenotype. Embryos were selected, anaesthetised and mounted for analysis by confocal timelapse microscopy. Analysis commenced at approximately 24hpf and was conducted by two methods: either still images were obtained approximately every two hours, or images were obtained every two minutes for a period of two hours.

A total of 20 morphant primordia were studied. Our previous analysis in wildtype embryos indicated that the incorporation of the separated cells into the primordium had completed by approximately 26-somite stage or shortly thereafter. In control embryos the primordium had coalesced and migrated to approximately somite 6 by 24hpf. Of the 20 embryos examined only two had completed coalescence in two hours or less after the start of timelapse microscopy (data not shown). A further four primordia had completed coalescence by four hours after the commencement of timelapse analysis (Figure 20a-a"). However, the majority of primordia (n=14) had failed to unite within 4 hours (Figure 20b-c"). Therefore in the majority of cases primordium coalescence had failed to occur approximately eight hours after completion of the process in control embryos. In all embryos examined (n=20) the separated cells were found either at the boundaries of somites one and two, or somites two and three. These are the same locations that separated cells were identified during primordium coalescence in control embryos (Chapter 5).

Interestingly short interval timelapse microscopy (periodicity of 2 minutes) of a subset of embryos revealed that in all the embryos examined with a split primordium phenotype the separated cells appeared highly protrusive and displayed wheeling behaviour suggesting that they were motile (n=6). Though the cells displayed migratory characteristics they appeared to make no net gains with regard to migration along the horizontal myoseptum (Figure 20d-e, Supplemental Data; S6, S7). A behaviour also observed in control embryos before fusion (see Chapter 5). Unlike control embryos however the main body of the morphant primordia, which

also appear protrusive and migratory, failed to migrate towards the separated cells resulting in a failure to unify.

**Figure 20: Retarded migration of the primordium in *cxcr7b* morphant embryos results in a failure to coalesce**

Confocal timelapse analysis of *cxcr7b* morphant primordia displaying the split primordium phenotype. All images are lateral views with anterior to the left and dorsal up.

(a-c") Confocal images of *cxcr7b* morphant embryos at 2 hour intervals from 24hpf. The migration of the main body of the primordium is greatly retarded such that it takes a great deal longer to move posteriorly to incorporate the separated cells (white arrowheads) (a-a") or else it fails to incorporate the separated cells over the 4-hour period examined (b-c") (See **Supplemental Data S6-S7**)

(d-e) Timelapse analysis of *cxcr7b* morphant primordia with a periodicity of two minutes. The main body of the primordium and the separated cells (white arrowheads) display ruffling membranes and motile behaviour. However, neither group of cells migrate along the horizontal myoseptum (See **Supplemental Data S8-S9**).

All scale bars are 50μm. Abbreviations: **mp**, migrating primordium; **S1**, somite 1; **S2**, somite 2; **S3**, somite 3.

**Figure 20**

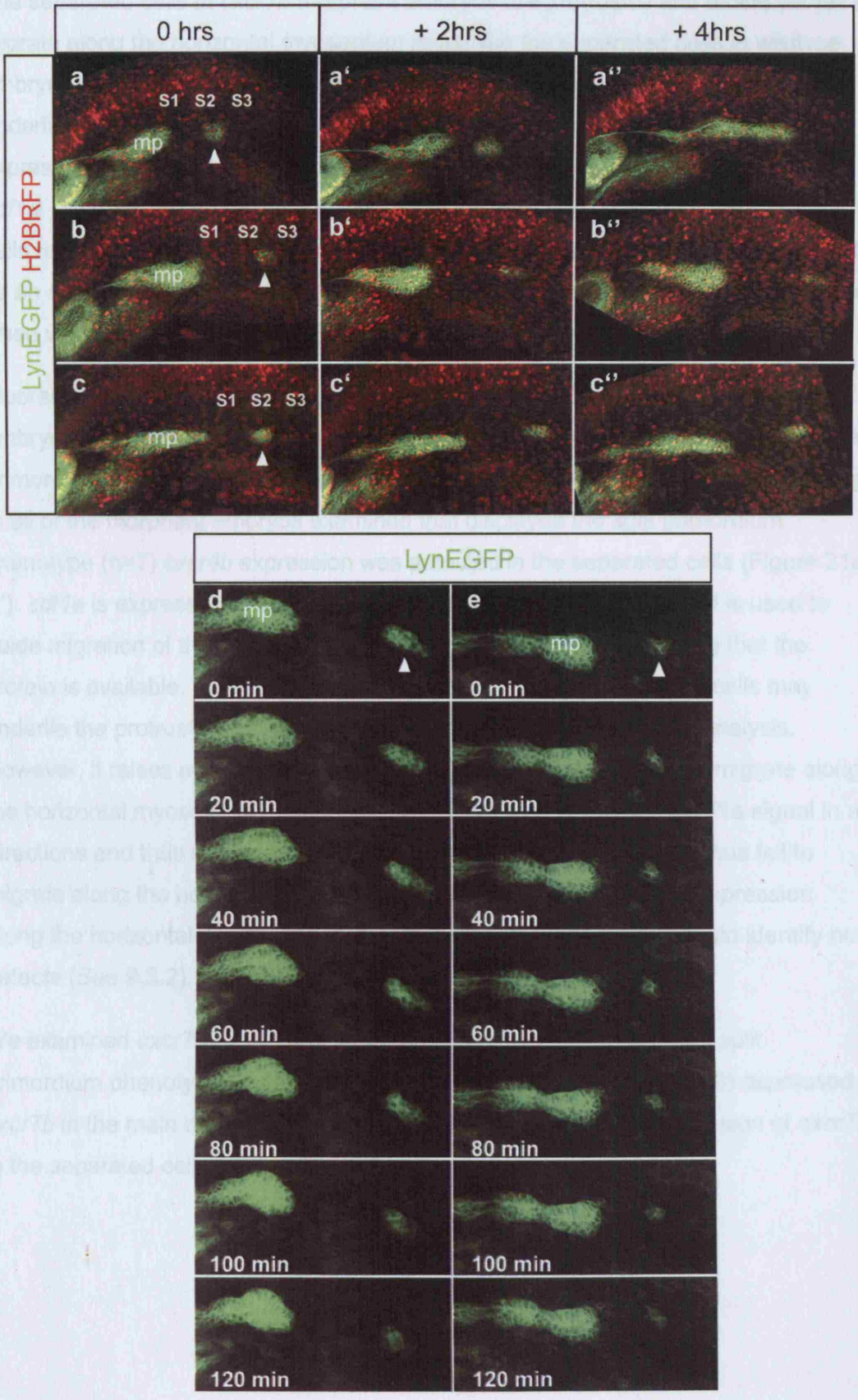
0 hrs
+ 2hrs
+ 4hrs
LynEGFP H2BRFP
a
a'
a''
b
b'
b''
c
c'
c''
S1 S2 S3
mp
LynEGFP
d
e
0 min
20 min
40 min
60 min
80 min
100 min
120 min

### 6.3.6 Separated cells express *cxcr4b*

The separated cells in *cxcr7b* morphant embryos are protrusive and motile yet fail to migrate along the horizontal myoseptum much like the separated cells in wildtype embryos prior to fusion with the main primordium. We were curious as to what underlies the protrusive activity of these cells. One possibility is that these cells express *cxcr4b* and the protrusive activity is in response to signalling mediated by *sdf1a*. In control embryos there is a very small time-window in which the separated cells remain distinct from the main primordium. *cxcr7b* morphant embryos provided us an opportunity to examine expression of *cxcr4b* in the separated cells at a period when we can be confident that SDF1a is present to guide migration.

Fluorescent *in situ* hybridisation was performed on CldnB:LynEGFP transgenic embryos injected with *cxcr7b* morpholino at 28hpf. The LynEGFP expressed by the primordium was detected post *in situ* hybridisation using anti-GFP antibody staining. In all of the morphant embryos examined that displayed the split primordium phenotype (n=7) *cxcr4b* expression was detected in the separated cells (Figure 21a-c"). *sdf1a* is expressed on the horizontal myoseptum at this stage and is used to guide migration of the primordium from approximately 22hpf indicating that the protein is available. Therefore, expression of *cxcr4b* in the separated cells may underlie the protrusive and migratory abilities revealed by timelapse analysis. However, it raises an interesting question as to why these cells fail to migrate along the horizontal myoseptum? One possibility is that they detect the SDF1a signal in all directions and thus cannot determine which direction to migrate and thus fail to migrate along the horizontal myoseptum. We have examined sdf1a expression along the horizontal myoseptum in *cxcr7b* morphant embryos and could identify no defects (See 9.3.2).

We examined *cxcr7b* expression in morphant embryos displaying the split primordium phenotype as outlined above. All primordia examined (n=6) expressed *cxcr7b* in the main body of the primordium with no appreciable expression of *cxcr7b* in the separated cells (Figure 21d-d").

**Figure 21: Separated cells of the primordium express *cxcr4b* but not *cxcr7b*.**

Expression of *cxcr4b* and *cxcr7b* in *cxcr7b* morphant primordia. All images are lateral views with anterior to the left and dorsal up.

(a-c") *cxcr4b* expression in *cxcr7b* morphant primordia. Expression of *cxcr4b* is detectable in the separated cells (white arrowheads) of *cxcr7b* morphant primordia that display the split primordium phenotype. (d-d") *cxcr7b* expression in *cxcr7b* morphant primordia. No appreciable expression of *cxcr7b* could be identified in the separated cells (white arrowheads) and the expression in the trailing region of the main body of the primordium was maintained.

Abbreviations: **mp**, migrating primordium. The primordium is outlined in all cases. The scale bar is 50μm.

**Figure 21**

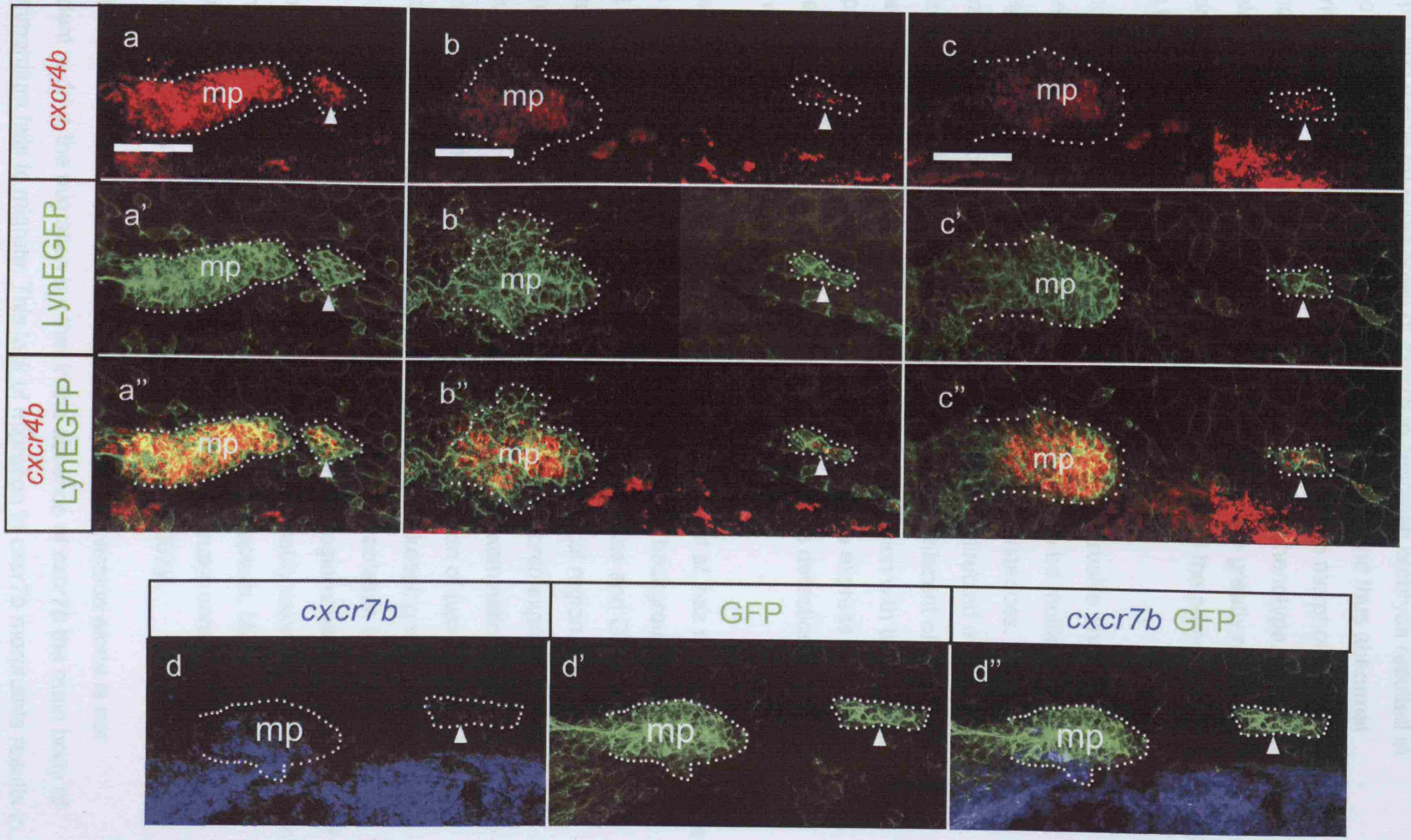
cxcr4b
LynEGFP
cxcr4b LynEGFP
a
b
c
a'
b'
c'
a''
b''
c''
mp
cxcr7b
GFP
cxcr7b GFP
d
d'
d''

## 6.4 Discussion

Morpholino mediated knockdown of *cxcr7b* in zebrafish embryos resulted in abnormal migration of the posterior lateral primordium and thus abnormal distribution of the neuromasts. Closer examination of the morphology of morphant primordia identified the presence of a split primordium phenotype. Confocal timelapse analysis revealed that morphant primordia are greatly retarded with regard to migration. As a consequence the main body of the primordium fails to fuse with the separated cells.

In morphant embryos the separated cells are highly protrusive and send out protrusions in all directions. Furthermore, they appear to be motile displaying a wheeling behaviour and they are able to migrate short distances. However, the migratory abilities of the separated cells fail to produce directed migration along the horizontal myoseptum. The protrusive behaviour is reminiscent of that observed in the separated cells of wildtype embryos prior to their fusion with the main body of the primordium. We have shown that the separated cells express *cxcr4b*. It is therefore likely that the protrusive response is due to the detection of *sdf1a* expressed along the horizontal myoseptum.

These are intriguing results as recent work by Gilmour *et al.* has shown that wildtype cells transplanted into the *Odysseus* (*cxcr4b* -/-) mutant background move to the front of the primordium where they rescue migration (Haas and Gilmour, 2006). These transplantation experiments also identified a critical region of approximately 20μm at the leading edge of the primordium in which *cxcr4b* expressing cells can rescue migration (Haas and Gilmour, 2006). From our examination of the split cells in *cxcr7b* morphant embryos it is apparent that expression of *cxcr4b* alone is not sufficient to drive migration. However, our results are in keeping with observations from the Gilmour lab. The Gilmour lab has utilised laser ablation to ablate strips of cells in various regions of the primordium. When small regions behind the very tip of the primordium are ablated the lead cells, which presumably express *cxcr4b*, remain protrusive yet fail to progress along the horizontal myoseptum. Migration of the tip remains stalled until the trailing cells of the primordium make contact (5$^{th}$ European Zebrafish Genetics and Development Meeting (Haas, 2007)).

Our results have not only demonstrated that *cxcr4b* expression alone is not sufficient to drive the migration but that in the absence of *cxcr7b* the main body of the primordium fails to migrate. This lack of migration in *cxcr7b* morphants results in the failure of the primordium to complete coalescence. Thus the expression of

CXCR7b in the trailing cells of the primordium is required for migration along the horizontal myoseptum to occur.

In support of our results two recent papers on the role of *cxcr7b* in zebrafish posterior lateral line primordium migration using a different morpholino sequence against *cxcr7b* have also identified a split primordium phenotype (Dambly-Chaudiere et al., 2007; Valentin et al., 2007). Interestingly the paper by Dambly-Chaudiere *et al.* displays a small group of separated cells that have migrated to approximately somite 9; in this case the cell cluster contains several *cxcr7b* expressing cells at the trailing edge thus constituting a mini primordium (Dambly-Chaudiere et al., 2007). This result lends further support to our finding that *cxcr7b* is required for the normal migration of the primordium. It also suggests that the cells of the posterior lateral line primordium must be polarised in order to successfully migrate with expression of *cxcr4b* in leading cells and *cxcr7b* in the trailing cells. One possibility is that expression of *cxcr7b* modifies the response of the primordium to the *sdf1a* stripe on the horizontal myoseptum thereby facilitating directional migration. An alternative possibility is that *cxcr7b* expressing cells exert a force to drive the migration of the primordium.

# Chapter 7: The role of *cxcr7b* in guiding primordium migration

## 7.1 Introduction

Our initial analysis of *cxcr7b* morphant primordia had identified ventral migration of the primordium occurring between somite one and somite three approximately at the region of the pectoral fin.

Study of the published literature revealed that both David *et al.* and Li *et al.* had identified ventral migration phenotypes in *sdf1a* morphant embryos (David et al., 2002; Li et al., 2004). Lee *et al.* demonstrated that the majority of *sdf1a* morphant embryos display ventral migration of the primordium between somites one and four (Li et al., 2004). Furthermore, ventral migration phenotypes have been observed in the *smooth-muscle omitted* (*smu*), *chameleon* (*con*), and *fused somites/tbx24* (*fss*) mutants that lack portions of the *sdf1a* pathway due to the absence of the horizontal myoseptum (David et al., 2002; Haas and Gilmour, 2006). In addition, David *et al.* display an image of an *sdf1a* morphant embryo with a neuromast positioned at the approximate region of the pectoral fin bud (David et al., 2002).

Interestingly, two groups have examined the migration of the posterior lateral line primordium in the *cxcr4b* null *Odysseus* (*Ody*) mutant. While migration of the primordium is described as retarded, neither mention a ventral migration phenotype (Haas and Gilmour, 2006; Li et al., 2004), though Li *et al.* have published an image that looks very similar to the ventral migration phenotype we observe (Li et al., 2004) (Figure 6b). Furthermore, analysis of *cxcr4b* morphant embryos by Li *et al.* identifies several cases of ventral migration (Li et al., 2004). Additionally, the Medaka mutant *kazura* (*kaz*), which encodes a *cxcr4* mutation, frequently displays ventral migration (Yasuoka et al., 2004).

In light of this information we were curious as to why the primordium migrates ventrally and what the relationship between *cxcr4b*, *cxcr7b* and *sdf1a* could be.

## 7.2 Aims

In this chapter we aimed to characterise the ventral migration defect and used confocal timelapse microscopy to study the behaviour of the primordium during ventral migration. In addition we examined the potential roles of *cxcr7b* and *cxcr4b* in guiding migration of the primordium

## 7.3 Results

### 7.3.1 Ventrally located primordia

As discussed in Chapter 6 the primordia of *cxcr7b* morphant embryos often took up locations on the yolk; typically between somite one and somite three. This is the region of the forming pectoral fin bud. Published data also indicated that ventral migration of the primordium occurred when *sdf1a* or *cxcr4b* function was absent (David et al., 2002; Li et al., 2004; Yasuoka et al., 2004). We were therefore curious as to what extent the phenotypes were similar.

Embryos were either injected at one-cell stage with the *sdf1a*, or *cxcr7b*, morpholino, or were collected from natural spawning of *cxcr4b* (*Ody*) mutant fish. The embryos were allowed to develop to 28hpf and were analysed by *in situ* hybridisation using *hmx3* as a marker for the posterior lateral line. It has been shown that PGCs are scattered throughout the embryo when *cxcr4b* function is abrogated (Dumstrei et al., 2004). Thus to positively identify *cxcr4b* mutant embryos *nanos-3'UTR*, a marker for the primordial germ cells (PGCs) (Dumstrei et al., 2004), was used in combination with *hmx3*.

*cxcr7b* morphant embryos displayed similar levels of ventral migration to those we had observed previously (Chapter 6) (Figure 22c-d). We observed that in both *cxcr4b* mutant and *sdf1a* morphant embryos the primordia displayed morphology indicating ventral migration (Figure 22e-h). In strong phenotypes the entire primordium was found to be on the yolk while in weaker phenotypes only part of the primordium had projected ventrally. The effect was weakest in *cxcr4b* mutant embryos which showed ventral protuberances coming out from the primordium toward the yolk however the main body of the primordium remained on the horizontal myoseptum (Figure 22e-f). This may explain why the phenotype has not been reported previously. In *sdf1a* morphant embryos the effect was strikingly strong. The primordia typically appeared to have migrated ventrally onto the yolk at approximately the region of the pectoral fin before continuing posteriorly on the yolk toward the region of the gonad (Figure 22g-h).

These observations suggested to us that when the *sdf1a*/*cxcr4b*/*cxcr7b* G-protein coupled receptor pathways are compromised the primordium migrates ventrally away from the horizontal myoseptum. We were therefore intrigued as to whether the ventral migration was a result of active migration of the primordium toward the pectoral fin.

**Figure 22: Ventral migration of the primordium occurs in *cxcr4b* mutants and *sdf1a*, and *cxcr7b*, morphants**

Primordia were visualised by *hmx3 in situ* hybridisation at 28hpf. Images a and b are lateral views with anterior to the left and dorsal up. All other images are dorsal views with anterior to the left.

(a-b) The primordia of control embryos have migrated along the horizontal myoseptum to approximately somite 10 . (c-d) *cxcr7b* morphant primordia have migrated onto the yolk in the region of the forming pectoral fin. (e-f) *cxcr4b* mutant embryos exhibit a ventral migration phenotype in the region of the pectoral fin though the effect is weaker than *cxcr7b* morphants. (g-h) A similar ventral migration phenotype is seen in *sdf1a* morphant embryos. The effect is the most severe when compared with loss of *cxcr4b* or *cxcr7b* as the primordium migrates ventrally and continues posteriorly on the yolk towards the region of the gonad.

The scale bar is 50μm. The primordium is indicated by black arrows.

**Figure 22**

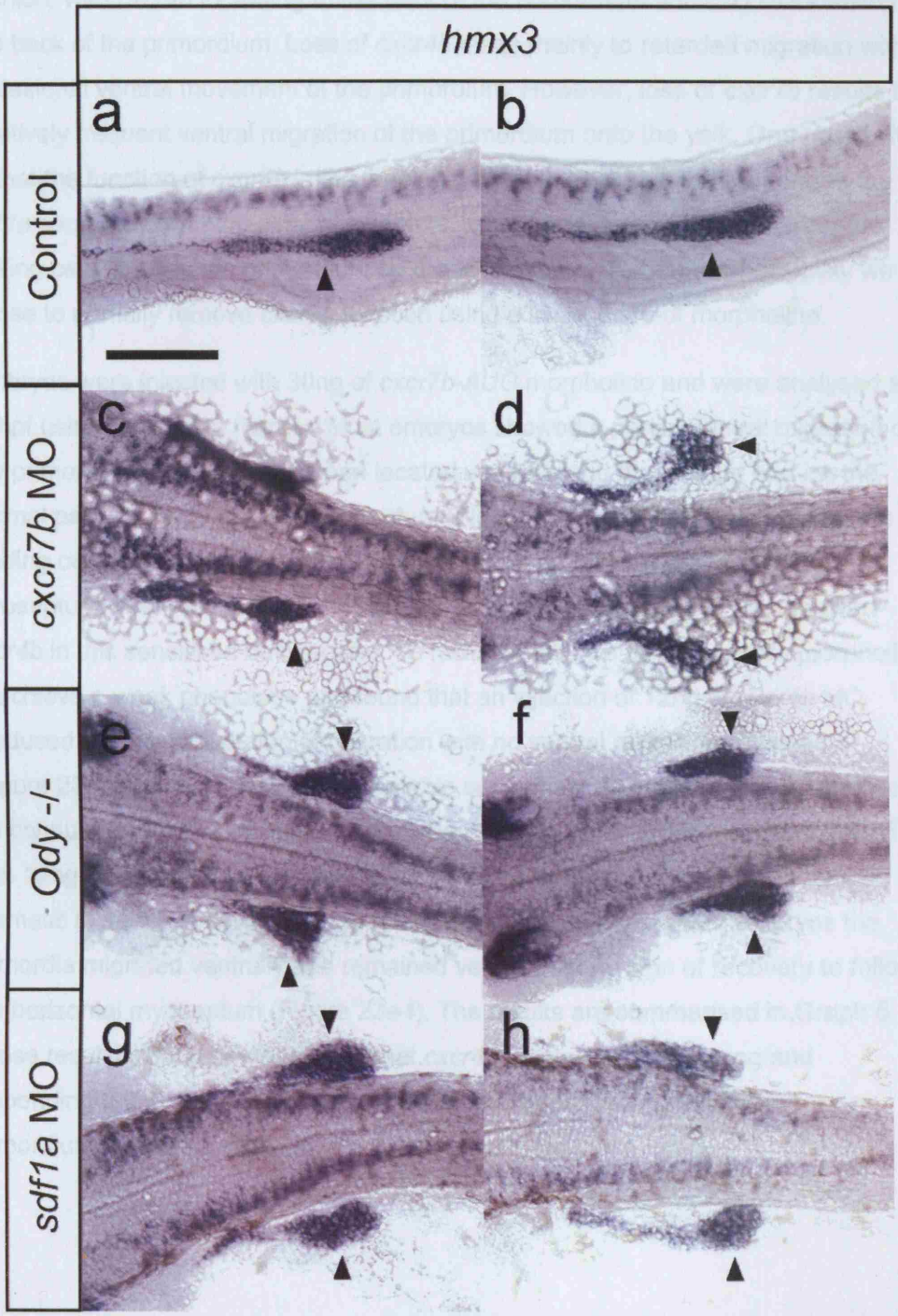

### 7.3.4 Assessment of the relative contribution of *cxcr4b* and *cxcr7b* in guiding primordium migration

The two chemokine receptors *cxcr7b* and *cxcr4b* are expressed in a complimentary fashion, with *cxcr4b* localising to the front of the primordium and *cxcr7b* localising to the back of the primordium. Loss of *cxcr4b* leads mainly to retarded migration with occasional ventral movement of the primordium. However, loss of *cxcr7b* results in relatively frequent ventral migration of the primordium onto the yolk. One possibility is that the function of *cxcr4b* in the leading cells is to seek out and respond to the *sdf1a* source on the horizontal myoseptum. Meanwhile, *cxcr7b* is required in the trailing cells to keep the primordium on the *sdf1a* stripe. To test this possibility we chose to partially remove *cxcr7b* function using a lower dose of morpholino.

Embryos were injected with 30ng of *cxcr7b-AUG* morpholino and were analysed at 28hpf using *hmx3* as a marker. Most embryos showed a partial ventral migration of the primordium with the trailing part located ventrally and the leading part on the normal path on the horizontal myoseptum (Figure 23c-d). This suggested that the leading cells were capable of responding to *sdf1a* present on the horizontal myoseptum. We were therefore curious as to what would happen if we removed *cxcr4b* in this sensitised background. To facilitate this, we titrated *cxcr4b* morpholino to achieve a weak phenotype and found that an injection of 12ng of *cxcr4b* MO produced a weak retardation of migration with no ventral migration phenotype (Figure 23g-h). Having established suitable suboptimal dosages of the morpholinos we conducted double morpholino experiments by coinjecting 30ng of *cxcr7b-AUG* with 12ng of *cxcr4b* morpholino. When both morpholinos were used we observed a dramatic increase in severity of the phenotype. In double morphant embryos the primordia migrated ventrally and remained ventral with no sign of recovery to follow the horizontal myoseptum (Figure 23e-f). The results are summarised in Graph 5. These results clearly demonstrated that *cxcr4b* is required for sensing and responding to the *sdf1a* stripe while *cxcr7b* is responsible for keeping the primordium on the *sdf1a* stripe.

**Figure 23: Knockdown of *cxcr7b* and *cxcr4b* produces a combinatorial effect**

Primordium visualised by *hmx3 in situ* hybridisation at 28hpf. Images a and b are lateral views with anterior to the left and dorsal up. All other images are dorsal views with anterior to the left.

(a-b) The primordia of control embryos have migrated along the horizontal myoseptum to approximately somite 10. (c-d) Embryos administered 30ng of cxcr7b-AUG morpholino display a mild ventral migration phenotype wherein the trailing cells of the primordium are located ventrally while the lead cells remain associated with the horizontal myoseptum. (g-h) *cxcr4b* morphant embryos administered 12ng of morpholino display a retardation of migration with no ventral migration. (e-f) Embryos administered suboptimal doses of both *cxcr4b* and *cxcr7b* morpholinos show an increase in the severity of the ventral migration phenotype with the entire primordium being attracted ventrally toward the pectoral fin.

The scale bar is 200μm. The primordium is indicated by black arrowheads, ventral projections are denoted by black arrows.

**Graph 5: Effect of combined knockdown of *cxcr7b* and *cxcr4b* on primordium migration**

Single and double morphant embryos were examined at 28hpf and the phenotype of each primordia assessed and assigned to one phenotype category (n= number of primordia).

Figure 23

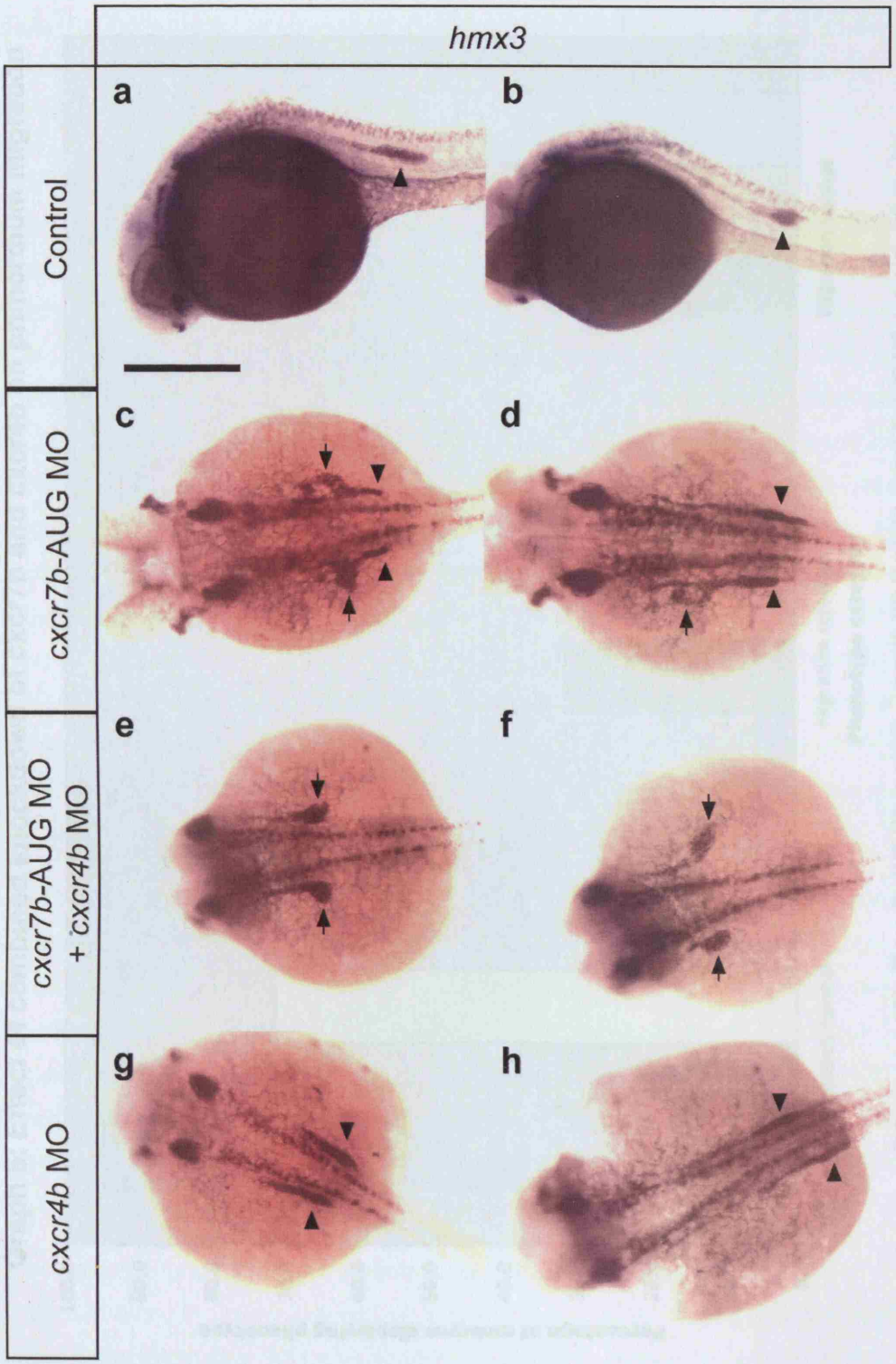
hmx3
Control
cxcr7b-AUG MO
cxcr7b-AUG MO + cxcr4b MO
cxcr4b MO
a
b
c
d
e
f
g
h

**Graph 5: Effect of combined knockdown of cxcr7b and cxcr4b on primordium migration**

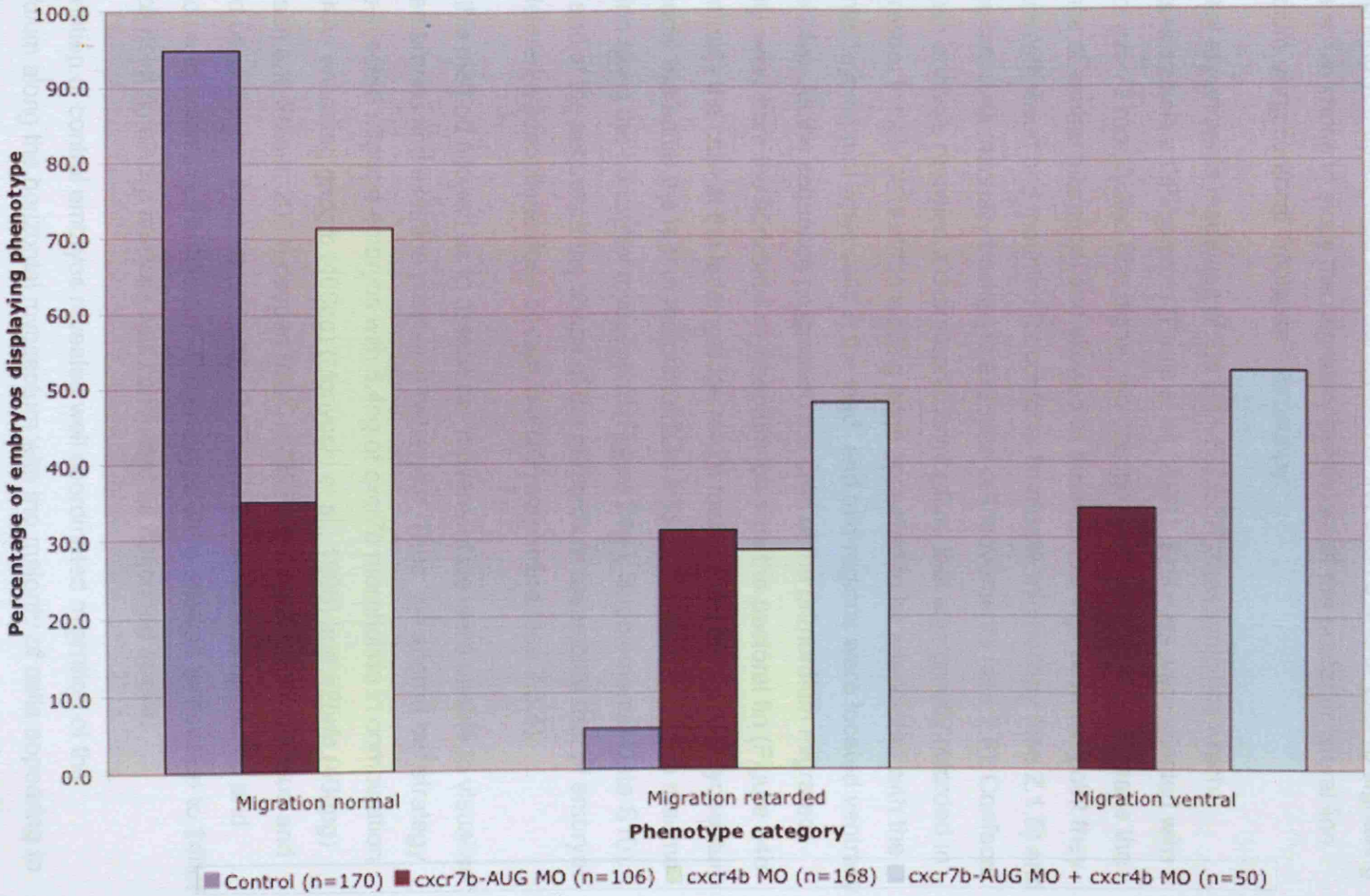

### 7.3.5 Aberrant location of the primordium is due to ventralward migration

As the movement of the primordium to assume a ventral position appeared to be a robust phenotype associated with abrogation of the *cxcr7b* and/or *cxcr4b* signalling pathways, we chose to study the migratory behaviour of the posterior lateral line primordium using confocal timelapse microscopy.

Our initial experiments made use of the H2A.F/Z:GFP transgenic line which expresses a nuclear GFP protein (Pauls et al., 2001). Embryos were injected with 8.4ng of *cxcr7b* morpholino (the higher morpholino dose was used to increase the incidence of ventral migration) and allowed to develop to 24hpf at which point they were anaesthetised and mounted for confocal timelapse microscopy (see 2.1.5) and the resultant data manually tracked to examine cell movements (see 2.6). Confocal timelapse analysis revealed a dysmorphic primordium that was greatly retarded in its migration. Initially cells at the leading edge appeared to be associated with the horizontal myoseptum while cells in the lead- and mid-regions were located ventrally (Figure 24a). As the sequence progressed the cells of the primordium migrated ventrally away from the horizontal myoseptum towards the pectoral fin (Figure 24b-f). Eventually the cells at the leading edge return towards the horizontal myoseptum and shortly thereafter the rest of the primordium follows the leading part to resume migration along the horizontal myoseptum (Figure 24g-j; Supplemental Data S10). At the end of the sequence the shape of the primordium resembled that of embryos administered a suboptimal dose of *cxcr7b-AUG* morpholino (see 7.3.4).

While this method allowed us to assess cell movement we were unable to visualise cell membranes and examine protrusive behaviour. Thus, we altered our strategy and co-injected wildtype embryos with 8.4ng of *cxcr7b* morpholino in combination with RNAs encoding *gapgfp* (400pg) (Moriyoshi et al., 1996) and *h2brfp* (400pg) (Megason and Fraser, 2003) capped RNA. H2BRFP localises to the nucleus and allowed us to trace cell movement while GAPGFP is membrane anchored and allowed us to assess cell behaviour. The embryos were allowed to develop to 24hpf at which point timelapse analysis was conducted as described above.

Examination of control embryos revealed well coordinated migration of the primordium along the horizontal myoseptum with the majority of cells appearing to migrate in approximately the same direction with similar speeds: excluding those cells being deposited at the trailing edge of the primordium (Figure 25a-e; Supplemental Data; S11).

In morphant embryos the cells at the periphery of the primordium appeared to be abnormally protrusive. At the start of the sequences the primordia seemed to be associated with the horizontal myoseptum (Figure 25f, k). As time progressed the cells in the leading and mid regions migrated ventrally towards the pectoral fin and do not return to the horizontal myoseptum during the period analysed (Figure 25g-j, l-o; Supplemental Data S12-S13) resulting in a morphology reminiscent of the more severe ventral migration phenotypes observed by *hmx3 in situ* hybridisation (Figure 24; Figure 25). It is apparent that the ventral movement of the primordium towards the pectoral fin is an active migratory process and may also indicate that *cxcr7b* is required to keep the primordium on the horizontal myoseptum as in its absence the primordium strays off course.

**Figure 24: Inhibition of *cxcr7b* results in aberrant migratory behaviour**

Confocal timelapse analysis of an H2A.F/Z:GFP transgenic embryo injected with *cxcr7b* morpholino. All images are lateral views with anterior to the left and dorsal up. The confocal image and cumulative cell tracing data for each time point are shown. The coloured arrows in the cell trace data indicate the direction of cell movement at that time-point. The timelapse sequence can be found in **Supplemental Data S10**.

(a-f) The cells of the mid region of the primordium migrate toward the pectoral fin and appear to drag the lead cells away from the horizontal myoseptum. (g-j) As the sequence progresses the lead cells of the primordium return to the midline followed shortly by the trailing cells.

The scale bar is 50μm. The primordium is outlined in all cases. Abbreviations: **pfb**, pectoral fin bud.

Figure 24


0 min
20 min
40 min
60 min
80 min
100 min
120 min
140 min
160 min
180 min
pfb
a
b
c
d
e
f
g
h
i
j

**Figure 25: *cxcr7b* morphant primordia actively migrate toward the pectoral fin**

Timelapse analysis of control and *cxcr7b* morphant embryos expressing GAPGFP and H2BRFP. All images are lateral views with anterior to the left and dorsal up. The confocal image and cumulative cell tracing data for each time point are shown. The coloured arrows in the cell trace data indicate the direction of cell movement at that time-point. Timelapse images can be found in **Supplemental Data S11, S12 and S13**.

(a-e) Control primordia show normal migration along the horizontal myoseptum.

(f-o) Cells in the lead and mid regions of *cxcr7b* morphant embryos display active migration away from the horizontal myoseptum and towards the pectoral fin bud this results in the ventral movement of the primordium.

The scale bar is 50μm. The primordium is outlined in all cases. Abbreviations: **pfb**, pectoral fin bud.

**Figure 25**

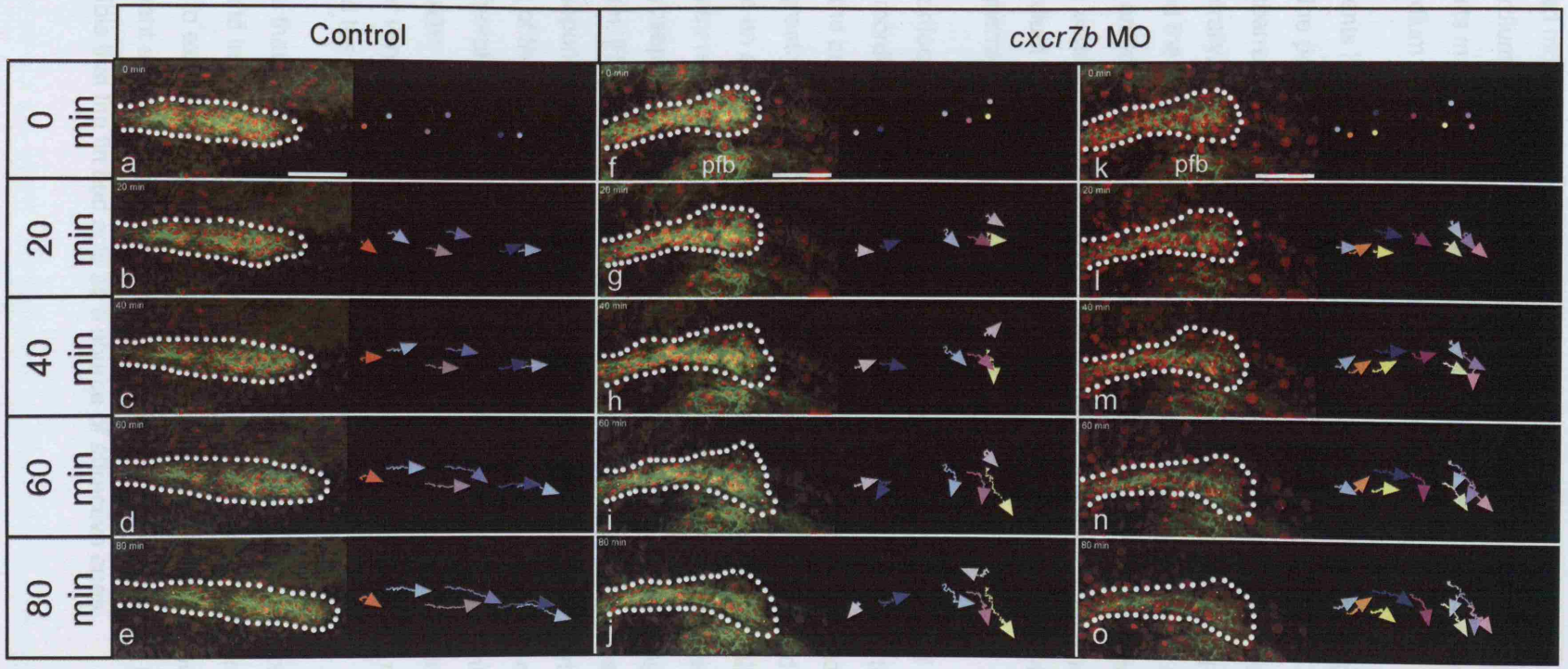
Control
cxcr7b MO
0 min
20 min
40 min
60 min
80 min
a
b
c
d
e
f
g
h
i
j
k
l
m
n
o
pfb
pfb

## 7.4 Discussion

We have used morpholino mediated knockdown of *cxcr7b* in order to examine its role in primordium migration. Thus we have demonstrated that a loss of *cxcr7b* function results in two major phenotypes: retarded migration (and as a result failure of the primordium to coalesce) and ventral migration.

Our experiments have demonstrated a requirement for *cxcr7b* in guiding the migration of the primordium. In its absence migration of the primordium is greatly retarded or aberrant. In cases of aberrant migration the primordium typically migrates ventrally. This may suggest that *cxcr7b* plays a role in keeping the trailing and deposited the cells of the primordium on the horizontal myoseptum and in its absence the primordium is attracted to exogenous cues. Alternatively, *cxcr7b* may play a role in establishing the polarity of the primordium and in its absence the cells of the primordium are thrown into disarray altering their migratory behaviour and resulting in aberrant migration.

By utilising confocal timelapse microscopy to study the cell behaviour of *cxcr7b* morphant primordia we have been able to demonstrate that the cells at the periphery of the primordium are abnormally protrusive; however, primordium migration is greatly retarded. In addition, ventral migration of the primordium appears to be an active process. Our data also indicates that occasionally the primordium may recover and return to the horizontal myoseptum. The return to the horizontal myoseptum appears to be instigated by the cells at the leading edge of the primordium. This suggests that polarity is maintained and that the leading cells are able to respond to SDF1a. Our analysis is limited to a relatively short period in the migration of the primordium and we have been unable to image the entire migration of morphant primordia (as the anaesthesia wears off when embryos are imaged for longer periods) therefore we do not know how the primordium behaves before or after ventral migration occurs in all cases. Some variability, or recovery, may be due to the variable effects of morpholino knockdown.

It may also be that *cxcr7b* is required to hold the primordium onto the horizontal myoseptum and in its absence the primordium not only struggles to migrate but may also respond to exogenous cues present in its environment. As the primordia of *cxcr7b* morphant embryos typically migrate ventrally in the region of the pectoral fin bud it is possible that the fin bud acts as a source of attractive cues.

# Chapter 8: Role of fibroblast growth factors in guiding the migration of the posterior lateral line primordium

## 8.1 Introduction

In the previous chapter we demonstrated that when the CXC-type G-protein coupled receptor signalling, mediated by *cxcr7b*, *cxcr4b* or *sdf1a*, is abrogated the posterior lateral line primordium migrates ventrally toward the pectoral fin bud. In all of the experimental conditions we have used we have never observed any dorsally located primordia. Based upon our observations we hypothesised that an additional chemoattractant emanated from the forming pectoral fin. However, the primordium only appears to respond to this exogenous chemoattractant when signalling mediated by *cxcr7b*, *cxcr4b* or *sdf1a* is perturbed. Thus we were curious as to the identities of these potential chemoattractants.

A possible chemoattractive cue could be fibroblast growth factors (FGFs). FGF mediated signalling has a well-established role in limb formation and patterning (Li and Muneoka, 1999; Sun et al., 2002; Webb et al., 1997)(See (Martin, 1998; Tickle and Munsterberg, 2001) for review) and pectoral fin formation of zebrafish (Fischer et al., 2003; Norton et al., 2005). In addition, FGFs have been implicated as chemoattractants in a wide variety of developmental processes including: *Drosophila* trachea formation (Ribeiro et al., 2002) and air sac migration (Sato and Kornberg, 2002), mouse germ cell migration (Takeuchi et al., 2005), sex myoblast migration in *C. elegans* (Burdine et al., 1997), *Ciona* heart formation (Davidson et al., 2005), and cancer cell motility (Bange et al., 2002).

The compound SU5402 (3-[(3-(2-carboxyethyl)-4-methylpyrrol-2-yl)methylene]-2-indolinone) is a potent inhibitor of FGF-receptor kinase activity (Mohammadi et al., 1997) and has been shown to be effective in the treatment of zebrafish embryos (Abe et al., 2007; Leger and Brand, 2002; Roehl and Nusslein-Volhard, 2001) where it abolishes downstream expression of the ETS-type transcription factors *polyomavirus enhancer activator 3* (*pea3*) and *ETS related molecule* (*erm*) (Roehl and Nusslein-Volhard, 2001).

## 8.2 Aims

In this chapter we will use *in situ* hybridisation to demonstrate the presence of FGF signalling molecules within the primordium and pectoral fin. Furthermore, we will use

the chemical antagonist SU5402 to study the role of FGF signalling in primordium migration in parallel with *cxcr4b*, *cxcr7b* and *sdf1a* knockdowns.

## 8.3 Results

### 8.3.1 Differential expression of *fgfr1* and *fgf10* in the developing posterior lateral line

Previous work in the lab had examined the expression profiles of several FGFs and FGFRs and had identified expression of *fgf10* and its known receptor *fgfr1* (Eswarakumar et al., 2005) in the primordium. To determine the spatial and temporal expression pattern of both genes a detailed *in situ* hybridisation timecourse was performed on wildtype embryos at various stages.

We identified expression of *fgf10* and *fgfr1* in both the pectoral fin and posterior lateral line primordium (Figure 26). *fgfr1* expression is found throughout the pectoral fin, lateral line primordium, interneuromast cells and neuromast precursors (Figure 26a-d), however, expression in the primordium appears to be polarised such that expression is stronger in the trailing cells of the primordium (Figure 26c-d). Similarly, we were able to identify *fgf10* expression within the pectoral fin, though a smaller domain than *fgfr1* (Figure 26a-b, e-f), and throughout the migratory primordium (Figure 26g-h). However, *fgf10* expression was absent from other structures of the posterior lateral line and does not appear to show the same polarisation as *fgfr1* (Figure 26c-d, g-h).

**Figure 26: Expression of *fgfr1* and its ligand *fgf10* in the posterior lateral line primordium and pectoral fin**

Expression of *fgfr1* and *fgf10* detected by *in situ* hybridisation in 28hpf wildtype embryos. Images a-b and e-f are dorsal views with anterior to the left. All other images are lateral views with anterior to the left and dorsal up.

(a-b) *fgfr1* expression is present throughout the forming pectoral fin bud; identifiable as a domain on the yolk sack extending from approximately somite one to somite three. (c-d) Additional *fgfr1* expression can be found throughout the migrating primordium, interneuromast cells and neuromast precursors; however, expression in the primordium is graded with strongest expression identifiable in the trailing cells.

(e-h) Expression of *fgf10* is present in the pectoral fin, though a smaller domain than *fgfr1*, and throughout the migrating primordium.

Scale bars are 25μm. The primordium is outlined where visible. Abbreviations: **S1**, somite 1; **S3**, somite 3; **mp**, migrating primordium; **pfb**, pectoral fin bud; **nm**, neuromast precursors; **inc**, interneuromast cells.

**Figure 26**

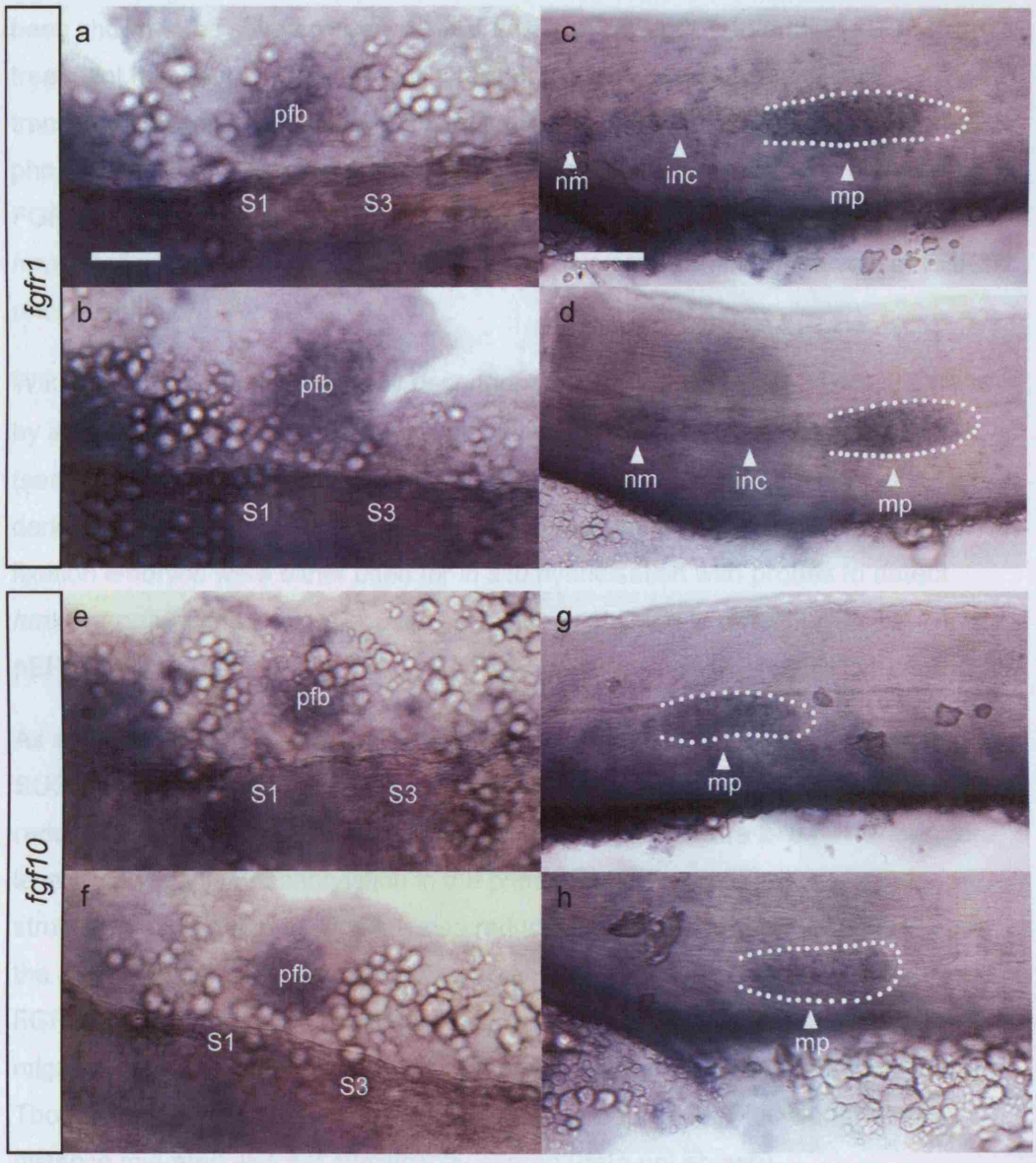

### 8.3.2 Effect of chemical inhibition of FGF signalling on the formation and migration of the primordium.

Having identified expression of both an FGF ligand and receptor in the posterior lateral line primordium, and pectoral fin bud, we were curious as to whether they could play a role in the migration of the primordium.

Expression of *hmx3* in the otic vesicle of the zebrafish *fgf8* mutant *acerebellar* has been shown to be severely reduced (Adamska et al., 2000). In addition SU5402 treatment has been shown to result in dramatically reduced levels of *pea3* transcription (Raible and Brand, 2001; Roehl and Nusslein-Volhard, 2001) and ERK phosphorylation (Mohammadi et al., 1997). Therefore, we confirmed the inhibition of FGF signalling, as a result of SU5402 treatment, by *in situ* hybridisation to detect *hmx3* and *pea3* transcription, and antibody staining to examine the levels of ERK1/2 phosphorylation.

Wildtype embryos were manually dechorionated and treated from 24-somite stage by incubation in a 1%DMSO 0.65x Danieau's solution containing 32μM SU5402 (see 2.1.3) or the same solution without SU5402. Embryos were incubated in the dark at 28.5°C and allowed to develop to approximately 24hpf stage. Following fixation embryos were either used for *in situ* hybridisation with probes to detect *hmx3* or *pea3* transcription, or used for antibody staining to detect levels of pERK1/2.

As expected levels of *pea3* transcription were reduced in embryos treated with SU5402 (Figure 27a-c), in addition, the levels of *hmx3* expression were greatly reduced in the otic vesicle of SU5402 treated embryos (Figure 27d-f). Furthermore, levels of ERK1/2 phosphorylation in the primordium (Figure 27g-i), and other structures (data not shown), were also reduced in SU5402 treated embryos. Thus the SU5402 treatment was deemed to be an effective method to reduce the levels of FGF signalling. In addition, we examined the effect of SU5402 treatment on the migration of the posterior lateral line primordium using *hmx3 in situ* hybridisation. Though the primordium had a more elongated appearance (Figure 28a-b) the distance migrated was not significantly altered (data not shown).

To assess whether FGF mediated signalling could be responsible for the ventral migration phenotypes observed in *cxcr7b* and *sdf1a* morphants embryos were injected at one-cell stage with either *cxcr7b* MO (8.4ng) or *sdf1a* MO (10ng). In addition, *cxcr4b* mutants (*Ody* -/-) embryos were collected by natural spawning of mutant adults. Embryos were allowed to develop to approximately 24-somite stage

at which time they were treated as described above. At 24hpf stage *in situ* hybridisation was conducted with the *hmx3* probe to identify the primordium. The experiment was repeated several times, however, the efficacy of treatment varied considerably most likely due to the instability of the stored SU5402. The stocks that produced the most effective treatment were made on the day of use. Furthermore, it has been speculated that SU5402 may be degraded rapidly by the embryo such that it is only effective for a short period equivalent to the formation of 1 somite in chick embryos, approximately 90 minutes (Baker et al., 2006; Pourquie, 2004); our treatments lasted approximately twice as long. However, it is likely that SU5402 treatment was effective at the concentration and period we have used as demonstrated by Figure 27.

Following *in situ* hybridisation primordia were examined by compound microscopy and classified according to phenotype. The results of a typical experiment in which SU5402 treatment was deemed to be effective are shown in Graph 6. We observed that in the cases of *cxcr7b*, and *sdf1a*, morphants and *Ody* -/- embryos treated with SU5402 there was a reduction in the percentage of embryos displaying the ventral migration phenotype (Graph 6) with the primordium migrating along the horizontal myoseptum to approximately somite 4 or somite 5 (Figure 28e, g, i). A reduction in the incidence of ventral migration was consistently observed though to differing degrees in all experiments (data not shown). Statistical analysis conducted using GraphPad Prism software on two such experiments for *cxcr7b* morphant embryos identified a statistically significant decrease in the ventral migration phenotype, from 29.0%±10.6 to 2.0%±0.3 in embryos treated with SU5402 (Graph 7). Though SU5402 treatment of control embryos resulted in a more elongated appearance we could identify no significant effect on the migration of the primordium along the horizontal myoseptum in comparison to control embryos (data not shown).

In addition to the observed decrease in ventral migration of the primordium following SU5402 treatment we also observed an increase in the incidence of primordia that displayed the split primordium phenotype (Figure 28 f, h, j; Graph 8). Statistical analysis conducted on two such experiments for *cxcr7b* morphant embryos identified a statistically significant increase in the split primordium phenotype, from 10.0%±2.9 to 34.7%±13.7 in embryos treated with SU5402 (Graph 9). The split primordium phenotype suggests that very little or no migration of the primordium has occurred in these embryos. It may be that due to slight variations in the age of embryos within the populations used these embryos were treated with SU5402 prior to the completion of primordium coalescence and that SU5402 treatment has

inhibited the coalescence of the primordium. Unfortunately, time constraints have prevented further analysis of this effect. However, the results may suggest a requirement for FGF signalling in the initial coalescence of the primordium and the initiation of primordium migration.

**Figure 27: Demonstration of the efficacy of SU5402 treatment**

Demonstration of SU5402 treatment efficacy. Images a-c and g-l are lateral views with dorsal up. All other images are dorsal views with anterior to the left.

(a-c) *In situ* hybridisation to detect *pea3* transcription at 26hpf. (a) Control embryos show normal expression of pea3 in the migrating primordium. (b-c) Embryos treated with SU5402 show a marked decrease in the level of *pea3* transcription in the primordium.

(d-f) *hmx3* transcription detected by *in situ* hybridisation at 26hpf. (d) In control embryos *hmx3* is strongly expressed in the anterior of the otic vesicle. (e-f) SU5402 treated embryos show a dramatic reduction in levels of *hmx3* expression.

(g-i) Levels of phosphorylated ERK1/2 were detected by antibody staining of 26hpf embryos. (g) Untreated control embryos show normal levels of pERK1/2 in the primordium. (h-i) Levels of ERK1/2 phosphorylation are greatly reduced in embryos treated with SU5402.

Scale bars are 50μm. Regions of interest are outlined. Abbreviations: **mp**, migrating primordium; **ov**, otic vesicle.

**Figure 27**

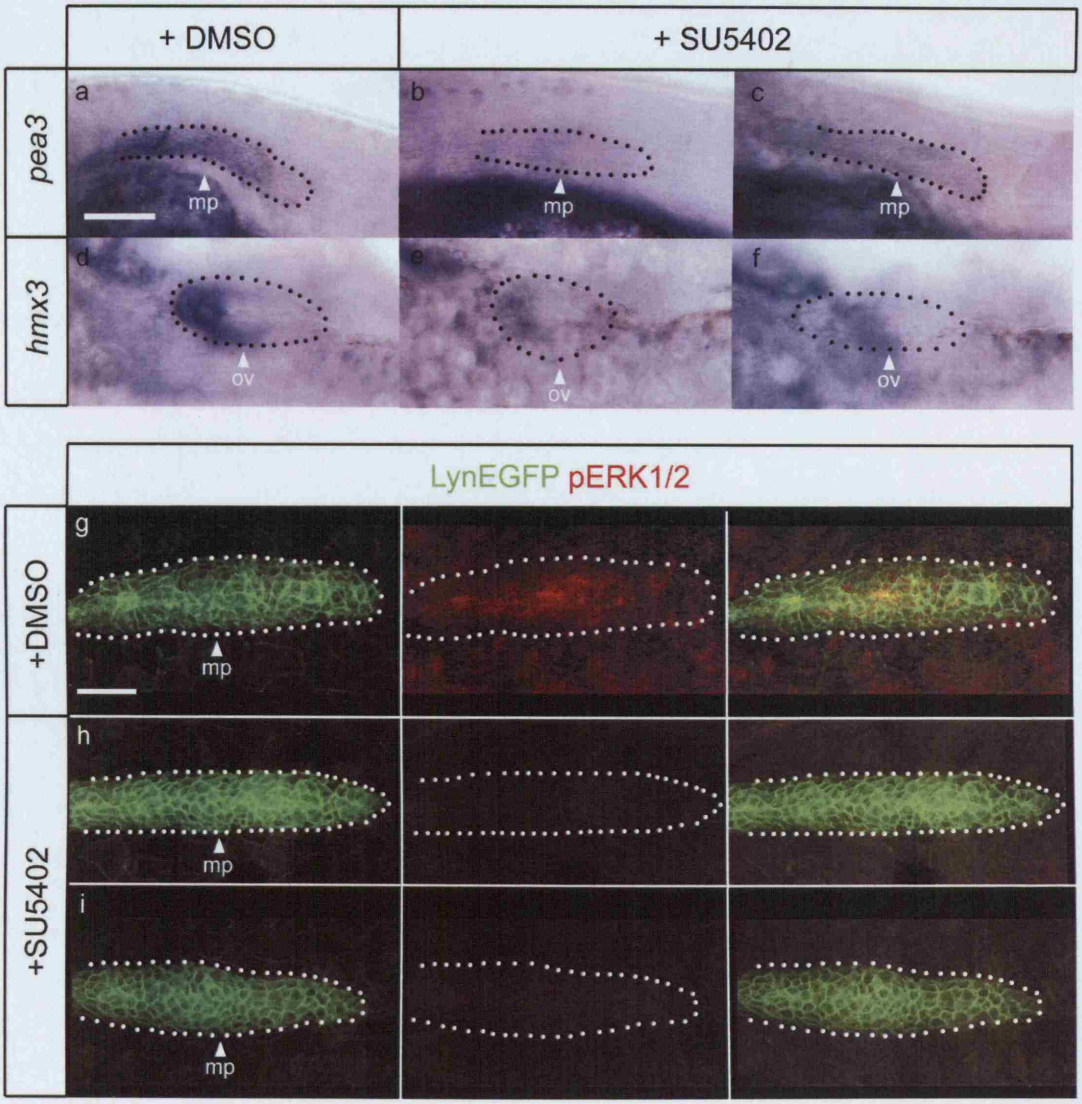
+ DMSO
+ SU5402
pea3
hmx3
a
b
c
d
e
f
mp
ov
LynEGFP pERK1/2
+DMSO
+SU5402
g
h
i

**Figure 28: Effect of SU5402 treatment on cxcr7b morphant primordia**

*hmx3 in situ* hybridisation on wildtype and *cxcr7b* morphant embryos in the presence and absence of SU5402. Images a and b are lateral views with anterior to the left and dorsal up. All other images are dorsal views with anterior to the left.

(a-d) *hmx3 in situ* hybridisation on wildtype embryos. (a-b) The primordia of untreated control embryos have migrated to approximately somite 6 or somite 7 by 24hpf. (c-d) In control embryos treated with SU5402 the primordia have migrated a similar distance.

(e-j) Embryos injected with *cxcr7b* morpholino that have not been treated with SU5402 display both ventral migration of the primordium and the split primordium phenotype. In contrast *cxcr7b* morphant embryos treated with SU5402 display a reduction in the incidence of ventral migration with the primordium remaining on the horizontal myoseptum. In addition, morphant embryos treated with SU5402 show an increase in the incidence and severity of the split primordium phenotype.

The scale bar is 25μm. Regions of interest are outlined. Abbreviations: **mp**, migrating primordium; **S3**, somite 3; **S4**, somite 4; **S6**, somites 6; **sc**, separated cells.

**Figure 28**

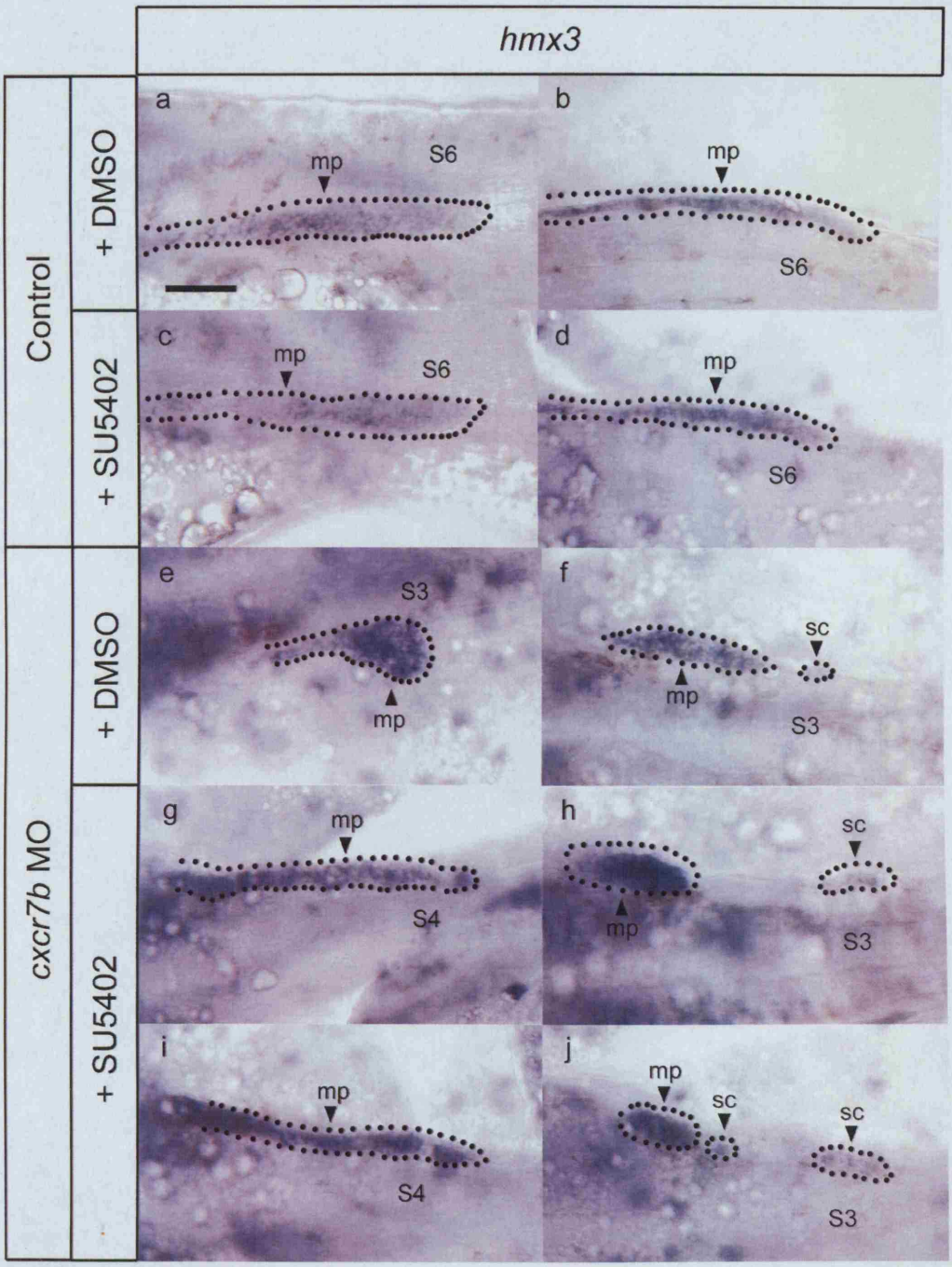
hmx3
Control
cxcr7b MO
+ DMSO
+ SU5402
+ DMSO
+ SU5402
a
b
c
d
e
f
g
h
i
j
mp
S6
S3
S4
sc

### Graph 6: Effect of SU5402 treatment on primordium migration

The morphology of individual primordia was examined at 24hpf by *in situ* hybridisation with the *hmx3* probe. Each primordium was categorised according to phenotype. Abbreviations: **n**, number of primordia examined.

### Graph 7: Effect of SU5402 treatment on ventral migration in *cxcr7b* morphants

The effect of SU5402 on primordium morphology of *cxcr7b* morphant was compared for statistical significance using a paired one-tailed t-test. As only two experiments were available both sets of data were entered twice. T-test p-values: 1=0.3586, 2=0.0068. A p-value <0.05 was taken as statistically significant.

Graph 6: Effect of SU5402 treatment on primordium migration

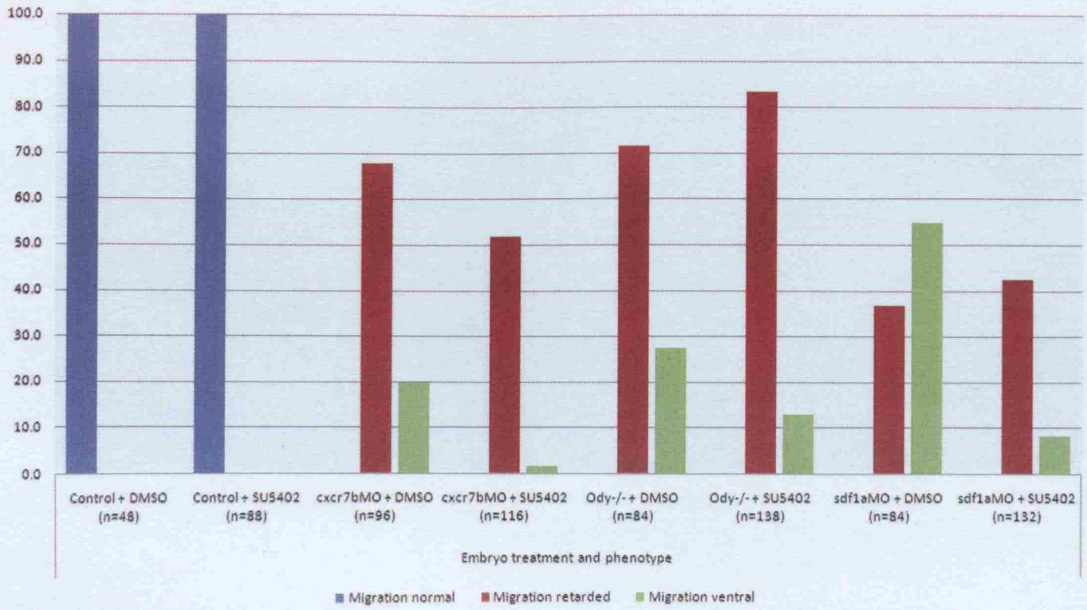


Graph 7: Effect of SU5402 treatment on ventral migration in cxcr7b morphants

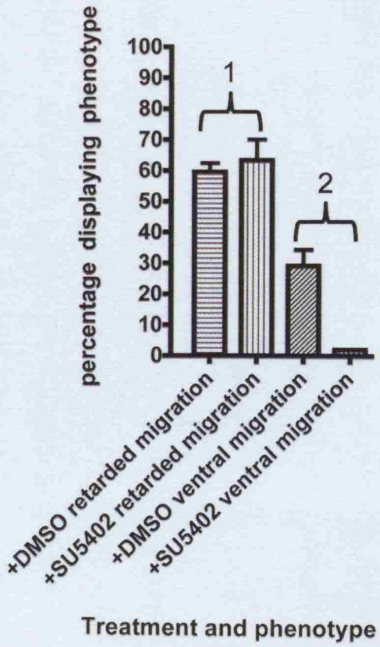

**Graph 8: Effect of SU5402 treatment on the coalescence of the primordium**

The morphology of individual primordia was examined at 24hpf by *in situ* hybridisation with the *hmx3* probe. Each primordium was assigned to one phenotype category. Abbreviations: **n**, number of primordia examined.

**Graph 9: Effect of SU5402 treatment on incidence of split primordia**

The effect of SU5402 on primordium coalescence in *cxcr7b* morphant was compared for statistical significance using a paired one-tailed t-test. As only two experiments were available both sets of data were entered twice. T-test p-values: 1=0.0097. A p-value <0.05 was taken as statistically significant.

Graph 8: Effect of SU5402 treatment on the coalescence of the primordium

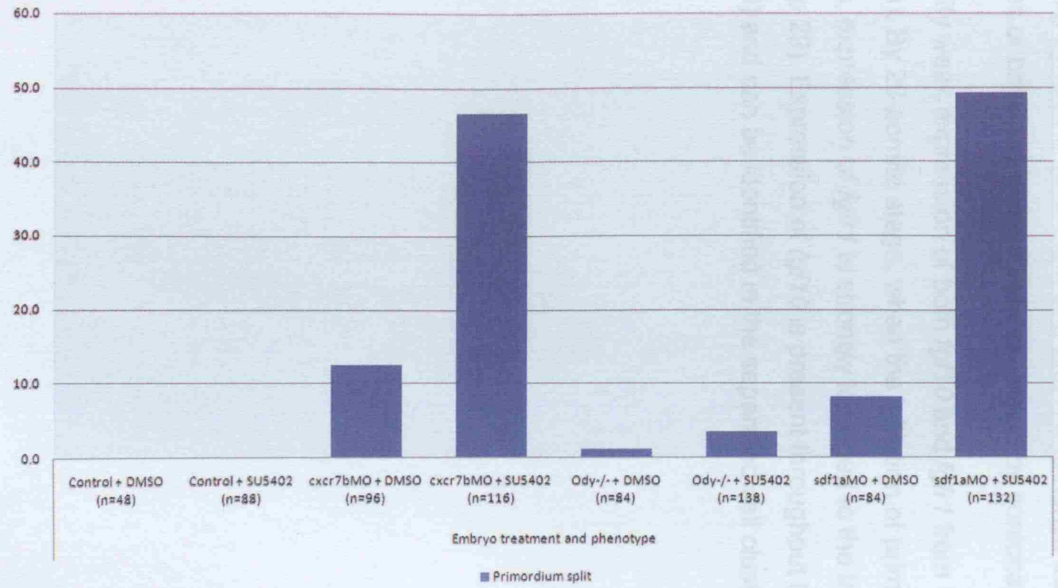


Graph 9: Effect of SU5402 treatment on the incidence of split primordia

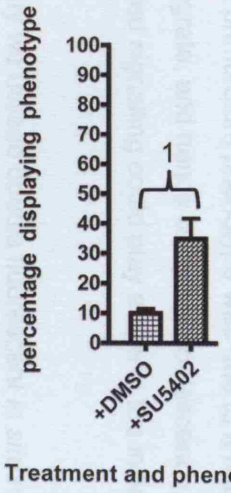

### 8.3.3 FGF mediated signalling may play a role in the initiation of primordium migration

Surprisingly SU5402 treatment of *cxcr7b* morphant embryos resulted in a significant increase in the incidence of the split primordium phenotype. As we had previously concluded that the split primordium phenotype was due to a failure of the main body of the primordium to migrate, and hence complete coalescence, we were curious as to whether FGF mediated signalling could play a role in the initial migration of the primordium.

To assess this possibility we utilised double fluorescent *in situ* hybridisation to examine the expression profiles of *fgf10* and *fgfr1* during the initiation of primordium migration. CldnB:LynEGFP embryos were fixed at two somite intervals from approximately 18-somite stage to 28-somite stage and *in situ* hybridisation conducted to detect *fgf10* and *fgfr1*. Following *in situ* hybridisation antibody staining was performed to detect LynEGFP (see 2.3.3 and 2.3.4) and hence the primordium. The expression profiles of both genes were then examined by confocal microscopy.

We were able to identify weak expression of both *fgf10* and *fgfr1* from 18-somite stage (data not shown). By 26-somite stage, when the initiation of primordium migration commences, expression of *fgfr1* is strongly localised to the trailing cells of the primordium (Figure 29). Expression of *fgf10* is present throughout the primordium (Figure 29) and can be identified in the separated cell clusters (n=3) (Figure 29c-c').

**Figure 29: *fgf10* and *fgfr1* expression during the initial stages of primordium migration**

Expression of *fgfr1* and *fgf10* in wildtype embryos at approximately 26-somite stage. All images are lateral views with anterior to the left and dorsal up.

(a-c') Expression of *fgfr1* localises strongly to the trailing region of the primordium during the initiation of primordium migration. *fgf10* is expressed throughout the primordium and can be detected in the separated cell clusters (white arrowheads).

The scale bar in a and b is 100μm, a', b' and c is 50μm, and c' is 25μm. The primordium is outlined in all cases. Abbreviations: **mp**, migrating primordium. a', b' and c' are high power images of a, b and c respectively.

**Figure 29**

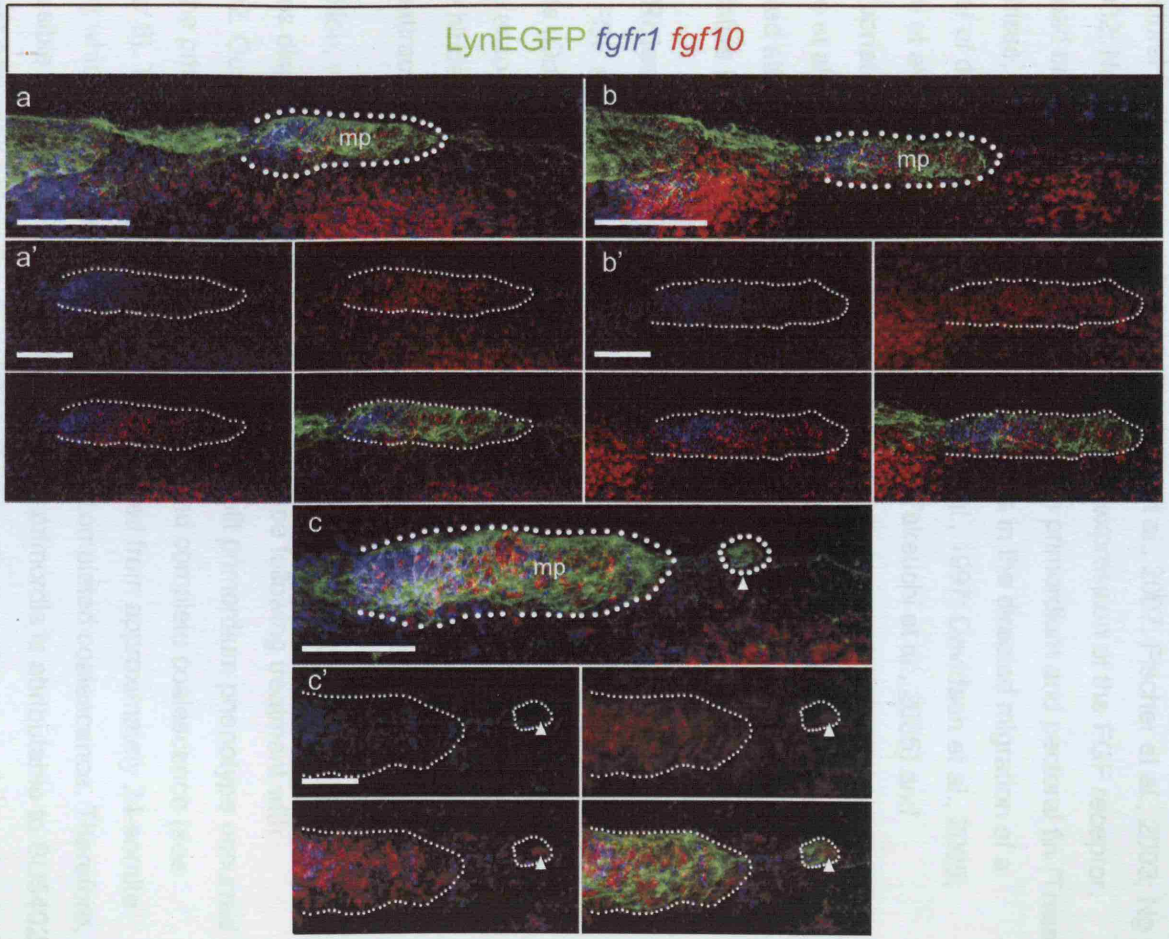

## 8.4 Discussion

Abrogation of *cxcr7b*, *cxcr4b* or *sdf1a* mediated signalling leads to the ventral migration of the primordium at the region of the pectoral fin bud. Confocal timelapse microscopy has shown that ventral migration is an active process suggesting that the primordium was responding to a cue emanating from the pectoral fin bud. Study of the published literature suggested multiple fibroblast growth factors were required for pectoral fin development in zebrafish (Abe et al., 2007; Fischer et al., 2003; Ng et al., 2002; Nomura et al., 2006). In addition, the expression of the FGF receptor, *fgfr1*, had been noted in the posterior lateral line primordium and pectoral fin (Thisse and Thisse, 2005). FGFs have established roles in the directed migration of a number of developmental systems (Burdine et al., 1997; Davidson et al., 2005; Ribeiro et al., 2002; Sato and Kornberg, 2002; Takeuchi et al., 2005) and inappropriate signalling has been noted in the metastasis of human breast cancers (Bange et al., 2002). FGF signalling, therefore, appeared to be a candidate for the observed attraction of the primordium to the pectoral fin and we conducted speculative investigations.

### 8.4.1 Roles for FGF signalling in primordium migration

When FGF signalling is inhibited in *cxcr7b*, or *sdf1a*, morphant embryos, or *cxcr4b* mutants (*Ody* -/-) the incidence of ventral migration is reduced. The primordia remain associated with the horizontal myoseptum, however, their migration is greatly hindered. This suggests that the ventral migration phenotype is likely due to chemoattraction resulting from FGF receptor mediated signalling.

In addition, we observed a significant increase in the proportion of *cxcr7b* morphant embryos displaying the split primordium phenotype following treatment with SU5402. Our previous work indicated that the split primordium phenotype occurred when the primordium failed to begin migration and complete coalescence (see Chapter 6). The SU5402 treatment was conducted from approximately 24-somite stage at which point not all primordia may have completed coalescence. Therefore, it is possible that the increased incidence of split primordia is attributable to SU5402 treatment occurring before the completion of primordium coalescence in a subset of the embryos treated. This could indicate a possible motorgenic role for FGF signalling in the initial stages of primordium formation and migration. This is an intriguing possibility, unfortunately, time constraints have prevented further investigation at this time. In support of this hypothesis we have identified expression of *fgf10* and *fgfr1* in a polarised fashion within the early primordium. This places the

ligand in the leading region of the primordium and the receptor in the trailing region. Assuming that activation of the receptor results in migration towards the strongest source of ligand, this could indicate a role for FGF receptor mediated signalling in the initiation of primordium migration. If such a role for FGF signalling does exist it is most likely secondary to the CXC-type GPCR mediated pathways as we do not observe any hindrance of the migration in the control primordia treated with SU5402.

Though we have been able to provide evidence that FGF signalling may play a role in the initial coalescence and migration of the primordium to conclusively prove such a role would require a great deal more work. It would be necessary to characterise which of the 27 FGFs, and seven FGF receptors, present in the zebrafish genome (Itoh, 2007) are expressed by the primordium and/or pectoral fin. Once characterisation was complete it would be necessary to determine which receptor and ligand combinations are involved in the initiation of migration. Such a project cannot be pursued due to time constraints. However, the role of FGF signalling in primordium migration may prove an interesting topic for further study especially as the Xu lab has access to an *hsp70:dnfgfr1-EGFP* transgenic line (Lee et al., 2005). The *hsp70:dnfgfr1-EGFP* line contains a heat-shock inducible dominant negative form of FGFR1 tagged with EGFP. The heat-shock promoter should make it possible to analyse the temporal requirement for FGF signalling in the formation of the primordium and initiation of migration. However, this has the caveat that other FGF receptors, or ligands, may be involved in primordium formation; the signalling of which would be unaffected in this line.

# Chapter 9: Elucidation of CXCR7b function

## 9.1 Introduction

Loss of *cxcr7b* function has a detrimental effect on the ability of posterior lateral line primordium to migrate. We were therefore interested in whether we could elucidate the molecular mechanisms underlying the function of CXCR7b. Thus we came to consider the methods available to us that could further our investigations.

## 9.2 Aims

The work presented in this chapter was conducted in an effort to improve our understanding of how CXCR7b elicits its effects in the embryo. Of particular interest to us was whether SDF1a interacts with CXCR7b; at the time that this work was initiated *cxcr7b* was an orphan receptor. In an effort to support our hypothesis that SDF1a could be a ligand for CXCR7b we chose to examine the effect of *cxcr7b* morpholino on the migration of the primordial germ cells (PGCs); a second system known to require *cxcr4b*, and *sdf1a*, for successful migration (Doitsidou et al., 2002; Dumstrei et al., 2004). The results of which lead us to further examine the interaction between SDF1a and CXCR7b in zebrafish.

In addition, we have attempted to examine the spatial requirement for *cxcr7b* within the migrating primordium and particularly what the effect of expression of *cxcr7b* in the leading part of the primordium might be. The expression of *cxcr4b* and *cxcr7b* is largely exclusive we have therefore investigated whether *cxcr4b* and *cxcr7b* are capable of regulating one another's expression by examining their expression profiles within mutant and morphant primordia.

## 9.3 Results

### 9.3.1 *cxcr7b* morpholino treatment results in scattering of the primordial germ cells

*cxcr7b* was originally identified as the orphan G-protein coupled receptor *rdc1*. RDC1 had no known ligand. However, both RDC1 and CXCR4 had been implicated as cofactors that facilitated human immunodeficiency virus (HIV) entry of cells (Doranz et al., 1999; Feng et al., 1996; Shimizu et al., 2000). This suggested to us a sufficiently similar extracellular domain in both RDC1 and CXCR4 that HIV was capable of binding both. Combined with the overlapping expression domains of the two receptors in the posterior lateral line and the close proximity of *sdf1a* and *rdc1* expression along the horizontal myoseptum, and in the hindbrain and other tissues

(data not shown), we considered the possibility that SDF1a could be a ligand for RDC1. This possibility was considered worthy of investigation as it would allow us to assign a ligand to the orphan receptor RDC1 and provide evidence that both CXCR4b and RDC1 responded to the same ligand in the posterior lateral line.

In zebrafish the migration of the primordial germ cells requires *cxcr4b* and *sdf1a* expression (Doitsidou et al., 2002; Dumstrei et al., 2004). As we had shown a requirement for *cxcr7b* in primordium migration we were curious as to whether *cxcr4b*, *sdf1a* and *cxcr7b* could represent a conserved signalling system and whether it could play a role in PGC migration. This was of particular interest as a role for *cxcr7b* in PGC development could constitute circumstantial evidence that SDF1a was a ligand for CXCR7b, thereby making this line of investigation worth pursuing. To test this theory we examined the effect of *cxcr7b* morpholino treatment on the migration of the PGCs.

Embryos were injected at one-cell stage with morpholinos against *cxcr4b* (12ng), *cxcr7b* (8.4ng), or *sdf1a* (10ng) and allowed to develop to 24hpf at which point *in situ* hybridisation was performed using a probe to detect the *nanos1-3'UTR* transcripts present exclusively in the PGCs (Koprunner et al., 2001).

In all cases where embryos were treated with morpholino against *cxcr4b* (n=37), *cxcr7b* (n=50) or *sdf1a* (n=47) the PGCs were scattered throughout the embryo, though the degree of scatter was variable (Figure 30c-h). These results were confirmed by coinjection of morpholino with *gfp-nos1–3'UTR* RNA, consisting of GFP fused to the 3' UTR of the *nanos1* gene (Koprunner et al., 2001), to visualise the location of the PGCs in live embryos (data not shown).

Expression of *cxcr4b* can be readily identified in the primordial germ cells from approximately one-somite stage (Doitsidou et al., 2002). Therefore we attempted to identify expression of *cxcr7b* in the PGCs over a range of stages from one-cell stage to 24hpf by *in situ* hybridisation. We were unable to identify specific expression of *cxcr7b* within the PGCs (data not shown). At this point we entered into collaboration with the laboratory of Dr Erez Raz (Max-Planck-Institute for Biophysical Chemistry, Germany) and did not pursue study of the PGCs further.

**Figure 30: Scattering of the primordial germ cells in *cxcr4b*, *cxcr7b* and *sdf1a* morphant embryos.**

Primordial germ cells were detected using expression of *nanos-3'UTR* as a marker at 24hpf. Images of the head are dorsal views with anterior to the left; all other images are lateral views with anterior to the left and dorsal up.

(a-b) Wildtype embryos display normal localisation of the PGCs to the gonad. The *nanos-3'UTR* transcripts cannot be identified elsewhere in the embryo. (c-h) In embryos treated with morpholino against *cxcr4b*, *sdf1a* or *cxcr7b* the PGCs are scattered throughout the embryo with few PGCs arriving at the correct location in the gonad.

Scale bars are 50μm. Black arrowheads indicate primordial germ cells.

**Figure 30**

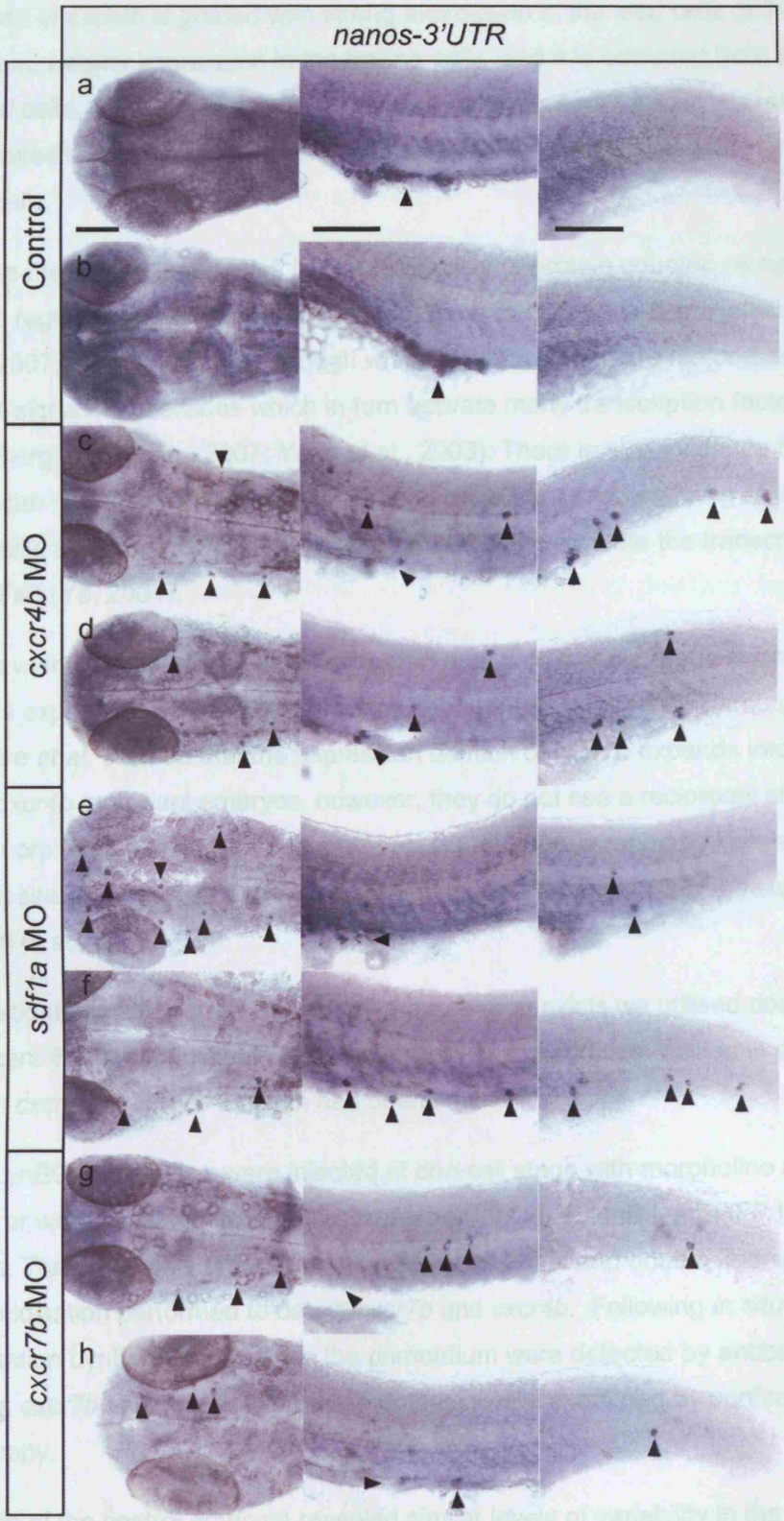

### 9.3.2 *cxcr4b* and *cxcr7b* do not regulate one another's expression

Expression of *cxcr4b* and *cxcr7b* is broadly complimentary and largely exclusive. Expression of *cxcr4b* is graded with strong expression in the lead cells of the primordium, weaker expression in the trailing cells, and it is excluded from the deposited cells. Conversely, *cxcr7b* expression is graded with strong expression in the deposited and trailing cells of the primordium while it is excluded from the leading cells.

As well as their established roles in cellular motility G-protein coupled receptors are known to regulate growth, differentiation and gene transcription (Spiegelberg and Hamm, 2007). The G-proteins, through which GPCRs signal, are major modulators of MAPK signalling cascades which in turn activate many transcription factors (Spiegelberg and Hamm, 2007; Yang et al., 2003). There is also evidence that GPCRs can modulate histone acetylation and gene transcription (Kang et al., 2005). Additionally, CXC-type GPCRs have been shown to up regulate the transcription factor NFκB (Ye, 2001).

Thus we wished to determine whether *cxcr4b* and *cxcr7b* could regulate one another's expression. This was particularly important as a report by Dambly-Chaudière *et al.* claimed that the expression domain of *cxcr7b* expands into leading cells in *cxcr4b* morphant embryos, however, they do not see a reciprocal effect in *cxcr7b* morphants (Dambly-Chaudiere et al., 2007). Also, a report by Valentin *et al.* does not see any effect on *cxcr7b* expression in *cxcr4b* mutant (*Ody* -/-) embryos (Valentin et al., 2007).

To investigate whether cross regulation of expression exists we utilised double fluorescent *in situ* hybridisation to detect *cxcr4b* and *cxcr7b* expression in embryos in which *cxcr4b* or *cxcr7b* function had been inhibited.

CldnB:LynEGFP embryos were injected at one-cell stage with morpholino against *cxcr7b*, or were collected from natural spawning of *Ody* /CldnB:LynEGFP transgenic mutants. The embryos were allowed to develop to 28hpf and double fluorescent *in situ* hybridisation performed to detect *cxcr7b* and *cxcr4b*. Following *in situ* hybridisation LynEGFP and hence the primordium were detected by antibody staining. *cxcr7b* and *cxcr4b* expression domains were examined by confocal microscopy.

Analysis of the control embryos revealed similar levels of variability in the expression domains of *cxcr4b* and *cxcr7b* described previously (see 4.3.3) (Figure 31a-c). Our examination of *Ody* -/-embryos could identify no substantial alteration in

the expression domains (Figure 30d-f), even when the ventral migration phenotype was observed (Figure 30f). Similarly, the primordia of embryos injected with *cxcr7b* morpholino displayed no obvious alteration in the expression domains of either receptor even in ventrally migrated primordia (Figure 31g-h). In cases where *cxcr7b* morphant embryos displayed the split primordium phenotype it is difficult to ascertain whether alterations in the expression have occurred due to the drastically different morphology of the morphant primordium (Figure 31e). However, the expression domains are not substantially different to the expression domains of embryos prior to 26-somite stage in which the primordium has not begun to migrate (see Chapter 5).

CXCR4 and CXCR7 have both been shown to be activated by SDF1/CXCL12 (Balabanian et al., 2005; Bleul et al., 1996; Burns et al., 2006; Oberlin et al., 1996). As a result *sdf1a* is assumed to be the ligand for *cxcr4b* and *cxcr7b* in zebrafish (Dambly-Chaudiere et al., 2007; David et al., 2002; Li et al., 2004; Valentin et al., 2007). We were therefore curious as to whether knockdown of *cxcr4b* or *cxcr7b* affected the expression of *sdf1a* along the horizontal myoseptum. *Ody-/-* embryos, or embryos injected with *cxcr7b* morpholino, were examined at 24hpf and 28hpf for expression of *sdf1a*. We were unable to identify any defects in the *sdf1a* stripe in either case (data not shown) indicating that the migratory defects do not stem from defects in the *sdf1a* pathway.

**Figure 31: *cxcr7b* and *cxcr4b* do not regulate each other at the transcriptional level**

Expression of *cxcr4b* and *cxcr7b* in embryos at 28hpf. All images are lateral views with anterior to the left and dorsal up.

(a-c) Control embryos display the normal level of variability in the expression domains of *cxcr4b* and *cxcr7b*. (d-f) *Ody* -/- embryos show no obvious alteration in the transcription domains of either *cxcr4b* or *cxcr7b*, even in cases where the primordium has migrated ventrally. (g-i) A similar conservation of the expression profiles of *cxcr4b* and *cxcr7b* is observed in embryos injected with *cxcr7b* morpholino.

The primordium is outlined in all cases. Separated cells are indicated by white arrowheads. The scale bar is 25μm.

**Figure 31**

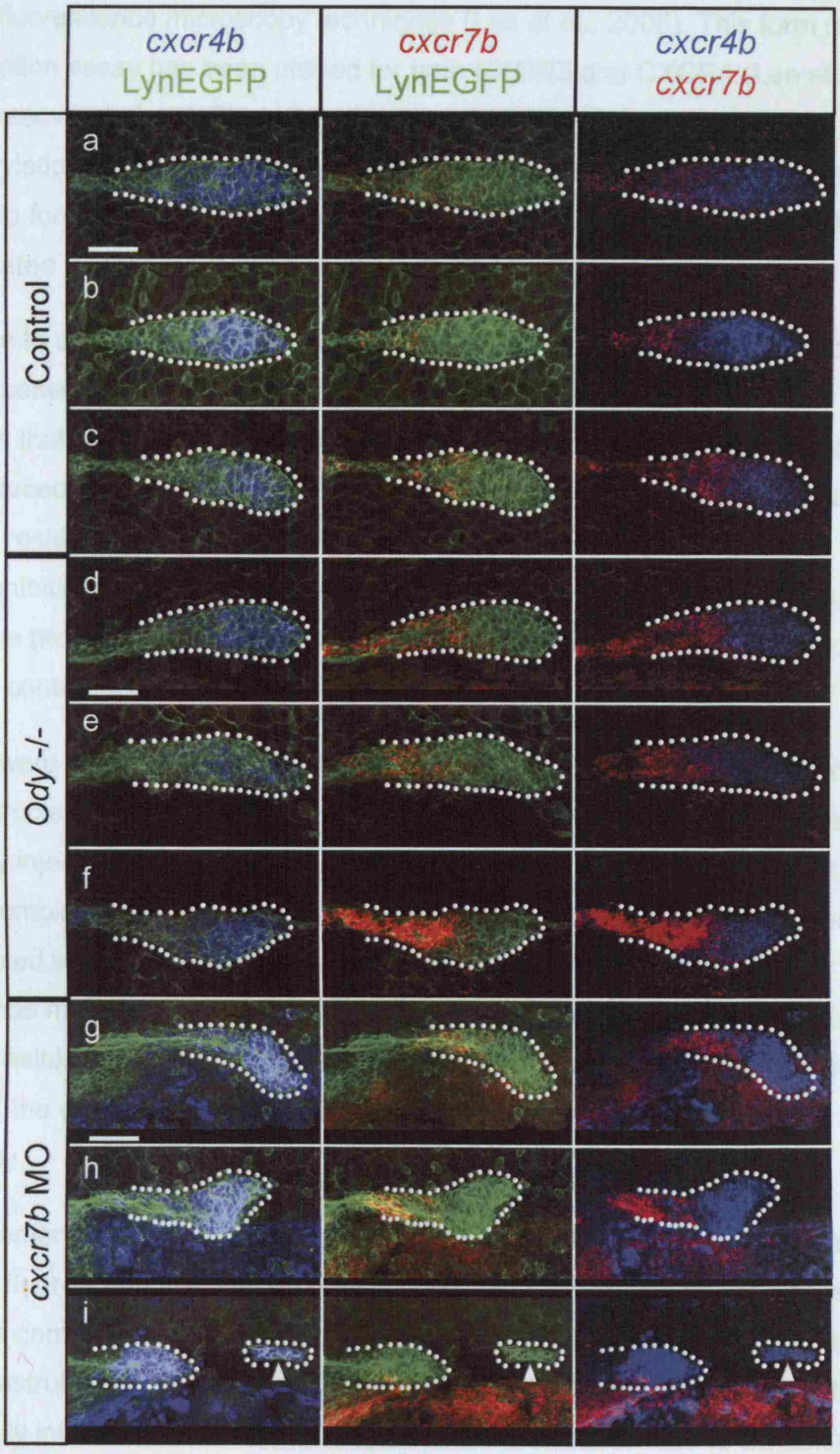
cxcr4b
LynEGFP
cxcr7b
LynEGFP
cxcr4b
cxcr7b
Control
Ody -/-
cxcr7b MO
a
b
c
d
e
f
g
h
i

### 9.3.4 Internalisation of CXCR7b fusion protein by SDF1a

Internalisation assays utilise the direct fusion of a fluorophore to the carboxy-terminus of GPCRs (Lee et al., 2006). It is then possible to directly observe the internalisation of the GPCR-fusion protein in response to ligand binding using a range of fluorescence microscopy techniques (Lee et al., 2006). This form of internalisation assay has been utilised for both CXCR3 and CXCR4 (Lee et al., 2006; Tarasova et al., 1997). Internalisation of GPCRs is dependent upon phosphorylation of serine/threonine residues in the C-terminal tail; deletion of these residues to form truncated GPCRs can inhibit receptor internalisation and has been demonstrated for CXCR4 (Haribabu et al., 1997).

We chose to utilise an internalisation assay to determine whether an interaction occurred between CXCR7b and SDF1a in zebrafish embryos. Two *cxcr7b* constructs that were C-terminally tagged with *eyfp*, *cxcr7beyfp* and *cxcr7bΔceyfp* were produced. One of which was C-terminally truncated to remove serine and threonine residues thought to be necessary for internalisation (Amara et al., 1997) thereby inhibiting internalisation and acting as a negative control (*cxcr7bΔceyfp*). In addition we produced a full-length *rfp* C-terminally tagged *cxcr4b* construct to act as a positive control (*cxcr4brfp)*.

Embryos were injected at one-cell stage with ~400pg of RNA encoding one of the four constructs; *CXCR7bEYFP, cxcr7bΔceyfp,* or *cxcr4brfp.* The embryos were then mosaically injected into one cell of an eight-cell stage embryo with RNA encoding *sdf1a* in combination with Cascade Blue lysinated dextran (CBLD). Control embryos were injected with CBLD alone. Live embryos were monitored regularly by fluorescence microscopy to determine the point at which the fluorescent proteins were first visible. Once the fluorescent proteins were visible, approximately at 1000-cell stage, the embryos were mounted and examined by confocal timelapse microscopy.

In control embryos expressing CXCR4bRFP, or CXCR7bEYFP, injected with CBLD alone, the fluorescently tagged proteins localised to the cell membrane as well as subcellular compartments (Figure 32a-f). This distribution was maintained before the onset of gastrulation. At ~50% epiboly stage both CXCR4bRFP and CXCR7bEYFP are normally internalised and showed cytoplasmic distribution due to an unknown endogenous internalisation activity present in gastrula embryos. Thus there is a very narrow time window in which to assay for internalisation in response to a source of SDF1a. We have nevertheless demonstrated the internalisation of CXCR4bRFP and CXCR7bEYFP by coinjection with RNA encoding sdf1a before gastrulation. The

effectiveness of ectopic expression of sdf1a was assessed by coinjecting RNA for *sdf1a* and *gfp-nos1-3'UTR*. The *gfp-nos1-3'UTR* expressing PGCs were scattered throughout the embryos (data not shown).

Experimental embryos of approximately the same stage injected with both CBLD and *sdf1a* RNA show a decrease in membrane localisation of the fluorescent proteins (Figure 32g-l), however, we do not have a method to quantify this apparent decrease. The experiment was repeated using the CXCR7bΔCEYFP construct which showed localisation to the membrane both in the presence and absence of *sdf1a* RNA (Figure 33). Currently there are no antibodies available that recognise zebrafish SDF1a thus we have been unable to demonstrate a colocalisation of SDF1a with the internalised tagged proteins. Therefore we cannot be certain that the internalisation of CXCR4bRFP and CXCR7bEYFP is directly due to expression of SDF1a and not as an indirect result of the over-expression of SDF1a.

**Figure 32: Expression of *sdf1a* RNA results in internalisation of CXCR4bRFP and CXCR7bEYFP**

Cellular localisation of CXCR4bRFP and CXCR7BEYFP in the presence and absence of SDF1a.

(a-f) CXCR4bRFP, or CXCR7bEYFP, in the presence of CBLD the fluorescently tagged proteins localise to the cell membrane as well as intracellular vesicles. (g-l) In embryos expressing CXCR4bRFP, or CXCR7bEYFP, in the presence of CBLD and *sdf1a* RNA the tagged protein appeared to show a decrease in the levels of protein found on the cell membrane and an increase in levels inside the cell (g-l).

The scale bar is 25μm. Abbreviations: **CBLD**, Cascade Blue lysinated dextran.

**Figure 32**

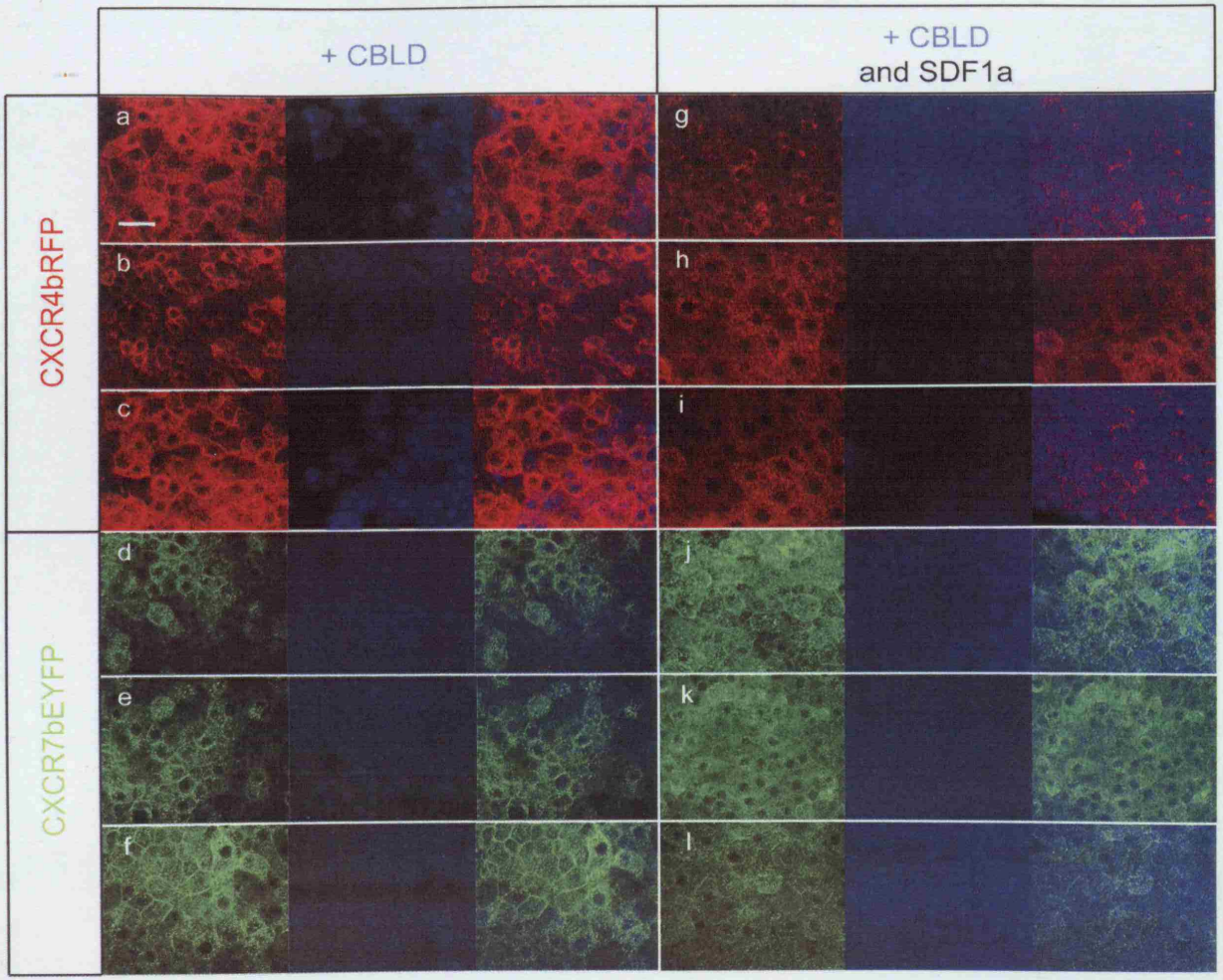

**Figure 33: CXCR7bΔCEYFP remains on the cell membrane in the presence of SDF1a**

Cellular localisation of CXCR7bΔCEYFP in the presence and absence of SDF1a.

(a-c) CXCR7bΔCEYFP in the presence of CBLD the tagged protein localises to the cytoplasmic membrane as well as intracellular vesicles. (d-f) In embryos expressing CXCR7bΔCEYFP in the presence of CBLD and *sdf1a* RNA the fluorescent protein remains associated with the cell.

The scale bar is 25μm. Abbreviations: **CBLD**, Cascade Blue lysinated dextran.

**Figure 33**

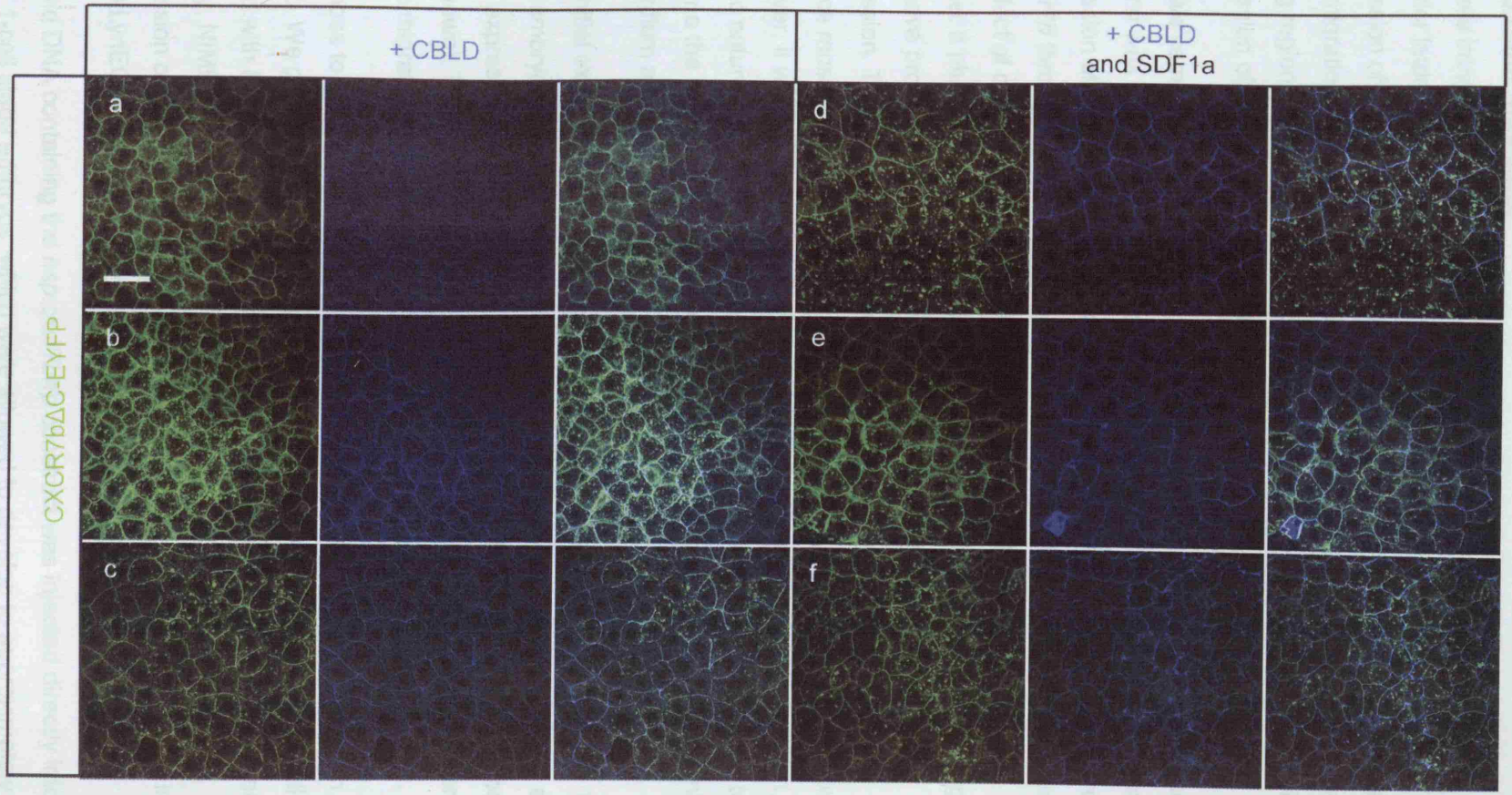

### 9.3.5 Ectopic expression of CXCR7bRFP on the pathway blocks primordium migration

We were intrigued as to the spatial requirement for *cxcr7b* expression in the posterior lateral line primordium. Of particular interest was whether we could induce expression of *cxcr7b* in the separated cells and whether this would be sufficient to drive migration of these cells. In addition, since *cxcr7b* expression is restricted to the trailing region of the primordium we were intrigued as to what would happen if expression of *cxcr7b* could be induced throughout the primordium.

Thus we came to consider the strategies available to us to examine these questions. The first was injection of RNA encoding CXCR7bRFP. This would allow widespread expression of CXCR7bRFP and would allow us to examine the effect of expression of *cxcr7b* throughout the primordium. In addition, it may have allowed us to examine the effect of *cxcr7b* expression in the separated cells. However, determining whether a phenotype was due to expression in the primordium or surrounding tissue may have proved difficult. The alternative was to use heat-shock inducible expression. This would require the injection of a DNA construct which would produce mosaic expression the location of which we would have no control over. However, it would facilitate temporal control of *cxcr7b* expression. In addition, the mosaic nature of expression could prove advantageous as it would allow us to examine the effect of expression of *cxcr7b* within subpopulations of cells within the primordium and separated cells.

Our initial experiments utilised injection of RNA encoding CXCR7bRFP into 1-cell stage embryos. Unfortunately, we found that the RNA was rapidly degraded and by 20hpf expression of CXCR7bRFP could no longer be detected in the embryos (data not shown). Thus we were unable to examine the effect of CXCR7bRFP expression on the migrating primordium and this line of enquiry was not pursued further.

We chose to continue our investigations utilising a heat-shock inducible form of *cxcr7b*. We generated a heat-shock inducible full-length CXCR7b C-terminally tagged with RFP, under the control of the *hsp70* heat-shock promoter (Dr Sebastian Gerety, NIMR) (see 2.2.13). This construct allowed us to temporally control expression of CXCR7bRFP and examine its effect on primordium migration in live CldnB:LynEGFP embryos.

Plasmid DNA containing the *hsp:cxcr7brfp* construct was injected directly into the cell of 1-cell stage embryos, which were allowed to develop to approximately 22hpf. Embryos were then heat-shocked at 37°C for one hour and returned to 28.5°C. The

embryos were monitored by fluorescence microscopy to detect the expression of CXCR7bRFP. The DNA construct yielded highly mosaic expression. Embryos expressing the construct were mounted for confocal timelapse analysis with a periodicity of either two minutes or approximately two hours.

The mosaic expression of the construct rarely resulted in detectable expression in the posterior lateral line. However, when expression of CXCR7bRFP was detectable within the primordium it appeared to have little impact on its migration (Figure 33a-c; Supplemental Data S14-S16), even when expressed in the mid and leading regions of the primordium (Figure 34a-c). On one occasion we observed expression of CXCR7bRFP at the leading edge of the primordium where it did not seem to inhibit migration of the primordium. However, the construct did not appear to localise to the membrane in these cells and appeared to be held in intracellular compartments (Figure 34c; Supplemental Data S15). It may therefore be that transport of CXCR7bRFP to the cell membrane is regulated in the leading cells which prevent it from exerting an effect.

In addition to expression of CXCR7bRFP in the primordium we frequently observed expression in the somites. The somitic expression presented some intriguing phenotypes. Expression either side of the horizontal myoseptum did not appear to have an effect on migration and the primordium migrated with grossly normal speed and cell behaviour (Figure 35a-b). However, when CXCR7bRFP was expressed on the pathway the primordium appeared to stall when it encountered regions of ectopic expression of CXCR7bRFP (Figure 35c-f), or produced membrane protrusions and actively moved to avoid the region of expression (Fig 35e-f; Supplemental Data S17-S18). In one severe case where posterior-ward migration was blocked by a region of CXCR7BRFP expression the primordium turned and migrated anteriorly (Figure 35f; Supplemental Data S18). Assuming that the fluorescently tagged version of CXCR7b is functional these results are intriguing as in combination they suggest that CXCR7b expression on the *sdf1a* pathway can block migration. This lends support to the proposal that CXCR7b binds and internalises SDF1a in the trailing region of the primordium making it unavailable to CXCR4b thereby generating a gradient of SDF1a (Dambly-Chaudiere et al., 2007).

**Figure 34: Ectopic expression of CXCR7bRFP on the pathway blocks primordium migration**

Timelapse images of CldnB:LynEGFP embryos expressing CXCR7bRFP. All images are lateral views with anterior to the left and dorsal up.

(a-c) Expression of CXCR7bRFP in the mid and leading regions of the primordium does not appear to adversely affect primordium migration. (c) However, when CXCR7bRFP is present at the leading edge of the primordium it does not appear to localise to the membrane and instead seems to be maintained in intracellular compartments.

The scale bar is 50 μm. Insets in c are high power images of the leading cells of the primordium. White arrows indicate the primordium; white arrowheads denote CXCR7bRFP expression in the primordium. a, b and c relate to **Supplemental Data S17, S18** and **S19** respectively.

Figure 34

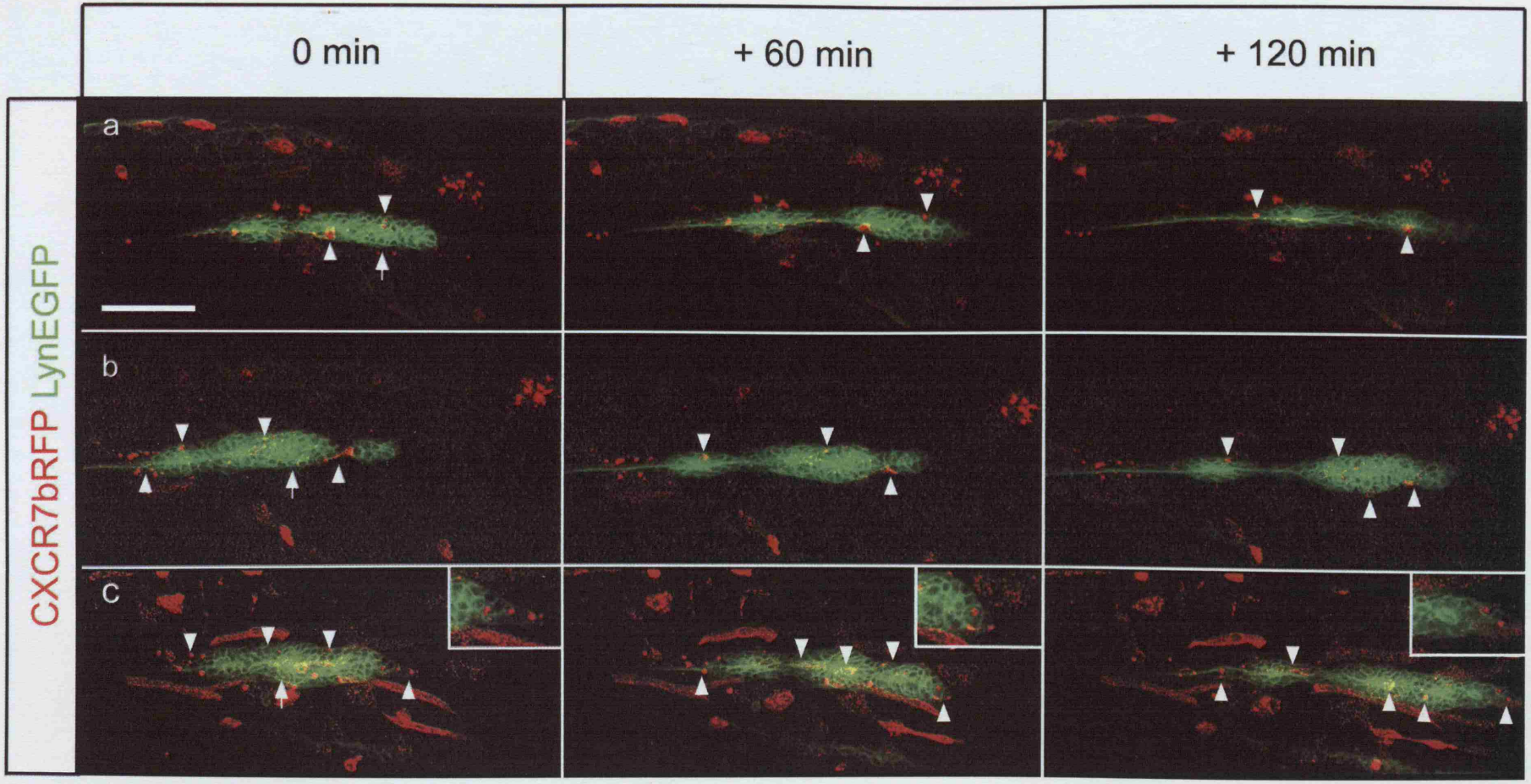

**Figure 35: Ectopic expression of CXCR7bRFP on the pathway blocks primordium migration**

Timelapse images of CldnB:LynEGFP embryos expressing CXCR7bRFP. All images are lateral views with anterior to the left and dorsal up.

(a-b) Ectopic expression of CXCR7bRFP lateral to the normal migration pathway does not hinder migration. (c-f) When CXCR7bRFP is located on the horizontal myoseptum it blocks migration. This causes the primordium to find alternative pathways to avoid the regions of expression. (f) In an extreme case the pathway is completely blocked and the primordium migrates ventrally before returning anteriorly.

The scale bar is 50 μm. Abbreviations: **mp**, migrating primordium. White arrowheads indicate CXCR7bRFP expression on the horizontal myoseptum. e and f relate to **Supplemental Data S17** and **S18** respectively.

Figure 35

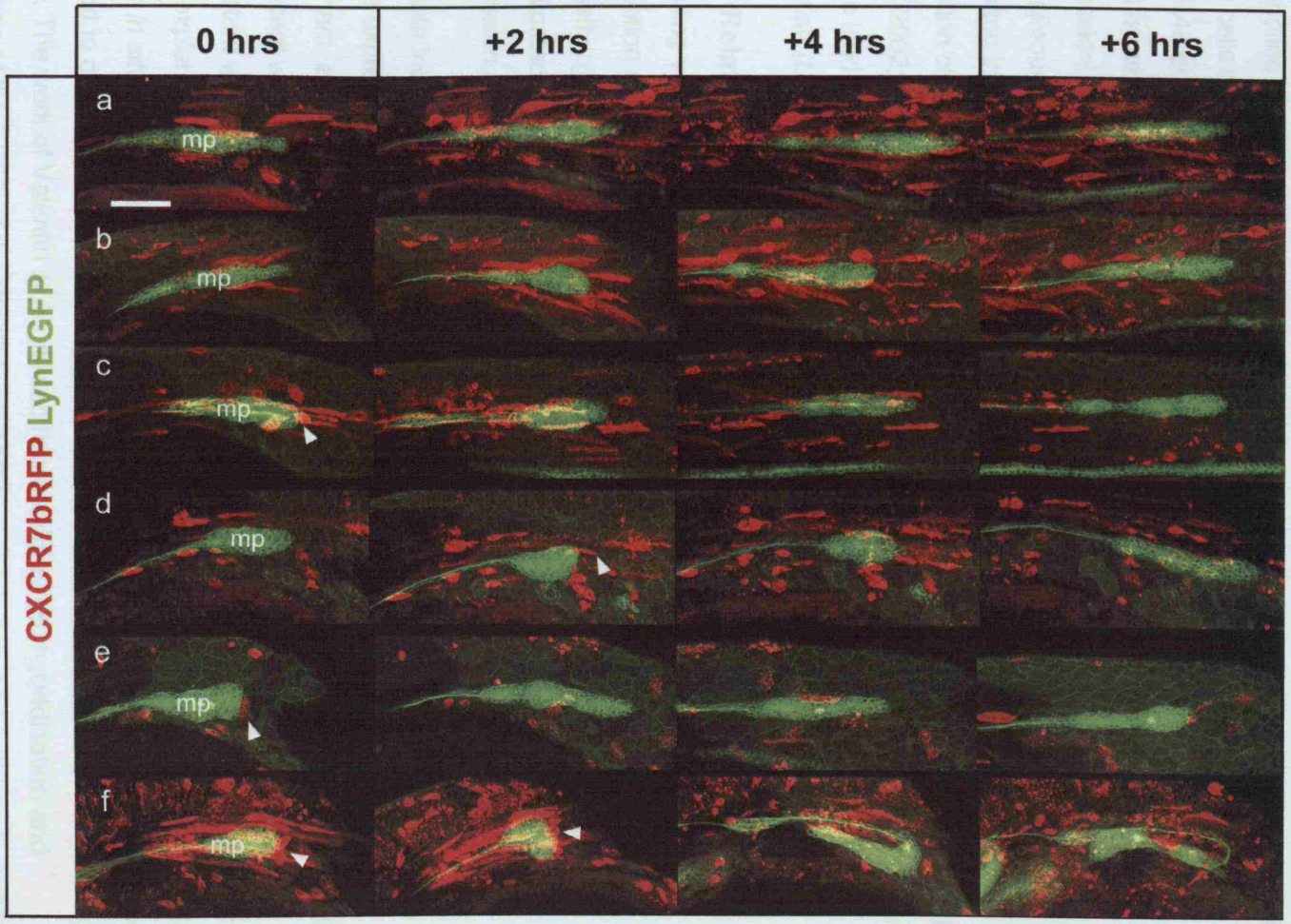

## 9.4 Discussion

In this chapter we have presented the results of our investigations to elucidate the mechanisms by which CXCR7b functions in zebrafish.

### 9.4.1 A role for *cxcr7b* in primordial germ cell migration

Morpholino knockdown of CXCR7b synthesis results in scattering of the primordial germ cells throughout the embryo in a phenotype reminiscent of knockdown of CXCR4b or SDF1a function (Doitsidou et al., 2002; Knaut et al., 2003). How this effect is mediated remains uncertain. We have been unable to demonstrate expression of *cxcr7b* in the PGCs, a result confirmed by our collaborators (Boldajipour, 2008 in press). However, it may suggest a conserved mechanism operating in both the PGCs and posterior lateral line migration. Furthermore, the migration of the PGCs and primordium are reliant on the chemokine SDF1a (David et al., 2002; Doitsidou et al., 2002; Knaut et al., 2003; Li et al., 2004). Therefore our results lend support to the assumption that SDF1a is a ligand for CXCR7b in zebrafish (Dambly-Chaudiere et al., 2007; Valentin et al., 2007).

### 9.4.2 Relationship between *cxcr7b* and *cxcr4b*

Signalling via GPCRs has documented effects on gene expression via histone acetylation and MAPK activation of transcription factors (Kang et al., 2005; Spiegelberg and Hamm, 2007; Yang et al., 2003; Ye, 2001). Therefore we have investigated whether *cxcr4b* and *cxcr7b* are capable of regulating one another's expression.

Our data indicate that *cxcr4b* and *cxcr7b* do not regulate one another's expression as the expression domains of *cxcr4b* and *cxcr7b* in *Odysseus* mutant, and *cxcr7b* morphant, embryos appear largely unchanged. While this result does not agree with the recent work of Dambly-Chaudiere *et al.* (Dambly-Chaudiere et al., 2007) it is consistent with the observations of Valentin *et al.* (Valentin et al., 2007). The most likely explanation is that Dambly-Chaudiere *et al.* examined expression using single colour *in situ* hybridisation to detect expression of *cxcr4b* or *cxcr7b* without a reliable method to distinguish the primordium from other tissues (Dambly-Chaudiere et al., 2007). The work of Valentin *et al.* utilised fluorescent *in situ* hybridisation and detection of the EGFP of the CldnB:LynEGFP transgenic line (Valentin et al., 2007), a similar method to our work, which allows more reliable identification of the primordium and higher resolution.

Although cross regulation at the level of expression may not exist between the two receptors evidence has been presented for an interaction at the protein level

between CXCR4 and CXCR7 which results in the formation of heterodimers with altered signalling properties *in vitro* (Sierro et al., 2007). Though the *in vitro* environment may not truly replicate the *in vivo* situation, considering the overlapping expression domains of *cxcr4b* and *cxcr7b* in the posterior lateral line primordium there may be a role for heterodimerisation, and regions of altered signalling properties, in primordium migration a possibility certainly worthy of further study.

### 9.4.2 A ligand for CXCR7b

When we commenced our studies *cxcr7b* was an orphan receptor; it has since been shown to bind SDF1 (CXCL12), ITAC (CXCL11) and an unidentified ligand secreted by plasmacytoid dendritic cells (Balabanian et al., 2005; Burns et al., 2006; Infantino et al., 2006; Proost et al., 2007). It has therefore been assumed that SDF1a is a ligand of CXCR7b in zebrafish (Dambly-Chaudiere et al., 2007; Valentin et al., 2007). However, it remains to be proven and additional ligands may be involved in primordium migration.

We have attempted to demonstrate an interaction between CXCR7b and SDF1a *in vivo* as the ligand(s) for CXCR7b must be resolved in order to examine the roles of CXCR4b, CXCR7b and SDF1a in primordium migration effectively. We have been able to show a correlation between the presence of SDF1a and internalisation of CXCR7b. However, we are unable to definitively demonstrate a direct association between the two events. The elucidation of the ligands for CXCR7b will require further work to determine their identity and whether they play roles in primordium migration.

### 9.4.3 Ectopic expression of CXCR7bRFP on the pathway hinders primordium migration

By utilising heat-shock inducible expression of CXCR7bRFP we have been able to examine the effect of ectopic CXCR7b expression on the migration of the posterior lateral line primordium. Our preliminary analyses indicate that ectopic CXCR7bRFP is well tolerated within the primordium and does not appear to adversely affect primordium migration. However, the mosaic nature of the expression may mean that the number of cells expressing CXCR7bRFP is not sufficient to effect migration. When CXCR7bRFP is expressed at the very leading edge of the primordium it appears to be retained in intracellular vesicles away from the cell membrane. This could suggest trafficking of CXCR7bRFP is regulated in these cells preventing it from exerting an effect on primordium migration.

In addition, ectopic expression of CXCR7bRFP in the somites, other than within the horizontal myoseptum, does not effect the migration of the primordium. However, when CXCR7bRFP is expressed on the migration pathway it causes migration to stall as the primordium seeks out an alternative route thus avoiding the CXCR7bRFP region in order to continue its posterior-ward migration. This could indicate that CXCR7b has a role in absorbing SDF1a from the environment, thereby creating the directional nature of primordium migration in the apparent absence of a ligand gradient as suggested by Dambly-Chaudière *et al.* (Dambly-Chaudiere et al., 2007). In any case the relationship between *sdf1a*, *cxcr4b* and *cxcr7b* is worthy of, and will require, further investigation.

The Xu lab has developed an *hmx3:gal4* transgenic zebrafish line thus it should be possible to drive expression of CXCR4b or CXCR7b throughout the primordium by designing constructs that place *cxcr4b*, or *cxcr7b*, under the transcriptional regulation of the *uas* promoter (Scheer and Campos-Ortega, 1999). Unfortunately time constraints prevent these avenues from being pursued at this time.

# Chapter 10: General discussion

## 10.1 *cxcr7*

We set out with the aim of identifying genes that could be involved in establishing directionality in a multicellular migratory system. To do this we chose to utilise the migration of the zebrafish posterior lateral line primordium. In order to identify potential genes we conducted an *in situ* hybridisation screen. As a result of the screening process we were able to identify five genes with differential expression patterns one of which was the EST cb900. Subsequent sequence analysis identified cb900 as the orphan GPCR RDC1. RDC1 has since been shown to bind the CXC-type chemokine ligands CXCL11 (ITAC) and CXCL12 (SDF1) (Burns et al., 2006; Proost et al., 2007) (Balabanian et al., 2005). As the binding of CXC-type chemokine ligands is the defining property of a CXC-type chemokine receptor, RDC1 has been renamed CXCR7 (Burns et al., 2006; Proost et al., 2007) (Balabanian et al., 2005). Two *cxcr7* genes have been identified in the zebrafish genome and named *cxcr7a* and *cxcr7b* (Miyasaka et al., 2007); cb900 pertains to *cxcr7b* (ZFIN). Our conclusion that the EST cb900 is the chemokine receptor CXCR7 is in agreement with the published work of Dambly-Chaudiere *et al.* (Dambly-Chaudiere et al., 2007).

## 10.2 Initiation of primordium migration

Using confocal timelapse microscopy we have been able to conduct detailed study of the initial stages of the migration of the posterior lateral line primodium, a hereto little examined process in zebrafish. Our analysis has demonstrated that the primordium forms from several distinct parts; the main primordium and lateral line ganglion form from the lateral line placode posterior to the otic vesicle. In addition, we have identified small clusters of cells posterior to the main primordium which are derived from the posterior lateral line placode, as indicated by their expression of the marker for this tissue *hmx3*. These separated cell clusters display membrane protrusions and are capable of migrating short distances but fail to make significant progress along the horizontal myoseptum. *In situ* hybridisation revealed that both the main primordium and separated cell clusters express the chemokine receptor *cxcr4b* at a time when *sdf1a* is expressed along the horizontal myoseptum. This suggested that the protrusive activity was due to the cells responding to SDF1a, however, expression of *cxcr4b* alone does not appear to be sufficient to drive directional migration. Intriguingly, *in situ* hybridisation revealed that expression of *cxcr7b* in the trailing region of the primordium correlated well with the initiation of directed migration along the horizontal myoseptum. Furthermore, by using

morpholino mediated knockdown of *cxcr7b* we have been able to demonstrate that the main primodium and separated cells remain protrusive in the absence of *cxcr7b* but fail to migrate along the horizontal myoseptum. This led us to conclude that *cxcr7b* has a role in the initiation of the directed migration of the primordium along the horizontal myoseptum.

In addition, we have been able to demonstrate that the incorporation of the separated cells correlates with an increase in the migration speed of the primordium along the horizontal myoseptum. This raises the intriguing possibility that the separated cells may have a specific function in guiding the migration of the primordium. This role could potentially be similar to that of the distal tip-cells in the formation of the *C. elegans* gonad (Lehmann, 2001) or tip-cells in the migration of *Drosophila* tracheal cells to form the tracheal branches (Ribeiro et al., 2002). These tip-cells are specialised cells that act to guide the migration of other cells associated with them, as such they have specific behavioural characteristics. Work conducted in the Gilmour lab has shown that when wild-type cells transplanted into the *Odysseus* mutant background move to the tip of the primordium they can organise the rest of the primordium and rescue migration. Furthermore, when *Ody* -/- cells are transplanted into a wild-type background they are excluded from the leading positions but are capable of migrating with the primordium (Haas and Gilmour, 2006). In addition, laser ablation work in the Gilmour lab has shown that when cells are ablated behind the leading edge of the primordium the migration of the leading cells stalls until the main primordium regains contact ( 5$^{th}$ European Zebrafish Meeting (Haas, 2007)). This is reminiscent of the behaviour of the separated cells prior to fusion with the main primordium.

However, our tracking data indicates that the separated cells do not remain at the leading edge of the primordium which may indicate that they are not tip-cells. But due to the difficulties of cell tracking we cannot exclude the possibility and further work will be required to analyse the function of the separated cells in primordium migration. To address these questions there are a number of potential avenues available. Mosaic expression of fluorescent constructs to achieve expression in the separated cells may facilitate easier tracking of their movements. It may also be possible to conduct a further *in situ* hybridisation screen to identify specific markers for the separated cells. This would allow the location of the cells to be determined in the primordium following coalescence. It may also be possible to use genetic ablation (Pisharath et al., 2007) to specifically remove the separated cells to examine their role in migration. Additionally, it may be possible to use laser ablation

to destroy the separated cells. However, both methods have the caveat that cell debris, or damage to the *sdf1a* stripe, may also adversely effect migration.

## 10.3 Role of *cxcr7b* in primordium migration

The chemokine receptor *cxcr4b* and its ligand, *sdf1a*, are known to be required for the successful migration of the primordium (David et al., 2002; Li et al., 2004). In addition, the receptor CXCR7 has been shown to bind SDF1 (Balabanian et al., 2005; Burns et al., 2006; Wang et al., 2007). CXCR7 has also been shown to increase the adhesion of cells to their substrate *in vitro* (Burns et al., 2006) and may have a role in increasing tumour cell adhesion (Miao et al., 2007). *In situ* hybridisation analysis revealed that the zebrafish homologue of CXCR7, *cxcr7b*, is expressed in the trailing region of the primordium, the deposited interneuromast cells and neuromast precursors. This expression is complementary to *cxcr4b* but with a broad region of overlap. We were thus intrigued as to the function of *cxcr7b* in guiding primordium migration. Morpholino mediated knockdown of *cxcr7b* resulted in retardation of primordium migration and ventral migration at approximately the region of the forming pectoral fin bud. We have demonstrated that the ventral migration phenotype also occurs in embryos deficient for *sdf1a* or *cxcr4b*. However, the effect is most severe when *sdf1a* function is abrogated and least severe when *cxcr4b* function is compromised. This suggests that there may be a greater requirement for *cxcr7b* function for successful migration of the primordium than for *cxcr4b*. Furthermore, partial knockdown of *cxcr4b* and *cxcr7b* alone and in combination revealed that while *cxcr4b* has a role in guiding primordium migration *cxcr7b* is required to hold the primordium onto the *sdf1a* pathway, and may have a role in increasing cell adhesion (Burns et al., 2006; Miao et al., 2007), and loss of both receptors results in a severe ventral migration toward the pectoral fin. In addition, confocal timelapse analysis of the behaviour of *cxcr7b* morphant primordia revealed that the ventral migration of the primordium is an active process wherein the primordium fails to remain associated with the *sdf1a* stripe.

The consistent ventral migration phenotype led us to consider whether the aberrant migration could be due to attractive cues emanating from the primordium. Our preliminary studies to elucidate these attractive cues revealed the presence of *fgf10* and *fgfr1* expression in the primordium during the migration initiation period and within the migrating primordium. By using chemical inhibition of FGFR signalling in backgrounds deficient for *cxcr4b*, *cxcr7b* or *sdf1a* we were able to demonstrate that the ventral migration phenotype could be attributed to FGFR signalling. Thus it may be that FGF signalling is involved in the initial stage of migration of the primordium

and the continued migration of the primordium along the horizontal myoseptum. However, it is likely that FGF signalling is secondary to GPCR mediated guidance of the migration as we do not observe migration defects when FGF signalling alone is inhibited. Although as both GPCR and FGFR signalling pathways commonly activate the MAPK pathway it is feasible that there is interplay between the two receptor pathways to control migration and/or gene regulation. Indeed the concept of interplay between GPCRs and receptor tyrosine kinases (including FGFRs) is well established and may even occur through interactions between the two receptors (Delcourt et al., 2007).

Elucidation of the role of FGF signalling in primordium migration and any interplay between the two receptors will require a great deal of further work. It will be necessary to characterise which FGFs and FGFRs are expressed by the primordium, when they are expressed and where within the primordium. It may be possible to utilise the *hsp:dn-fgfr1-egfp* transgenic line to temporally disrupt FGFR function to dissect the requirement for FGF signalling during the formation and migration of the posterior lateral line primordium. However, interactions between CXCR7b and CXCR4b may also play roles in primordium migration and elucidating which effects are due to which signalling pathways or interplays between the signalling pathways may prove technically challenging.

## 10.4 Mode of action of CXCR7b

CXCR7 has been shown to interact with CXCL11 (ITAC) (Burns et al., 2006; Proost et al., 2007), CXCL12 (SDF1) (Balabanian et al., 2005; Burns et al., 2006) and potentially additional unknown ligands (Infantino et al., 2006). In our efforts to determine the mode of action of CXCR7b we have utilised an internalisation assay to demonstrate an interaction between CXCR7b and SDF1a. Our results indicate that CXCR7b is internalised as a result of *sdf1a* expression. In light of the growing evidence for interactions between CXCR7 and SDF1 (Balabanian et al., 2005; Burns et al., 2006; Sierro et al., 2007; Wang et al., 2007) it seems reasonable to assume that SDF1a is a ligand of CXCR7b in the posterior lateral line system. However, it is also possible that additional ligands exist that may be involved in the guidance of primordium migration. Furthermore, the domain of co-expression of *cxcr4b* and *cxcr7b* in the primordium may also result in heterodimerisation of the receptors with functional consequences (Sierro et al., 2007).

In our pursuit of the functional role of CXCR7b we have demonstrated that CXCR7b function is required for the migration of the primordial germ cells, however, we have

been unable to demonstrate expression of *cxcr7b* in the PGCs. This result has been confirmed by our collaborators who have shown that *cxcr7b* morphant cells transplanted into wild-type embryos show normal migration to the gonad. In addition, the Raz lab has been able to show that cells expressing CXCR7b internalise SDF1a thereby making it unavailable to CXCR4b. Indeed they have proposed that *cxcr7b* expression in somitic tissue is required to absorb excess SDF1a and helps to confine the PGCs to the region of *sdf1a* expression in the gonad. When CXCR7b function is abrogated the SDF1a gradient fails to establish and the PGCs fail to move efficiently toward the gonad (Boldajipour, 2008 in press)

This role for CXCR7b in ligand sequestration fits well with our own data examining the effect of CXCR7bRFP over-expression induced by heat-shock. We have demonstrated that expression of CXCR7bRFP on the migration pathway stalls the migration of the primordium while it searches for a route around the CXCR7bRFP expressing region. If CXCR7b is indeed acting to internalise SDF1a it may be that migration stalls as the primordium is unable to detect the normal source of SDF1a. In the context of the wild-type primordium it may well be that CXCR7b functions in the trailing region of the primordium to absorb SDF1a produced by the horizontal myoseptum thereby creating a ligand gradient which prevents the primordium migrating in the wrong direction. In effect this would create a ligand gradient that moves with the primordium forcing forward migration.

From our data and that of the Raz laboratory it appears that CXCR7b acts to sequester SDF1a. In addition the Raz group have been able to demonstrate that CXCR7 activity does not result in an increase in intracellular calcium (Boldajipour, 2008 in press), this is in agreement with published work by other groups (Burns et al., 2006; Sierro et al., 2007) and provides further evidence that CXCR7 may function as an atypical GPCR similar to DARC and CCX-CKR (Comerford et al., 2007; Hansell et al., 2006). However, it remains unclear whether this is the sole function of CXCR7 and in light of recent evidence for altered signalling properties when CXCR4 and CXCR7 are co-expressed (Sierro et al., 2007) the function of CXCR7 may be context specific.

Our finding that CXCR7b is required for the migration of the PGCs also raises the question of whether CXCR7, CXCR4 and SDF1 could form a conserved signalling method in other species and migration systems. It could prove informative to study the role of CXCR7 in the migration of PGCs in mice, which have also been shown to require SDF1 and CXCR4 (Ara et al., 2003). Unfortunately, a recent report on the mouse *Cxcr7* knockout did not examine this question (Sierro et al., 2007).

Intriguingly, the *Cxcr7* knockout appears to develop reasonably normally with no reported defects in vascularisation or blood cell maturation; however, the mice do die shortly after birth due to heart formation defects (Sierro et al., 2007). Further study of the mouse knockout will no doubt prove useful to the study of CXCR7 function. In addition, SDF1 signalling through CXCR7 has been shown to lead to increased chemotaxis in T-lymphocytes (Balabanian et al., 2005). It may therefore be that CXCR7 has functions in the chemotaxis of other leukocyte cells and its role in immune responses warrants further investigation.

Further study of the spatial requirement for *cxcr7b* within the migrating primordium may also prove informative as to its function. As the Xu lab has developed an *hmx3:gal4-gfp* transgenic line it may be possible to obtain expression throughout the primordium, or in sub-populations of cells within the primordium, by placing CXCR7b under the transcriptional regulation of the UAS promoter (Scheer and Campos-Ortega, 1999). If over-expression of CXCR7b can be achieved throughout the primordium, and our theory that CXCR7b functions to internalise SDF1a is correct, one would expect that migration would be hindered due to the internalisation of SDF1a preventing it from interacting with CXCR4b. Alternatively, it may be that over-expression of CXCR7b throughout the primordium would increase migration speed as the chemokine gradient at the leading edge would be dramatically increased. It may also be possible to express CXCR7b in a subset of the separated cells by mosaic expression in which case it may be possible to create a miniature primordium capable of migrating along the horizontal myoseptum without the main primordium.

## 10.5 Conclusions and model

Based upon our findings, and in the light of the work of other groups, we suggest the following model for the role of *cxcr7b* in the migration of the posterior lateral line primordium of zebrafish.

Our data indicate that the receptor *cxcr4b* and its ligand, *sdf1a*, are expressed for approximately 2 hours prior to the start of primordium migration. In addition, the separated cells express *cxcr4b* and though they show migratory activity they fail to migrate along the horizontal myoseptum. This indicates that *cxcr7b* is required for the migration of the primordium and failure to migrate results in failure to complete coalescence. These results were confirmed by our timelapse studies of *cxcr7b* morphant embryos which showed that in the absence of *cxcr7b* migration of the primordium is greatly hindered. The ventral migration phenotype we observe in

*cxcr7b* morphants also indicates that *cxcr7b* has a role in holding the primordium onto the *sdf1a* pathway.

Furthermore, *cxcr7b* morphant phenotypes are more reminiscent of those observed for *sdf1a* morphants and *sdf1a* mutants (David et al., 2002; Haas and Gilmour, 2006; Li et al., 2004; Valentin et al., 2007), combined with published data indicating that SDF1 binds CXCR7 (Balabanian et al., 2005; Burns et al., 2006) and that of our collaborators, we propose that CXCR7b and CXCR4b share SDF1a as a ligand. CXCR7 has been shown to bind SDF1 with a tenfold higher affinity than CXCR4 (Balabanian et al., 2005) and work in the Raz lab has shown that CXCR7b expression promotes internalisation of SDF1a (Boldajipour, 2008 in press).

Thus we propose that expression of *cxcr7b* in the trailing cells of the primordium acts to internalise SDF1a produced by the horizontal myoseptum. The internalisation of SDF1a acts to reinforce the directional movement of the primordium as the lead cells seek out higher ligand concentrations resulting in directional movement of the primordium along the horizontal myoseptum. In addition, the trailing cells, which continue to express *cxcr7b*, act to maintain low levels of SDF1a behind the migrating primordium and act as a physical barrier to migration along the horizontal myoseptum in the wrong direction (Figure 36).

If an antibody against the zebrafish form of SDF1a were available it would be intriguing to examine the distribution of SDF1a along the horizontal myoseptum to determine whether a gradient is established and whether SDF1a is internalised by cells expressing CXCR7b. However, this is not possible at this point as antibodies against SDF1a are not available in zebrafish.

However, if CXCR7 and CXCR4 do indeed form heterodimers with altered signalling characteristics as has been suggested (Sierro et al., 2007) it may be that CXCR7b performs slightly different functions in the different regions of the primordium. In addition CXCR7 has been implicated in increasing cell adhesion and promoting cell survival in prostate cancer (Wang et al., 2007) and the MDA breast cancer cell line (Burns et al., 2006) *in vitro*. It could prove informative to study the role of *cxcr7b* in the INCs and neuromasts following deposition. However, study of this is difficult as the poor migration of the primordium when *cxcr7b* is deficient prevents the deposition of INCs and neuromasts. Over-expression of CXCR4b or CXCR7b in different regions of the primordium may prove informative as to whether they interact and produce altered cell behaviours. It may also be possible to conditionally knockdown or over-express the receptors once primordium migration has begun

using the heat-shock inducible Cre/Lox recombinase system (Le et al., 2007). This could facilitate the study of the role of CXCR7b in the INCs and neuromasts.

To conclude, our work on the role of *cxcr7b* in the migration of the posterior lateral line has revealed an essential role for *cxcr7b* in the migration of a multicellular system. However, a great deal more work is required to further analyse the exact mechanism through which *cxcr7b* exerts its influence especially as this role may be context dependant.

**Figure 36: A model for CXCR7b function in posterior lateral line migration**

(a-c) A schematic model of the proposed mode of CXCR7b function in the zebrafish posterior lateral line.

(a) Prior to expression of *cxcr7b*, *cxcr4b* is expressed by the leading part of the primordium and the separated cells where it acts to internalise sdf1a. This leads to local reductions in SDF1a but the cells sense high SDF1a in both directions and therefore fail to migrate.

(b) CXCR7b expression in the trailing cells acts to further internalise SDF1a reinforcing the SDF1a gradient at the leading edge. The cells at the leading edge can now only detect SDF1a in one direction and so commence directional migration along the horizontal myoseptum in response and collect the separated cells as they do so.

(c) As the migration continues the primordium deposits interneuromast cells in its wake that act to maintain low levels of SDF1a behind the primordium and act as a physical barrier that prevents the primordium moving in the wrong direction.

**Figure 36**

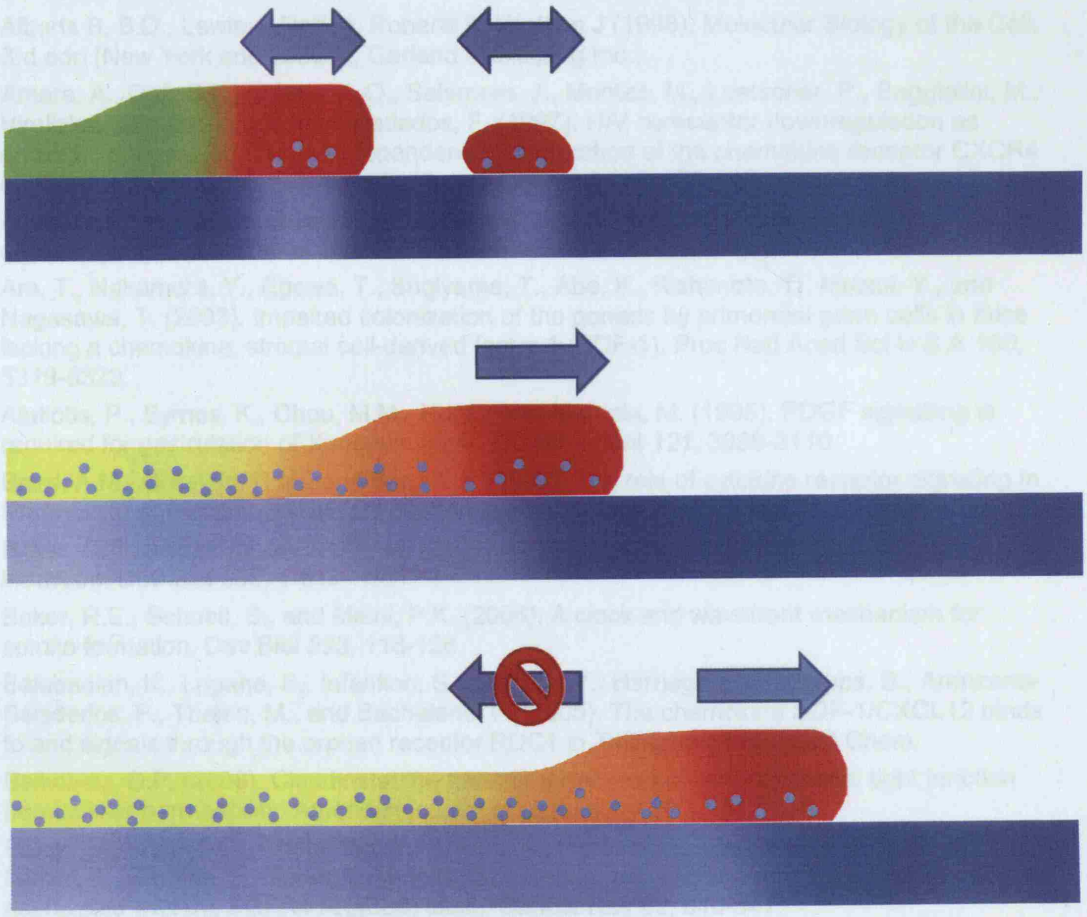

# Bibliography


Abe, G., Ide, H., and Tamura, K. (2007). Function of FGF signaling in the developmental process of the median fin fold in zebrafish. Dev Biol *304*, 355-366.

Adamska, M., Leger, S., Brand, M., Hadrys, T., Braun, T., and Bober, E. (2000). Inner ear and lateral line expression of a zebrafish Nkx5-1 gene and its downregulation in the ears of FGF8 mutant, ace. Mech Dev *97*, 161-165.

Affolter, M., and Weijer, C.J. (2005). Signaling to cytoskeletal dynamics during chemotaxis. Dev Cell *9*, 19-34.

Alberts B, B.D., Lewis J, Raff M, Roberts K, Watson J (1998). Molecular Biology of the Cell, 3rd edn (New York and London, Garland Publishing Inc.).

Amara, A., Gall, S.L., Schwartz, O., Salamero, J., Montes, M., Loetscher, P., Baggiolini, M., Virelizier, J.L., and Arenzana-Seisdedos, F. (1997). HIV coreceptor downregulation as antiviral principle: SDF-1alpha-dependent internalization of the chemokine receptor CXCR4 contributes to inhibition of HIV replication. J Exp Med *186*, 139-146.

Andermann, P., Ungos, J., and Raible, D.W. (2002). Neurogenin1 defines zebrafish cranial sensory ganglia precursors. Dev Biol *251*, 45-58.

Ara, T., Nakamura, Y., Egawa, T., Sugiyama, T., Abe, K., Kishimoto, T., Matsui, Y., and Nagasawa, T. (2003). Impaired colonization of the gonads by primordial germ cells in mice lacking a chemokine, stromal cell-derived factor-1 (SDF-1). Proc Natl Acad Sci U S A *100*, 5319-5323.

Ataliotis, P., Symes, K., Chou, M.M., Ho, L., and Mercola, M. (1995). PDGF signalling is required for gastrulation of Xenopus laevis. Development *121*, 3099-3110.

Baird, A.M., Gerstein, R.M., and Berg, L.J. (1999). The role of cytokine receptor signaling in lymphocyte development. Current opinion in immunology *11*, 157-166.

Baker, C.V., and Bronner-Fraser, M. (2001). Vertebrate cranial placodes I. Embryonic induction. Dev Biol *232*, 1-61.

Baker, R.E., Schnell, S., and Maini, P.K. (2006). A clock and wavefront mechanism for somite formation. Dev Biol *293*, 116-126.

Balabanian, K., Lagane, B., Infantino, S., Chow, K.Y., Harriague, J., Moepps, B., Arenzana-Seisdedos, F., Thelen, M., and Bachelerie, F. (2005). The chemokine SDF-1/CXCL12 binds to and signals through the orphan receptor RDC1 in T lymphocytes. J Biol Chem.

Balkovetz, D.F. (2006). Claudins at the gate: determinants of renal epithelial tight junction paracellular permeability. American journal of physiology *290*, F572-579.

Bange, J., Prechtl, D., Cheburkin, Y., Specht, K., Harbeck, N., Schmitt, M., Knyazeva, T., Muller, S., Gartner, S., Sures, I., *et al.* (2002). Cancer progression and tumor cell motility are associated with the FGFR4 Arg(388) allele. Cancer Res *62*, 840-847.

Bastock, R., and Strutt, D. (2007). The planar polarity pathway promotes coordinated cell migration during Drosophila oogenesis. Development *134*, 3055-3064.

Berchiche, Y.A., Chow, K.Y., Lagane, B., Leduc, M., Percherancier, Y., Fujii, N., Tamamura, H., Bachelerie, F., and Heveker, N. (2007). Direct assessment of CXCR4 mutant conformations reveals complex link between receptor structure and G(alpha)(i) activation. J Biol Chem *282*, 5111-5115.

Blelloch, R., Anna-Arriola, S.S., Gao, D., Li, Y., Hodgkin, J., and Kimble, J. (1999). The gon-1 gene is required for gonadal morphogenesis in Caenorhabditis elegans. Dev Biol *216*, 382-393.

Bleul, C.C., Farzan, M., Choe, H., Parolin, C., Clark-Lewis, I., Sodroski, J., and Springer, T.A. (1996). The lymphocyte chemoattractant SDF-1 is a ligand for LESTR/fusin and blocks HIV-1 entry. Nature *382*, 829-833.

Boilly, B., Vercoutter-Edouart, A.S., Hondermarck, H., Nurcombe, V., and Le Bourhis, X. (2000). FGF signals for cell proliferation and migration through different pathways. Cytokine Growth Factor Rev *11*, 295-302.

Boldajipour, B., Mahabaleshwar, H, Reichman-Fried, M, Kardash, E, Blaser, H, Minina, S, Wilson, D, Xu, Q, Raz,E (2008 in press). Control of chemokine-guided cell migration by ligand sequestration. Cell.

Bonner, J.T. (1970). Induction of stalk cell differentiation by cyclic AMP in the cellular slime mold Dictyostelium discoideum. Proc Natl Acad Sci U S A *65*, 110-113.

Bouley, R., Sun, T.X., Chenard, M., McLaughlin, M., McKee, M., Lin, H.Y., Brown, D., and Ausiello, D.A. (2003). Functional role of the NPxxY motif in internalization of the type 2 vasopressin receptor in LLC-PK1 cells. Am J Physiol Cell Physiol *285*, C750-762.

Brelot, A., Heveker, N., Pleskoff, O., Sol, N., and Alizon, M. (1997). Role of the first and third extracellular domains of CXCR-4 in human immunodeficiency virus coreceptor activity. J Virol *71*, 4744-4751.

Bulenger, S., Marullo, S., and Bouvier, M. (2005). Emerging role of homo- and heterodimerization in G-protein-coupled receptor biosynthesis and maturation. Trends Pharmacol Sci *26*, 131-137.

Burdine, R.D., Chen, E.B., Kwok, S.F., and Stern, M.J. (1997). egl-17 encodes an invertebrate fibroblast growth factor family member required specifically for sex myoblast migration in Caenorhabditis elegans. Proc Natl Acad Sci U S A *94*, 2433-2437.

Burns, J.M., Summers, B.C., Wang, Y., Melikian, A., Berahovich, R., Miao, Z., Penfold, M.E., Sunshine, M.J., Littman, D.R., Kuo, C.J., *et al.* (2006). A novel chemokine receptor for SDF-1 and I-TAC involved in cell survival, cell adhesion, and tumor development. J Exp Med *203*, 2201-2213.

Busillo, J.M., and Benovic, J.L. (2007). Regulation of CXCR4 signaling. Biochim Biophys Acta *1768*, 952-963.

Cernuda-Cernuda, R., and Garcia-Fernandez, J.M. (1996). Structural diversity of the ordinary and specialized lateral line organs. Microscopy research and technique *34*, 302-312.

Chakravarty, P., Suthar, T.P., Coppock, H.A., Nicholl, C.G., Bloom, S.R., Legon, S., and Smith, D.M. (2000). CGRP and adrenomedullin binding correlates with transcript levels for calcitonin receptor-like receptor (CRLR) and receptor activity modifying proteins (RAMPs) in rat tissues. Br J Pharmacol *130*, 189-195.

Chalasani, S.H., Sabelko, K.A., Sunshine, M.J., Littman, D.R., and Raper, J.A. (2003). A chemokine, SDF-1, reduces the effectiveness of multiple axonal repellents and is required for normal axon pathfinding. J Neurosci *23*, 1360-1371.

Charest, P.G., and Firtel, R.A. (2007). Big roles for small GTPases in the control of directed cell movement. Biochem J *401*, 377-390.

Cherla, R.P., and Ganju, R.K. (2001). Stromal cell-derived factor 1 alpha-induced chemotaxis in T cells is mediated by nitric oxide signaling pathways. J Immunol *166*, 3067-3074.

Chong, S.W., Emelyanov, A., Gong, Z., and Korzh, V. (2001). Expression pattern of two zebrafish genes, cxcr4a and cxcr4b. Mech Dev *109*, 347-354.

Chung, C.Y., Funamoto, S., and Firtel, R.A. (2001). Signaling pathways controlling cell polarity and chemotaxis. Trends in biochemical sciences *26*, 557-566.

Comerford, I., Litchfield, W., Harata-Lee, Y., Nibbs, R.J., and McColl, S.R. (2007). Regulation of chemotactic networks by 'atypical' receptors. Bioessays *29*, 237-247.

Cook, J.S., Wolsing, D.H., Lameh, J., Olson, C.A., Correa, P.E., Sadee, W., Blumenthal, E.M., and Rosenbaum, J.S. (1992). Characterization of the RDC1 gene which encodes the canine homolog of a proposed human VIP receptor. Expression does not correlate with an increase in VIP binding sites. FEBS Lett *300*, 149-152.

Dambly-Chaudiere, C., Cubedo, N., and Ghysen, A. (2007). Control of cell migration in the development of the posterior lateral line: antagonistic interactions between the chemokine receptors CXCR4 and CXCR7/RDC1. BMC developmental biology *7*, 23.

David, N.B., Sapede, D., Saint-Etienne, L., Thisse, C., Thisse, B., Dambly-Chaudiere, C., Rosa, F.M., and Ghysen, A. (2002). Molecular basis of cell migration in the fish lateral line: role of the chemokine receptor CXCR4 and of its ligand, SDF1. Proc Natl Acad Sci U S A *99*, 16297-16302.

Davidson, B., Shi, W., and Levine, M. (2005). Uncoupling heart cell specification and migration in the simple chordate Ciona intestinalis. Development *132*, 4811-4818.

Davy, A., and Soriano, P. (2005). Ephrin signaling in vivo: look both ways. Dev Dyn *232*, 1-10.

Delcourt, N., Bockaert, J., and Marin, P. (2007). GPCR-jacking: from a new route in RTK signalling to a new concept in GPCR activation. Trends Pharmacol Sci *28*, 602-607.

Devreotes, P., and Janetopoulos, C. (2003). Eukaryotic chemotaxis: distinctions between directional sensing and polarization. J Biol Chem *278*, 20445-20448.

Doitsidou, M., Reichman-Fried, M., Stebler, J., Koprunner, M., Dorries, J., Meyer, D., Esguerra, C.V., Leung, T., and Raz, E. (2002). Guidance of primordial germ cell migration by the chemokine SDF-1. Cell *111*, 647-659.

Doranz, B.J., Orsini, M.J., Turner, J.D., Hoffman, T.L., Berson, J.F., Hoxie, J.A., Peiper, S.C., Brass, L.F., and Doms, R.W. (1999). Identification of CXCR4 domains that support coreceptor and chemokine receptor functions. J Virol *73*, 2752-2761.

Dormann, D., and Weijer, C.J. (2003). Chemotactic cell movement during development. Curr Opin Genet Dev *13*, 358-364.

Dormann, D., and Weijer, C.J. (2006). Chemotactic cell movement during Dictyostelium development and gastrulation. Curr Opin Genet Dev *16*, 367-373.

Draper, B.W., Morcos, P.A., and Kimmel, C.B. (2001). Inhibition of zebrafish fgf8 pre-mRNA splicing with morpholino oligos: a quantifiable method for gene knockdown. Genesis *30*, 154-156.

Draper, B.W., Stock, D.W., and Kimmel, C.B. (2003). Zebrafish fgf24 functions with fgf8 to promote posterior mesodermal development. Development *130*, 4639-4654.

Duchek, P., and Rorth, P. (2001). Guidance of cell migration by EGF receptor signaling during Drosophila oogenesis. Science *291*, 131-133.

Duchek, P., Somogyi, K., Jekely, G., Beccari, S., and Rorth, P. (2001). Guidance of cell migration by the Drosophila PDGF/VEGF receptor. Cell *107*, 17-26.

Dumstrei, K., Mennecke, R., and Raz, E. (2004). Signaling pathways controlling primordial germ cell migration in zebrafish. J Cell Sci *117*, 4787-4795.

Egea, J., and Klein, R. (2007). Bidirectional Eph-ephrin signaling during axon guidance. Trends Cell Biol *17*, 230-238.

Ekker, S.C., and Larson, J.D. (2001). Morphant technology in model developmental systems. Genesis *30*, 89-93.

Eswarakumar, V.P., Lax, I., and Schlessinger, J. (2005). Cellular signaling by fibroblast growth factor receptors. Cytokine Growth Factor Rev *16*, 139-149.

Fan, G.H., Lapierre, L.A., Goldenring, J.R., Sai, J., and Richmond, A. (2004a). Rab11-family interacting protein 2 and myosin Vb are required for CXCR2 recycling and receptor-mediated chemotaxis. Mol Biol Cell *15*, 2456-2469.

Fan, M., Rhee, J., St-Pierre, J., Handschin, C., Puigserver, P., Lin, J., Jaeger, S., Erdjument-Bromage, H., Tempst, P., and Spiegelman, B.M. (2004b). Suppression of mitochondrial respiration through recruitment of p160 myb binding protein to PGC-1alpha: modulation by p38 MAPK. Genes & development *18*, 278-289.

Fanto, M., and McNeill, H. (2004). Planar polarity from flies to vertebrates. J Cell Sci *117*, 527-533.

Feng, Y., Broder, C.C., Kennedy, P.E., and Berger, E.A. (1996). HIV-1 entry cofactor: functional cDNA cloning of a seven-transmembrane, G protein-coupled receptor. Science *272*, 872-877.

Ferguson, S.S. (2001). Evolving concepts in G protein-coupled receptor endocytosis: the role in receptor desensitization and signaling. Pharmacological reviews *53*, 1-24.

Fischer, S., Draper, B.W., and Neumann, C.J. (2003). The zebrafish fgf24 mutant identifies an additional level of Fgf signaling involved in vertebrate forelimb initiation. Development *130*, 3515-3524.

Fredriksson, R., Lagerstrom, M.C., Lundin, L.G., and Schioth, H.B. (2003). The G-protein-coupled receptors in the human genome form five main families. Phylogenetic analysis, paralogon groups, and fingerprints. Molecular pharmacology *63*, 1256-1272.

Funamoto, S., Meili, R., Lee, S., Parry, L., and Firtel, R.A. (2002). Spatial and temporal regulation of 3-phosphoinositides by PI 3-kinase and PTEN mediates chemotaxis. Cell *109*, 611-623.

Futahashi, Y., Komano, J., Urano, E., Aoki, T., Hamatake, M., Miyauchi, K., Yoshida, T., Koyanagi, Y., Matsuda, Z., and Yamamoto, N. (2007). Separate elements are required for

ligand-dependent and -independent internalization of metastatic potentiator CXCR4. Cancer science *98*, 373-379.

Gerhardt, H., Golding, M., Fruttiger, M., Ruhrberg, C., Lundkvist, A., Abramsson, A., Jeltsch, M., Mitchell, C., Alitalo, K., Shima, D., *et al.* (2003). VEGF guides angiogenic sprouting utilizing endothelial tip cell filopodia. J Cell Biol *161*, 1163-1177.

Gilmour, D. (2005). Dynamic cell-cell interactions regulate migration behaviour during zebrafish sensory nervous development. In BSCB/BSDB Annual Spring Meeting 2005 (York).

Gilmour, D., Knaut, H., Maischein, H.M., and Nusslein-Volhard, C. (2004). Towing of sensory axons by their migrating target cells in vivo. Nat Neurosci *7*, 491-492.

Gilmour, D.T., Maischein, H.M., and Nusslein-Volhard, C. (2002). Migration and function of a glial subtype in the vertebrate peripheral nervous system. Neuron *34*, 577-588.

Godenschwege, T.A., Hu, H., Shan-Crofts, X., Goodman, C.S., and Murphey, R.K. (2002). Bi-directional signaling by Semaphorin 1a during central synapse formation in Drosophila. Nat Neurosci *5*, 1294-1301.

Goidl, E.A., Chassy, B.M., Love, L.L., and Krichevsky, M.I. (1972). Inhibition of aggregation and differentiation of Dictyostelium discoideum by antibodies against adenosine 3':5'-cyclic monophosphate diesterase. Proc Natl Acad Sci U S A *69*, 1128-1130.

Gompel, N., Cubedo, N., Thisse, C., Thisse, B., Dambly-Chaudiere, C., and Ghysen, A. (2001). Pattern formation in the lateral line of zebrafish. Mech Dev *105*, 69-77.

Gospodarowicz, D., Jones, K.L., and Sato, G. (1974). Purification of a growth factor for ovarian cells from bovine pituitary glands. Proc Natl Acad Sci U S A *71*, 2295-2299.

Grant, K.A., Raible, D.W., and Piotrowski, T. (2005). Regulation of latent sensory hair cell precursors by glia in the zebrafish lateral line. Neuron *45*, 69-80.

Haas, P., Colombelli, J, Stelzer, E, Gilmour D (2007). Reciprorocal interaction between leading and following cells ensures directed tissue migration. Paper presented at: 5th European Zebrafish Genetics and Development Meeting (Amsterdam).

Haas, P., and Gilmour, D. (2006). Chemokine signaling mediates self-organizing tissue migration in the zebrafish lateral line. Dev Cell *10*, 673-680.

Hansell, C.A., Simpson, C.V., and Nibbs, R.J. (2006). Chemokine sequestration by atypical chemokine receptors. Biochem Soc Trans *34*, 1009-1013.

Haribabu, B., Richardson, R.M., Fisher, I., Sozzani, S., Peiper, S.C., Horuk, R., Ali, H., and Snyderman, R. (1997). Regulation of human chemokine receptors CXCR4. Role of phosphorylation in desensitization and internalization. J Biol Chem *272*, 28726-28731.

Heesen, M., Berman, M.A., Benson, J.D., Gerard, C., and Dorf, M.E. (1996). Cloning of the mouse fusin gene, homologue to a human HIV-1 co-factor. J Immunol *157*, 5455-5460.

Heesen, M., Berman, M.A., Charest, A., Housman, D., Gerard, C., and Dorf, M.E. (1998). Cloning and chromosomal mapping of an orphan chemokine receptor: mouse RDC1. Immunogenetics *47*, 364-370.

Hiratsuka, S., Kataoka, Y., Nakao, K., Nakamura, K., Morikawa, S., Tanaka, S., Katsuki, M., Maru, Y., and Shibuya, M. (2005). Vascular endothelial growth factor A (VEGF-A) is involved in guidance of VEGF receptor-positive cells to the anterior portion of early embryos. Molecular and cellular biology *25*, 355-363.

Hollway, G.E., Bryson-Richardson, R.J., Berger, S., Cole, N.J., Hall, T.E., and Currie, P.D. (2007). Whole-somite rotation generates muscle progenitor cell compartments in the developing zebrafish embryo. Dev Cell *12*, 207-219.

Horuk, R. (2001). Chemokine receptors. Cytokine Growth Factor Rev *12*, 313-335.

Huang, C., Jacobson, K., and Schaller, M.D. (2004). MAP kinases and cell migration. J Cell Sci *117*, 4619-4628.

Hubbard, E.J., and Greenstein, D. (2000). The Caenorhabditis elegans gonad: a test tube for cell and developmental biology. Dev Dyn *218*, 2-22.

Iijima, M., and Devreotes, P. (2002). Tumor suppressor PTEN mediates sensing of chemoattractant gradients. Cell *109*, 599-610.

Infantino, S., Moepps, B., and Thelen, M. (2006). Expression and Regulation of the Orphan Receptor RDC1 and Its Putative Ligand in Human Dendritic and B Cells. J Immunol *176*, 2197-2207.

Itoh, M., and Chitnis, A.B. (2001). Expression of proneural and neurogenic genes in the zebrafish lateral line primordium correlates with selection of hair cell fate in neuromasts. Mech Dev *102*, 263-266.

Itoh, N. (2007). The Fgf families in humans, mice, and zebrafish: their evolutional processes and roles in development, metabolism, and disease. Biological & pharmaceutical bulletin *30*, 1819-1825.

Itoh, N., and Ornitz, D.M. (2004). Evolution of the Fgf and Fgfr gene families. Trends Genet *20*, 563-569.

Ji, T.H., Grossmann, M., and Ji, I. (1998). G protein-coupled receptors. I. Diversity of receptor-ligand interactions. J Biol Chem *273*, 17299-17302.

Johnson, D.E., and Williams, L.T. (1993). Structural and functional diversity in the FGF receptor multigene family. Advances in cancer research *60*, 1-41.

Johnson, M.S., Robertson, D.N., Holland, P.J., Lutz, E.M., and Mitchell, R. (2006). Role of the conserved NPxxY motif of the 5-HT2A receptor in determining selective interaction with isoforms of ADP-ribosylation factor (ARF). Cell Signal *18*, 1793-1800.

Jones, L.C., Okino, S.T., Gonda, T.J., and Whitlock, J.P., Jr. (2002). Myb-binding protein 1a augments AhR-dependent gene expression. J Biol Chem *277*, 22515-22519.

Jones, S.W., Brockbank, S.M., Mobbs, M.L., Le Good, N.J., Soma-Haddrick, S., Heuze, A.J., Langham, C.J., Timms, D., Newham, P., and Needham, M.R. (2006). The orphan G-protein coupled receptor RDC1: evidence for a role in chondrocyte hypertrophy and articular cartilage matrix turnover. Osteoarthritis Cartilage.

Jordan, B.A., and Devi, L.A. (1999). G-protein-coupled receptor heterodimerization modulates receptor function. Nature *399*, 697-700.

Kalatskaya, I., Schussler, S., Blaukat, A., Muller-Esterl, W., Jochum, M., Proud, D., and Faussner, A. (2004). Mutation of tyrosine in the conserved NPXXY sequence leads to constitutive phosphorylation and internalization, but not signaling, of the human B2 bradykinin receptor. J Biol Chem *279*, 31268-31276.

Kang, J., Shi, Y., Xiang, B., Qu, B., Su, W., Zhu, M., Zhang, M., Bao, G., Wang, F., Zhang, X., *et al.* (2005). A nuclear function of beta-arrestin1 in GPCR signaling: regulation of histone acetylation and gene transcription. Cell *123*, 833-847.

Kantor, D.B., Chivatakarn, O., Peer, K.L., Oster, S.F., Inatani, M., Hansen, M.J., Flanagan, J.G., Yamaguchi, Y., Sretavan, D.W., Giger, R.J., *et al.* (2004). Semaphorin 5A is a bifunctional axon guidance cue regulated by heparan and chondroitin sulfate proteoglycans. Neuron *44*, 961-975.

Kapas, S., and Clark, A.J. (1995). Identification of an orphan receptor gene as a type 1 calcitonin gene-related peptide receptor. Biochem Biophys Res Commun *217*, 832-838.

Keller, R. (2005). Cell migration during gastrulation. Curr Opin Cell Biol *17*, 533-541.

Kilian, B., Mansukoski, H., Barbosa, F.C., Ulrich, F., Tada, M., and Heisenberg, C.P. (2003). The role of Ppt/Wnt5 in regulating cell shape and movement during zebrafish gastrulation. Mech Dev *120*, 467-476.

Kimble, J.E., and White, J.G. (1981). On the control of germ cell development in Caenorhabditis elegans. Dev Biol *81*, 208-219.

Kimmel, C.B., Ballard, W.W., Kimmel, S.R., Ullmann, B., and Schilling, T.F. (1995). Stages of embryonic development of the zebrafish. Dev Dyn *203*, 253-310.

Klagsbrun, M., and Eichmann, A. (2005). A role for axon guidance receptors and ligands in blood vessel development and tumor angiogenesis. Cytokine Growth Factor Rev *16*, 535-548.

Knaut, H., Blader, P., Strahle, U., and Schier, A.F. (2005). Assembly of trigeminal sensory ganglia by chemokine signaling. Neuron *47*, 653-666.

Knaut, H., Steinbeisser, H., Schwarz, H., and Nusslein-Volhard, C. (2002). An evolutionary conserved region in the vasa 3'UTR targets RNA translation to the germ cells in the zebrafish. Curr Biol *12*, 454-466.

Knaut, H., Werz, C., Geisler, R., and Nusslein-Volhard, C. (2003). A zebrafish homologue of the chemokine receptor Cxcr4 is a germ-cell guidance receptor. Nature *421*, 279-282.

Kobilka, B.K. (2007). G protein coupled receptor structure and activation. Biochim Biophys Acta *1768*, 794-807.

Kobilka, B.K., and Deupi, X. (2007). Conformational complexity of G-protein-coupled receptors. Trends Pharmacol Sci *28*, 397-406.

Konijn, T.M., van de Meene, J.G., Chang, Y.Y., Barkley, D.S., and Bonner, J.T. (1969). Identification of adenosine-3',5'-monophosphate as the bacterial attractant for myxamoebae of Dictyostelium discoideum. Journal of bacteriology *99*, 510-512.

Koprunner, M., Thisse, C., Thisse, B., and Raz, E. (2001). A zebrafish nanos-related gene is essential for the development of primordial germ cells. Genes & development *15*, 2877-2885.

Kruger, R.P., Aurandt, J., and Guan, K.L. (2005). Semaphorins command cells to move. Nat Rev Mol Cell Biol *6*, 789-800.

Krull, C.E., Lansford, R., Gale, N.W., Collazo, A., Marcelle, C., Yancopoulos, G.D., Fraser, S.E., and Bronner-Fraser, M. (1997). Interactions of Eph-related receptors and ligands confer rostrocaudal pattern to trunk neural crest migration. Curr Biol *7*, 571-580.

Kucia, M., Jankowski, K., Reca, R., Wysoczynski, M., Bandura, L., Allendorf, D.J., Zhang, J., Ratajczak, J., and Ratajczak, M.Z. (2004). CXCR4-SDF-1 signalling, locomotion, chemotaxis and adhesion. J Mol Histol *35*, 233-245.

Kulbe, H., Levinson, N.R., Balkwill, F., and Wilson, J.L. (2004). The chemokine network in cancer--much more than directing cell movement. Int J Dev Biol *48*, 489-496.

Laguerre, L., Soubiran, F., Ghysen, A., Konig, N., and Dambly-Chaudiere, C. (2005). Cell proliferation in the developing lateral line system of zebrafish embryos. Dev Dyn.

Le, X., Langenau, D.M., Keefe, M.D., Kutok, J.L., Neuberg, D.S., and Zon, L.I. (2007). Heat shock-inducible Cre/Lox approaches to induce diverse types of tumors and hyperplasia in transgenic zebrafish. Proc Natl Acad Sci U S A *104*, 9410-9415.

Ledent, V. (2002). Postembryonic development of the posterior lateral line in zebrafish. Development *129*, 597-604.

Lee, S., Howell, B., and Kunapuli, P. (2006). Cell imaging assays for G protein-coupled receptor internalization: application to high-throughput screening. Methods in enzymology *414*, 79-98.

Lee, Y., Grill, S., Sanchez, A., Murphy-Ryan, M., and Poss, K.D. (2005). Fgf signaling instructs position-dependent growth rate during zebrafish fin regeneration. Development *132*, 5173-5183.

Lefkowitz, R.J., and Shenoy, S.K. (2005). Transduction of receptor signals by beta-arrestins. Science *308*, 512-517.

Leger, S., and Brand, M. (2002). Fgf8 and Fgf3 are required for zebrafish ear placode induction, maintenance and inner ear patterning. Mech Dev *119*, 91-108.

Lehmann, R. (2001). Cell migration in invertebrates: clues from border and distal tip cells. Curr Opin Genet Dev *11*, 457-463.

Levoye, A., Dam, J., Ayoub, M.A., Guillaume, J.L., and Jockers, R. (2006). Do orphan G-protein-coupled receptors have ligand-independent functions? New insights from receptor heterodimers. EMBO reports *7*, 1094-1098.

Li, Q., Shirabe, K., and Kuwada, J.Y. (2004). Chemokine signaling regulates sensory cell migration in zebrafish. Dev Biol *269*, 123-136.

Li, Q., Shirabe, K., Thisse, C., Thisse, B., Okamoto, H., Masai, I., and Kuwada, J.Y. (2005). Chemokine signaling guides axons within the retina in zebrafish. J Neurosci *25*, 1711-1717.

Li, S., and Muneoka, K. (1999). Cell migration and chick limb development: chemotactic action of FGF-4 and the AER. Dev Biol *211*, 335-347.

Libert, F., Parmentier, M., Lefort, A., Dinsart, C., Van Sande, J., Maenhaut, C., Simons, M.J., Dumont, J.E., and Vassart, G. (1989). Selective amplification and cloning of four new members of the G protein-coupled receptor family. Science *244*, 569-572.

Libert, F., Parmentier, M., Lefort, A., Dumont, J.E., and Vassart, G. (1990). Complete nucleotide sequence of a putative G protein coupled receptor: RDC1. Nucleic Acids Res *18*, 1917.

Lin, F., Sepich, D.S., Chen, S., Topczewski, J., Yin, C., Solnica-Krezel, L., and Hamm, H. (2005). Essential roles of G{alpha}12/13 signaling in distinct cell behaviors driving zebrafish convergence and extension gastrulation movements. J Cell Biol *169*, 777-787.

Lopez-Schier, H., and Hudspeth, A.J. (2005). Supernumerary neuromasts in the posterior lateral line of zebrafish lacking peripheral glia. Proc Natl Acad Sci U S A *102*, 1496-1501.

Luttrell, L.M. (2002). Activation and targeting of mitogen-activated protein kinases by G-protein-coupled receptors. Canadian journal of physiology and pharmacology *80*, 375-382.

Marchese, A., and Benovic, J.L. (2001). Agonist-promoted ubiquitination of the G protein-coupled receptor CXCR4 mediates lysosomal sorting. J Biol Chem *276*, 45509-45512.

Marchese, A., Chen, C., Kim, Y.M., and Benovic, J.L. (2003). The ins and outs of G protein-coupled receptor trafficking. Trends in biochemical sciences *28*, 369-376.

Martin, G.R. (1998). The roles of FGFs in the early development of vertebrate limbs. Genes & development *12*, 1571-1586.

Martinez, A., Kapas, S., Miller, M.J., Ward, Y., and Cuttitta, F. (2000). Coexpression of Receptors for Adrenomedullin, Calcitonin Gene-Related Peptide, and Amylin in Pancreatic beta-Cells. Endocrinology *141*, 406-411.

Megason, S.G., and Fraser, S.E. (2003). Digitizing life at the level of the cell: high-performance laser-scanning microscopy and image analysis for in toto imaging of development. Mech Dev *120*, 1407-1420.

Mellado, M., Rodriguez-Frade, J.M., Vila-Coro, A.J., Fernandez, S., Martin de Ana, A., Jones, D.R., Toran, J.L., and Martinez, A.C. (2001a). Chemokine receptor homo- or heterodimerization activates distinct signaling pathways. Embo J *20*, 2497-2507.

Mellado, M., Vila-Coro, A.J., Martinez, C., and Rodriguez-Frade, J.M. (2001b). Receptor dimerization: a key step in chemokine signaling. Cellular and molecular biology (Noisy-le-Grand, France) *47*, 575-582.

Mellitzer, G., Xu, Q., and Wilkinson, D.G. (1999). Eph receptors and ephrins restrict cell intermingling and communication. Nature *400*, 77-81.

Metcalfe, W.K. (1985). Sensory neuron growth cones comigrate with posterior lateral line primordial cells in zebrafish. J Comp Neurol *238*, 218-224.

Metcalfe, W.K., Kimmel, C.B., and Schabtach, E. (1985). Anatomy of the posterior lateral line system in young larvae of the zebrafish. J Comp Neurol *233*, 377-389.

Miao, Z., Luker, K.E., Summers, B.C., Berahovich, R., Bhojani, M.S., Rehemtulla, A., Kleer, C.G., Essner, J.J., Nasevicius, A., Luker, G.D., *et al.* (2007). CXCR7 (RDC1) promotes breast and lung tumor growth in vivo and is expressed on tumor-associated vasculature. Proc Natl Acad Sci U S A *104*, 15735-15740.

Milligan, G., Canals, M., Pediani, J.D., Ellis, J., and Lopez-Gimenez, J.F. (2006). The role of GPCR dimerisation/oligomerisation in receptor signalling. Ernst Schering Foundation symposium proceedings *2*, 145-161.

Mirkovic, I., and Mlodzik, M. (2006). Cooperative activities of drosophila DE-cadherin and DN-cadherin regulate the cell motility process of ommatidial rotation. Development *133*, 3283-3293.

Miyasaka, N., Knaut, H., and Yoshihara, Y. (2007). Cxcl12/Cxcr4 chemokine signaling is required for placode assembly and sensory axon pathfinding in the zebrafish olfactory system. Development *134*, 2459-2468.

Mohammadi, M., McMahon, G., Sun, L., Tang, C., Hirth, P., Yeh, B.K., Hubbard, S.R., and Schlessinger, J. (1997). Structures of the tyrosine kinase domain of fibroblast growth factor receptor in complex with inhibitors. Science *276*, 955-960.

Molyneaux, K., and Wylie, C. (2004). Primordial germ cell migration. Int J Dev Biol *48*, 537-544.

Montell, D.J. (2003). Border-cell migration: the race is on. Nat Rev Mol Cell Biol *4*, 13-24.

Montero, J.A., Kilian, B., Chan, J., Bayliss, P.E., and Heisenberg, C.P. (2003). Phosphoinositide 3-kinase is required for process outgrowth and cell polarization of gastrulating mesendodermal cells. Curr Biol *13*, 1279-1289.

Moriyoshi, K., Richards, L.J., Akazawa, C., O'Leary, D.D., and Nakanishi, S. (1996). Labeling neural cells using adenoviral gene transfer of membrane-targeted GFP. Neuron *16*, 255-260.

Murphy, A.M., Lee, T., Andrews, C.M., Shilo, B.Z., and Montell, D.J. (1995). The breathless FGF receptor homolog, a downstream target of Drosophila C/EBP in the developmental control of cell migration. Development *121*, 2255-2263.

Nagel, M., Tahinci, E., Symes, K., and Winklbauer, R. (2004). Guidance of mesoderm cell migration in the Xenopus gastrula requires PDGF signaling. Development *131*, 2727-2736.

Nasevicius, A., and Ekker, S.C. (2000). Effective targeted gene 'knockdown' in zebrafish. Nature genetics *26*, 216-220.

Neves, S.R., Ram, P.T., and Iyengar, R. (2002). G protein pathways. Science *296*, 1636-1639.

Ng, J.K., Kawakami, Y., Buscher, D., Raya, A., Itoh, T., Koth, C.M., Rodriguez Esteban, C., Rodriguez-Leon, J., Garrity, D.M., Fishman, M.C., *et al.* (2002). The limb identity gene Tbx5 promotes limb initiation by interacting with Wnt2b and Fgf10. Development *129*, 5161-5170.

Nishio, M., Watanabe, K., Sasaki, J., Taya, C., Takasuga, S., Iizuka, R., Balla, T., Yamazaki, M., Watanabe, H., Itoh, R., *et al.* (2007). Control of cell polarity and motility by the PtdIns(3,4,5)P3 phosphatase SHIP1. Nat Cell Biol *9*, 36-44.

Nishiumi, F., Komiya, T., and Ikenishi, K. (2005). The mode and molecular mechanisms of the migration of presumptive PGC in the endoderm cell mass of Xenopus embryos. Development, growth & differentiation *47*, 37-48.

Nomura, R., Kamei, E., Hotta, Y., Konishi, M., Miyake, A., and Itoh, N. (2006). Fgf16 is essential for pectoral fin bud formation in zebrafish. Biochem Biophys Res Commun *347*, 340-346.

Norton, W.H., Ledin, J., Grandel, H., and Neumann, C.J. (2005). HSPG synthesis by zebrafish Ext2 and Extl3 is required for Fgf10 signalling during limb development. Development *132*, 4963-4973.

Oberlin, E., Amara, A., Bachelerie, F., Bessia, C., Virelizier, J.L., Arenzana-Seisdedos, F., Schwartz, O., Heard, J.M., Clark-Lewis, I., Legler, D.F., *et al.* (1996). The CXC chemokine SDF-1 is the ligand for LESTR/fusin and prevents infection by T-cell-line-adapted HIV-1. Nature *382*, 833-835.

Orsini, M.J., Parent, J.L., Mundell, S.J., Benovic, J.L., and Marchese, A. (1999). Trafficking of the HIV coreceptor CXCR4. Role of arrestins and identification of residues in the c-terminal tail that mediate receptor internalization. J Biol Chem *274*, 31076-31086.

Owen, H.R., Elser, M., Cheung, E., Gersbach, M., Kraus, W.L., and Hottiger, M.O. (2007). MYBBP1a is a novel repressor of NF-kappaB. Journal of molecular biology *366*, 725-736.

Pauls, S., Geldmacher-Voss, B., and Campos-Ortega, J.A. (2001). A zebrafish histone variant H2A.F/Z and a transgenic H2A.F/Z:GFP fusion protein for in vivo studies of embryonic development. Dev Genes Evol *211*, 603-610.

Pisharath, H., Rhee, J.M., Swanson, M.A., Leach, S.D., and Parsons, M.J. (2007). Targeted ablation of beta cells in the embryonic zebrafish pancreas using E. coli nitroreductase. Mech Dev *124*, 218-229.

Poliakov, A., Cotrina, M., and Wilkinson, D.G. (2004). Diverse roles of eph receptors and ephrins in the regulation of cell migration and tissue assembly. Dev Cell *7*, 465-480.

Popowicz, G.M., Schleicher, M., Noegel, A.A., and Holak, T.A. (2006). Filamins: promiscuous organizers of the cytoskeleton. Trends in biochemical sciences *31*, 411-419.

Pourquie, O. (2004). The chick embryo: a leading model in somitogenesis studies. Mech Dev *121*, 1069-1079.

Procko, E., and McColl, S.R. (2005). Leukocytes on the move with phosphoinositide 3-kinase and its downstream effectors. Bioessays *27*, 153-163.

Proost, P., Mortier, A., Loos, T., Vandercappellen, J., Gouwy, M., Ronsse, I., Schutyser, E., Put, W., Parmentier, M., Struyf, S., *et al.* (2007). Proteolytic processing of CXCL11 by CD13/aminopeptidase N impairs CXCR3 and CXCR7 binding and signalling and reduces lymphocyte and endothelial cell migration. Blood.

Raible, F., and Brand, M. (2001). Tight transcriptional control of the ETS domain factors Erm and Pea3 by Fgf signaling during early zebrafish development. Mech Dev *107*, 105-117.

Ribeiro, C., Ebner, A., and Affolter, M. (2002). In vivo imaging reveals different cellular functions for FGF and Dpp signaling in tracheal branching morphogenesis. Dev Cell *2*, 677-683.

Ridley, A.J., Schwartz, M.A., Burridge, K., Firtel, R.A., Ginsberg, M.H., Borisy, G., Parsons, J.T., and Horwitz, A.R. (2003). Cell migration: integrating signals from front to back. Science *302*, 1704-1709.

Robu, M.E., Larson, J.D., Nasevicius, A., Beiraghi, S., Brenner, C., Farber, S.A., and Ekker, S.C. (2007). p53 activation by knockdown technologies. PLoS genetics *3*, e78.

Roehl, H., and Nusslein-Volhard, C. (2001). Zebrafish pea3 and erm are general targets of FGF8 signaling. Curr Biol *11*, 503-507.

Rohde, L.A., and Heisenberg, C.P. (2007). Zebrafish gastrulation: cell movements, signals, and mechanisms. International review of cytology *261*, 159-192.

Rovati, G.E., Capra, V., and Neubig, R.R. (2007). The highly conserved DRY motif of class A G protein-coupled receptors: beyond the ground state. Molecular pharmacology *71*, 959-964.

Sahly, I., Andermann, P., and Petit, C. (1999). The zebrafish eya1 gene and its expression pattern during embryogenesis. Dev Genes Evol *209*, 399-410.

Samakovlis, C., Hacohen, N., Manning, G., Sutherland, D.C., Guillemin, K., and Krasnow, M.A. (1996). Development of the Drosophila tracheal system occurs by a series of morphologically distinct but genetically coupled branching events. Development *122*, 1395-1407.

Sapede, D., Gompel, N., Dambly-Chaudiere, C., and Ghysen, A. (2002). Cell migration in the postembryonic development of the fish lateral line. Development *129*, 605-615.

Sapede, D., Rossel, M., Dambly-Chaudiere, C., and Ghysen, A. (2005). Role of SDF1 chemokine in the development of lateral line efferent and facial motor neurons. Proc Natl Acad Sci U S A *102*, 1714-1718.

Sato, M., and Kornberg, T.B. (2002). FGF is an essential mitogen and chemoattractant for the air sacs of the drosophila tracheal system. Dev Cell *3*, 195-207.

Scheer, N., and Campos-Ortega, J.A. (1999). Use of the Gal4-UAS technique for targeted gene expression in the zebrafish. Mech Dev *80*, 153-158.

Schumacher, S., Gryzik, T., Tannebaum, S., and Muller, H.A. (2004). The RhoGEF Pebble is required for cell shape changes during cell migration triggered by the Drosophila FGF receptor Heartless. Development *131*, 2631-2640.

Seifert, J.R., and Mlodzik, M. (2007). Frizzled/PCP signalling: a conserved mechanism regulating cell polarity and directed motility. Nature reviews *8*, 126-138.

Sela-Donenfeld, D., and Wilkinson, D.G. (2005). Eph receptors: two ways to sharpen boundaries. Curr Biol *15*, R210-212.

Servant, G., Weiner, O.D., Herzmark, P., Balla, T., Sedat, J.W., and Bourne, H.R. (2000). Polarization of chemoattractant receptor signaling during neutrophil chemotaxis. Science *287*, 1037-1040.

Shih, J., and Fraser, S.E. (1995). Distribution of tissue progenitors within the shield region of the zebrafish gastrula. Development *121*, 2755-2765.

Shimizu, N., Soda, Y., Kanbe, K., Liu, H.Y., Mukai, R., Kitamura, T., and Hoshino, H. (2000). A putative G protein-coupled receptor, RDC1, is a novel coreceptor for human and simian immunodeficiency viruses. J Virol *74*, 619-626.

Shoji, W., Yee, C.S., and Kuwada, J.Y. (1998). Zebrafish semaphorin Z1a collapses specific growth cones and alters their pathway in vivo. Development *125*, 1275-1283.

Sierro, F., Biben, C., Martinez-Munoz, L., Mellado, M., Ransohoff, R.M., Li, M., Woehl, B., Leung, H., Groom, J., Batten, M., *et al.* (2007). Disrupted cardiac development but normal hematopoiesis in mice deficient in the second CXCL12/SDF-1 receptor, CXCR7. Proc Natl Acad Sci U S A *104*, 14759-14764.

Signoret, N., Oldridge, J., Pelchen-Matthews, A., Klasse, P.J., Tran, T., Brass, L.F., Rosenkilde, M.M., Schwartz, T.W., Holmes, W., Dallas, W., *et al.* (1997). Phorbol esters and SDF-1 induce rapid endocytosis and down modulation of the chemokine receptor CXCR4. J Cell Biol *139*, 651-664.

Smith, S.C., Lannoo, M.J., and Armstrong, J.B. (1990). Development of the mechanoreceptive lateral-line system in the axolotl: placode specification, guidance of migration, and the origin of neuromast polarity. Anatomy and embryology *182*, 171-180.

Sokol, N.S., and Cooley, L. (2003). Drosophila filamin is required for follicle cell motility during oogenesis. Dev Biol *260*, 260-272.

Solnica-Krezel, L. (2006). Gastrulation in zebrafish -- all just about adhesion? Curr Opin Genet Dev *16*, 433-441.

Spiegelberg, B.D., and Hamm, H.E. (2007). Roles of G-protein-coupled receptor signaling in cancer biology and gene transcription. Curr Opin Genet Dev *17*, 40-44.

Sprague, J., Bayraktaroglu, L., Clements, D., Conlin, T., Fashena, D., Frazer, K., Haendel, M., Howe, D.G., Mani, P., Ramachandran, S., *et al.* (2006). The Zebrafish Information Network: the zebrafish model organism database. Nucleic Acids Res *34*, D581-585.

Springael, J.Y., Urizar, E., and Parmentier, M. (2005). Dimerization of chemokine receptors and its functional consequences. Cytokine Growth Factor Rev *16*, 611-623.

Sreedharan, S.P., Robichon, A., Peterson, K.E., and Goetzl, E.J. (1991). Cloning and expression of the human vasoactive intestinal peptide receptor. Proc Natl Acad Sci U S A *88*, 4986-4990.

Starz-Gaiano, M., and Lehmann, R. (2001). Moving towards the next generation. Mech Dev *105*, 5-18.

Starz-Gaiano, M., and Montell, D.J. (2004). Genes that drive invasion and migration in Drosophila. Curr Opin Genet Dev *14*, 86-91.

Stebler, J., Spieler, D., Slanchev, K., Molyneaux, K.A., Richter, U., Cojocaru, V., Tarabykin, V., Wylie, C., Kessel, M., and Raz, E. (2004). Primordial germ cell migration in the chick and mouse embryo: the role of the chemokine SDF-1/CXCL12. Dev Biol *272*, 351-361.

Stone, L. (1922). Experiments on the development of the cranial ganglia and the lateral sense organs in Amblystoma punctatum. J Exp Zool *35*, 421-496.

Stone, L. (1928). Primitive lines in Amblystoma and their relation to the migratory lateral line primordia. J Comp Neurol *45*, 169-190.

Stone, L. (1933). The development of lateral-line sense organs in amphibians observed in living and vital-stained preparations. J Comp Neurol *57*, 507-540.

Stumm, R., and Hollt, V. (2007). CXC chemokine receptor 4 regulates neuronal migration and axonal pathfinding in the developing nervous system: implications for neuronal regeneration in the adult brain. Journal of molecular endocrinology *38*, 377-382.

Su, M., Merz, D.C., Killeen, M.T., Zhou, Y., Zheng, H., Kramer, J.M., Hedgecock, E.M., and Culotti, J.G. (2000). Regulation of the UNC-5 netrin receptor initiates the first reorientation of migrating distal tip cells in Caenorhabditis elegans. Development *127*, 585-594.

Summerton, J. (1999). Morpholino antisense oligomers: the case for an RNase H-independent structural type. Biochim Biophys Acta *1489*, 141-158.

Sun, X., Mariani, F.V., and Martin, G.R. (2002). Functions of FGF signalling from the apical ectodermal ridge in limb development. Nature *418*, 501-508.

Sun, X., Meyers, E.N., Lewandoski, M., and Martin, G.R. (1999). Targeted disruption of Fgf8 causes failure of cell migration in the gastrulating mouse embryo. Genes & development *13*, 1834-1846.

Svetic, V., Hollway, G.E., Elworthy, S., Chipperfield, T.R., Davison, C., Adams, R.J., Eisen, J.S., Ingham, P.W., Currie, P.D., and Kelsh, R.N. (2007). Sdf1a patterns zebrafish melanophores and links the somite and melanophore pattern defects in choker mutants. Development *134*, 1011-1022.

Takeuchi, Y., Molyneaux, K., Runyan, C., Schaible, K., and Wylie, C. (2005). The roles of FGF signaling in germ cell migration in the mouse. Development *132*, 5399-5409.

Tamagnone, L., and Comoglio, P.M. (2004). To move or not to move? Semaphorin signalling in cell migration. EMBO reports *5*, 356-361.

Tarasova, N.I., Stauber, R.H., Choi, J.K., Hudson, E.A., Czerwinski, G., Miller, J.L., Pavlakis, G.N., Michejda, C.J., and Wank, S.A. (1997). Visualization of G protein-coupled receptor trafficking with the aid of the green fluorescent protein. Endocytosis and recycling of cholecystokinin receptor type A. J Biol Chem *272*, 14817-14824.

Tavner, F.J., Simpson, R., Tashiro, S., Favier, D., Jenkins, N.A., Gilbert, D.J., Copeland, N.G., Macmillan, E.M., Lutwyche, J., Keough, R.A., *et al.* (1998). Molecular cloning reveals that the p160 Myb-binding protein is a novel, predominantly nucleolar protein which may play a role in transactivation by Myb. Molecular and cellular biology *18*, 989-1002.

Thirumurugan, K., Sakamoto, T., Hammer, J.A., 3rd, Sellers, J.R., and Knight, P.J. (2006). The cargo-binding domain regulates structure and activity of myosin 5. Nature *442*, 212-215.

Thisse, B., Heyer, V., Lux, A., Alunni, V., Degrave, A., Seiliez, I., Kirchner, J., Parkhill, J.P., and Thisse, C. (2004). Spatial and temporal expression of the zebrafish genome by large-scale in situ hybridization screening. Methods Cell Biol *77*, 505-519.

Thisse, B., and Thisse, C. (2005). Functions and regulations of fibroblast growth factor signaling during embryonic development. Dev Biol *287*, 390-402.

Tickle, C., and Munsterberg, A. (2001). Vertebrate limb development--the early stages in chick and mouse. Curr Opin Genet Dev *11*, 476-481.

Ueda, Y., Neel, N.F., Schutyser, E., Raman, D., and Richmond, A. (2006). Deletion of the COOH-terminal domain of CXC chemokine receptor 4 leads to the down-regulation of cell-to-cell contact, enhanced motility and proliferation in breast carcinoma cells. Cancer Res *66*, 5665-5675.

Ulrich, F., Concha, M.L., Heid, P.J., Voss, E., Witzel, S., Roehl, H., Tada, M., Wilson, S.W., Adams, R.J., Soll, D.R., *et al.* (2003). Slb/Wnt11 controls hypoblast cell migration and morphogenesis at the onset of zebrafish gastrulation. Development *130*, 5375-5384.

Valentin, G., Haas, P., and Gilmour, D. (2007). The Chemokine SDF1a Coordinates Tissue Migration through the Spatially Restricted Activation of Cxcr7 and Cxcr4b. Curr Biol.

Van Haastert, P.J., and Devreotes, P.N. (2004). Chemotaxis: signalling the way forward. Nat Rev Mol Cell Biol *5*, 626-634.

Van Itallie, C.M., and Anderson, J.M. (2006). Claudins and epithelial paracellular transport. Annual review of physiology *68*, 403-429.

Vila-Coro, A.J., Rodriguez-Frade, J.M., Martin De Ana, A., Moreno-Ortiz, M.C., Martinez, A.C., and Mellado, M. (1999). The chemokine SDF-1alpha triggers CXCR4 receptor dimerization and activates the JAK/STAT pathway. Faseb J *13*, 1699-1710.

von Philipsborn, A., and Bastmeyer, M. (2007). Mechanisms of gradient detection: a comparison of axon pathfinding with eukaryotic cell migration. International review of cytology *263*, 1-62.

Wang, H.U., and Anderson, D.J. (1997). Eph family transmembrane ligands can mediate repulsive guidance of trunk neural crest migration and motor axon outgrowth. Neuron *18*, 383-396.

Wang, H.Y., Liu, T., and Malbon, C.C. (2006). Structure-function analysis of Frizzleds. Cell Signal *18*, 934-941.

Wang, J., Shiozawa, Y., Wang, J., Wang, Y., Jung, Y., Pienta, K.J., Mehra, R., Lober, R., and Taichman, R.S. (2007). The role of CXCR7/RDC1 as a chemokine receptor for CXCL12/ SDF-1 in prostate cancer. J Biol Chem.

Watanabe, S., Mabuchi, K., Ikebe, R., and Ikebe, M. (2006). Mechanoenzymatic characterization of human myosin Vb. Biochemistry *45*, 2729-2738.

Webb, S.E., Lee, K.K., Tang, M.K., and Ede, D.A. (1997). Fibroblast growth factors 2 and 4 stimulate migration of mouse embryonic limb myogenic cells. Dev Dyn *209*, 206-216.

Weidinger, G., Wolke, U., Koprunner, M., Klinger, M., and Raz, E. (1999). Identification of tissues and patterning events required for distinct steps in early migration of zebrafish primordial germ cells. Development *126*, 5295-5307.

Westerfield, M. (1995). The Zebrafish Book (University Of Oregon Press).

Wilkinson, D.G. (2001). Multiple roles of EPH receptors and ephrins in neural development. Nat Rev Neurosci *2*, 155-164.

Wilson, S., Wilkinson, G., and Milligan, G. (2005). The CXCR1 and CXCR2 receptors form constitutive homo- and heterodimers selectively and with equal apparent affinities. J Biol Chem *280*, 28663-28674.

Winklbauer, R. (1989). Development of the lateral line system in Xenopus. Progress in neurobiology *32*, 181-206.

Wolman, M.A., Liu, Y., Tawarayama, H., Shoji, W., and Halloran, M.C. (2004). Repulsion and attraction of axons by semaphorin3D are mediated by different neuropilins in vivo. J Neurosci *24*, 8428-8435.

Xiao, Z., Zhang, N., Murphy, D.B., and Devreotes, P.N. (1997). Dynamic distribution of chemoattractant receptors in living cells during chemotaxis and persistent stimulation. J Cell Biol *139*, 365-374.

Xu, Q., Mellitzer, G., Robinson, V., and Wilkinson, D.G. (1999). In vivo cell sorting in complementary segmental domains mediated by Eph receptors and ephrins. Nature *399*, 267-271.

Yang, S.H., Sharrocks, A.D., and Whitmarsh, A.J. (2003). Transcriptional regulation by the MAP kinase signaling cascades. Gene *320*, 3-21.

Yang, X., Dormann, D., Munsterberg, A.E., and Weijer, C.J. (2002). Cell movement patterns during gastrulation in the chick are controlled by positive and negative chemotaxis mediated by FGF4 and FGF8. Dev Cell *3*, 425-437.

Yasuoka, A., Hirose, Y., Yoda, H., Aihara, Y., Suwa, H., Niwa, K., Sasado, T., Morinaga, C., Deguchi, T., Henrich, T., *et al.* (2004). Mutations affecting the formation of posterior lateral line system in Medaka, Oryzias latipes. Mech Dev *121*, 729-738.

Ye, R.D. (2001). Regulation of nuclear factor kappaB activation by G-protein-coupled receptors. Journal of leukocyte biology *70*, 839-848.

Yoon, C., Kawakami, K., and Hopkins, N. (1997). Zebrafish vasa homologue RNA is localized to the cleavage planes of 2- and 4-cell-stage embryos and is expressed in the primordial germ cells. Development *124*, 3157-3165.

Zhang, X., Ibrahimi, O.A., Olsen, S.K., Umemori, H., Mohammadi, M., and Ornitz, D.M. (2006). Receptor specificity of the fibroblast growth factor family. The complete mammalian FGF family. J Biol Chem *281*, 15694-15700.

Zlotnik, A. (2006). Chemokines and cancer. International journal of cancer *119*, 2026-2029.

# Appendix

## Supplementary data

S1; S2; S3: Timelapse series of the initiation of posterior lateral line primordium migration.

S4a-c: Tracked timelapse series examining the initiation of the posterior lateral line primordium. Images relate to S1.

S5a-c: Tracked timelapse series examining the initiation of the posterior lateral line primordium. Images relate to S3.

S6; S7; S8; S9: Timelapse series examining the behaviour of *cxcr7b* morphant primordia displaying the split primordium phenotype.

S10: Timelapse series examining of a *cxcr7b* morphant primordium displaying the ventral migration phenotype.

S11: Timelapse analysis of primordium migration in a control embryo.

S12; S13: Timelapse analysis of *cxcr7b* morphant primordia displaying the ventral migration phenotype.

S14; S15; S16: Timelapse series examining the effect of CXCR7bRFP expression in the posterior lateral line primordium on cell behaviour.

S17; S18: Timelapse series examining the effect of CXCR7bRFP expression on the migration pathway on the behaviour of the posterior lateral line primordium.